REFERENCE ONLY

UNIVERSITY OF LONDON THESIS

Degree PhD Year 2006 Name of Author A U. A B

The incorporation of sulfur, oxygen and nitrogen containing organic molecules into triosmium clusters

Abul Basar Ali

A thesis submitted to the University of London for the partial fulfilment for the requirement for the degree of doctor of philosophy.

Department of Chemistry
University College London (UCL)

June 2006

ProQuest LLC
789 East Eisenhower Parkway
P.O. Box 1346
Ann Arbor, MI 48106-1346

Abstract

This thesis describes the oxidative addition reactions of sulfur, oxygen and nitrogen containing organic molecules into triosmium clusters. The products were formed by C-H, O-H, N-H and S-S bond cleavage.

The direct reaction of dibenzyl disulfide, di(2-thienyl)disulfide and di-*tertiary*-butyl disulfide with cluster $[Os_3(MeCN)_2(CO)_{10}]$ yielded their respective unsymmetrical thiolato derivatives: $[Os_3(\mu\text{-}SCH_2Ph)_2(CO)_{10}]$, $[Os_3(\mu\text{-}S^tBu)_2(CO)_{10}]$ and $[Os_3(\mu\text{-}SC_4H_3S_2)_2(CO)_{10}]$ in high yields with the cleavage of the S-S bond. Only dibenzyl disulfide gave a second cluster $[Os_3(\mu\text{-}H)(S_2CH_2Ph)(CO)_{10}]$, which retained the S-S bond. Thermal treatment of $[Os_3(\mu\text{-}SCH_2Ph)_2(CO)_{10}]$ gave the symmetrical isomer in which both sulfur ligands bridged the same pair of osmium atoms. The interconversion of isomers of the unsymmetrical form of $[Os_3(\mu\text{-}SCH_2Ph)_2(CO)_{10}]$, related by inversion at sulfur, gave Ea = 61.5± 2.0 kJ mol^{-1}, determined by NMR methods.

The direct reaction of 8-hydroxyquinoline with $[Os_3(MeCN)_2(CO)_{10}]$ employing various reaction conditions yielded both mono-, tri- and tetra-nuclear compounds: $[Os(C_9H_6NO)_2(CO)_2]$, $[Os_3(C_9H_6NO)_2(CO)_8]$, $[Os_3(\mu\text{-}H)(C_9H_6NO)(CO)_9]$ and $[Os_4(\mu\text{-}H)(C_9H_6NO)(CO)_{11}]$. Three isomers of complex $[Os(C_9H_6NO)_2(CO)_2]$ were observed.

Reactions between osmium carbonyl and phenols substituted with both electron-donating or accepting substituents always gave the dienone structures $[Os_3(\mu\text{-}H)_2(\mu\text{-}OC_6H_4X)(CO)_9]$ (X = OH, F, OMe) in preference to the alternative aromatic form. The variable-temperature NMR spectra of $[Os_3(\mu\text{-}H)_2(\mu\text{-}OC_6H_4OMe)(CO)_9]$ show both the hydrides and the carbonyl ligands are mobile. Attempts to link clusters were only successful with hydroquinone which gave $[Os_6(\mu\text{-}H)_3(\mu\text{-}OC_6H_3O)(CO)_{19}]$. However with aminophenol, reaction was always preferred at the amine in preference to the hydroxyl group. Benzoquinone gave a unique cluster $[Os_3(\mu\text{-}H)(\mu\text{-}OC_6H_5O)(CO)_{10}]$.

Finally we have shown how the direct reaction of $[Os_3(MeCN)_2(CO)_{10}]$ with 4,4-dipyridyl disulfide yields the linked cluster $[Os_6(\mu\text{-}H)_2(\mu\text{-}C_5H_3NS_2C_5H_3N)(CO)_{20}]$ leaving the S-S bond intact. The S-S cleavage occurs by treating $[Os_6(\mu\text{-}H)_2(\mu\text{-}C_5H_3NS_2C_5H_3N)(CO)_{20}]$ further with $[Os_3(MeCN)_2(CO)_{10}]$ to give $[Os_9(\mu\text{-}H)_2(NC_5H_3S)_2(CO)_{30}]$. The initial reaction always takes place at the pyridine ligands followed by S-S cleavage. The reaction of 4-mercaptopyridine gave a linked cluster $[Os_6(\mu\text{-}H)_2(NC_5H_3S)(CO)_{20}]$. All these reactions were carried out at room temperature.

For my mum and dad, and my brothers and sisters

"The most powerful legacy in life is to enable others. Let them be the best they can be." Ghandi

Acknowledgements

I would like to thank my supervisor Professor A. J. Deeming, not only for his invaluable help, guidance, support and encouragement during the course of this research but also for carrying out the crystal structures and the gNMR simulations. I would also like to thank Dr D. A. Tocher for determining the crystal structure of $[Os_3(\mu\text{-}H)_2(OC_6H_3OMe)(CO)_9]$ and Dr A. E. Aliev for help with the variable-temperature NMR work.

My thanks to Professor S. E. Kabir and Dr A. Mottalib for tea and discussions on the political situation of Bangladesh and also to Mr John Hill for mass spectroscopic work. Thanks to all those in chemistry who have provided so much fun and entertainment: Caroline, Catherine, Sarah, Karim, Shervin, Warren and Jade, and many more. Thank you all!

Finally I would like to thank my family for their help and support throughout my life. Thanks to my nephews and niece, Tasnimul, Saiyed, Bokkor, Asad, Yusuf, Amena, Hamza, Hafiz and Hanifa for their smiles! Thanks go to Shelly for being a life-long friend, a great teacher but more importantly for being a wonderful person.

Table of Contents

Chapter 1. Chemistry of triosmium cluster $[Os_3(CO)_{12}]$

1.1 Introduction

The chemistry of osmium carbonyl clusters has come a long way since its birth in the 1940s. The chemistry of arene clusters, which is still in its infancy, has attracted considerable interest in the last few years. It has recently begun to emerge as an important entity within the field of organometallic chemistry, even though the root of this subject dates back as far as the late 1950s. This introduction will describe a few key triosmium clusters, which have been important in the development of the subject.

1.2 The cluster $[Os_3(CO)_{12}]$ 1.1

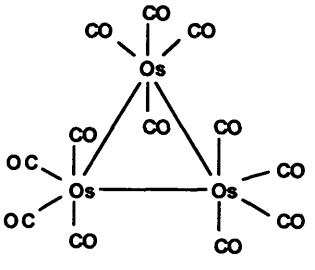

Dodecacarbonyltriosmium $[Os_3(CO)_{12}]$ **1.1** is the fundamental starting material for the syntheses of triosmium clusters. Larger osmium clusters can be synthesised from it.

Clusters may be defined in a variety of ways, but they are generally considered by inorganic chemists as compounds in which three or more metal atoms are incorporated into a molecule involving significant metal-metal bonding. The area of triosmium clusters has grown rapidly over the last 30 years. A comprehensive review of triosmium cluster chemistry appeared in 1986,[1] along with others on the general chemistry of osmium.[2,3,4] The yellow cluster **1.1**, easily prepared from OsO_4,[5] is triangular with D_{3h} symmetry with six axial CO ligands and six equatorial CO ligands in the Os_3 plane. Cluster **1.1** is highly stable thermally and in the air. Previously, **1.1** was synthesised using a high boiling inert solvent such as xylene, which gave low yields as well as some contamination with the cubane compound $[Os_4O_4(CO)_{12}]$.[6] $[Os_3(CO)_{12}]$ is prepared in excellent yield by treating OsO_4 with CO in ethanol.[7] The ruthenium cluster $[Ru_3(CO)_{12}]$ was synthesised from $RuCl_3$ using zinc dust as a reducing agent, as orange crystals which darken on exposure to sunlight and air over a prolonged period.[8]

$$3OsO_4 + 24CO \longrightarrow Os_3(CO)_{12} + 12CO_2$$

The average Os–Os bond distance in **1.1** is 2.877(3) Å. The average Os–C (axial) distance of 1.946(6) Å is marginally longer than the average Os–C (equatorial) distance of 1.912(7) Å. The difference between these lengths (0.034 Å) is only just greater than three times the standard deviation of the measurement (0.02 Å), so the difference is not a great significant. However, we would expect axail Os-C bonds to be longer because axial co-ordination of CO is weaker as these ligands are competing for available *d*–orbitals for back bonding. Each osmium atom is co-ordinated to four terminal ligands and bonds to two other metal atoms, thus giving an eighteen valence-electron shell [$d^8 + (4 \times 2) + (2 \times 1)$]. The complex is therefore *saturated* and fairly unreactive at low temperatures towards reactions that involve either Os-Os or Os-C bond cleavage. However at higher temperatures CO fluxionality is observed by variable temperature NMR, in which there is CO migration over all CO sites.

The osmium carbonyl bonds are relatively strong (ca. 201 kJ mol^{-1}),[9] so in order to introduce a ligand on to the metal cluster by cleavage of an osmium carbonyl bond, a

large activation energy is required. The stability and inertness of cluster **1.1** initially caused synthetic problems because the need for high temperature procedures prevented all but the most robust products from being obtained. Various synthetic routes have been developed enabling reactions to be carried out at lower temperatures.

The direct reactions of $[Os_3(CO)_{12}]$ **1.1** with halogens such as X_2 (X = Cl, Br, I), yield the non-cyclic complexes $[Os_3(CO)_{12}X_2]$ which can be converted to the triangular complexes $[Os_3(CO)_{10}X_2]$ on heating.[10,11]

$$Os_3X_2(CO)_{12} \xrightarrow{\text{Heat}} Os_3X_2(CO)_{10} + 2CO$$

The ring-closed hydrido derivative $[Os_3HX(CO)_{10}]$ has been synthesised by treating $[Os_3Cl_2(CO)_{12}]$ with sodium borohydride.[12] Better yields are obtained by treating $[Os_3(\mu\text{-}H)_2(CO)_{10}]$ with allyl chloride.

$$Os_3Cl_2(CO)_{12} \xrightarrow{NaBH_4} Os_3HCl(CO)_{10}$$

Of the triad Fe, Ru and Os, it has been found that osmium clusters rarely adopt structures with bridging CO ligands, whereas ruthenium is more likely to form a bridging CO structure. Iron clusters have an even stronger tendency to form carbonyl bridges as $[Fe_3(CO)_{12}]$ contains two bridging CO ligands observed by both IR and X-ray diffraction.[13] This could be because the larger radii of the heavier elements disfavour carbonyl bridges. Wade has devised an updated version of bond enthalpy data which systematize these structural differences (**Table 1.1**).[14] An increase in the stability of metal-metal bonds on descending a triad is paralleled by an increase in the stability of metal carbonyl bonds. Therefore discussion about stability of **1.1** must consider both factors, not just the metal-metal bonds.[15] The X-ray crystal structure of $[Fe_3(CO)_{12}]$ was determined by Wei and Dahl in 1969. In a subsequent publication they explained the history of the problem associated with determining the structure of $[Fe_3(CO)_{12}]$.[16]

Table 1.1 The bond enthalpy data for triad clusters.[14]

	$[Fe_3(CO)_{12}]$	$[Ru_3(CO)_{12}]$	$[Os_3(CO)_{12}]$
E(M-M) kJ/ mol^{-1}	65	78	94
E(M-CO) kJ/mol^{-1}	126	182	201

1.3 Clusters $[Os_3(MeCN)(CO)_{11}]$ and $[Os_3(MeCN)_2(CO)_{10}]$

The triosmium complexes $[Os_3(MeCN)(CO)_{11}]$ **1.2** and $[Os_3(MeCN)_2(CO)_{10}]$ **1.3** are easily synthesised by treating $[Os_3(CO)_{12}]$ with trimethylamine *N*-oxide (Me_3NO) and acetonitrile (MeCN). The trimethylamine *N*-oxide oxidises the carbonyl ligands on triosmium to carbon dioxide leaving trimethylamine or acetonitrile to fill the vacant co-ordination site.[17,18] The mechanism involves initial nucleophilic attack of Me_3NO at the carbon of the coordinated CO so the reagent is only useful when the CO are susceptible to nucleophilic attack.

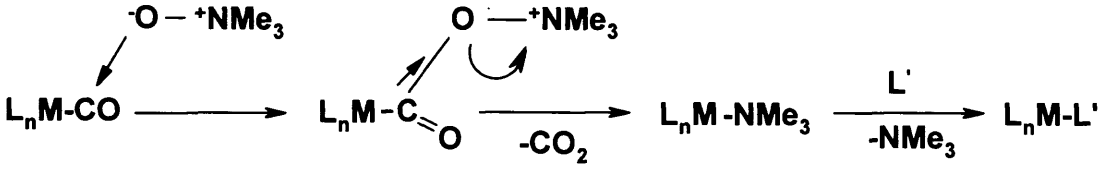

Substitution of a carbonyl ligand using amine N-oxide in the presence of a ligand L'

Trimethylamine is a very poor ligand and can be easily displaced by acetonitrile to give clusters **1.2** and **1.3**. The acetonitrile ligands of $[Os_3(MeCN)(CO)_{11}]$ **1.2** and $[Os_3(MeCN)_2(CO)_{10}]$ **1.3** are labile[19] and are readily substituted by other potential ligands.[18,20] Whether **1.2** or **1.3** is obtained is controlled by the amount of amine oxide added and each may be formed successively and quantitatively although more care is normally needed to form **1.2** without contamination with **1.3**.[21,22,23] Treatment with an excess of Me_3NO/MeCN does not give the *tris*-product.

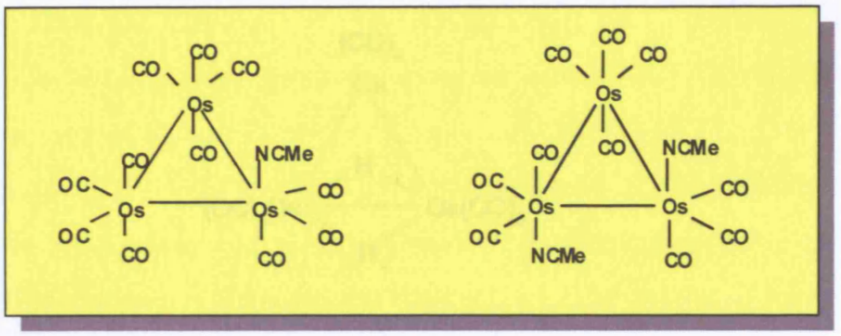

1.2 **1.3**

The osmium compounds **1.2** and **1.3** may be stored indefinitely, whereas the ruthenium analogues $[Ru_3(CO)_{11}(MeCN)]$ **1.4** and $[Ru_3(CO)_{10}(MeCN)_2]$ **1.5** are best used without isolation since they are only stable at –20 °C or below.[24] In each case silica is used to absorb any excess of Me_3NO before using the cluster for a reaction, since an excess leads to decomposition or side reactions. Clusters **1.2** and **1.3** are stable enough to be separated by Thin Layer Chromatography (TLC) in the presence of MeCN or by HPLC.[25] More recently it has been found that both clusters **1.2** and **1.3** can be easily prepared by broad-band UV irradiation of an acetonitrile solution of **1.1** for one and two hours respectively.[26] The ruthenium analogues of **1.4** and **1.5** can be synthesised in the same way.[26] This offers a simple and high yield route to the highly versatile substituted clusters, without the use of any oxidant (Me_3NO). The replacement of a third carbonyl ligand has not been achieved for **1.3** using either photolysis or the use of an excess of trimethylamine *N*–oxide and MeCN. However, the protonated form of the tris(acetonitrile) complex of triosmium $[Os_3(\mu\text{-}H)_2(MeCN)_3(CO)_9][CF_3SO_3]_2$ has been obtained by another method.[27] Interestingly, the photolysis method using an excess of trimethylamine *N*–oxide and MeCN has been successful for $[Ru_3(CO)_{12}]$ to give $[Ru_3(MeCN)_3(CO)_9]$.[28]

1.4 Cluster $[Os_3(\mu\text{-}H)_2(CO)_{10}]$

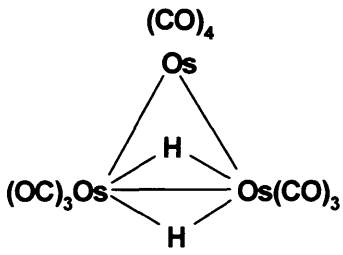

1.6

1.4.1 Structure and properties of $[Os_3(\mu\text{-}H)_2(CO)_{10}]$

Several triosmium clusters are known in which the ligands and metal–metal single bonds do not provide an eighteen-valence electron shell about each metal. Such complexes are *unsaturated.* The most studied of these electron-deficient triosmium clusters is the purple compound $[Os_3(\mu\text{-}H)_2(CO)_{10}]$ **1.6**, which is easily prepared by the hydrogenation of $[Os_3(CO)_{12}]$ **1.1** [29] or $[Os_3(CO)_{10}(MeCN)_2]$ **1.3** under mild conditions.[23] Osmium–osmium double bonds are commonly drawn to represent this unsaturation, the rationale being that metal atoms in such complexes will share an electron to complete their valence shell. However the force constant measurements associated with the bridged pair of osmium atoms support the no-direct-bond picture for the $Os(\mu\text{-}H)_2Os$ bridge.[30] Photoelectron spectroscopy (PES) and molecular orbital (MO) calculations support this view.[31]

The structure of cluster **1.6** has been established by both X-ray and neutron diffraction.[1] Carbon–13 NMR saturation–transfer studies have given rates for slow localised exchange at each $Os(CO)_3$ group, and the ^{17}O quadrupolar coupling constant has been determined.[32]

1.4.2 Chemistry of $[Os_3(\mu\text{-}H)_2(CO)_{10}]$

Whatever the electronic structure of $[Os_3(\mu\text{-}H)_2(CO)_{10}]$ **1.6**, it certainly shows unsaturation in its reactions with the simple donor molecule L (L = CO, H_2, MeCN, etc.). If CO is bubbled through a purple solution of $[Os_3(\mu\text{-}H)_2(CO)_{10}]$, a yellow solution of $[Os_3(\mu\text{-}H)_2(CO)_{10}L]$ **1.7** (L = CO) is formed, and if N_2 is bubbled through this solution the decacarbonyl **1.6** is regenerated.[33,34] In addition cluster **1.7** can add another CO with elimination of H_2 to give complex **1.1**. The cluster **1.6** undergoes many reactions, for example, nucleophilic addition, electrophilic addition and insertion (**Scheme 1.1**).

The initial adduct **1.7** can be isolated with many different ligands (tertiary phosphines, isonitriles, MeCN or PhCN), but often adducts of this type react to give insertion products. The crystal structures of the tertiary phosphine derivatives and many others have been determined. The structures relate closely to that of $[Os_3(CO)_{12}]$ **1.1**, with an axial terminal hydride replacing one CO ligand. Examples in which there is insertion into Os–H bonds for alkynes, alkenes, ketenes, R_2CN_2, $Ph_2C{=}S$, isocyanates (RNCO), azides (RN_3), isonitriles and nitriles have been reported.[1,2] The loss of CO or H_2 are alternatives to insertion. The loss of CO regenerates unsaturated species of type $[Os_3(\mu\text{-}H)_2(CO)_9L]$ **1.9**, a reaction that can occur thermally but may also be photochemically induced.

The ruthenium analogue of the dihydrido species $[Ru_3(\mu\text{-}H)_2(CO)_{10}]$ **1.11**, which had evaded chemists for many years, was finally synthesised in high yield by broadband UV irradiation of a dichloromethane solution of $[Ru_3(CO)_{12}]$ under an atmosphere of hydrogen. The deep orange dihydridotriruthenium cluster has been characterised by IR and ^1H NMR spectroscopy.[35] Further irradiation of the dichloromethane solution of **1.11** under hydrogen leads to the generation of the known tetranuclear hydrido cluster $[Ru_4(\mu\text{-}H)_4(CO)_{12}]$.[5] The tetranuclear hydrido cluster is the product of the thermal treatment of $[Ru_3(CO)_{12}]$ with H_2. It is interesting to note that there is a marked difference between the reactivity of **1.6** and **1.11** with simple donor ligands.

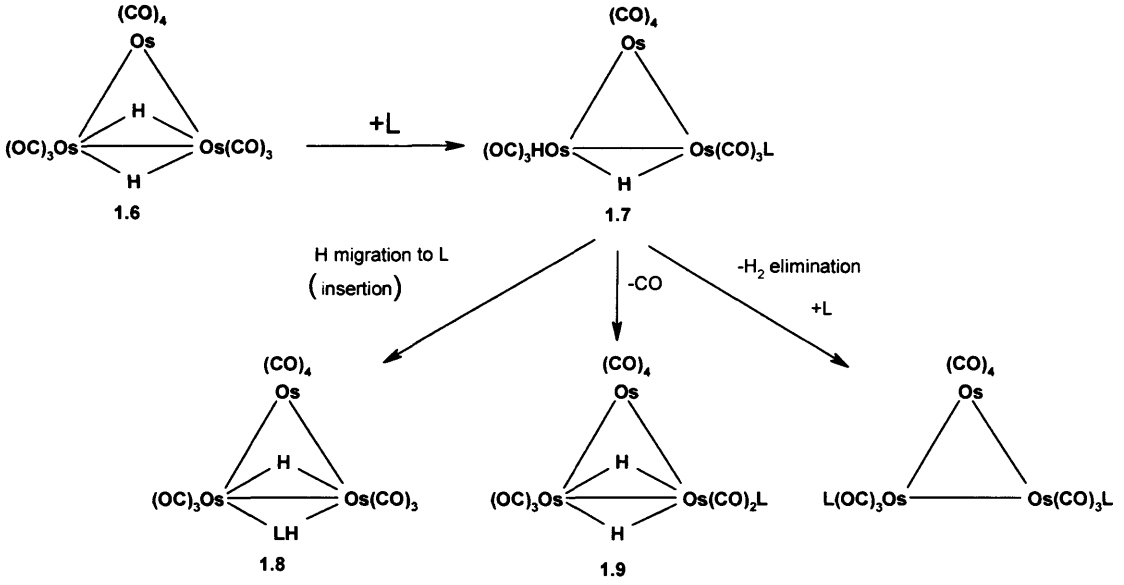

Scheme 1.1. Shows the chemistry of the unsaturated cluster $[Os_3(\mu\text{-}H)_2(CO)_{10}]$ 1.6.

The treatment of **1.11** with phenylacetylene (HC≡CPh) only gives the acetylide derivative $[Ru_3(\mu\text{-}H)(\mu\text{-}\eta^2\text{-}C_2Ph)(CO)_{10}]$, whereas for **1.6**, the vinyl cluster $[Os_3(\mu\text{-}H)(\mu\text{-}\sigma,\pi\text{-}CH{=}CHPh)(CO)_{10}]$ is formed in addition to $[Os_3(\mu\text{-}H)(\mu\text{-}\eta^2\text{-}C_2Ph)(CO)_{10}]$. This demonstrates the difference in metal-metal and other M-X bond strengths in ruthenium and osmium cluster compounds.[25]

1.5 Monofunctional ligands

The reactivity of alcohols (ROH), thiols (RSH), amines (NH_2R) and primary phosphines (PH_2R) has been extensively studied. Alcohols and thiols both react with dodecacarbonyltriosmium at high temperatures to give complexes of the type $[Os_3(\mu\text{-}H)(\mu\text{-}OR)(CO)_{10}]$ **1.12** [36] or $[Os_3(\mu\text{-}H)(\mu\text{-}SR)(CO)_{10}]$ **1.13**.[37] Complexes of these types have been characterized by infrared, ^1H NMR and X-ray diffraction. [38] These complexes have been recently synthesised by Leadbeater using a milder method at room temperature by UV or visible photolysis.[15] Leadbeater has also shown that prolonged photolysis of the reaction mixture of $[Ru_3(CO)_{12}]$ and RSH leads to the known sulphido cluster $[Ru_3(\mu_3\text{–}S)(CO)_{10}]$.[15] Since the completion of these experiments, a general pattern has emerged. It has been found that if there are two

hydrogens on a heteroatom both may be transferred to the metal, as in the reaction of H_2S with $[Os_3(CO)_{12}]$ **1.1**, to give the sulfur-capped cluster $[Os_3(\mu\text{-}H)_2(\mu_3\text{-}S)(CO)_9]$.[39] The transfer of two hydrogens to a molecule of triosmium cluster, is now known for olefins,[39,40,41,42] benzene,[39] trialkylphosphines,[43] hydrogen sulphide [39] and many other compounds.

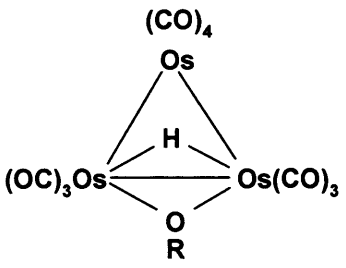

1.12

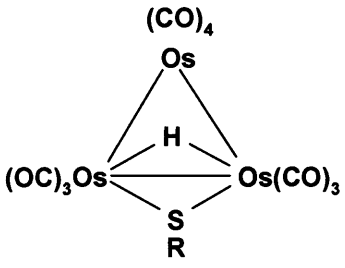

1.13

1.5.1 Reactions of $[Os_3(CO)_{12}]$ with arenes

There is considerable interest in the analogy between arenes bound to metal clusters and the interaction of arenes with metal surfaces. The interaction of arene ligands with clusters has been of great interest for many years. Clusters with one or more arene ligands present are known to exist with nuclearities ranging from three to eight.[44] In general, arene ligands tend to co-ordinate in one of two main bonding modes, either the terminal (η^6) or the face capping ($\mu_3\text{-}\eta^2\text{:}\eta^2\text{:}\eta^2$). Compounds with these bonding modes can and sometimes do interconvert, but the factors affecting the relative stabilities of these bonding modes have not been fully determined.[44]

The complex $[Os_3(\mu_3\text{-}\eta^2\text{:}\eta^2\text{:}\eta^2\text{-}C_6H_6)(CO)_9]$ **1.14** was the first example of an arene facially bound to a triosmium cluster or any other metal atom cluster. It was successfully synthesised by Johnson and Lewis *et al.* in 1985,[45] **Scheme 1.2**. The hexaruthenium complex $[Ru_6C(\eta^6\text{-}C_6H_6)(\mu_3\text{-}\eta^2\text{:}\eta^2\text{:}\eta^2\text{-}C_6H_6)(CO)_{11}]$ was reported at the same time. **Scheme 1.2** illustrates the different routes to complex **1.14**. Complex **1.14** can be synthesised using either compound **1.3** or **1.6** as the starting material to give a triply-bridging cyclohexadienyl complex $[Os_3(\mu\text{-}H)(\mu_3\text{-}\eta^2\text{:}\eta^1\text{:}\eta^2\text{-}C_6H_7)(CO)_9]$ **1.15**. This was also prepared several years earlier by Johnson *et al.*[46] by the reaction of **1.6** with cyclohexa-1,3-diene. A hydride ion can be abstracted from the facially

bound dienyl complex **1.15** using the trityl cation, $[Ph_3C]^+$ to give the cationic benzene cluster $[Os_3(\mu\text{-}H)(\mu_3\text{-}\eta^2\text{:}\eta^2\text{:}\eta^2\text{-}C_6H_6)(CO)_9]^+$. This can be treated with the non-coordinating base 1,8-diazobicyclo[5.4.0]undec-7-ene (DBU). This results in the deprotonation of the metal triangle to give the neutral μ_3–benzene triosmium cluster **1.14**.

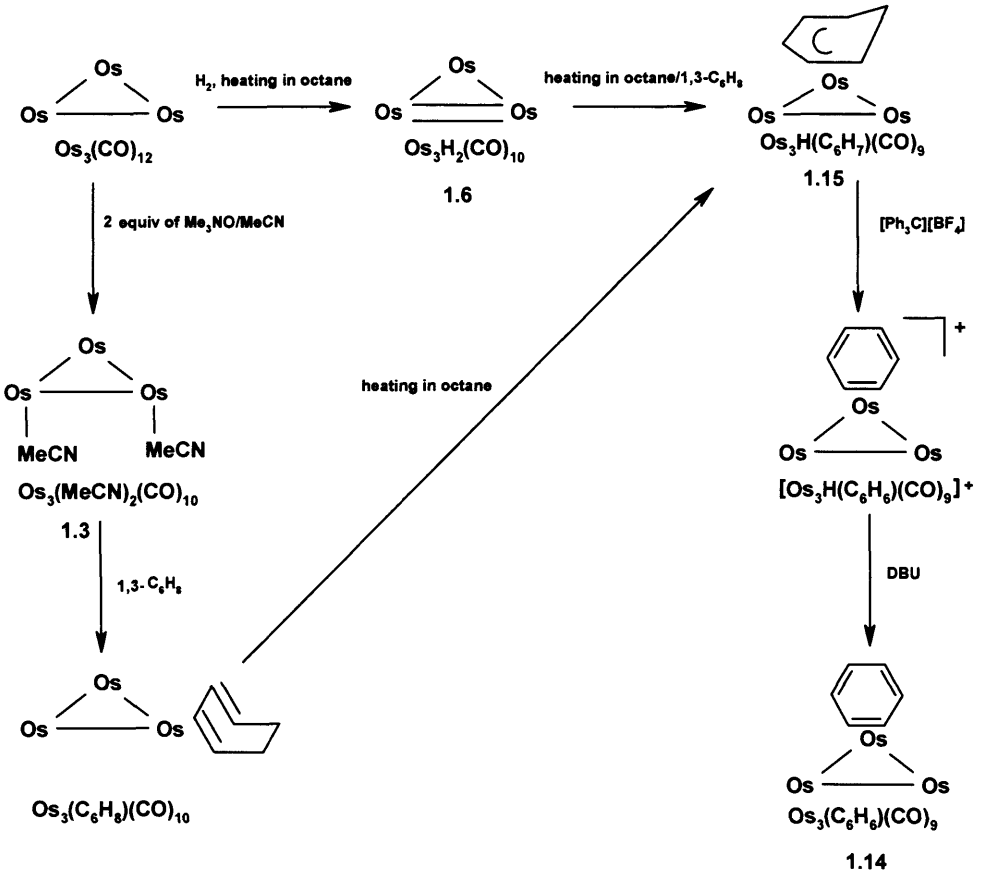

Scheme 1.2. Shows the synthesis of cluster 1.14.

The ruthenium analogue of **1.14** was synthesised five years later using the ruthenium analogue of **1.5**[47] since $[Ru_3(\mu\text{-}H)_2(CO)_{10}]$ **1.11** was not available then and had only recently been synthesised.[35] The $[Ru_3(\mu_3\text{-}C_6H_6)(CO)_9]$ cluster can also be made directly from $[Ru_3(CO)_{12}]$ and cyclohexa-1,3-diene in the presence of trimethylamine *N*-oxide.[48] This direct-method synthesis does not work for **1.1**. This is probably because ruthenium is more reactive than osmium which once again demonstrates the difference in reactivity between the two clusters.

Further reactions can be carried out on complex **1.14** as illustrated in **Scheme 1.3**. All the clusters mentioned have been characterized by infrared and ^{1}H NMR spectroscopy and X-ray diffraction.[45,46,47,48] The complex $[Os_3(CO)_9(\mu_3\text{-}\eta^2\text{:}\eta^2\text{:}\eta^2\text{-}C_6H_6)]$ **1.14** has been subjected to *ab initio* MO calculations.[49] It has been shown that the benzene interacts with the metal by a combination of donation and back-donation. There is evidence that the H atoms lie out of the C_6 plane away from the Os_3 triangle and there is some evidence of bond length alternation in the C_6 ring. The barrier to the internal rotation of the benzene over the osmium triangle has been estimated to be 66.5 kJ mol^{-1}.[49]

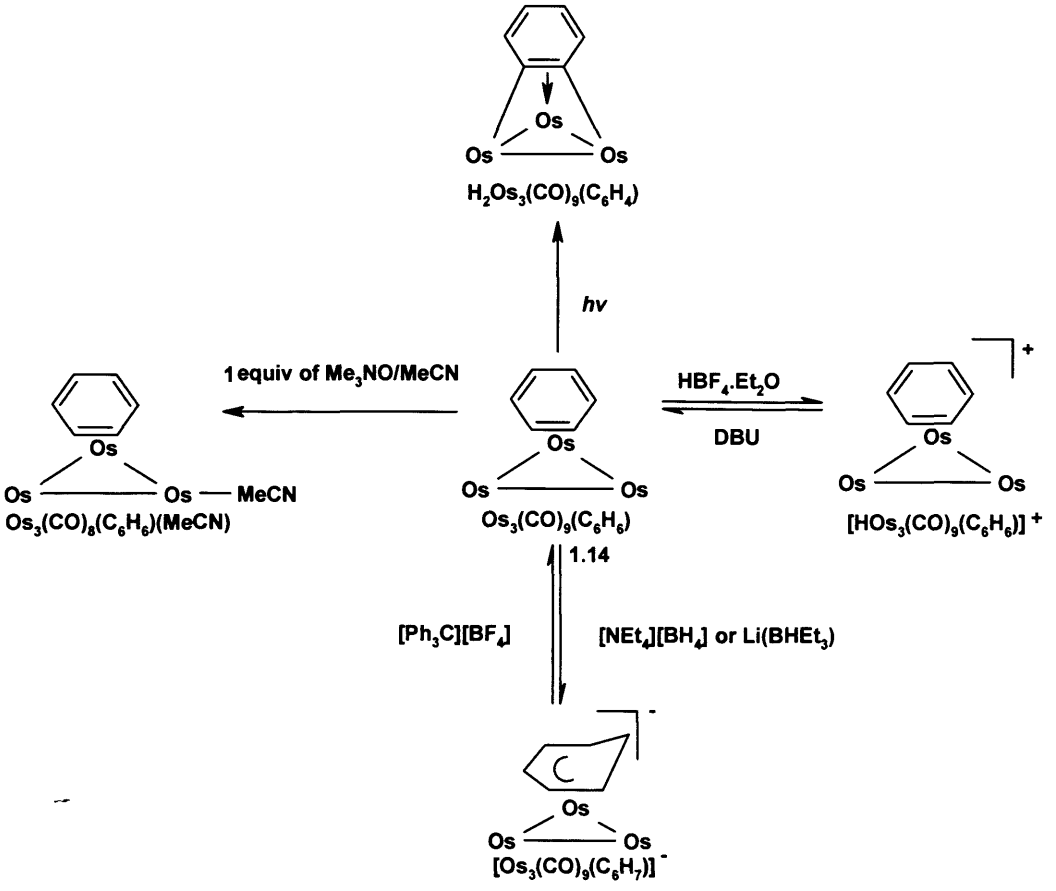

Scheme 1.3. Shows the reactions of cluster 1.14

1.5.2 Reactions of triosmium clusters with phenols

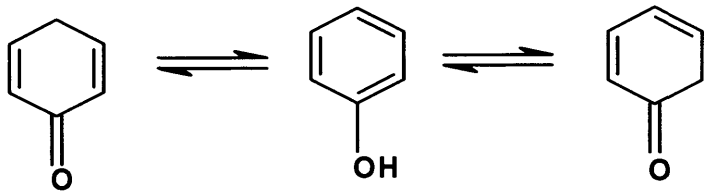

Phenol

In the area of triosmium cluster chemistry, there has been relatively little work reported on the reactivity of phenols with the cluster $[Os_3(CO)_{12}]$ **1.1**. Phenol (C_6H_6O) can in principle exist in three tautomeric forms, related by 1,3-hydrogen shifts as shown above. Because of the aromaticity of phenol, the central form shown (the classical description of phenol) is by far the most stable.

Deeming and Azam carried out the first experiment of phenol with cluster **1.1** in 1976.[49] They were interested in the successive transfer of hydrogen atoms from the ligand to metal. The Deeming group had previously shown that the treatment of aniline with $[Os_3(CO)_{12}]$ **1.1** at a high temperature results in a yellow crystalline complex $[Os_3(\mu\text{-}H)_2(C_6H_4NH)(PhNH_2)(CO)_8]$, which reacts with carbon monoxide to give the derivatives $[Os_3(\mu\text{-}H)_2(C_6H_4NH)(CO)_9]$ **1.15** and $[Os_3(\mu\text{-}H)(HNPh)(CO)_{10}]$ **1.16**.[50] If the original reaction of **1.1** with neat aniline is carried out with carbon monoxide passing through the solution, the decacarbonyl **1.16** is the major product. Complex **1.15** can also be obtained by heating **1.16** in a refluxing nonane solution under nitrogen. The compound **1.15** may be regarded as a double oxidative addition product, the second oxidative addition being an *ortho*-metallation. However, visible photolysis of compound **1.16** at room temperature leads to $[Os_3(\mu\text{-}H)_2(NPh)(CO)_9]$, which is an isomer of **1.15** in which both hydride ligands are derived from the NH_2 group. All the complexes have been characterized by mass spectroscopy, elemental analysis and ^1H NMR.[50] All the data suggest that the nitrogen lone-pairs rather than the π-electrons of arene, are used in the initial bonding to metals. Corresponding reactions with *p*-fluoroaniline and *p*-methylaniline have also been carried out giving similar derivatives to those of aniline.[50]

Phenol reacts with compound **1.1** to give the μ_2-phenolato complex $[Os_3(\mu\text{-}H)(\mu_2\text{-}OPh)(CO)_{10}]$ **1.17**, which loses CO on thermolysis at 150 °C in refluxing nonane to give $[Os_3(\mu\text{-}H)_2(OC_6H_4)(CO)_9]$ **1.18**. This compound is formed by the transfer of a hydrogen atom to osmium from the 2-position of the benzene ring in addition to the transfer of H from the OH group.[49]

The direct reaction of **1.1** with phenol at 170-185 °C gives $[Os_3(\mu_2\text{-}OPh)_2(CO)_{10}]$ as well as **1.17** and **1.18**, and the reaction of 2-isopropyl- or 2-benzyl-phenol gives the substituted analogues of **1.18**. It was initially thought that since complex **1.15** is related to **1.18** by an isoelectronic replacement of NH by O, both compounds **1.15** and **1.18** would be isostructural. This was later proved inaccurate since complexes derived from ketens and aldehydes showed very strong analogies with **1.18** and were well characterised as keto species.[51] This implies the clusters were bridged by a carbon atom rather than an oxygen atom. This was later shown by the X-ray crystal structure of 2-benzylphenol derivative, which clearly showed that a carbon rather than oxygen atom of the μ_3-ligand was bridging. The phenol molecule had been trapped in its dienone form.[52] The bond length data obtained from $[Os_3(\mu\text{-}H)_2(OC_6H_3CH_2Ph)(CO)_9]$ **1.19** supports a dienone structure, as there was an alternation of the bond lengths around the diene part of the ring. One C-C bond was essentially single (1.52 Å) and the C-O bond length (1.28 Å) indicated a double bond.[52] Conversely, the crystal structure of the aniline derivative $[Os_3(\mu\text{-}H)_2(HNC_6H_3F)(CO)_9]$ **1.20** clearly showed the ring to be aromatic with C-C bond distances in the range of 1.35-1.42 Å, which is a big contrast to the bond lengths of **1.19**.[52] **Scheme 1.4** shows the different products obtained from **1.1** with phenol and aniline.

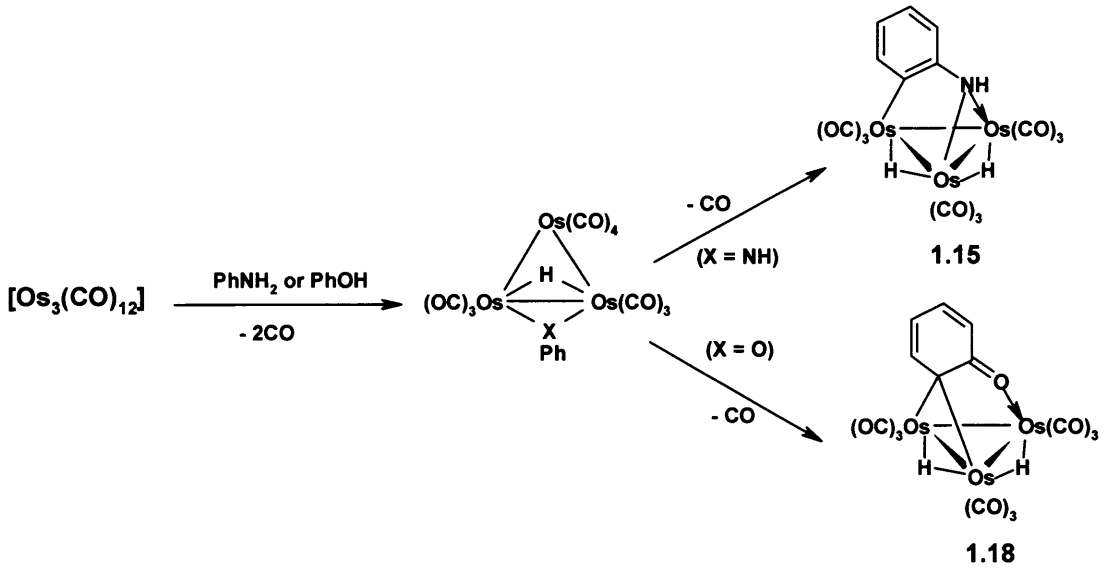

Scheme 1.4. The chemistry of phenol and aniline.

To date there has only been one report of the reaction of $[Ru_3(CO)_{12}]$ with phenol.[53] This is very surprising, considering the reactivity of ruthenium clusters is generally much greater than osmium. When $[Ru_3(CO)_{12}]$ is treated with an excess of phenol in boiling cyclohexane, the complex $[Ru_6(\mu\text{-}H)_2(\mu\text{-}C_6H_4O)(CO)_{16}]$ **1.21** is obtained in 30% yield as black crystals. This complex has been fully characterized.[53] The structure of **1.21** is very unusual as it has little resemblance to the osmium analogues. There is some resemblance in that *ortho*-metallation has occurred to give the C_6H_4O ligand. The cluster has a puckered 'raft' arrangement of ruthenium atoms, in which only one ruthenium atom has not bonded to the $\mu\text{-}OC_6H_4$ ligand (**Figure 1.1**).

The C_6H_4O ligand in **1.21** counts as a 10-electron donor (6 electrons are from the aromatic π-system, one electron is donated by the *ortho*-metallated carbon and three electrons are from the μ-OR unit). This together with the electrons of 2 H, 16 CO ligands and 6 ruthenum atoms, gives a total electron count of 92-electrons. This is two more than would be required to fulfil the 18-electron rule for all of the ruthenium ions. An electron excess of this kind has been observed in earlier work on structures by Sundberg.[54]

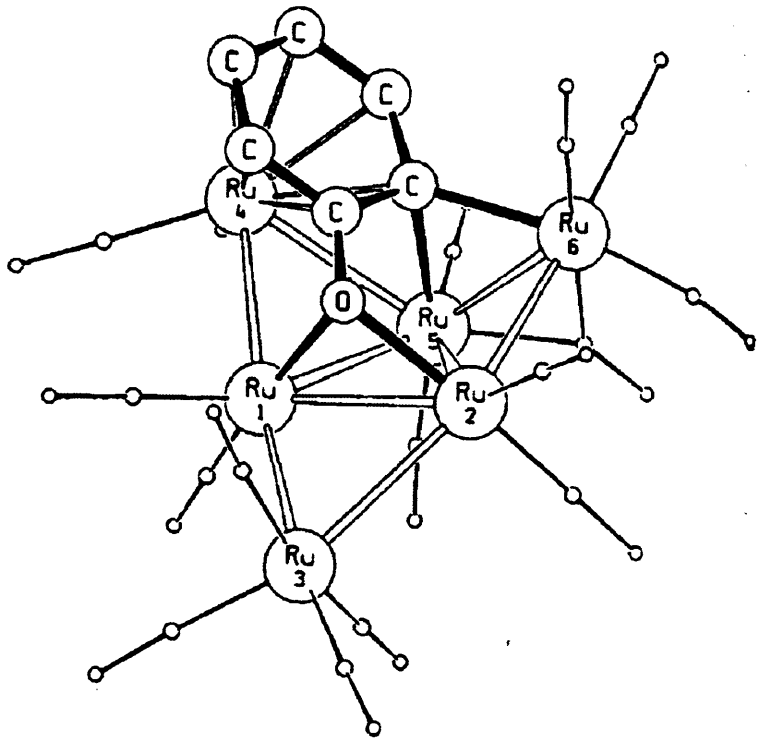

Figure 1.1. The molecular structure of $[Ru_6(\mu\text{-}H)_2(\mu\text{-}C_6H_4O)(CO)_{16}]$ 1.21.

1.6 Arene groups as bridges between clusters

There are examples in the literature where arene ligands act as bridges between clusters.[55] Other clusters are linked by capping ligands which use their available non-bonding electrons to link trinuclear chalcogenido clusters.[1] For example, the cluster $[Ru_3(\mu\text{-}H)_2(\mu_3\text{–}S)(CO)_9]$ in refluxing heptane or on treatment with UV, trimerises with a loss of CO to give $[Ru_3(\mu\text{-}H)_2(\mu_4\text{–}S)(CO)_8]_3$ which contains three μ_4-S ligands, linking three quite distinct Ru_3 clusters.[56] Other clusters of higher nuclearities can be formed by dimerisation, for example cluster $[Os_3(\mu_3\text{–}S)_2(CO)_9]$ loses CO under UV to give $[Os_6(\mu_3\text{–}S)_4(CO)_{16}]$.[57]

To date there has only been two reports of arenes acting as a bridge between clusters; one by Deeming [52] and the other by Brodie.[58] Deeming reported the structure of complex $[Os_6(\mu\text{-}H)_3(C_6H_3O)(CO)_{19}]$ **1.22** from the reaction of **1.1** with quinol. It was initially assumed that the compound was a mixture. However the easy movement of

the band on the TLC plate (SiO_2) indicated the lack of free OH groups. Careful division of the TLC band into fractions showed that the band was homogeneous and not two individual Os_3 clusters. The structure has been proposed on the evidence of infrared, electron ionisation and ^1H NMR spectroscopy methods.[52]

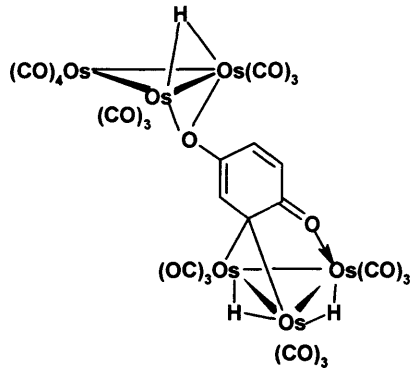

1.22

Brodie obtained the orange complex [{Os_3(μ-H)(CO)$_9$}(μ-$SC_5H_3NCO_2$){Os_3(μ-H)(CO)$_{10}$}] **23** by irradiating a dichloromethane solution of [{Os_3(μ-H)(CO)$_{10}$}$_2$(μ-$SC_5H_3NCO_2$)] for 8 minutes using a tungsten lamp. The complex has been fully characterised.[58] It appears that the chemistry of the arene group acting as a bridge between clusters is still in its infancy. This is very surprising since there are numerous reactions of arene with clusters. Thus, this area of chemistry has a huge potential for development.

1.7 Fluxional behaviour

Fluxionality plays a very important part in triosmium chemistry. Studies centred on CO mobility in [$Os_3(CO)_{12}$] and simple substituted derivatives, have established two major mechanisms for CO site exchange. One is the *turnstile* and the other the *merry-go-round* process. The term *turnstile* implies the synchronous exchange of one *axial* carbonyl with two *equatorial* carbonyl ligands, without the transfer of carbonyl ligands between metal centres. This could be considered to be a localised process. The term *merry-go-round* implies delocalised exchange, where CO ligands migrate around

two or more metal centres via bridging CO in an ordered manner. The overall scrambling mechanism in osmium clusters remains unclear. However, it probably involves the combination of both *turnstile* and *merry-go-round* mechanisms. It is widely accepted that the exchange mechanisms at the highest temperatures are entirely delocalised over all CO groups and metal atoms in the molecule.[59] The use of $[^{187}Os_3(CO)_{12}]$ has shown that CO ligands migrate over all three metal centres.

It has been found that fluxional behaviour can be constrained by substituents, as in the case of $[Os_3(CO)_{12-x}\{P(OMe)_3\}_x]$ (x = 1-4)[60] and $[Os_3(PMe_2Ph)_2(CO)_{10}]$,[61,62] where carbonyl ligands are substituted by phosphine or phosphite ligands. This means only limited carbonyl scrambling is possible, since such ligands tend to occupy equatorial terminal sites in trinuclear clusters and show little preference for either bridging or axial terminal coordination modes. This is in agreement with studies published in literature, that bulky ligands generally adopt equatorial positions in Os_3 clusters.[63,64,65] The converse is true for small ligands such as H and CH_3CN which coordinate axially as terminal ligands.[66]

There are many examples of hydride migration between metal centres, which are routinely observed by variable-temperature ^1H NMR methods.[67] We have shown in Chapter 4 the mobility of the hydride ligands in cluster $[Os_3(\mu\text{-}H)_2(OC_6H_3OMe)(CO)_9]$. Interestingly the cluster $[Os_3(Ph_2P\text{-}2\text{-}NC_5H_4)(CO)_{10}]$ underwent pyridine migration between the two osmium atoms while the phosphine was locked in place at the third atom.[68]

Chapter 2. The reactions of triosmium clusters with disulfides

2.1 Introduction

The S-S bond plays a very important role both in biology and in industry. In biology the S-S linkage can occur between two separate peptide strands linking them via covalent bonding. It is also structurally important in hair and nails. The disulfide bonds between cysteines in two different peptide chains link the otherwise separated chains together and help to stabilize the three-dimensional conformation of proteins.[69]

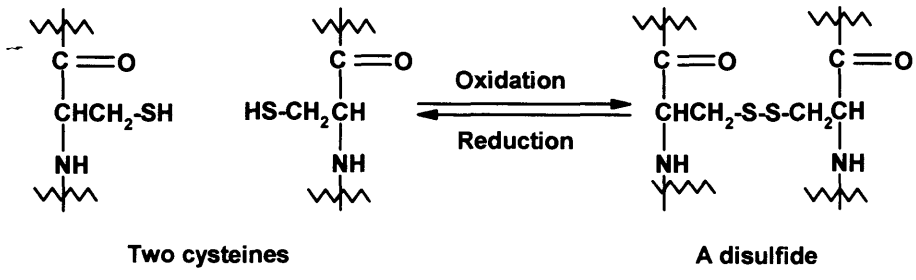

Scheme 2.1. The formation of a disulfide bond within a protein.

The S-S cross-linkage plays a very big role in the rubber industry. Both natural and synthetic rubbers are soft and thus difficult to handle on a large-scale production line. This can be overcome by hardening the rubber by a process called vulcanisation, discovered in 1839 by Charles Goodyear. Vulcanisation involves heating the crude polymer with few percent by weight of sulfur. The sulfur forms disulfide bridges between the polymer chains, cross-linking them, which means they can no longer slip over one another, **Figure 2.1**. This results in a much harder rubber with greatly improved resistance to wear, which is easy to handle on a large scale production line.[70]

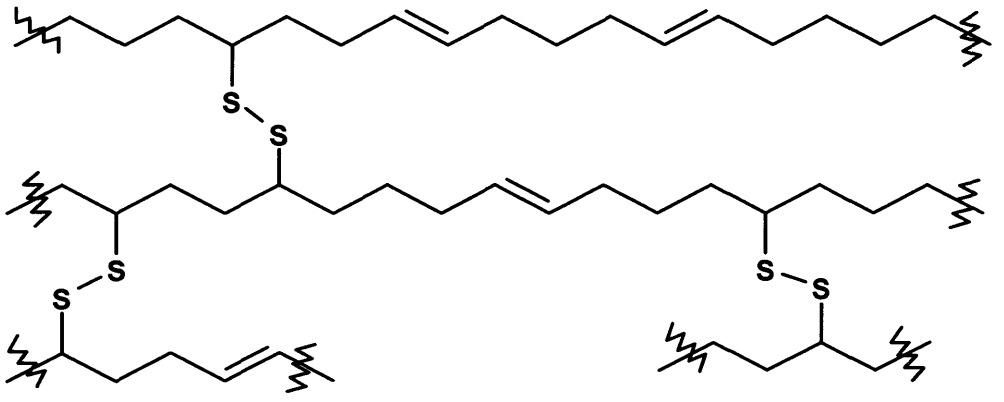

Figure 2.1. Sulfur cross-linked chains resulting in the hardening of rubber.

When metal carbonyl clusters react with electron-pair donors, one of two things can usually happen: either ligand substitution or degradation of the cluster via cleavage of the metal-metal bonds.[71,72,73,74] The simplest types of such ligands are those bonded to metal atoms through a single atom of a main-group element, such as the chalcogens (S, Se and Te) or the pnicogens (N, P and As). The group may be a single atom (E) or a group (ER, ER_2 *etc*). Furthermore if the added donor can serve as a bridging ligand (ligands such as those above which can bridge by acting as 2 to 6 electron donors), it could help to maintain the integrity of the molecule even when there has been extensive cleavage of the metal-metal bonded cluster framework.[75]

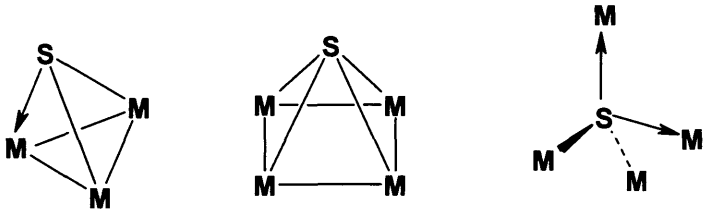

4-electron donor 4-electron donor 6-electron donor

The chalcogen ligands containing sulfur and selenium frequently coordinate as bridging multielectron-pair donors.[76,77] The chemistry of osmium and ruthenium with sulfur ligands is vast, especially in higher clusters in which the sulfur atom bonds to three, four, five or more metal atoms. The whole subject has been reviewed and the synthesis of key compounds described in detail by Adams.[78,79,80] However reports of the chemistry of disulfide derivatives of triosmium clusters are very limited in the literature. In 1982, Lewis *et al.* reported the first reactions of $[Os_3(MeCN)(CO)_{11}]$ with the compound R_2E_2 (E = S, R = Me, Ph and CH_2Ph) to give clusters of type $[Os_3(\mu\text{-}ER)_2(CO)_{10}]$, which were partially characterised based on their spectroscopic properties, but there were errors in the structure assigned.[81] Arce and Deeming *et al.* in 1991 and again in 1994 explored diselenium and some disulfide reactions of $[Os_3(MeCN)_2(CO)_{10}]$ with MeSeSeMe, PhSeSePh[82] and PySSPy.[83] Other bridging RSeSeR ligands have been observed for platinum(IV) complexes which are stable because they are incapable of oxidative addition. With triosmium clusters there is only tentative evidence for an intact RSSR or RSeSeR bridge as the cleavage of the chalcogen-chalcogen bond occurs readily.[84]

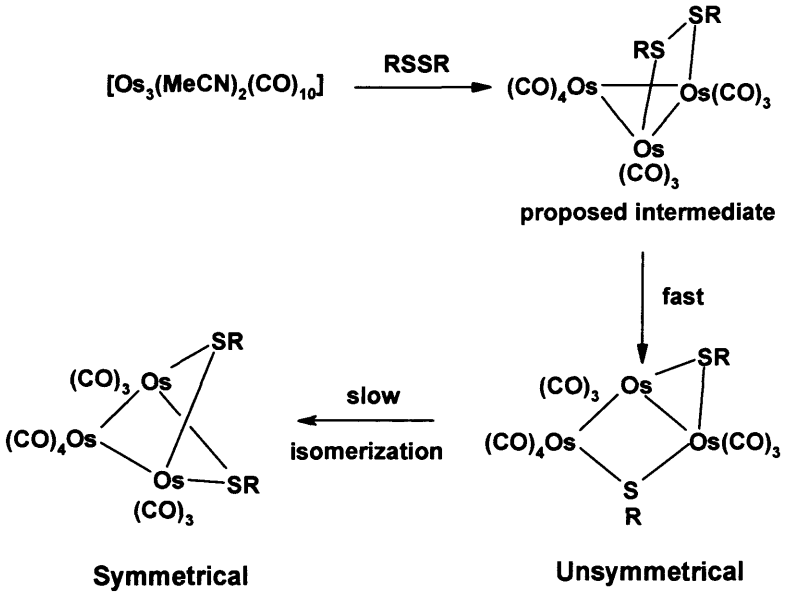

Scheme 2.2. The proposed reaction pathway for the formation of isomers.

It was previously postulated, although not established by Deeming and co-workers, that the formation of clusters of type $[Os_3(\mu\text{-}ER)_2(CO)_{10}]$ must occur via a transient intermediate state which probably retained the chalcogenide bond, *i.e.* the S-S bond remained intact **(Scheme 2.2)**. The formation of the unsymmetrical isomer with inequivalent SR ligands rather than the thermodynamically stable symmetrical isomer, probably relates to the ease of transfer of a RS group to a second Os-Os edge as the S-S bond is cleaved.

We wanted to study in detail the reaction of $[Os_3(MeCN)_2(CO)_{10}]$ with disulfides, in the hope of isolating the proposed intermediate species. Further we wished to establish the possible formation of isomers of decacarbonyl derivatives and carry out detailed variable low-temperature ^1H NMR spectroscopy studies of the isomers to see if they interconvert in solution. We also wanted to see what happened with more bulky disulfides, since it was previously reported by Lewis that the ^{t}BuSS^{t}Bu reaction did not take place due to the large bulk of the ^{t}BuS ligand. He reported that the reaction only led to the fragmentation of the Os_3 unit.[81] We have now re-examined those reactions. Herein, we report very interesting results, which adds significantly to our understanding of these systems. More recently we observed the retention of the S-S bond of 4,4-dipyridyl disulfide in its reaction with a triosmium cluster. These results will be discussed in Chapter 5.

2.2 Results and Discussion

2.2.1 Oxidative addition of dibenzyl disulfide to triosmium clusters

(a) With $[Os_3(MeCN)_2(CO)_{10}]$

The yellow labile cluster $[Os_3(MeCN)_2(CO)_{10}]$ reacted with dibenzyl disulfide ($PhCH_2SSCH_2Ph$) in dichloromethane at room temperature over several hours to give, after TLC separation, the clusters $[Os_3(\mu\text{-}H)(\mu\text{-}SSCH_2Ph)(CO)_{10}]$ **2.1** (4%) and $[Os_3(\mu\text{-}SCH_2Ph)_2(CO)_{10}]$ **2.2** (86%). Higher yields of cluster **2.2** can be obtained by using a longer reaction time. Cluster **2.2** is an analogue of $[Os_3(SePh)_2(CO)_{10}]$ [81,83] and $[Os_3(SeMe)_2(CO)_{10}]$.[82] Cluster **2.1** is of the well known type $[Os_3(\mu\text{-}H)(SR)(CO)_{10}]$,[83] but as far as we know it is the first example of an SSR complex of this type. Compound **2.1** was obtained in a very low yield which may have been the result of there being some $PhCH_2SSH$ as an impurity in the commercial $PhCH_2SSCH_2Ph$ used. We made no attempt to establish its origin or to remove this thiol from the disulfide we used, to test whether this was the real origin.

(b) With $[Os_3(\mu\text{-}H)_2(CO)_{10}]$

Many sulfur-substituted derivatives of the unsaturated purple cluster $[Os_3(\mu\text{-}H)_2(CO)_{10}]$ have been prepared. In some earlier work the Deeming group have shown that the direct reaction of sulfur with $[Os_3(\mu\text{-}H)_2(CO)_{10}]$ yielded $[Os_3(\mu\text{-}H)_2(\mu_3\text{-}S)(CO)_9]$.[85] We therefore applied this method to the study of disulfides. The purple cluster $[Os_3(\mu\text{-}H)_2(CO)_{10}]$ and an excess of benzyl disulfide in heptane gave $[Os_3(\mu\text{-}H)(\mu\text{-}SCH_2Ph)(CO)_{10}]$ **2.3** in 21% yield as yellow crystals. No other reaction was observed at room temperature and no other product could be characterised.

2.2.2 Characterisation of dibenzyl disulfide products

The IR and ^1H NMR spectroscopic data for compounds **2.1** to **2.3** is given in **Tables 1.1** and **1.2**, found at the end of this chapter. Cluster **2.1** gave three signals in the ^1H

NMR spectrum in the ratio of 1:2:5: a high-field hydride singlet at δ -17.50, a CH_2 singlet at δ 3.48 and Ph multiplets between δ 7.21-7.28. The mass spectrum of cluster **2.1** showed its parent molecular ion *m/z* = 1012 (based on ^{192}Os) corresponding to the formulation of $[Os_3(\mu\text{-}H)(\mu\text{-}SSCH_2Ph)(CO)_{10}]^+$. The IR spectrum in this region was similar to those of other clusters of the type $[Os_3(\mu\text{-}H)(\mu\text{-}SR)_2(CO)_{10}]$. The IR υ(CO) spectrum of cluster $[Os_3(\mu\text{-}SCH_2Ph)_2(CO)_{10}]$ **2.2** was likewise similar to those of $[Os_3(\mu\text{-}ER)_2(CO)_{10}]$ (E = S, R = Me, Ph and E = Se, R = Ph, Me),[36,37] where the E.A.N rule is obeyed by the ligand (E) acting as a 3-electron donor.

The ^1H NMR spectrum of **2.3** exhibited three signals in the ratio 1:2:5. A characteristic high-field hydride signal at δ -14.67 (s), a CH_2 singlet at δ 3.57 and phenyl complex multiplets between δ 7.22–7.38. The EI mass spectrum gave *m/z* = 980 (calc. 980) based on ^{192}Os, and the successive loss of ten CO ligands was observed. The bridging sulfur in the case above, was acting as a three-electron donor to give a total electron count of 48, thus making it a fully saturated cluster. The infrared and ^1H NMR spectrums were similar to those known for the decacarbonyl species of the type $[Os_3(\mu\text{-}H)(\mu\text{-}X)(CO)_{10}]$ (X = SR and OMe).[86, 87] The main evidence we have found for **2.1** was the mass spectrum and its non-equivalence to the closely similar cluster **2.3**.

2.2.3 Thermal and photochemical studies of cluster 2.2

In an attempt to discover whether cluster $[Os_3(\mu\text{-}SCH_2Ph)_2(CO)_{10}]$ **2.2** loses CO to give other species, the carbonyl derivative was refluxed in cyclohexane for 4 hours. After careful TLC separation, the only species isolated was the new decacarbonyl derivative $[Os_3(\mu\text{-}SCH_2Ph)_2(CO)_{10}]$ **2.4** in 40% yield. Cluster **2.4** is an isomer of **2.2**. However, when a solution of **2.2** was refluxed in nonane for 15 minutes, it gave considerable decomposition. The only product isolated was the known sulfido bridged cluster $[Os_3(\mu\text{-}S)_2(CO)_9]$ **2.5**.[88]

The unsymmetrical cluster **2.2** can in principle be one of four isomers (**Figure 2.2**) based on the structures established for $[Os_3(\mu\text{-}SMe)_2(CO)_{10}]$ *etc.* In addition the

symmetrical isomer **2.4** with equivalent $PhCH_2S$ has been successfully isolated via the thermolysis method. In view of isomers produced by thermal methods, an attempt was made to see if similar reactions occurred photochemically, since this commonly gives other isomers. An advantage of the photochemical method is that reactions tend to go cleanly by avoiding thermal decomposition and tend to give different products from thermal methods. A toluene solution of **2.2** was irradiated using a mercury UV lamp at room temperature for 5 hours. However only the known sulfido bridged cluster $[Os_3(\mu\text{-}S)_2(CO)_9]$ **2.5** was isolated, along with some starting material, so this approach was not developed further.

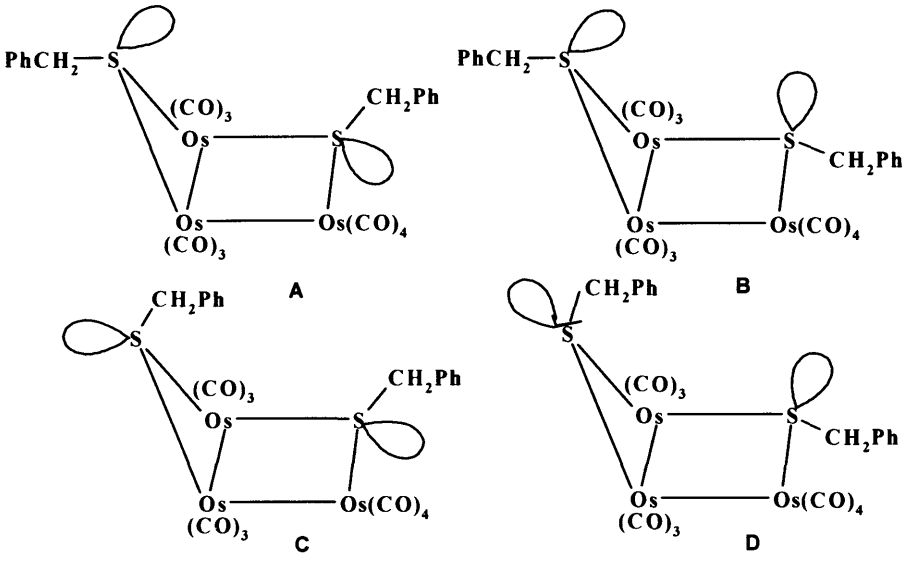

Figure 2.2. Shows the four possible isomers of $[Os_3(\mu\text{-}SCH_2Ph)_2(CO)_{10}]$ 2.2.

2.2.4 Characterisation of thermal and photochemical products

The thermolysis of **2.2** in cyclohexane yielded the isomer $[Os_3(\mu\text{-}SCH_2Ph)_2(CO)_{10}]$ **2.4** with equivalent CH_2Ph ligands. The IR data differs greatly between the two isomers, indicating a large structural change in the interconversion of one isomer to the other. Lewis *et al.* had originally proposed that the isomers had the same metal framework but only differed by inversion at sulfur. The mass spectra of both isomers **2.2** and **2.4** showed the parent molecular ion *m/z* = 1102 (based on ^{192}Os),

corresponding to $[Os_3(\mu\text{-}SCH_2Ph)_2(CO)_{10}]$.$^+$ The ^1H NMR spectrum (**Table 1.2**) was consistent with the structure giving two CH_2 proton signals at δ 4.16 and 3.55 for the unsymmetrical isomer **2.2** and only one signal at δ 4.49 for the symmetrical isomer **2.4**. This implies that there is a plane of symmetry in cluster **2.4** unlike **2.2**. The ^1H NMR signals of cluster **2.2** appeared slightly broad at room temperature. This prompted us to carry out a variable low-temperature ^1H NMR investigation on the unsymmetrical cluster, since for any one of the four isomers **A** to **D** there should be four CH_2 signals rather than the two observed (**Figure 2.2**).

2.2.5 V.T. ^1H NMR study of $[Os_3(\mu\text{-}SCH_2Ph)_2(CO)_{10}]$ 2.2

Having carefully examined the ^1H NMR spectrum of cluster **2.2**, it was clear that one of the CH_2 signals was broader than the other at room temperature. This prompted us to investigate the variable low-temperature ^1H NMR spectra. On cooling the $CDCl_3$ solution to 173 K, we observed a complete change from the room temperature NMR spectrum, as both the singlets at δ 4.16 and 3.55 produced multiplets, which broadened and eventually gave rise to a complex spectra consistent with two isomers. Each isomer showed four signals (some overlapping) for the CH_2 protons (Figure 2.3), consistent with a major and a minor isomer, which were in equilibrium in the ratio of 4:1 at approximately 173K. As the temperature was slowly raised, the signals of the minor isomer started to broaden faster than those of the major isomer as expected for exchange between them. All signals were broadened out at 198 K and then slowly started to reform as two AB quartets at 230 K and above. The exchanging isomers are likely to be related by having different configurations at a SR group of the cluster. From **Figure 2.2** we knew that there were four possible isomers. However, the variable-temperature spectra showed evidence of only two forms in the solution, which led us to ask, *which two isomers were present in the variable-temperature spectra?* Sulfur inversion can in principle take place both at the closed and the open sulfur edges. However if inversion occurred at both sulfur centres, this would have given rise to a complex ^1H NMR spectrum consisting of more signals, with four signals for each CH_2 proton, giving a total of 16 signals in total. As only two isomers were observed in the variable low-temperature ^1H NMR, we can conclude that inversion was taking place at one sulfur centre only. This raises another question,

which sulfur is inverting? We will discuss this later in the light of the X-ray diffraction structure. Nevertheless it has previously been noted that for species where both solid-state and solution data are available, the favoured isomer in solution is usually the one which resembles the solid-state structure most closely.[89]

We have further evidence for the inversion of sulfur by simulation of the ^{1}H NMR spectra using a commercial program. This simulation program allowed observed data (experimental data) to be matched with simulated data (theoretical data) based on defined exchange behaviour; see **Figure 2.4** for the simulated variable-temperature spectra. The correspondence of simulated with observed spectra was not as exact as it might have been since as well as varying the rate of exchange with the temperature, there were changes in the chemical shifts of the eight signals, and these could not be modelled precisely at the temperatures where the signals were broad. Nonetheless the rate constants for the sulfur inversion in cluster **2.2** were obtained from a simulation of the methylene region of the variable-temperature ^{1}H NMR spectra. The rate constant obtained was used to calculate the Arrhenius activation energy (E_a) for the sulfur inversion in cluster **2.2**, giving $E_a = 61.5 \pm 2.0$ kJ mol^{-1}. This implied that 61.5 $\pm$ 2.0 kJ mol^{-1} of energy is required for one sulfur to invert from one form to another. We have also calculated the activation parameter using the Eyring equation, which gave an activation enthalpy of $\Delta H^{\neq} = 61.4 \pm 2.0$ kJ mol^{-1} ($\Delta H^{\neq}$ is expected to correspond closely to the Arrhenius E_a, as is the case here).

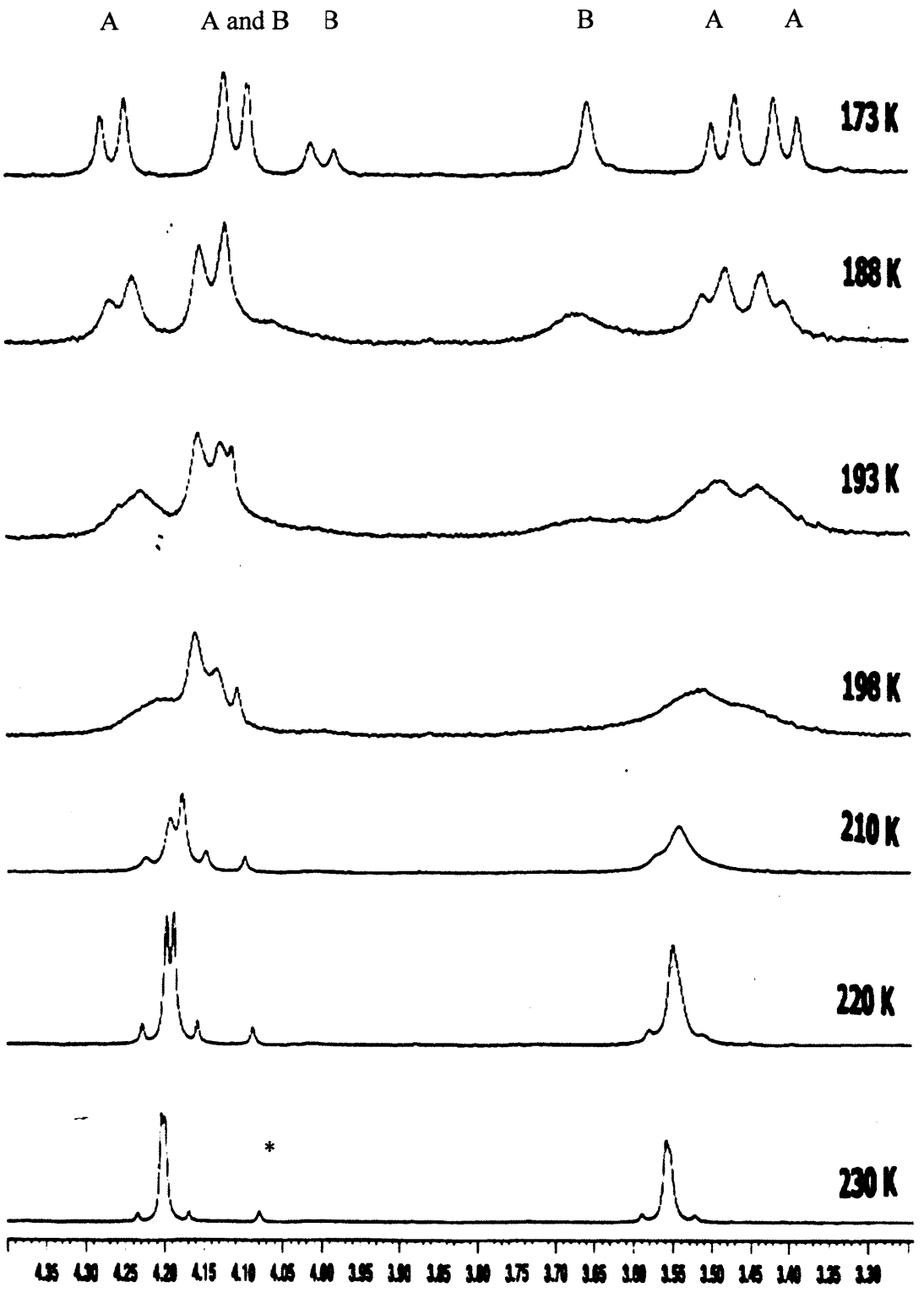

Figure 2.3. Observed ^1H NMR spectra (CH_2 region) for the two invertomers of unsymmetrical isomers of $[Os_3(\mu\text{-}SCH_2Ph)_2(CO)_{10}]$. Peak not assigned (*), probably a minor impurity. A= major isomer, B = minor isomer.

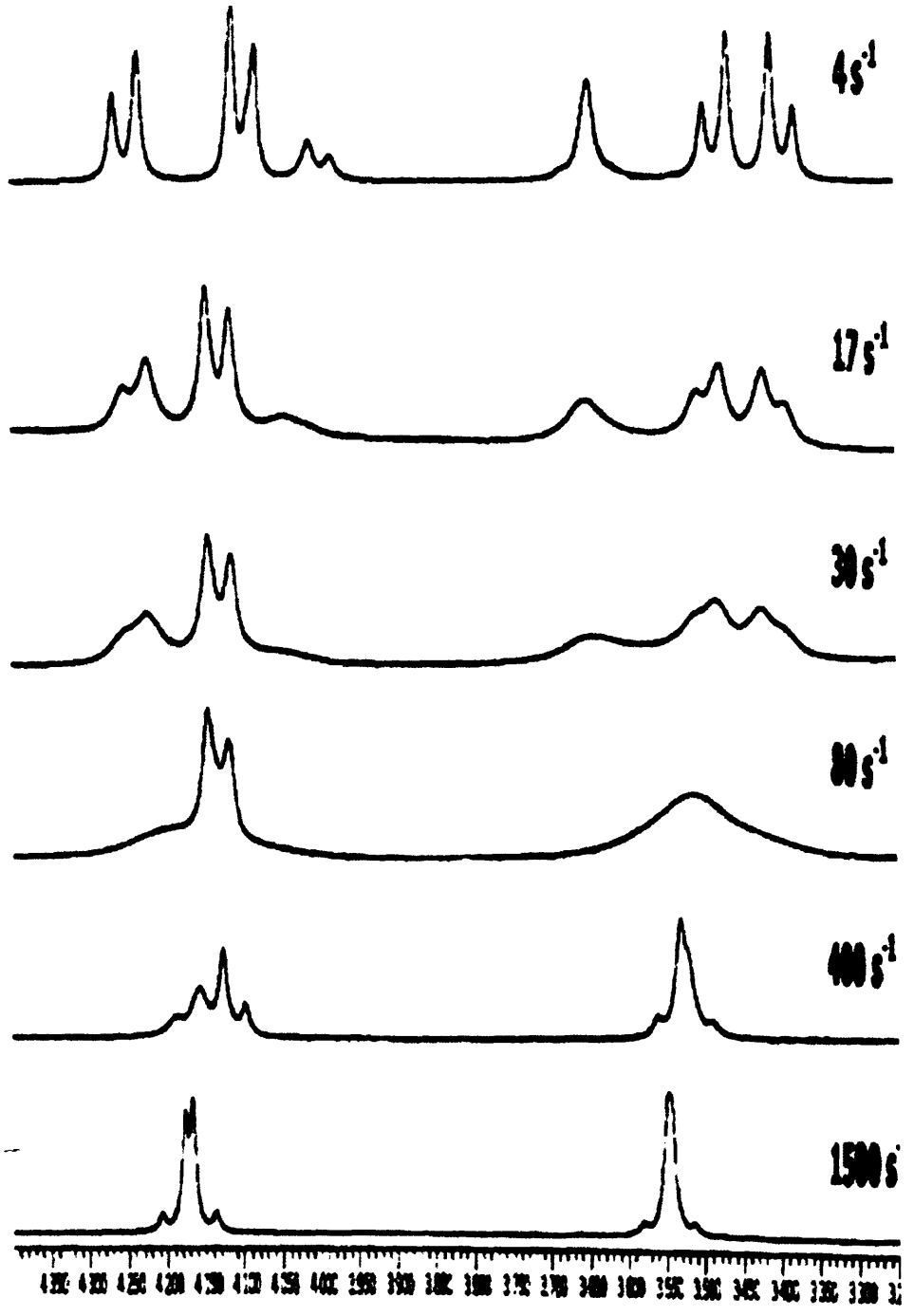

Figure 2.4. Simulated ^1H NMR spectra (CH_2 region) for the two invertomers of the unsymmetrical isomer of $[Os_3(\mu\text{-}SCH_2Ph)_2(CO)_{10}]$.

The inversion of sulfur at coordinated S-ligands is not a new phenomenon. It was first observed by Abel in 1966, using NMR spectroscopy,[90] and since then chalcogen inversion in a wide range of transition metals (including Cr, Mo, Re, Ru and W)[91,92,93,94] has been studied, and accurate inversion barriers have been calculated using both the Arrhenius and Eyring equations. Comparing the value of Ea for cluster **2.2** with those reported in literature for other transition metal complexes, we found an excellent match with our calculated value of 61.5 ± 2.0 kJ mol^{-1}. See **Table 2.3**.[95]

Table 2.3. Arrhenius activation parameters for pyramidal sulfur inversion in early transition metal complexes.[95]

Complex	Ea (kJ mol^{-1})
$[Cr(CO)_4(^tBuSCH_2CH_2SBu^t)]$	50.99 ± 1.23
$[Mo(CO)_4(^tBuSCH_2CH_2SBu^t)]$	46.63 ± 0.79
$[W(CO)_4(^tBuSCH_2CH_2SBu^t)]$	54.98 ± 0.71
$[W(CO)_4(^tPrSCH_2CH_2SPr^i)]$	57.38 ± 1.26
$[W(CO)_4(EtSCH_2CH_2SEt)]$	60.54 ± 1.33
$[W(CO)_4(MeSCH_2CH_2SMe)]$	65.53 ± 3.37

2.2.6 Oxidative addition reaction of di-tert-butyl disulfide

When the yellow labile cluster $[Os_3(MeCN)_2(CO)_{10}]$ was treated with di-*tert*-butyl disulfide in dichloromethane at room temperature, two yellow TLC bands were obtained, of which only one was characterised as $[Os_3(\mu\text{-}S^tBu)_2(CO)_{10}]$ **2.6** (82%). The ^{t}BuS derivative is an analogue of the dibenzyl disulfide derived cluster **2.2**. The infrared spectrum (**Table 1.1**) was very similar to that of cluster $[Os_3(\mu\text{-}SCH_2Ph)_2(CO)_{10}]$ **2.2**. The ^{1}H NMR spectrum (**Table 1.2**) showed two $C(CH_3)_3$ signals of equal intensity at δ 1.56 and 1.17 indicating an unsymmetrical isomer. Other weak $C(CH_3)_3$ signals might have indicated the presence of another minor isomer, but they were not characterised. Like **2.2**, the mass spectrum of the parent molecular ion was observed at *m/z* = 1034 (based on ^{192}Os) with the successive loss of ten carbonyl ligands.

2.2.7 Oxidative addition reaction of di(2-thienyl) disulfide

The reaction of $[Os_3(MeCN)_2(CO)_{10}]$ with di(2-thienyl) disulfide at room temperature after 4 hours of stirring, yielded the yellow decacarbonyl cluster $[Os_3(C_4H_3S_2)_2(CO)_{10}]$ **2.7** in high yield at 80%. Further reaction was not observed by refluxing the yellow cluster $[Os_3(C_4H_3S_2)_2(CO)_{10}]$ **2.7** in toluene. The υ(CO) frequencies of compound **2.7** were significantly higher than those of the dibenzyl disulfide analogue by an average of 8 cm^{-1} approximately. This implied that the osmium atoms in cluster **2.7** were much less electron-rich compared to those in compound **2.2**. This could be due to the two thienyl ligands pulling electrons away from the coordinated sulfur which in turn pulls electrons away from the osmium atoms, thus making them less electron-rich. The ^{1}H NMR spectrum showed the presence of 6 proton signals. The mass spectrum showed its parent molecular ion *m/z* = 1086 (calc. 1086), with the successive loss of ten carbonyl ligands consistent with the formulation of $[Os_3(C_4H_3S_2)_2(CO)_{10}]^+$, **Figure 2.5**. In cluster **2.4** the bridging sulfido ligands were acting as 3-electron donors giving a total count of 50-electrons, which implied the formation of a cluster with two metal-metal bonds in accordance with the 18-electron rule.

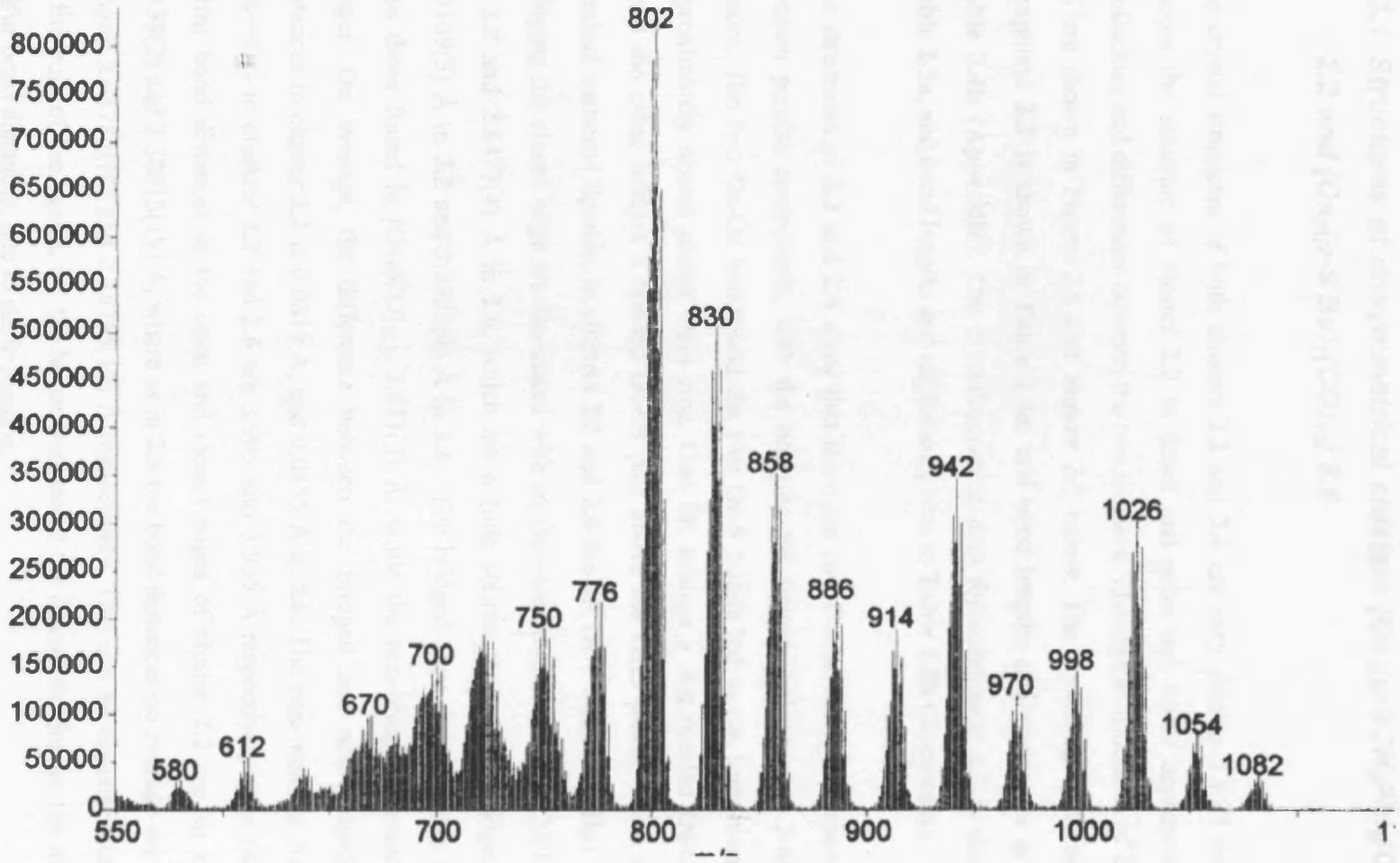

Figure 2.5. The E.I. mass spectrum of cluster $[Os_3(C_4H_3S_2)_2(CO)_{10}]$, showing the successive loss of ten carbonyl ligands.

2.3 Single-crystal X-ray structures

2.3.1 Structures of unsymmetrical clusters $[Os_3(\mu\text{-}SCH_2Ph)_2(CO)_{10}]$ 2.2 and $[Os_3(\mu\text{-}S^tBu)_2(CO)_{10}]$ 2.6

The crystal structures of both clusters **2.2** and **2.6** are very similar. I will therefore discuss the structure of cluster **2.2** in detail and point out where appropriate the similarities and differences between the two isomers. The crystal structures of **2.2** and **2.6** are shown in Figure 2.6 and **Figure 2.7** below. The crystallographic data for compound **2.2** is shown in **Table 2.4a**, and bond lengths and angles are given in **Table 2.4b** (**Appendix**). The crystallographic data for compound **2.3** is shown in **Table 2.5a**, and bond lengths and angles are given in **Table 2.5b** (**Appendix**).

The structures of **2.2** and **2.6** show that there are two Os-Os bonds as expected for electron precise compounds, with the bridging SR ligands behaving as 3-electron donors. The two Os-Os bonds and the two Os-S bonds led to the formation of an approximately square planar Os_3S ring. One SR bridges a non-bonded Os-Os pair while the other bridges a bonded Os-Os pair above the Os_3S plane. There are ten terminal carbonyl ligands. In clusters **2.2** and **2.6** the SR (R = CH_2Ph or ^tBu) groups bridging the closed edge are associated with an Os—Os bond distance of 2.829(5) Å in **2.2** and 2.8477(4) Å in **2.6**, which are a little shorter than the unbridged edge 2.9109(5) Å in **2.2** and 2.9332(4) Å in **2.6**. The bridged edge distances are shorter than those found in $[Os_3(CO)_{12}]$, 2.877(3) Å, while the non-bridged distances are longer. On average, the difference between the bridged and non-bridged bond distances in cluster **2.2** is 0.0819 Å, and 0.0855 Å in **2.6**. The non-bonding distances (Os····Os) in clusters **2.2** and **2.6** are 3.905 and 3.936 Å respectively. The osmium-sulfur bond distances in the open and closed edges of cluster **2.2** are on average 2.439(2) and 2.38015(19) Å, where as in **2.6** the bond distances on average are a little longer: 2.45785(18) and 2.38765(19) Å respectively. This can be explained in terms of the bulk of the ligand, i.e. the larger the size of the ligand, the longer the metal to sulfur bond distances, due to steric reasons.

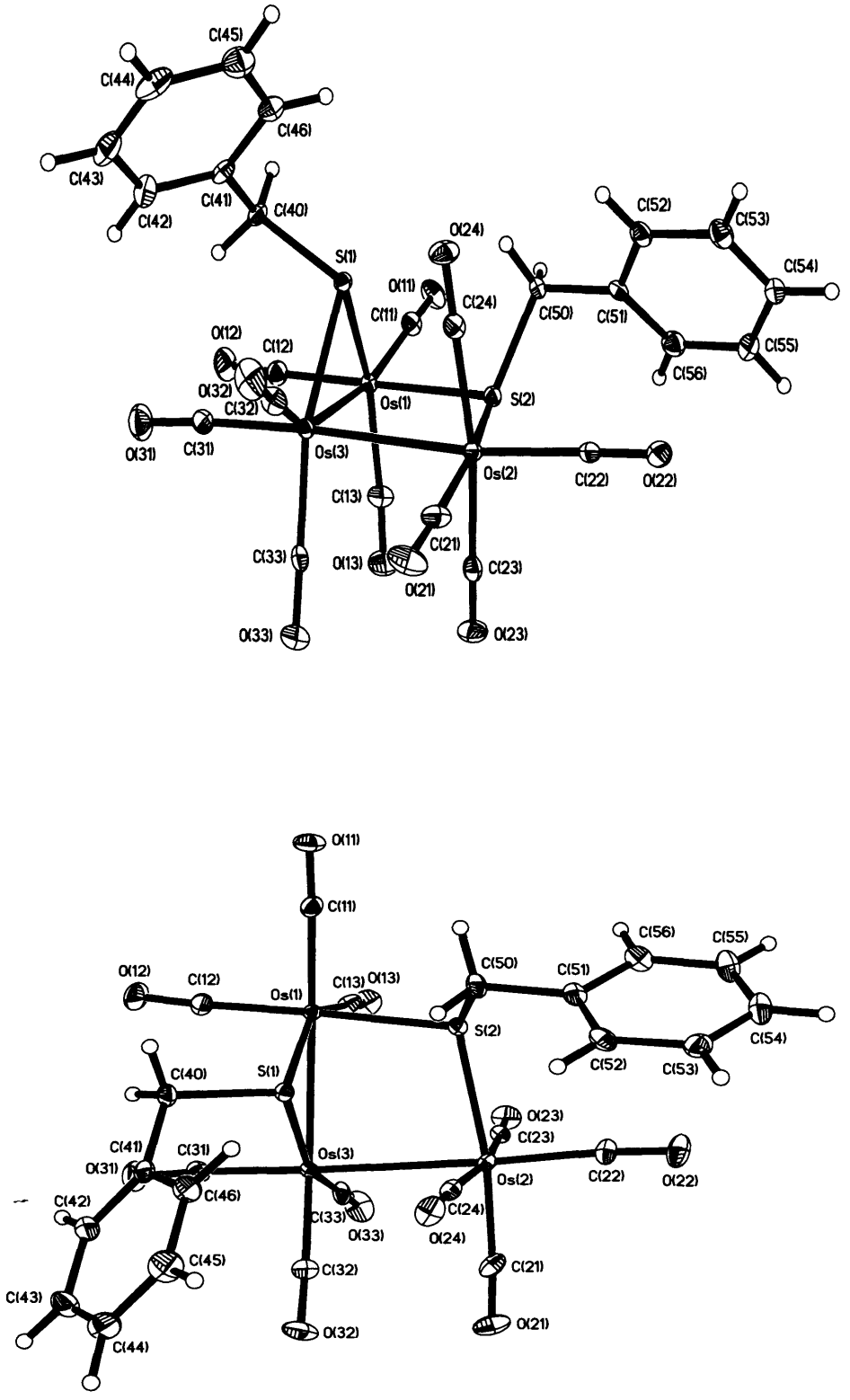

Figure 2.6. The molecular structure of the unsymmetrical cluster $[Os_3(\mu\text{-}SCH_2Ph)_2(CO)_{10}]$ 2.2. Two different projections are shown.

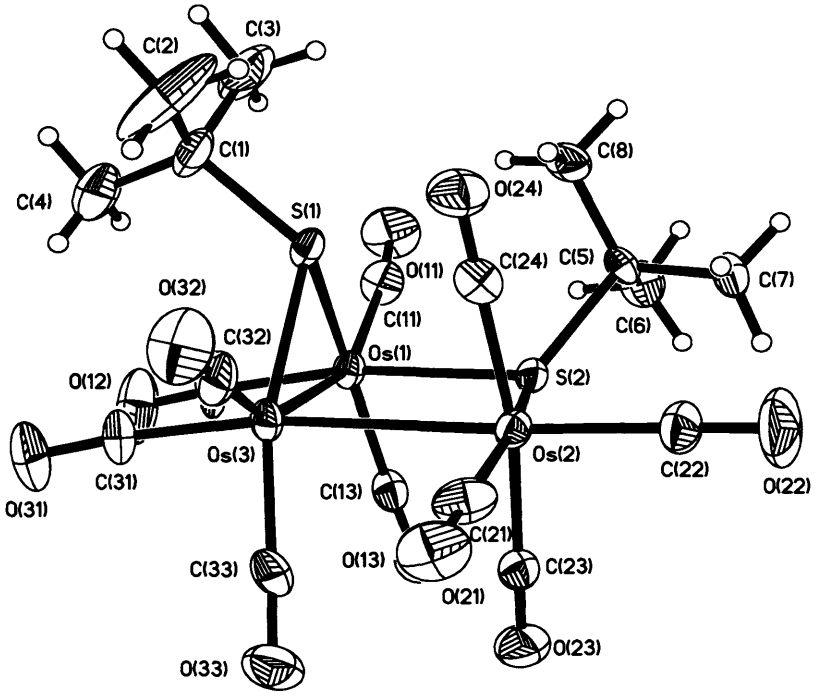

Figure 2.7. The molecular structure of the unsymmetrical cluster [$Os_3(\mu$-$S^tBu)_2(CO)_{10}$] 2.6. The structure is almost identical to that of cluster 2.2.

The carbon-sulfur and carbon-oxygen bond distances are approximately the same in each cluster as expected. We previously asked, *which two of the four possible isomers were present in the ^1H NMR spectra?* This can now be answered by looking at the solid-state structures of both **2.2** and **2.6**. We can definitely say that the major isomer in the solution is that with the benzyl group pointing away from the centre at S(1) and up at S(2) which corresponds to isomer **A**, **Figure 2.4**. We can also conclude from the variable-temperature data, that there is inversion at one sulfur. In the structure of **2.2**, the SR group on the closed edge Os(3)-Os(1) lies well above the Os_3 plane. An inversion at the sulfur S(1) atom would position the **R** group C(40) very close to an axial carbonyl ligand C(24)-O(24) of the $Os(CO)_4$ unit, making the inverted configuration less stable. However, there appears to be no reason why sulfur inversion cannot take place across the open edge S(2) of the cluster. As the **SR** group at the open edge is already pointing up C(50), there are no terminal CO ligands that could

place any steric hindrance affect for inversion in a downward direction, as shown by the crystal structure in **Figure 2.7**.

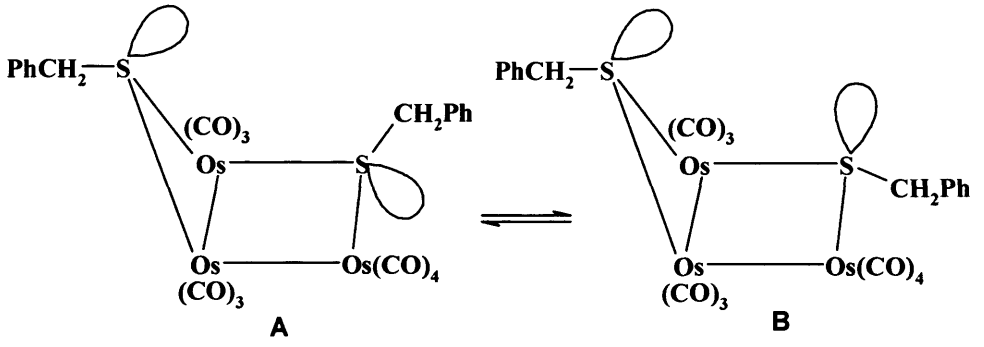

Scheme 2.3. Shows the rapid isomerisation process leading to the variable-temperature ^1H NMR spectra in Figure 2.6. It requires 61.5 ± 2.0 kJmol^{-1} of energy for the sulfur to invert from A to B.

2.3.2 Crystal structure of $[Os_3(\mu\text{-}SCH_2Ph)_2(CO)_{10}]$ 2.4

The crystal structure of isomer **2.4** is closely related to its analogue **2.2** and **2.6**. Again cluster **2.4** is a 50-electron compound containing two metal-metal bonds, see **Figure 2.8**. The crystallographic data for compound **2.4** is shown in **Table 2.6a** and bond lengths and angles are given in **Table 2.6b** (**Appendix**). Unlike isomers **2.2** and **2.6**, the $PhCH_2S$ ligands in **2.4** are bridging the same pair of non-bonded osmium atoms, thus giving rise to two non-bridged Os–Os bonds. This time sulfur S(1a) is below the Os_3 plane, while S(1) is above. Indeed there is a crystallographic mirror plane through the Os_3 atoms so that the two $PhCH_2S$ ligands are related by reflection through this mirror plane. The non-bridging metal-metal bond lengths are 2.8926(4) and 2.8917(4) Å respectively. The non-bonding Os···Os distance is 3.372 Å, which is significantly shorter than that in the isomers **2.2** and **2.6** by 0.533 and 0.564 Å respectively. There are ten terminal carbonyl ligands where the bond lengths are within the expected range. The osmium-sulfur bond lengths vary from 2.3-2.4 Å, which is almost the same as in isomers **2.4** and **2.6**.

The non-bonding angles of 106.35(5)° for Os(2)—S(2)—Os(1) in **2.2** and 106.38(7)° for Os(1)—S(2)—Os(2) in **2.6** are significantly different from those in **2.4**; Os(1)—S(1)—Os(2) and Os(2)—S(1a)—Os(1) are both 87.79(4)°. This is a significant difference of 18.56°, which is in agreement with the non-bonding distances. Similarly, the unbridged bond lengths in **2.2** and **2.6** are 2.9109(5) and 2.9332(4) Å which are slightly longer than those of **2.4**, which are 2.8917(4) and 2.8926(4) Å respectively. The unbridged bond distances in **2.4** are on average 0.01875 Å shorter than those in **2.2** and **2.6**, which is most probably due to the unusual shortening of the nonbonding distance of **2.4** by both SR ligands bridging the same pair of osmium atoms.

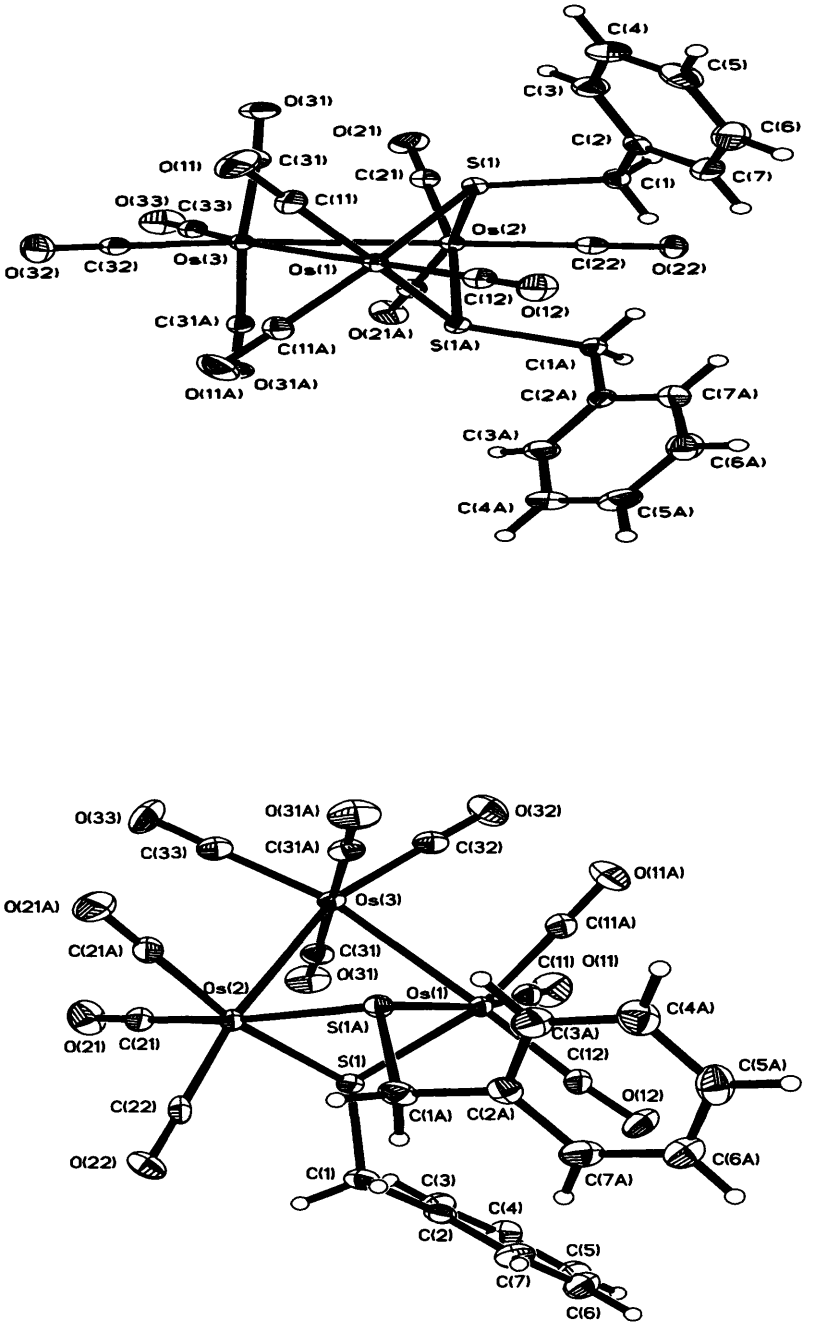

Figure 2.8. The molecular structure of the symmetrical isomer $[Os_3(\mu\text{-}SCH_2Ph)_2(CO)_{10}]$ 2.4, from two different orientations.

2.4 Conclusions

The direct reactions of the labile cluster $[Os_3(MeCN)_2(CO)_{10}]$ with a range of disulfides (dibenzyl disulfide, di(2-thienyl)disulfide and di-*tertiary*-butyl disulfide) at room temperature, yielded their respective triosmiumdecacarbonyl derivatives in high yield, with the cleavage of the S-S bond. In each case, the major product obtained was always the unsymmetrical isomer of their respective thiolato derivatives: $[Os_3(\mu\text{-}SCH_2Ph)_2(CO)_{10}]$ **2.2**, $[Os_3\{\mu\text{-}SC(CH_3)_3\}_2(CO)_{10}]$ **2.6** and $[Os_3(\mu\text{-}S_2C_4H_3)_2(CO)_{10}]$ **2.7**. In the case of dibenzyl disulfide, a second cluster was characterised which retained the S-S bond to give the cluster $[Os_3(\mu\text{-}H)(\mu\text{-}S_2CH_2Ph)(CO)_{10}]$ **2.1**.

Interestingly only cluster $[Os_3(\mu\text{-}SCH_2Ph)_2(CO)_{10}]$ **2.2** in refluxing cyclohexane, yielded the corresponding symmetrical isomer $[Os_3(\mu\text{-}SCH_2Ph)_2(CO)_{10}]$ **2.4**, where both the sulfur ligands bridged the same pair of osmium atoms. A variable-temperature ^1H NMR investigation of cluster **2.2** showed the presence of two isomers in solution, the major isomer having both **SR** ligands pointing up above the Os_3 plane, while the minor one had one pointing up and one pointing down, **Scheme 2.3**. The calculation of the Arrhenius activation energy for the inversion gave $E_a = 61.5 \pm 2.0$ kJ mol^{-1}, which was an excellent match with known values for sulfur inversion reported in literature. From both the variable-temperature data and crystal structure of **2.2**, we have provided strong evidence for the inversion of only one sulfur atom.

We have isolated the first example of a disulfide ligand which retained the sulfur-sulfur bond when coordinated to a triosmium cluster. We have also shown for the first time that bulkier ligands react in the same way with $[Os_3(MeCN)_2(CO)_{10}]$ as does non-bulkier ligands which were previously thought not possible. The chemistry of the bulkier ligands could be further developed by carrying out a detailed variable low-temperature NMR spectrum investigation on the inversion of sulfur. It would be very interesting to know if the bulkier ligands are also fluxional.

2.5 Experimental

2.5.1 General synthetic details

The bis-acetonitrile clusters $[Os_3(MeCN)_2(CO)_{10}]$ and $[Os_3(\mu\text{-}H)_2(CO)_{10}]$ were prepared by published methods.[18,29] The dibenzyl disulfide, di(2-thienyl) disulfide and *tert*-butyl disulfide were purchased from Aldrich plc and used without further purification. The ^1H NMR spectras were obtained from a Bruker AMX300 MHz or AMX400 MHz spectrometer and the data was processed using XWIN-NMR and X-WIN-PLOT. The variable-temperature ^1H NMR spectra were recorded from a mixture of dichloromethane/trifluoromethane solution and calibrated using CH_2Cl_2 as standard. Electron Ionisation (EI) mass spectra and Fast Atom Bombardment (FAB) were acquired by the UCL mass spectrometry service using ZAB instruments (MBNA matrix). IR spectra were recorded on a Shimadzu 8700 FT-IR spectrometer in a CaF_2 solution cell. Elemental analyses were performed by the micro analytical service at UCL. Preparative Thin Layer Chromatography (TLC) plates (silica gel 60 HF_{254} with fluorescent indicator E. Merck, Germany) were prepared as an aqueous slurry which was layered on glass and either dried in air or in the oven at 100 °C overnight before use.

2.5.2 Reaction of $[Os_3(MeCN)_2(CO)_{10}]$ with dibenzyl disulfide

The yellow cluster $[Os_3(MeCN)_2(CO)_{10}]$ (0.2063 g, 0.2199 mmol) and dibenzyl disulfide (0.1441 g, 0.5856 mmol, > 2 mol per mol Os_3) were dissolved in dichloromethane (25 cm^3) and the solution was stirred at room temperature under nitrogen for 3 hours and 30 minutes. The solution changed in colour from pale yellow to dark yellow. The IR spectra showed that there was no starting cluster remaining after this time. Removal of the solvent under reduced pressure and separation of the residue by TLC [SiO_2 ; eluent: light petroleum (40-60 °C)/dichloromethane (v/v 4/1)] gave two yellow bands, which were characterised as $[Os_3(\mu\text{-}H)(CO)_{10}(\mu\text{-}SSCH_2Ph)]$ **2.1** (0.0090 g, 4%) as yellow powder and $[Os_3(\mu\text{-}SCH_2Ph)_2(CO)_{10}]$ **2.2** (0.1858 g, 86%) also as yellow powder. Crystals of **2.2** were grown from a dichloromethane/heptane solution by slow evaporation at room temperature. The EA

for $[Os_3(\mu\text{-}SCH_2Ph)_2(CO)_{10}]$ **2.2**: Found: C, 26.46; H, 1.24; N, 0.00; S, 3.50. Calc. C, 26.13; H, 1.27; N, 0.00; S, 5.80.

2.5.3 Reaction of $[Os_3(\mu\text{-}H)_2(CO)_{10}]$ with dibenzyl disulfide

A solution of the unsaturated purple cluster $[Os_3(\mu\text{-}H)_2(CO)_{10}]$ (0.0849 g, 0.0989 mmol) and benzyl disulfide (0.0731 g, 0.2972 mmol, 3 mol per mol Os_3) was refluxed in heptane (20 cm^3) for 40 minutes. The solution changed colour from purple to yellow. The solvent was removed under vacuum and TLC was carried out using dichloromethane-petroleum spirit (40-60 °C) (1:3 by volume) as eluent. Three bands were obtained of which two have been identified as $[Os_3(\mu\text{-}H)(\mu\text{-}SCH_2Ph)(CO)_{10}]$ **2.3** (0.020 g, 21%) and the starting material $[Os_3(\mu\text{-}H)_2(CO)_{10}]$.

2.5.4 Synthesis of symmetrical isomer $[Os_3(\mu\text{-}SCH_2Ph)_2(CO)_{10}]$ 2.7

A solution of cluster $[Os_3(\mu\text{-}SCH_2Ph)_2(CO)_{10}]$ **2.2** (0.0201 g, 0.0854 mmol) was refluxed in cyclohexane (25 cm^3) for 4 hours. IR indicated a complete reaction. The TLC work–up as above, yielded 3 bands of which one has been fully characterised as $[Os_3(\mu\text{-}SCH_2Ph)_2(CO)_{10}]$ **2.4** (0.008 g, 40%), which gave yellow crystals after extraction with dichloromethane.

2.5.5 Thermal reaction of $[Os_3(\mu\text{-}SCH_2Ph)_2(CO)_{10}]$ 2.2 at a higher temperature

A solution of the compound **2.2** (0.1001 g, 0.0908 mmol) in nonane (20 cm^3) was heated under reflux for 15 minutes. Removal of the solvent and TLC work-up as above, gave the known cluster $[Os_3(\mu\text{-}S)_2(CO)_9]$ **2.5** in low yield. Other bands gave traces of uncharacterised white materials.

2.5.6 Photochemical treatment of $[Os_3(\mu\text{-}SCH_2Ph)_2(CO)_{10}]$ 2.2

A solution of $[Os_3(\mu\text{-}SCH_2Ph)_2(CO)_{10}]$ **2.2** (0.0520 g, 0.0472 mmol) in toluene (20 cm^3) was placed under a mercury UV lamp for 5 hours. The colour changed from yellow to dark yellow. The solvent was removed under reduced pressure and separation of the residue by TLC [SiO_2 ; eluent : light petroleum (40-60^{0}C)/dichloromethane (v/v 4/1)] gave three bands of which two have been characterised as $[Os_3(\mu\text{-}S)_2(CO)_9]$ **2.5** (< 2%) and the starting material $[Os_3(\mu\text{-}SCH_2Ph)_2(CO)_{10}]$ **2.2** (0.0201 g, 37%).

2.5.7 Reaction of $[Os_3(MeCN)_2(CO)_{10}]$ with di-tert-butyl disulfide

The yellow cluster $[Os_3(MeCN)_2(CO)_{10}]$ (0.2063 g, 0.2199 mmol) and 7 drops of di-*tert*-butyl disulfide, (added by pipette, > 2 mol per mol Os_3) were dissolved in dichloromethane (15 cm^3) and the solution was stirred at room temperature for 2 hours. The solution changed in colour from pale yellow to dark yellow. Spot TLC indicated no starting material. Removal of the solvent under reduced pressure and separation of the residue by TLC [SiO_2; eluent: hexane/dichloromethane (v/v 4/1 then increased to 4/2)] gave two yellow bands, one of which was characterised as $[Os_3\{\mu\text{-}SC(CH_3)_3\}_2(CO)_{10}]$ **2.6** (0.1858 g, 82%). Crystals were grown from a dichloromethane/hexane mixture by slow evaporation at room temperature. The EA for $[Os_3\{\mu\text{-}SC(CH_3)_3\}_2(CO)_{10}]$ **2.6**: Found: C, 20.69; H, 1.61; N, 0.00; S, 3.59. Calc. C, 21.00; H, 1.76; N, 0.00; S, 6.18.

2.5.8 Reaction of $[Os_3(MeCN)_2(CO)_{10}]$ with di(2-thienyl) disulfide

A solution of the bis-acetonitrile compound $[Os_3(MeCN)_2(CO)_{10}]$ (0.0861 g, 0.0920 mmol) in dichloromethane (25 cm^3) with an excess of di(2-thienyl) disulfide (0.0461 g, 0.200 mmol, 2 mol per mol Os_3) was stirred under nitrogen at room temperature for 4 hours. The solvent was removed under reduced pressure and TLC was carried out using eluent: dichloromethane/petroleum spirit (40-60 °C), 1:3 by volume. One bright yellow band was isolated which gave yellow crystals of $[Os_3(\mu\text{-}$

$S_2C_4H_3)_2(CO)_{10}]$ **2.7** (0.0800 g, 80%). The EA for $[Os_3(\mu\text{-}S_2C_4H_3)_2(CO)_{10}]$ **2.7**: Found: C, 19.88; H, 0.42; N, 0.00; S, 8.38. Calc. C, 19.89; H, 0.55; N, 0.00; S, 11.74.

An attempt at decarbonylating the cluster $[Os_3(\mu\text{-}S_2C_4H_3)_2(CO)_{10}]$ **2.7** (0.0201 g, 0.0194 mmol) in refluxing toluene (15 cm^3) after 1 hour, yielded a complicated mixture, which could not be separated satisfactorily for analysis.

TABLE 2.1

ν (CO) VALUES FOR THE DISULFIDE DERIVATIVES

Compounds		ν (CO) (cm^{-1})
$[Os_3(\mu\text{-}H)(\mu\text{-}SSCH_2Ph)(CO)_{10}]$[a]	**2.1**	2108 w 2067 s 2058 m 2022 vs 2017 m 1999 m 1989 m 1983 w
$[Os_3(\mu\text{-}SCH_2Ph)_2(CO)_{10}]$[b]	**2.2**	2112 w 2062 s 2043 w 2031 vs 1988 w 1976 w 1961 w 1955 vw
$[Os3(\mu\text{-}H)(\mu\text{-}SCH_2Ph)(CO)_{10}]$[a]	**2.3**	2090 w 2080 w 2054 s 2027 s 2018vs 1999 w 1987 m
$[Os_3(\mu\text{-}SCH_2Ph)_2(CO)_{10}]$[b]	**2.4**	2104 w 2065 vs 2055 w 2017 s 1886 w (br)
$[Os_3(\mu\text{-}S^tBu)_2(CO)_{10}]$ [a]	**2.6**	2109w 2069vs 2059s 2043m 2015m 1981w(br)
$[Os_3(\mu\text{-}S_2C_4H_3)_2(CO)_{10}]$[a]	**2.7**	2117 w 2070 m 2045 m 2037 vs 2018 w 1997 w 1989 vw 1968 vw 1962 vw

[a] Cyclohexane solution
[b] Dichloromethane solution
Br Broadband

TABLE 2.2

^{1}H NMR DATA FOR DISULFIDE DERIVATIVES

Compounds		δ ^{1}H NMR ($CDCl_3$)	Assignment	Coupling Constant (J/Hz)
$[Os_3(\mu\text{-}H)(\mu\text{-}SSCH_2Ph)(CO)_{10}]$[a]	**2.1**	3.48 (s)	CH_2	
		7.21-7.28 (m)	Ph	
		-17.47 (s)	OsH	
$[Os_3(\mu\text{-}H)(\mu\text{-}SCH_2Ph)_2(CO)_{10}]$[a]	**2.2**	7.07 (m)	Ph	
		4.16 (s)	CH_2	
		3.55 (s)	CH_2	
$[Os_3(\mu\text{-}H)(\mu\text{-}SCH_2Ph)(CO)_{10}]$	**2.3**	3.57 (s)	CH_2	
		7.22-7.38 (m)	Ph	
		-14.67 (s)	OsH	
$[Os_3(\mu\text{-}SCH_2Ph)_2(CO)_{10}]$	**2.4**	7.33(m)	Ph	
		4.49 (s)	CH_2	
$[Os_3(\mu\text{-}S^tBu)_2(CO)_{10}]$	**2.6**	1.56(s)	$(CH_3)_3$	
		1.17(s)	$(CH_3)_3$	
$[Os_3(\mu\text{-}S_2C_4H_3)_2(CO)_{10}]$[a]	**2.7**	7.28(dd)	H^3	*peaks buried by solvent peak*
		7.25(dd)	$H^{3'}$	*J= 6.02 other peaks not observed*
		7.19(dd)	H^1	*J= 3.60, 1.67*
		7.16(d)	$H^{1'}$	*J= 3.61, 1.65*
		6.98(d)	H^2	*J= 3.65, 1.64*
		6.96(d)	$H^{2'}$	*J= 3.66, 1.68*

Chapter 3. The reactions of 8-hydroxyquinoline with triosmium clusters

3.1 Introduction

There has been considerable interest in understanding the factors controlling the rates of the hydrodenitrification (HDN) of polynuclear heteroaromatic nitrogen heterocycles induced by transition-metal centres. Hydrodenitrification is the catalytic process by which nitrogen is removed as ammonia from petroleum, coal, oil and tar sands during refining to fuel and petrochemical feedstocks.[96] The intramolecular activation of C-H, N-H and C-N bonds of the nitrogen-containing aromatic heterocycles, indole and more recently quinoline by polynuclear transition metals, has been investigated and reviewed.[97,98,99,100,101]

The first report of unsaturated metal clusters containing quinolines was made by Rosenberg *et al.* in 1995.[102] The reaction of $[Os_3(CO)_{10}(MeCN)_2]$ with quinoline at 25°C afforded the complex $[Os_3(\mu\text{-}H)(\mu\text{-}\eta^2\text{-}C_9H_7N)(CO)_{10}]$. This complex thermally decarbonylates to give the unsaturated 46-electron cluster $[Os_3(\mu\text{-}H)(\mu_3\text{-}\eta^2\text{-}C_9H_6N)(CO)_9]$, **Scheme 3.1**. This route opened a new pathway for making unsaturated quinoline clusters. A range of other unsaturated quinoline clusters has now been successfully synthesised.[103] Research in this area over the last ten years has intensified, mainly because unsaturated clusters are rare and are generally much more reactive than their electron-precise counterparts.

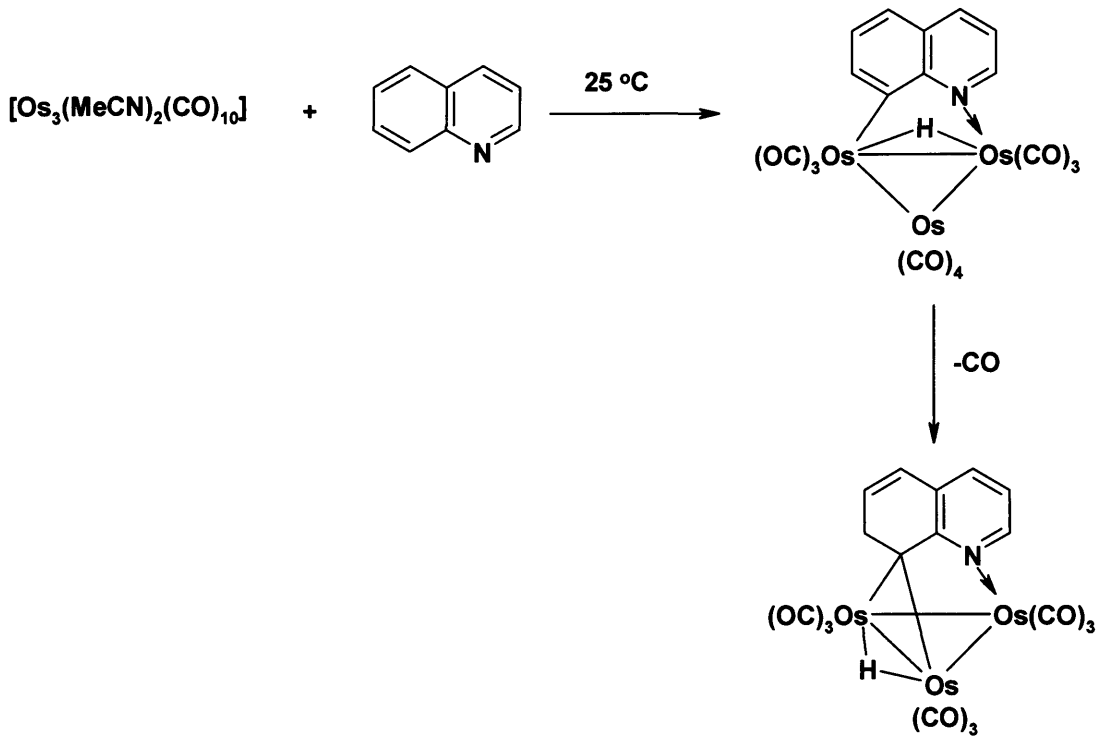

Scheme 3.1. The synthesis of unsaturated cluster $[Os_3(\mu\text{-}H)(\mu_3\text{-}\eta^2\text{-}C_9H_7N)(CO)_9]$.

The reaction of quinoline with $[Os_3(CO)_{12}]$ in refluxing nonane was reported by Choo Yin and Deeming in 1975.[104] They were interested in comparing the reaction of quinoline with that of pyridine. At high temperatures they did not observe the chemistry in **Scheme 3.1**. They also wanted to see whether metallation would take place at the 8-position of the quinoline ring since this would be different from metallation at the 2-position as observed for pyridine. They believed there was no reason why 8-metallation should not occur since carbon is β- to the N atom as was the case for aniline where metallation in the ring did occur.[105] Unfortunately, the only product they isolated was the decacarbonyl derivative $[Os_3(\mu\text{-}H)(C_9H_6NO)(CO)_{10}]$ with metallation at the 2-position only. The reaction in a sealed tube at a high temperature yielded only the dimer $[Os_2(C_9H_6N)_2(CO)_6]$ in low yield. They obtained similar products with iso-quinoline and 7-methylquinoline. The reason for this could be due to the very high reaction temperatures employed, as at very high temperatures only the most stable products can be obtained after degradation and decomposition of the less stable complexes. No evidence was found for 8-metallation by Choo Yin and Deeming. The labile cluster $[Os_3(MeCN)_2(CO)_{10}]$ was not known at that time, but in view of the chemistry established with this cluster (**Scheme 3.1**), it is likely that the

thermal reaction of $[Os_3(CO)_{12}]$ with quinoline involves a similar species and at 150 °C further transformations occur.

The intermolecular activation of the O-H bond of 8-hydroxyquinoline by triosmium clusters has not been studied so far. However studies on simple alcohols, phenols and hydroxypyridine *etc* with polynuclear transition-metal compounds have shown that activation of the OH group occurs. The hydrogen gets transferred to the metal with the ligands coordinating through available heteroatoms. In Chapter 2, we have shown how it is possible for one heteroatom to bridge several metal atoms. The deprotonated form of 8-hydroxyquinoline is a classical and much used chelating ligand in mononuclear coordination chemistry. We were interested in comparing the well-known behaviour of 8-hydroxyquinoline in mononuclear complexes with that in clusters.

In an attempt to prepare complexes containing two coordinated heteroatoms, we explored the reactions of $[Os_3(CO)_{12}]$, $[Os_3(\mu\text{-}H)_2(CO)_{10}]$ and $[Os_3(MeCN)_2(CO)_{10}]$ with 8-hydroxyquinoline. Previously in the reaction of quinoline, it has been shown that C-H activation occurs at the 8-position under mild conditions. However, as described above Deeming has shown that activation can also occur at the 2-position at a high temperature. In the absence of a CH group in the 8-position, we wished to establish whether activation takes place at the oxygen atom (with O-H cleavage) or at the carbon atom in the 2-position, with the transfer of the hydrogen to the metal leaving the hydroxy group uncoordinated. Alternatively a combination of these might occur leading to more complex cluster systems.

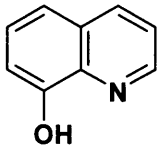

8-hydroxyquinoline

3.2 Results and Discussion

3.2.1 Reaction of 8-hydroxyquinoline with $[Os_3(CO)_{12}]$

The yellow cluster $[Os_3(CO)_{12}]$ reacted with an excess of 8-hydroxyquinoline in refluxing xylene to give one mononuclear complex $[Os(C_9H_6NO)_2(CO)_2]$ **3.1** (7%) and one trinuclear cluster $[Os_3(C_9H_6NO)_2(CO)_8]$ **3.2** (30%), along with a trace amount of the starting material $[Os_3(CO)_{12}]$. The ruthenium analogues of **3.1** and **3.2** were previously prepared by Doorn *et al.* by the direct reaction of 8-hydroxyquinoline with $[Ru_3(CO)_{12}]$ in refluxing THF over 24 hours.[106]

Interestingly, when $[Os_3(CO)_{12}]$ was treated with an excess of 8-hydroxyquinoline in xylene in a sealed Carius tube under vacuum by heating it in an oven at 180 °C, some orange crystals precipitated out. The crystals were separated and after TLC the remaining solution gave the yellow complex $[Os(C_9H_6NO)_2(CO)_2]$ **3.3** in trace amount (<2%), an isomer of complex **3.1**. The orange crystals were found to be a mixture of the known colourless tetranuclear cluster $[Os_4(\mu\text{-}H)_4(CO)_{12}]$[107] **3.4** and what appeared to be another isomer of both **3.1** and **3.3**. The crystalline mixture was separated further to give a pure sample of $[Os(C_9H_6NO)_2(CO)_2]$ **3.5** (76%). The known cluster **3.4** was initially reported by Moss in 1970,[108] Kaesz in 1975[109] and by Johnson in 1978,[110] by the direct reaction of $[Os_3(CO)_{12}]$ with hydrogen at high temperatures using inert solvents like octane and xylene. However, Roberto *et al.* showed that high yields of cluster **3.4** could be easily synthesised by hydrogenation under 1 atm of H_2 of silica-supported $[Os_3(CO)_{12}]$, by working at a lower temperature (100 °C).[111] This method was again modified by Roberto *et al.* to obtain almost 100% yields of **3.4**.[107] Naturally our interest focused on the hydroxyquinoline derivatives rather than the well-studied cluster **3.4**.

3.2.2 Spectroscopic characterisation of $[Os(C_9H_6NO)_2(CO)_2]$ 3.1

The EI mass spectrum of complex **3.1** showed its parent molecular ion with m/z = 536 corresponding to the formulation $[^{192}Os(C_9H_6NO)_2(CO)_2]^+$. The fragmentation pattern showed the successive loss of 2 CO mass units down to a residual ion m/z = 480

corresponding to $[^{192}Os(C_9H_6NO)_2]^+$ The IR spectrum (**Table 3.1**) showed absorptions at 2030(vs) and 1948(vs) cm^{-1}, corresponding to two terminal *cis* carbonyl ligands. There are three possible isomers of **3.1** with *cis* dicarbonyl geometries as shown below.

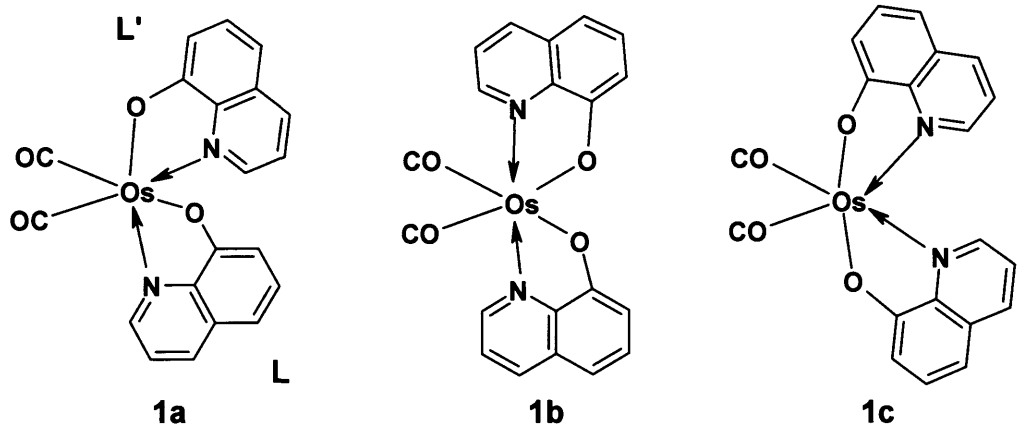

1a **1b** **1c**

The ^1H NMR spectrum, (**Figure 3.1** and **Table 3.2**), showed the presence of 12 equal intensity signals, indicating the formation of a mononuclear complex in which two different heteroatoms (nitrogen and oxygen) are *trans* to each other, as shown in **1a**. Conversely, if the same heteroatoms were *trans* to each other then we would only observe 6 proton signals for **1b** and **1c**, both of C_2 symmetry. A low-field doublet at δ 8.95 for H(2) with a small coupling (J = 4.50 Hz) was observed for the proton next to the electronegative nitrogen on one hydroxyquinolinato ligand **L**, as expected. However, we did not observe another proton signal in that region corresponding to the H(2) proton of the other ligand **L'**. Interestingly we observed another doublet in an upfield region at δ 7.12 with a small coupling (J = 4.60 Hz), which we have assigned to H(2) on **L'**. The small coupling constant was quite characteristic of an H(2) quinoline signal but the chemical shift was nearly 2 p.p.m. upfield of that normally found. We believe this upfield shift was due to ring current effects. The H-atoms in the plane of an aromatic ring are deshielded which accounts for arene hydrogens normally appearing at around δ 7 to 8. The electronegativity of the N-atom further deshields so the hydrogen atoms in the 2-position of pyridine and quinoline appear at around δ 9. In contrast H-atoms orientated perpendicularly above the plane of an

aromatic ring are shielded and hence their signals are shifted upfield. In **3.1** the 2-H in **L'** has shifted from about δ 9.0 to δ 7.12 by its fairly close approach to the heterocyclic ring of **L**. Therefore there is good ^{1}H NMR evidence of structure **1a** for compound **3.1**.

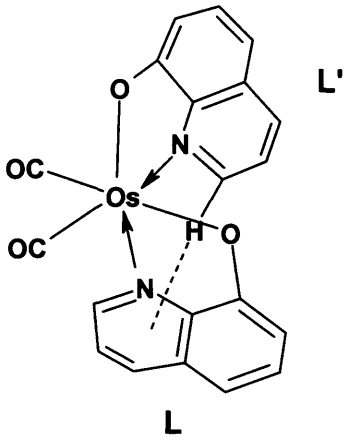

In addition to the above signals, we observed two doublets at δ 8.30 and 8.18 which have been assigned to H(4) **L** and H(4) **L'**. Two triplet signals due to H(6) and H(3) **L** were observed at δ 7.50 and 7.18 and those due to H(6) and H(3) **L'** were observed at δ 7.40 and 7.02. The remaining doublets were observed in the appropriate regions.

This same ring current phenomenon was observed for the ruthenium analogue of **3.1**,[106] and also for a complex of rhodium in which a quinoline proton in the 3-position was shielded by a nearby phenyl ring of triphenylphosphine.[112] This effect can be useful in considering the orientations of mutually *cis* ligands if one of them is aromatic.

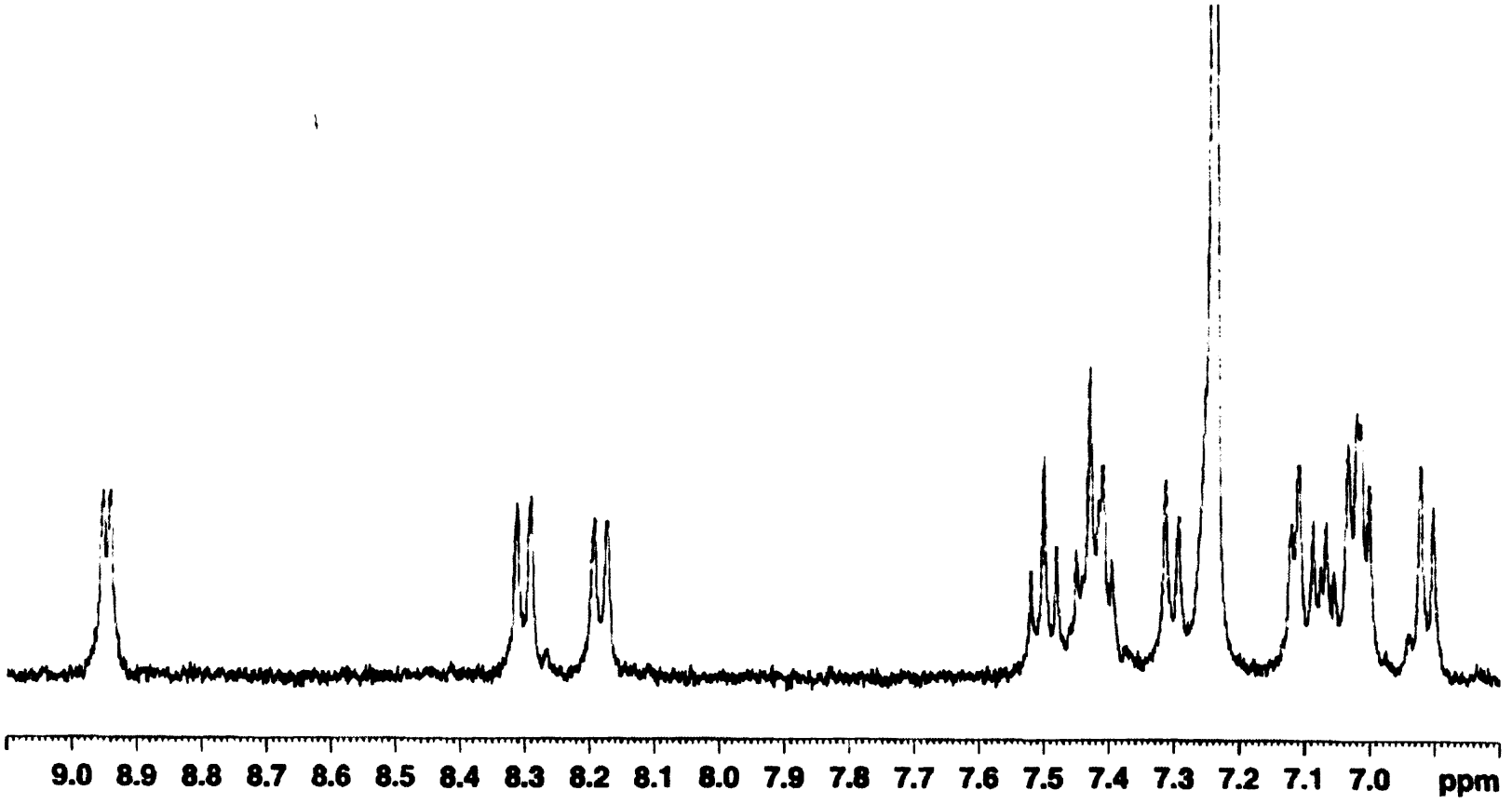

Figure 3.1. The ^{1}H NMR spectrum of $[Os(C_9H_6NO)_2(CO)_2]$ 3.1, showing the presence of 12 equal intensity proton signals.

3.2.2.1 X-ray crystal structure of $[Os(C_9H_6NO)_2(CO)_2]$ 3.1

The X-ray crystal structure of **3.1** is shown in **Figure 3.2**. Crystallographic data for compound **3.1** are given in **Table 3.3a** and bond lengths and angles are given in **Table 3.3b (Appendix)**. The solid-state structure shows two 8-hydroxyquinolinato rings bound to one osmium atom by the coordination of the nitrogen and oxygen lone pairs and the elimination of two protons. The osmium atom is in an oxidation state of +2, thus giving the complex a total electron count of 18. There are two terminal CO ligands. The nitrogen atom N(2) in one ring is coordinated *trans* to a terminal CO ligand C(2), while in the other ligand it is the oxygen O(3) that is coordinated *trans* to CO. The other two heteroatoms, N(1) and O(4), are almost *trans* to each other, as is implied by the ^{1}H NMR data (**Table 3.2**). Because of their different coordination positions it is worth comparing the geometries of **L** and **L'** since these are in different chemical environments. The Os(1)-N(2) bond length of 2.114(4) Å is longer than the Os(1)-N(1) bond by 0.043 Å. This could be due to N(2) being *trans* to a CO ligand which is a strong π acceptor and competes with the weakly π-accepting pyridine ring containing N(2). The other pyridine heteroatom N(1) is *trans* to oxygen, which does not compete as a π acceptor. There is a similar but somewhat smaller effect observed in the Os-O bonds, the one that is *trans* to CO being longer. The Os(1)-O(3) bond length of 2.086(3) Å is longer than the Os(1)-O(4) bond length of 2.054(3) Å. The bond angles of C(2)-Os(1)-N(2) and C(1)-Os(1)-O(3) are 175.89(19) and 174.69(16)° somewhat lower than 180°. The bond angle of O(4)-Os(1)-N(1) is 163.19(16)°, significantly less than 180°. Interestingly, the bond angles of O(4)-Os(1)-N(2), N(2)-Os(1)-O(3) and O(3)-Os(1)-N(1) are approximately 80°. These distortions from ideal octahedral geometry are the result of the small bite angles of the chelating ligands.

As we had predicted from the ^{1}H NMR spectrum, the proton H(12) at C(12) is pointing approximately towards the middle of the ring containing N(1), which accounts for its upfield shift due to ring-current effects (**Figure 3.3**). Since H(3) at C(3) is above C(1)O(1) rather than a pyridine ring, the ^{1}H NMR shift is normal. The aromatic nature of the ring remains relatively unperturbed, as evidenced by the similar bond distances for the carbon-carbon bonds.

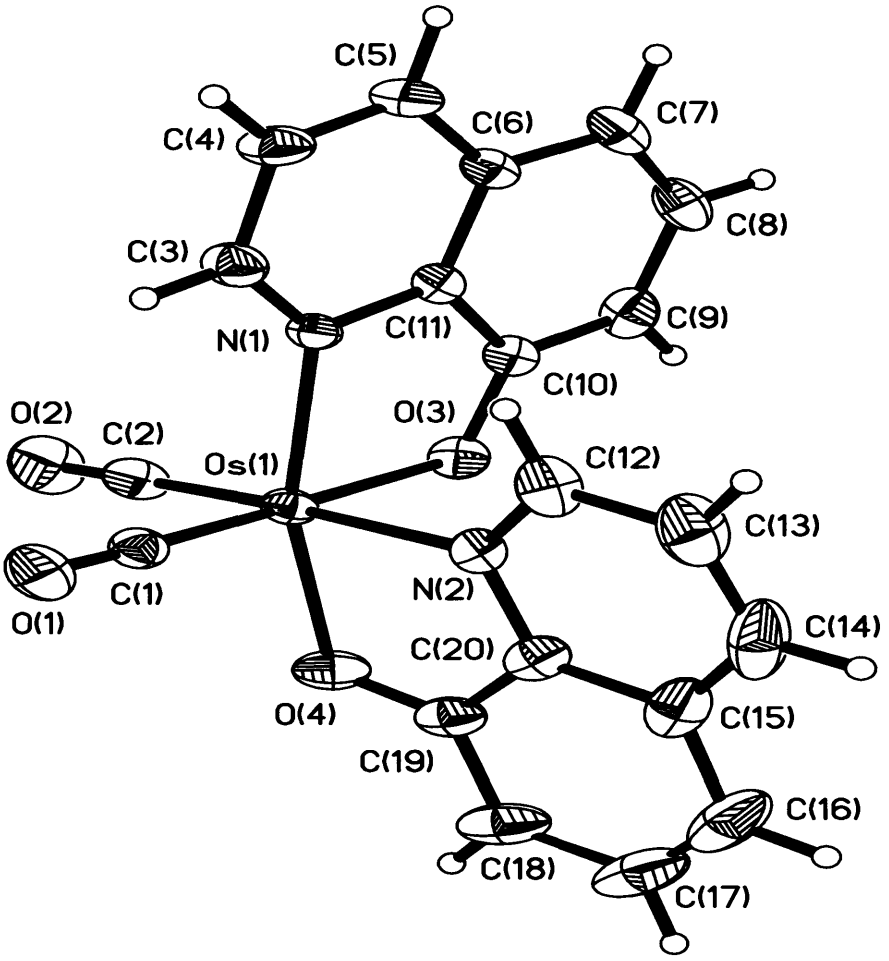

Figure 3.2. The molecular structure of $[Os(C_9H_6NO)_2(CO)_2]$ 3.1

Table 3.3. Selected bond lengths [Å] and angles [°] for $[Os(C_9H_6NO)_2(CO)_2]$ 3.1

Os(1)-C(1) = 1.857(6)	O(4)-Os(1)-N(2) = 80.33(15)
Os(1)-C(2) = 1.876(6)	N(2)-Os(1)-O(3) = 83.12(13)
Os(1)-O(3) = 2.086(3)	O(3)-Os(1)-N(1) = 79.63(13)
Os(1)-O(4) = 2.054(3)	C(1)-Os(1)-C(2) = 88.7 (2)
Os(1)-N(1) = 2.071(3)	C(2)-Os(1)-N(1) = 94.71(19)
Os(1)-N(2) = 2.114(4)	C(1)-Os(1)-O(4) = 97.29(17)

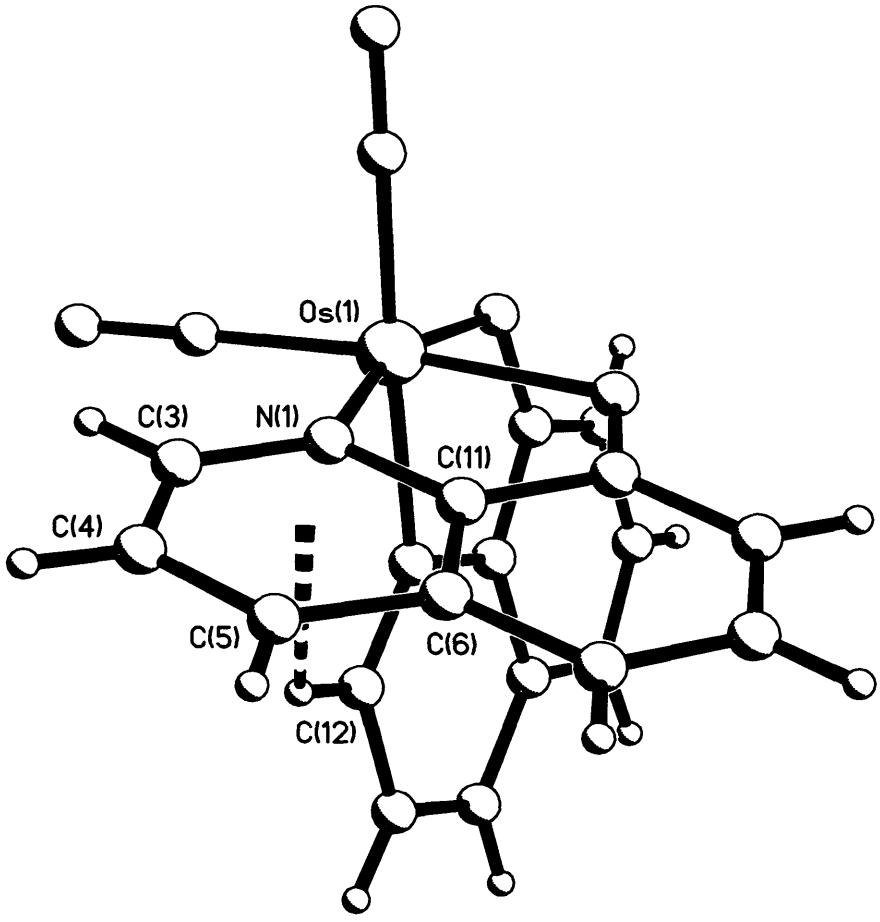

Figure 3.3. The solid state structure of [Os(C$_9$H$_6$NO)$_2$(CO)$_2$] 3.1, showing the H(12) proton at C(12) perpendicularly positioned below the pyridine ring containing N(1).

3.2.3 Spectroscopic characterisation of $[Os_3(C_9H_6NO)_2(CO)_8]$ 3.2

The EIMS spectrum showed its parent molecular ion m/z = 1088, corresponding to the formulation of $[^{192}Os_3(C_9H_6NO)_2(CO)_8]^+$. The fragmentation pattern showed the successive loss of eight CO ligands (**Figure 3.4**) with the presence of a minor impurity. The molecular formulation was also confirmed by elemental analysis. The ^1H NMR spectrum (**Table 3.2**) showed the presence of 6 proton signals, suggesting a molecule having C_2 symmetry with equivalent C_9H_6NO ligands. The spectrum resembled closely to those reported for other hydroxyquinolinato derivatives.[102] The characteristic doublet with small *ortho* coupling (J = 4.91 Hz) was observed at a low field for H(2) at δ 8.91, and the corresponding doublets and triplets were observed in the correct region of the spectrum. The infrared spectrum (**Table 3.1**) showed the presence of four CO absorptions around 2000 cm^{-1}, which were very different from those of any other triosmium quinoline derivative reported in literature thus far.[113]

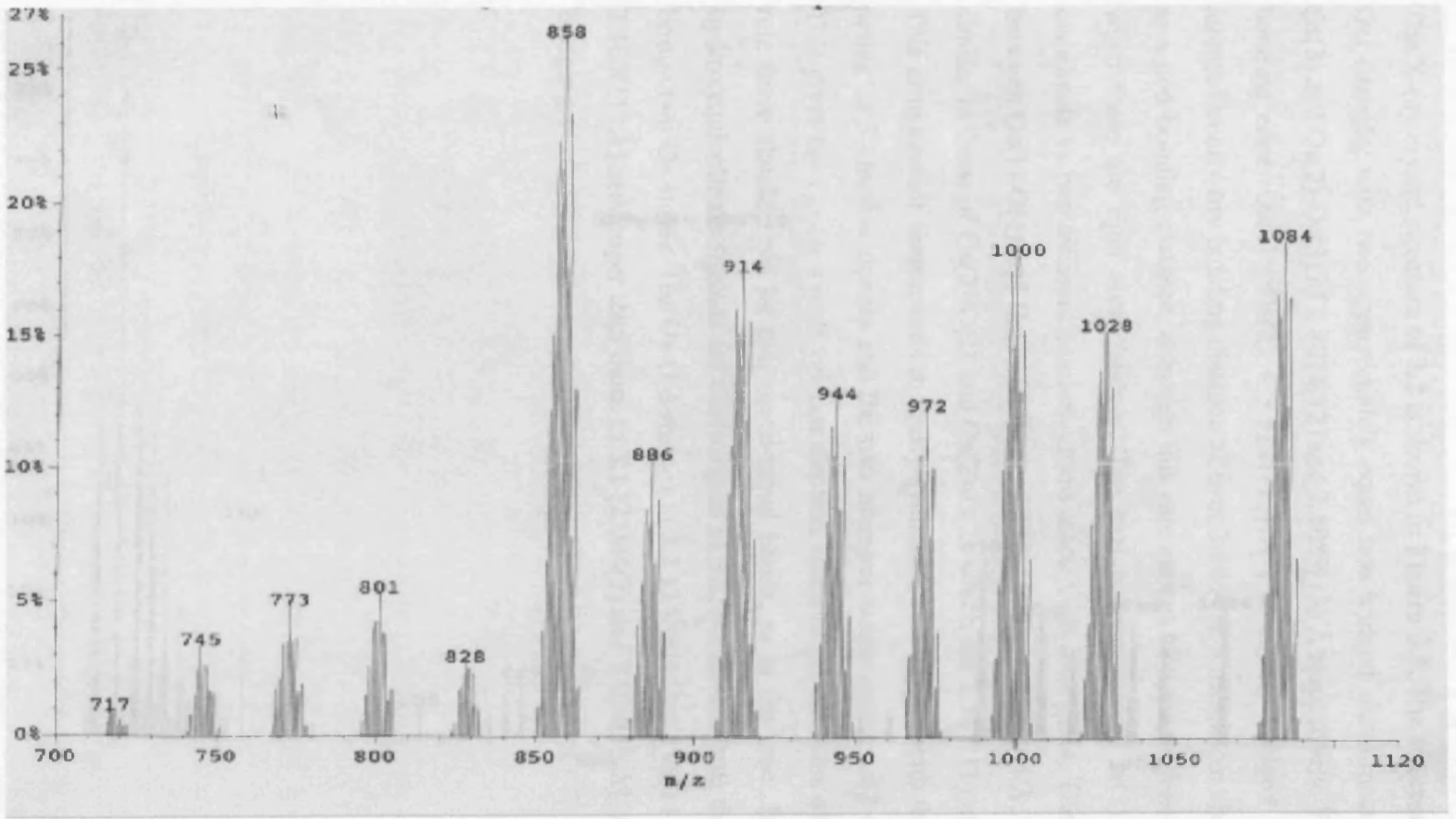

Figure 3.4. The EIMS of cluster $[Os_3(C_9H_6NO)_2(CO)_8]$ 3.2, showing the successive loss of eight CO ligands.

3.2.3.1 X-ray crystal structure of $[Os_3(C_9H_6NO)_2(CO)_8]$ 3.2

The X-ray crystal structure of **3.2** is shown in **Figure 3.5**. The structure consists of an Os_3 triangle, with two approximately equal non-bridged metal-metal bonds: Os(1)-Os(3) and Os(2)-Os(3) of 2.8014(12) and 2.8089(13) Å respectively. The longest non-bonding edge, Os(1)···Os(2) = 3.1221(13) Å , is doubly bridged by two oxygen atoms. Usually any bonding distance of over 3.00 Å in a triosmium cluster is regarded as a non-bonding distance, although this rule cannot be applied generally, especially when there are light atom bridges. The two nitrogen atoms N(1) and N(2) also coordinate to two different osmium atoms using their lone pairs. The bond distances between Os(1)-O(1) and Os(1)-O(2) are 2.138(11) and 2.198(11) Å, which are very similar to those of Os(2)-O(1) and Os(2)-O(2) which are 2.187(11) and 2.160(11) Å. This arrangement corresponds to nearly symmetrical bridging, with the oxygen atoms acting as 3-electron donors and the two nitrogen atoms acting as 2-electron donors. This gives the cluster a total valence electron count of 50. In terms of the 18-electron rule there should only be two metal-metal bonds, as is the case. Interestingly, the hydroxyquinolinato ligands are chelating as in **3.1**, but in this case the oxygen atoms bridge two Os atoms. The Os-O distances in **3.2** [2.138(11), 2.198(11), 2.187(11) and 2.160(11) Å] are longer than those in **3.1** [2.086(3) and 2.054(3) Å], as a result of the bridging.

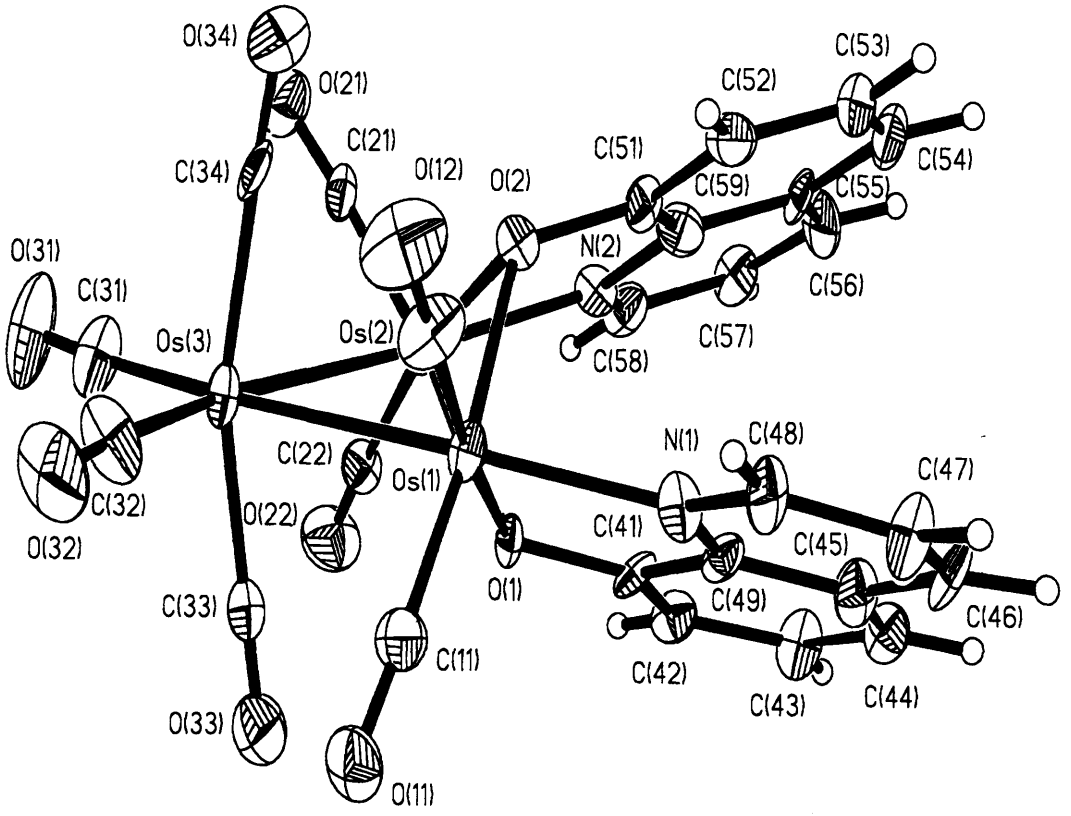

Figure 3.5. The molecular structure of $[Os_3(C_9H_6NO)_2(CO)_8]$ 3.2, showing the C_2 symmetry of the molecule.

The structure found for **3.2** is very similar to other osmium compounds, for example $[Os_3(OCH_3)_2(CO)_{10})]$ **3.9**,[114] $[Os_3(\mu\text{-}SCH_2Ph)_2(CO)_{10}]$ **2.1**, $[Os_3(\mu\text{-}S^tBu)_2(CO)_{10}]$ **2.6** (in Chapter 2) and the ruthenium nitrosyl cluster $[Ru_3(NO)_2(CO)_{10}]$ **3.10**,[115] where the nitrogen doubly bridges two ruthenium atoms. In compound **3.9**, the Os-Os bond distances are 2.815(3) and 2.823(3) Å respectively. The two bonding distances in **3.9** are longer than in **3.2**, whereas the non-bonding distance in **3.2** is longer than in **3.9** by 0.044 Å. The non-bonding Os···Os distances are largely controlled by the nature of the bridging ligands. The two Os-O-Os bond angles in **3.10** are approximately 95°, which is approximately the same as those found in **3.2** of 88°.

3.2.4 Spectroscopic characterisation of $[Os(C_9H_6NO)_2(CO)_2]$ isomer 3.5

The infrared spectrum of complex **3.5** in dichloromethane featured two strong carbonyl absorption bands at 2023(s) and 1945(s) cm^{-1}, somewhat lower than those for **3.1** but also indicative of two *cis* carbonyl ligands. The EI mass spectrum of complex **3.5** showed its parent molecular ion *m/z* = 536, corresponding to the formulation $[^{192}Os(C_9H_6NO)_2(CO)_2]^+$ (**Figure 3.6**). The ^1H NMR spectrum (**Figure 3.7.**) showed the presence of two equivalent 8-hydroxyquinolinato ligands. Of the three possible *cis* carbonyl isomers **1a-c**, this complex must be **1b** or **1c**. However, we could not distinguish between the two possible isomers on the basis of the spectroscopic data.

The ^1H NMR spectrum showed the characteristic downfield doublet for H(2) at δ 8.94 (J = 5.0 Hz), along with doublets and triplets in the appropriate regions of the spectrum for the other five protons, see **Table 3.2.**

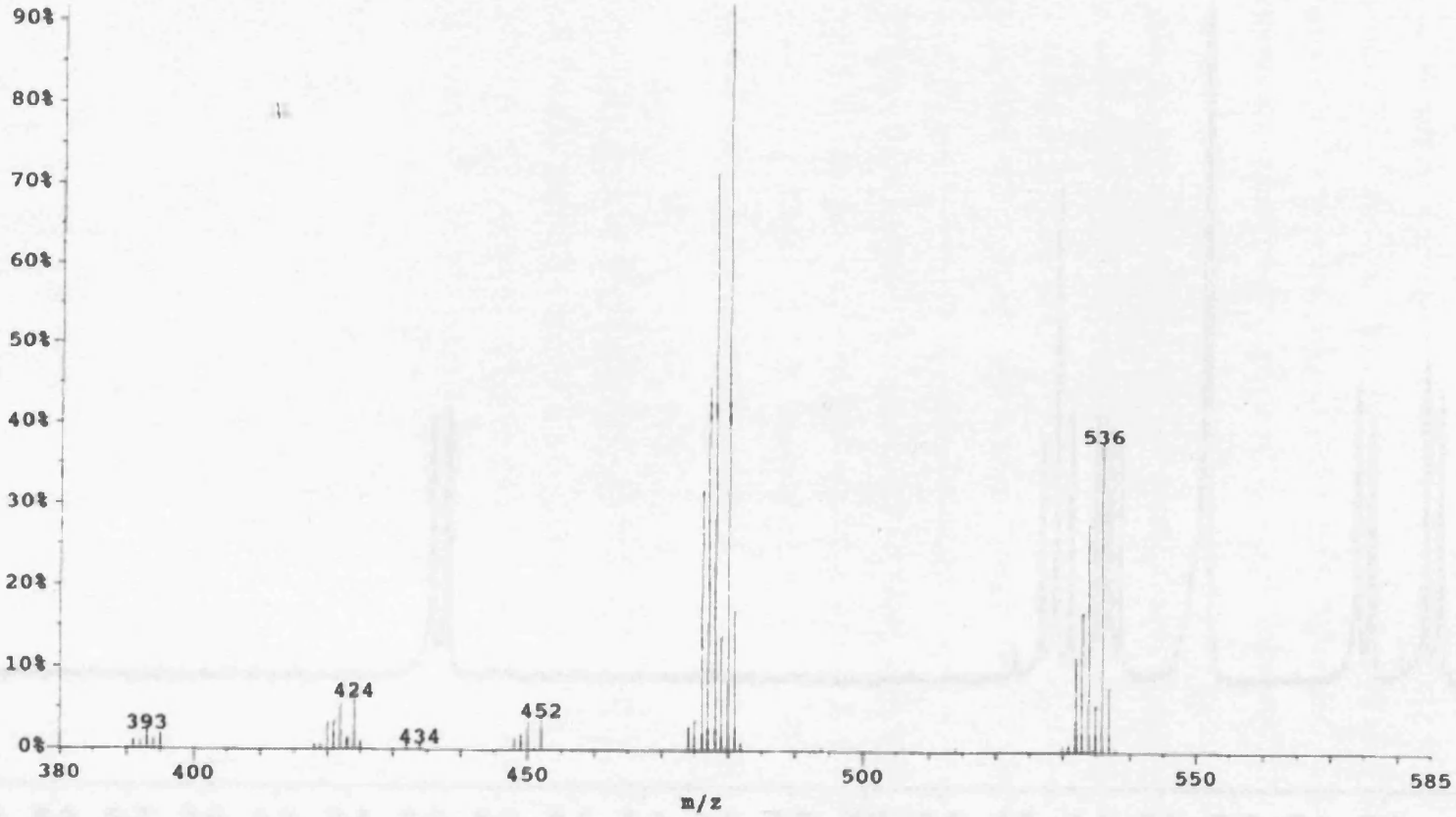

Figure 3.6. The EIMS of cluster $[Os(C_9H_6NO)_2(CO)_2]$ isomer 3.5

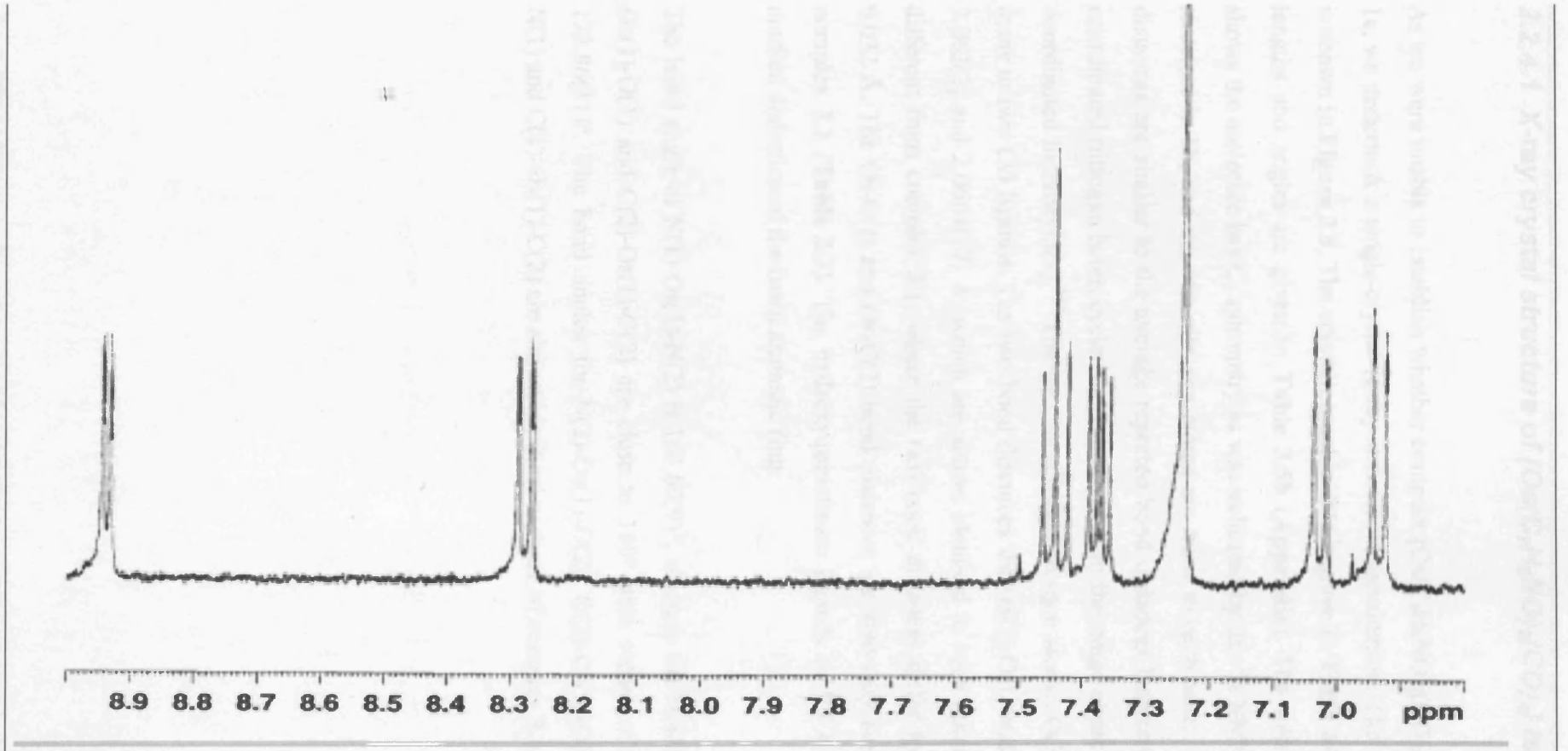

Figure 3.7. The ^{1}H NMR spectrum of $[Os(C_9H_6NO)_2(CO)_2]$ isomer 3.5, showing the six proton signals.

3.2.4.1 X-ray crystal structure of $[Os(C_9H_6NO)_2(CO)_2]$ isomer 3.5

As we were unable to establish whether complex $[Os(C_9H_6NO)_2(CO)_2]$ **3.5** was **1b** or **1c**, we undertook a single-crystal X-ray structure determination. The crystal structure is shown in **Figure 3.8**. The crystallographic data is given in **Table 3.4a** and the bond lengths and angles are given in **Table 3.5b** (**Appendix**). The solid-state structure shows the molecule has C_2 symmetry as was indicated by the ^1H NMR spectrum. The structure is **1b**, and the two nitrogen atoms are *trans* to each other. The Os-N bond distances are similar to the average reported bond distances between osmium and a coordinated nitrogen heterocycle (the values come in the range expected for nitrogen coordinated heterocycles).[116] The two coordinated oxygen atoms, O(3) and O(4), are *trans* to two CO ligands. The two bond distances for Os(1)-O(1) and Os(1)-O(2) are 2.062(2) and 2.0664(19) Å, which are almost identical to each other. This is quite different from complex **3.1**, where the two bond distances differ by approximately 0.032 Å. The Os-C(1) and Os-C(2) bond distances are also very similar to those of complex **3.1** (**Table 2.3**). The hydroxyquinolinato ligands in **3.3** do not show any marked distortion of the fused aromatic ring.

The bond angle of N(1)-Os(1)-N(2) is 163.60(9)°, whereas the bond angles of C(1)-Os(1)-O(1) and C(2)-Os(1)-O(2) are close to 180° with values of 175.95(10) and 173.86(11)°. The bond angles for N(2)-Os(1)-O(2), O(2)-Os(1)-O(1), O(1)-Os(1)-N(1) and C(1)-Os(1)-C(2) are almost identical to those of complex **3.1**.

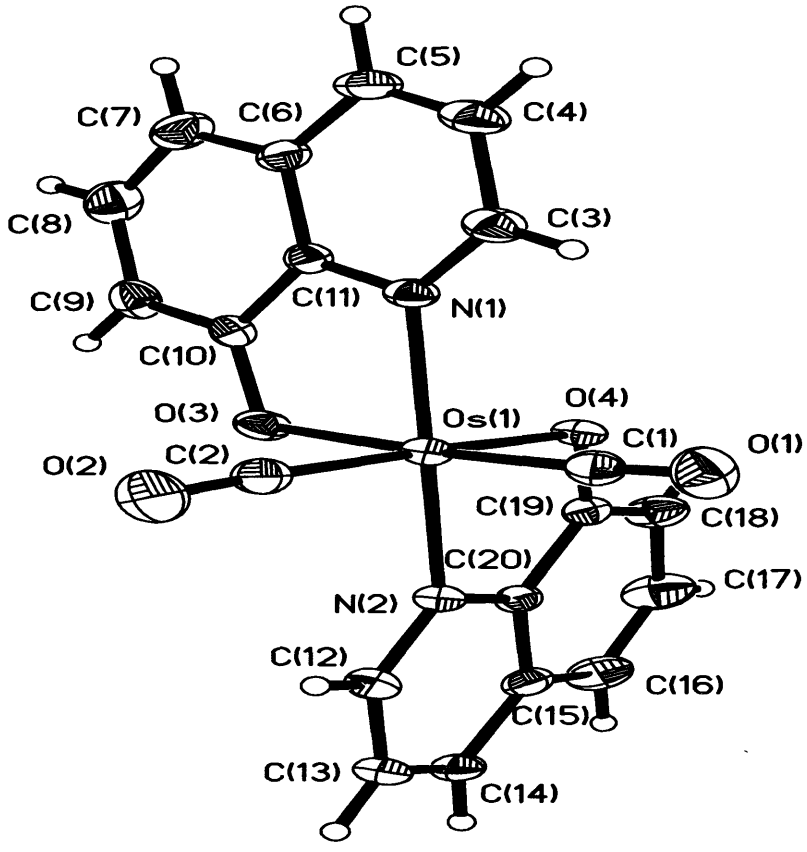

Figure 3.8. The molecular structure of $[Os(C_9H_6NO)_2(CO)_2]$ 3.5, showing C_2 symmetry.

3.2.5 Reactions of 8-hydroxyquinoline with $[Os_3(\mu\text{-}H)_2(CO)_{10}]$

On the evidence of the above reactions, the formation of 8-hydroxyquinoline products is highly dependent on the reaction conditions employed. We wished to carry out the reaction of 8-hydroxyquinoline with $[Os_3(\mu\text{-}H)_2(CO)_{10}]$, under milder conditions in the hope of isolating less stable 8-hydroxyquinoline products. We treated the unsaturated and more reactive cluster $[Os_3(\mu\text{-}H)_2(CO)_{10}]$ with an excess of 8-hydroxyquinoline in refluxing cyclohexane for 20 hours, after which time the reaction yielded the known cluster $[Os_4(\mu\text{-}H)_2(CO)_{13}]$ **3.6** (6%) and a new hydrido cluster $[Os_3(\mu\text{-}H)(C_9H_6NO)(CO)_9]$ **3.7** in a low yield (11%). No reaction occurred at room temperature after 5 hours of stirring.

However, the reaction of 8-hydroxyqunoline with $[Os_3(\mu\text{-}H)_2(CO)_{10}]$ in refluxing xylene gave $[Os_3(C_9H_6NO)_2(CO)_8]$ **3.2** (8%), $[Os_3(\mu\text{-}H)(C_9H_6NO)(CO)_9]$ **3.7** (35%) and a new tetranuclear cluster $[Os_4(\mu\text{-}H)(C_9H_6NO)(CO)_{11}]$ **3.8** (10%). We also obtained a trace amount of a mixture of both isomers **3.1** and **3.5**. The major product was the hydrido cluster **3.7**. It appears that more forcing conditions favour the formation of this cluster. This is rather unusual since it is difficult to see why cluster **3.7** was not formed in the direct reaction of $[Os_3(CO)_{12}]$ with 8-hydroxyquinoline. It is possible that the initial product formed in the reaction was $[Os_3(\mu\text{-}H)(C_9H_6NO)(CO)_9]$ **3.7** with O-H bond activation, which after prolonged heating lost a CO ligand with the addition of another 8-hydroxyquinoline molecule with the elimination of H_2 yields the cluster $[Os_3(C_9H_6NO)_2(CO)_8]$ **3.2**. The conditions we used for the reaction with $[Os_3(CO)_{12}]$ were more severe than those used for this reaction, and cluster **3.7** was the major product in this case.

Similarly, the direct reaction of $[Os_3(MeCN)](CO)_{11}]$ with 8-hydroxyquinoline in cyclohexane, only gave cluster $[Os_3(\mu\text{-}H)(C_9H_6NO)(CO)_9]$ **3.7** in a low yield (12%).

3.2.5.1 Spectroscopic characterisation of tri-and tetranuclear clusters

The known tetranuclear cluster $[Os_4(\mu\text{-}H)_2(CO)_{13}]$ **3.6** was characterised using IR, ^1H NMR and mass spectroscopy. The ^1H NMR spectrum showed the presence of only two hydride singlets at δ -20.57 and -21.44, in the ratio of 1:1. The EI mass spectrum showed a peak at m/z = 1134 (calcd. 1134), with the successive loss of thirteen CO ligands.

The EI mass spectrum of cluster **3.7** showed its parent molecular ion m/z = 973 corresponding to the formulation $[^{192}Os_3(\mu\text{-}H)(C_9H_6NO)(CO)_9].^+$ The fragmentation pattern showed the successive loss of 9 CO ligands. The infrared data is given in **Table 3.1** and the ^1H NMR data is in **Table 3.2**. The ^1H NMR spectrum showed a singlet at δ -10.09 for the hydride ligand, a downfield doublet at δ 9.19 for the H(2) proton, along with five other proton signals in the appropriate regions of the spectrum, corresponding to the coordinated 8-hydroxyquinolinato ligand.

The tetranuclear cluster $[Os_4(\mu\text{-}H)(C_9H_6NO)(CO)_{11}]$ **3.8**, was characterised by its IR, ^1H NMR spectrum, EI mass spectrum and single-crystal X-ray analysis. The EI mass spectrum showed its parent molecular ion peak at m/z = 1221, corresponding to the formulation of $[^{192}Os_4(\mu\text{-}H)(OC_9H_6N)(CO)_{11}]^+$ with the successive loss of 11 CO ligands. The IR data in **Table 3.1**, showed the presence of 11 signals in the terminal υ(CO) region of the spectrum, which implied a molecule with very low symmetry. The ^1H NMR data for **3.8 (Table 3.2)** are almost identical to those of all the other 8-hydroxyquinolinato derivatives, with a low-field doublet signal at δ 8.97 (J = 5.0 Hz) for H(2), and a doublet at δ 8.38 (J = 7.4 Hz) for H(4) with large coupling. The characteristic triplet and quartet, and the two doublets appear in the correct region of the spectrum, although in this case the two doublets due to H(5) and H(7) are slightly obscured by the solvent peak, thus making accurate assignment difficult. The hydride singlet appears at δ -13.32.

3.2.5.2 X-ray crystal structure of $[Os_3(\mu\text{-}H)(C_9H_6NO)(CO)_9]$ 3.7

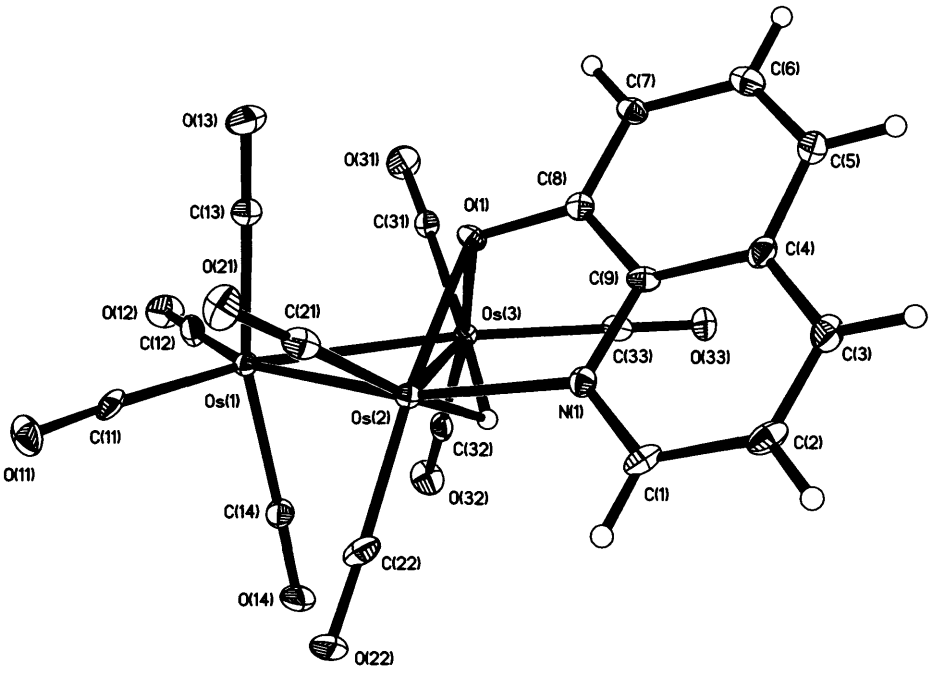

Figure 3.9. The solid-state structure of $[Os_3(\mu\text{-}H)(C_9H_6NO)(CO)_9]$ 3.7.

The solid-state structure of **3.7** is shown in **Figure 3.9**. Crystallographic data are given in **Table 3.5a** and bond lengths and angles are shown in **Table 3.6b** (**Appendix**). The structure consists of an Os_3 triangle with two approximately equal metal-metal bonds, Os(1)-Os(3) and Os(2)-Os(3) are 2.8162(5) and 2.8108(5) Å, and one slightly shorter metal-metal bond length of 2.7797(15) Å for Os(1)-Os(2). There are nine terminal CO ligands distributed so that four are attached to Os(1), three to Os(3) and two to Os(2). The organic ligand is coordinated to the cluster via the nitrogen lone pair and a doubly bridged oxygen atom, which bridges the same edge as the μ-H ligand, where the μ-H ligand is tucked well below the Os_3 plane. Interestingly, osmium clusters of the type $[Os_3(\mu\text{-}H)(\mu\text{-}X)(CO)_{10}]$ with only one bridging hydride ligand usually have two approximately equal metal-metal bond distances, along with one elongated metal-metal bond, usually the edge where the μ-hydride bridges the two metal atoms. In this case however, the situation is reversed because of the lower symmetry resulting from the coordinated pyridine. The ligand is

acting as a five-electron donor, thus making cluster **3.7** fully saturated with a total of 48 electrons.

The Os(2)-N(1) bond length of 2.147(8) Å is almost identical to that of cluster **3.2**, however it is slightly longer than those of the two mononuclear complexes **3.1** and **3.5**. The two Os(2)-O(1) and Os(3)-O(3) bond distances are 2.147(6) and 2.160(6) Å respectively, which are longer than those found in the related species $[Os_3(OCH_3)_3(CO)_{10}]$ **3.9** [114] and analogues **3.2** and **3.10**. The bond distances for C(1)-C(2) and C(2)-C(3) are 1.401(15) and 1.342(15) Å, which are typical values for aromatic C-C bonds. The bond angle of N(1)-Os(1)-O(1) is 77.4(3)°, which is similar to that of cluster **3.2** but slightly smaller than that of complex **3.1** and **3.3** by approximately 3°.

3.2.5.3 X-ray crystal structure of $[Os_4(\mu\text{-}H)(C_9H_6NO)(CO)_{11}]$ 3.8

The solid-state structure of **3.8** is shown in **Figure 3.10**. Crystallographic data are given in **Table 3.6a** and bond lengths and angles are shown in **Tables 3.7a** and **3.7b** (**Appendix**). The four osmium atoms are arranged in a 'butterfly' configuration, in which two triangles share a common edge [Os(3)-Os(4)]. There are five metal-metal bond distances, consisting of two short ones, Os(3)-Os(4) and Os(2)-Os(3) (2.8033(5) and 2.8295(5) Å); two medium bond distances for Os(2)-Os(4) and Os(1)-Os(4) (2.9605(5) and 2.9719(4) Å) and one elongated Os(1)-Os(3) bond distance of 3.0462(5) Å. The elongation in the metal-metal bond distances of osmium clusters is usually due to a bridging ligand, as is the case here where a μ-hydride bridges two atoms. Osmium atoms Os(2), Os(3) and Os(4) are each bound to three terminal carbonyl ligands, while Os(1) is only bound to two. So including all the metal-metal and hydrido ligand bondings, two osmium atoms, Os(2) and Os(4) are 6-coordinate, while Os(1) and Os(3) are both 7-coordinate, but 6-coordinate if the M-M vector associated with the hydride bridge is ignored. The 8-hydroxyquinolinato ligand is bound to the tetra-nuclear cluster by coordination of the nitrogen lone pair to Os(1), and with the oxygen atom doubly bridging the osmium atoms Os(1) and Os(2).

The Os(1)-N(1) bond distance is 2.110(6) Å. The bond angle of 78.6(2)° for O(1)-Os(1)-N(1), is in agreement with that of the related species **3.1**, **3.2**, **3.5**, **3.6** and **3.7**. The osmium bond angle fall in the range 55.508(10)° to 72.97(11)°, which is slightly lower than those found in $[Os_4(CO)_{12}H_3I]$.[117]

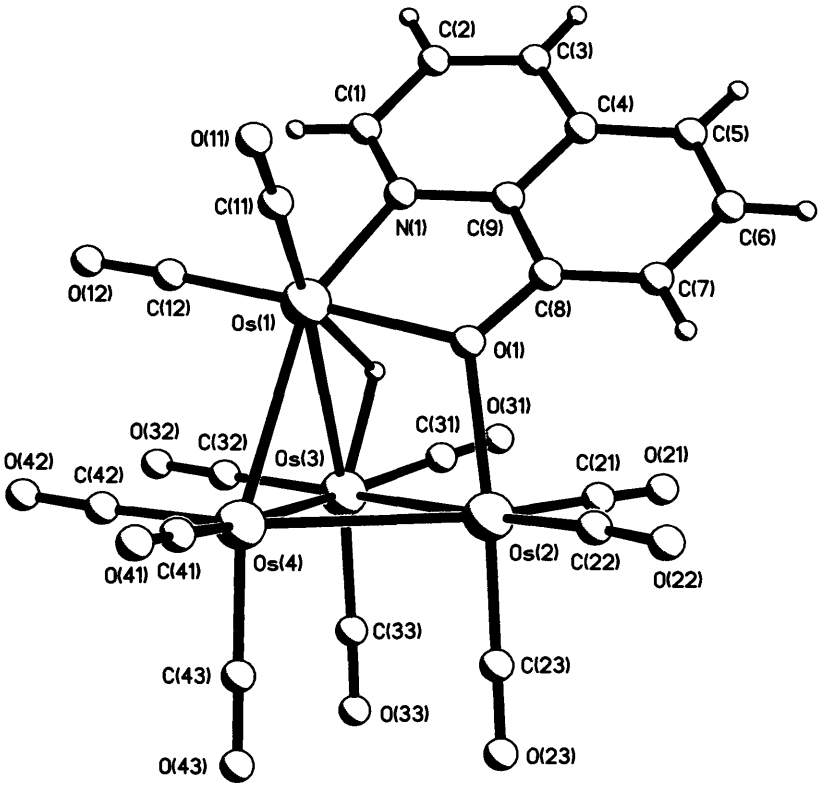

Figure 3.10. The solid-state structure of $[Os_4(\mu\text{-}H)(C_9H_6NO)(CO)_{11}]$ 3.8.

3.3 Conclusions

The chemistry of quinoline and its derivatives with triosmium clusters has been studied extensively as mentioned earlier. However, the reactions of 8-hydroxyquinoline with clusters have had little or no impact to date. We have now extended this area of research by exploring the reaction of triosmium clusters with 8-hydroxyquinoline ligand. We have observed that the direct reactions of 8-hydroxyquinoline with $[Os_3(CO)_{12}]$, in the various reaction conditions employed, yielded different products. The direct thermal reaction of $[Os_3(CO)_{12}]$ with 8-hydroxyquinoline yielded the mononuclear complex $[Os(C_9H_6NO)_2(CO)_2]$ **3.1** (where the oxygen and nitrogen atoms are *trans* to each other), along with the trinuclear cluster $[Os_3(C_9H_6NO)_2(CO)_8]$ **3.2** only. In complex **3.1** we have observed that the proton shift due to one of the H(2) atoms came at a much higher field ($\approx$ 2 p.p.m) than expected, and we have attributed this difference to the ring-current effects. Cluster **3.2**, has C_2 symmetry and consists of two oxygen atoms doubly bridging the same pair of osmium atoms. The ^1H NMR spectrum showed no effect like this in **3.1**. Conversely, carrying out the same reaction in a Carius tube yielded complex $[Os(C_9H_6NO)_2(CO)_2]$ **3.5**, an isomer of **3.1** (where the same heteroatoms are *trans* to each other), and a known tetranuclear cluster $[Os_4(\mu\text{-}H)_4(CO)_{12}]$ **3.4**.

The direct thermal reactions of 8-hydroxyquinoline with the purple unsaturated cluster $[Os_3(\mu\text{-}H)_2(CO)_{10}]$ in xylene yielded the mononuclear complex $[Os(C_9H_6NO)_2(CO)_2]$ **3.3**, the trinuclear cluster $[Os_3(\mu\text{-}H)(C_9H_6NO)(CO)_9]$ **3.7** and the tetranuclear cluster $[Os_4(\mu\text{-}H)(C_9H_6NO)(CO)_{11}]$ **3.8**. Only the trinuclear and the tetranuclear clusters have been characterised by IR, ^1H NMR spectrum, EI mass spectrum and X-ray crystallography. The above reactions gave a low yield when carried out in refluxing cyclohexane.

3.4 Experimental

3.4.1 General synthetic details

All of the reactions were carried out under nitrogen unless otherwise stated. The bis-acetonitrile cluster $[Os_3(MeCN)_2(CO)_{11}]$ and $[Os_3H_2(CO)_{10}]$ were prepared by published methods.[18,29] 8-Hydroxyquinoline was purchased from Aldrich plc and used without further purification. The ^1H NMR spectra were obtained from a Bruker AMX300 MHz or AMX400 MHz spectrometer and the data was processed using XWIN-NMR and X-WIN-PLOT. Electron Ionisation (EI), mass spectra and Fast Atom Bombardment (FAB) were acquired by the UCL mass spectrometry service. The IR spectra were recorded on a Shimadzu 8700 FT-IR spectrometer in a CaF_2 solution cell. Elemental analyses were performed by the micro analytical service at UCL. Preparative Thin Layer Chromatography (TLC) plates (silica gel 60 HF_{254} with fluorescent indicator E. Merck, Germany) were prepared as an aqueous slurry, which was layered on glass and either dried in the air or in the oven at 100 °C overnight before use.

3.4.2 Reaction of $[Os_3(CO)_{12}]$ with 8-hydroxyquinoline in refluxing xylene

A solution of the yellow cluster $[Os_3(CO)_{12}]$ (0.200 g, 0.221 mmol) and 8-hydroxyquinoline (0.2225 g, 1.534 mmol) in xylene (40 cm^3) was refluxed for 72 hours. The solution changed in colour from yellow to orange/yellow. Some yellow crystals were deposited at the bottom of the flask. The solvent was removed under vacuum and TLC was carried out using petroleum spirit (b.p. 40-60 °C): CH_2Cl_2 (3:1, v/v) as eluent. Three bands were isolated which have been identified as $[Os(C_9H_6NO)_2(CO)_2]$ **3.1** (0.008 g, 7%), $[Os_3(C_9H_6NO)_2(CO)_8]$ **3.2** (0.0350 g, 30%) and the starting material $[Os_3(CO)_{12}]$, which was obtained in trace amounts. Crystals of **3.2** were grown from a mixture of dichloromethane/heptane by slow evaporation at room temperature. The EA for $[Os_3(C_9H_6NO)_2(CO)_8]$ **3.2**: Found: C, 28.78; H, 1.15; N, 2.48. Calc, for C, 28.68; H, 1.11; N, 2.57.

3.4.3 Reaction of $[Os_3(CO)_{12}]$ with 8-hydroxyquinoline in a Carius tube in xylene

The yellow cluster $[Os_3(CO)_{12}]$ (0.2711 g, 0.2973 mmol) and 8-hydroxyquinoline (0.2622 g, 0.1808 mmol) were introduced into a Carius tube and xylene (20 cm^3) was added. Degassing was carried out by cooling the solution in liquid nitrogen while the vapour was pumped off. The Carius tube was then allowed to warm to room temperature in a closed vacuum. This process was repeated twice. The Carius tube was sealed at liquid nitrogen temperature then slowly warmed to room temperature and then placed in an oven at 180 °C for 71 hours. The colour of the solution changed from yellow to bright orange. Some orange crystals settled at the bottom of the Carius tube. The tube was cooled to room temperature and the glass seal was broken.

The orange crystals were separated by filtration, then the solvent was removed under reduced pressure and TLC was carried out on the yellow/orange solid using hexane: CH_2Cl_2 (3:1, v/v) as eluent. Two bands were isolated of which one has been partially characterised as the complex $[Os(C_9H_6NO)_2(CO)_2]$ **3.3** by IR only (<2 mg), an isomer of **3.1**.

The orange crystals were found to be a mixture of another isomer of complex **3.1** and the tetranuclear cluster $[Os_4(\mu\text{-}H)_4(CO)_{12}]$ **3.4**. The mixture was separated further by their solubility difference in dichloromethane, as the cluster $[Os_4(\mu\text{-}H)_4(CO)_{12}]$ **3.4** was more soluble in this. The isomer obtained was $[Os(C_9H_6NO)_2(CO)_2]$ **3.5** (0.1214 g, 36%). The EA for $[Os(C_9H_6NO)_2(CO)_2]$ **3.5**, Found: C, 45.01; H, 2.36; N, 5.05. Calc. C, 44.80; H, 2.20; N, 5.20.

3.4.4 Reaction of $[Os_3(\mu\text{-}H)_2(CO)_{10}]$ with 8-hydroxyquinoline in refluxing cyclohexane

A solution of the purple cluster $[Os_3(\mu\text{-}H)_2(CO)_{10}]$ (0.0563 g, 0.0656 mmol) and 8-hydroxquinoline (0.0574 g, 0.3958 mmol) in cyclohexane (15 cm^3) was refluxed for 20 hours. The solvent was removed under vacuum and TLC was carried out using petroleum spirit (b.p. 40-60 °C): CH_2Cl_2 (3:1, v/v) as eluent. Four significant bands were isolated of which three have been identified as $[Os_4(\mu\text{-}H)_2(CO)_{13}]$ **3.6** (0.0041 g, 6%), $[Os_3(\mu\text{-}H)(C_9H_6NO)(CO)_9]$ **3.7** (0.007 g, 11%) and a trace amount of the starting material $[Os_3(\mu\text{-}H)_2(CO)_{10}]$.

3.4.5 Reaction of $[Os_3(\mu\text{-}H)_2(CO)_{10}]$ with 8-hydroxyquinoline in refluxing xylene

The unsaturated cluster $[Os_3(\mu\text{-}H)_2(CO)_{10}]$ (0.0807 g, 0.0941 mmol) and 8-hydroxquinoline (0.0579 g, 0.3993 mmol) were refluxed in xylene (30 cm^3) for 1 hour and 50 minutes. The solution changed colour from purple to orange/yellow. The solvent was removed and TLC was carried out using petroleum spirit (b.p. 40-60 °C) : CH_2Cl_2 (3:1, v/v) as eluent. Four significant bands were isolated of which three have been identified as clusters: $[Os_3(C_9H_6NO)_2(CO)_8]$ **3.2** (0.0090 g, 8%) and $[Os_3(\mu\text{-}H)(C_9H_6NO)(CO)_9]$ **3.7** (ca. 0.040 g, 35%), which were previously synthesised from the thermal reactions of $[Os_3(CO)_{12}]$ or $[Os_3(\mu\text{-}H)_2(CO)_{10}]$ with 8-hydroxyquinoline, along with a new tetranucler cluster $[Os_4(\mu\text{-}H)(C_9H_6NO)(CO)_{11}]$ **3.8** (0.012 g, 10%). A mixture of complexes **3.1** and **3.5** was also obtained, but could not be separated.

3.4.6 Reaction of $[Os_3(MeCN)(CO)_{11}]$ with 8-hydroxyquinoline in refluxing xylene

The reactive cluster $[Os_3(MeCN)(CO)_{11}]$ (0.0310 g, 0.0334 mmol) and 8-hydroxyquinoline (0.0099 g, 0.0683 mmol) were refluxed in cyclohexane for 1 hour. The solution changed colour from yellow to orange. The solvent was removed and

TLC was carried out using dichloromethane/petroleum spirit (b.p. 40-60 °C) (4:3 v/v) as eluent to give cluster $[Os_3(\mu\text{-}H)(C_9H_6NO)(CO)_9]$ **3.7** (0.004 g, 12%).

Table 3.1. Selected infrared data for hydroxyquinoline derivatives.

Compounds	**υ(CO) (cm^{-1})**
$[Os(C_9H_6NO)_2(CO)_2]$ **3.1**[a]	2030vs, 1948vs
$[Os_3(C_9H_6NO)_2(CO)_8]$ **3.2**[a]	2079w, 1994vs, 1958vw, 1918w
$[Os(C_9H_6NO)_2(CO)_2]$ **3.3**[a]	2027vs, 1949vs
$[Os_4H_4(CO)_{12}]$ **3.4.**	2085m, 2068vs, 2020s, 1999m
$[Os(C_9H_6NO)_2(CO)_2]$ **3.5**[a]	2023vs, 1945vs
$[Os_3H(C_9H_6NO)(CO)_9]$ **3.7**[b]	2097w, 2058m, 2015vs, 2002m, 1994w 1986w, 1977vw, 1939w
$[Os_4H(C_9H_6NO)(CO)_{11}]$ **3.8**[b]	2092w, 2059vs, 2048m, 2033vs, 2009m 1998m, 1989s, 1976w, 1969vw, 1958vw(br) 1929vw(br).

[a] Cyclohexane solution. [b] Dichloromethane solution.

Table 3.2. The ^{1}H NMR data for 8-hydroxyquinoline.

Compound	Chemical shfits (δ)	Intensities (No. of H)	Assignment
$[Os(C_9H_6NO)_2(CO)_2]$ **3.1**	8.94(d)	1	H(2) L
	7.11(d)	1	H(2) L'
	7.07(t)	1	H(3) L
	7.02(t)	1	H(3) L'
	8.30(d)	1	H(4) L
	8.18(d)	1	H(4) L'
	7.40(d)	1	H(5) L
	7.30(d)	1	H(5) L'
	7.50(d)	1	H(6) L
	7.44(d)	1	H(6) L'
	7.00(d)	1	H(7) L
	6.91(d)	1	H(7) L'
$[Os_3(C_9H_6NO)_2(CO)_8]$ **3.2**	8.91(d)	2	H(2)
	6.96(t)	2	H(3)
	7.88(d)	2	H(4)
	6.78(d)	2	H(5)
	7.22(t)	2	H(6)
	6.73(d)	2	H(7)
$[Os_4H_4(CO)_{12}]$	-20.48	4	OsH
$[Os(C_9H_6NO)_2(CO)_2]$ **3.5**	8.94(dd)	1	H(2)
	7.42(t)	1	H(3)
	8.28(dd)	1	H(4)
	7.02(dd)	1	H(5)
	7.44(t)	1	H(6)
	6.93(dd)	1	H(7)
$[Os_4H_2(CO)_{13}]$ **3.6**	-20.57(s)	1	OsH
	-21.44(s)	1	OsH
$[Os_3H(C_9H_6NO)(CO)_9]$ **3.7**	9.19(d)	1	H(2)
	7.84(t)	1	H(3)
	8.25(d)	1	H(4)
	7.27(d)	1	H(5)
	7.89(t)	1	H(6)
	7.23(d)	1	H(7)
	-10.09(s)	1	OsH

Table 3.2. The ^{1}H NMR data for 8-hydroxyquinoline.

$[Os_4H(C_9H_6NO)(CO)_{11}]$ **3.8**	8.97(d)	1	H(2)
	8.38(d)	1	H(4)
	7.61(t)	1	H(3)
	7.44(t)	1	H(6)
	7.28(d)	1	H(5)
	7.23(d)	2	H(7)
	-10.09(s)	1	OsH

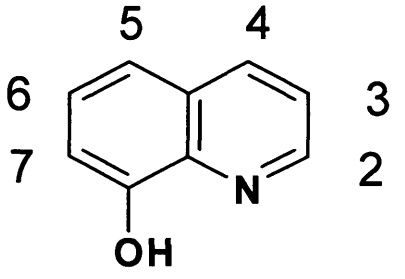

d =doublet, dd = double doublet, s = singlet and t= triplet, refer to the general shape of the multiplet.

Chapter 4. Reactions of triosmium clusters with mono and di-substituted phenols

4.1 Introduction

Transition metal complexes in which two or more metal atoms are bridged by one or more arene ligands, are few in comparison to the large number of mononuclear arene complexes. There is considerable interest in the interaction of arenes with metal clusters, as arene bridges can occur in a variety of coordination modes with almost all of the transition metal atoms of the periodic table.[118] In 1919, Hein[119] isolated the phenyl-chromium compound from $CrCl_3$ and PhMgBr. However, this was much later identified by Zeiss[120] as the $[Cr(\eta^6\text{-}C_6H_6)_2]^+$ cation. This can be reduced to give $[Cr(\eta^6\text{-}C_6H_6)_2]$.

The ability of Ag^+ ions to form an arene complex was discovered in the 1920s. However, it was not fully utilised until 1955, when Fischer and Hafner,[121] using the 'reducing Friedel-Craft method,' found an excellent synthesis for bis(η^6-benzene)chromium. This revolutionised the chemistry of bis(arene)metal complexes, and was soon followed by metal-arene carbonyl and other mixed derivatives.[118,122]

Molecular clusters of the general formulae [{L_mM}$_n$(μ-arene)] with $n \geq 3$, where an arene ligand is bonded to three or more metal atoms, are of great importance as possible model substances for arene chemisorptions on metal surfaces.[123] In Chapter 1, we gave some examples of the synthesis of osmium arene clusters. The phenyl ligand coordinates to cluster atoms by σ-bonding and is resistant to *β*-elimination to give benzyne. Aryl complexes are therefore amongst the most stable compounds containing M-C σ bonds. Much work has been done on mononuclear and binuclear arene complexes, however the chemistry of phenyl and related ligands as potential bridges between polynuclear metal atoms is still to be developed. Gladysz and co-workers[124,125] and others[126] have shown that when metal centres are linked via π-conjugated acetylide groups a high degree of electronic communication can be achieved. Multiple bonding between metal atoms and main group elements such as carbon and nitrogen is highly delocalised in nature, which allows for strong conjugation between metal and heteroatoms.

This chapter will focus on the coordination of phenol and mono-substituted phenol with both electron donating and withdrawing groups, with the trinuclear osmium clusters $[Os_3(CO)_{12}]$, $[Os_3(MeCN)_2(CO)_{10}]$ and $[Os_3(\mu\text{-}H)_2(CO)_{12}]$. We will look at the effect of phenols with both donating and withdrawing substituents on coordination to osmium clusters. There is considerable interest in the interaction of arenes with metal clusters as they can form numerous bonding modes with polynuclear metal clusters. We hope to coordinate a cluster at both substituents of a di-substituted arene in order to determine the degree of electronic communication between the metal centres linked *via* π-conjugated arene. Such complexes are very rare; to date only a few examples of this type of ligation have been reported.[127] Herein, we report the results of our findings and attempt to explain the nature of the metal-arene-metal interaction.

4.2 Results and Discussion

4.2.1 Phenol derivatives

The reaction of $[Os_3(CO)_{12}]$ **1.1** with phenol in refluxing xylene (143 °C), gave a mixture of products in low yields, which were separated by TLC. Five bands were obtained, of which two have been identified as $[Os_3(\mu\text{-}H)(OPh)(CO)_{10}]$ **4.1** (15%) and the starting material $[Os_3(CO)_{12}]$ **1.1**. The complex **4.1** was previously reported by Deeming *et al.*[128] Other products were present only in trace amounts and could not be characterized. The corresponding dihydride $[Os_3(\mu\text{-}H)_2(OC_6H_4)(CO)_9]$ **4.2** was not observed under the conditions we used.

However, when cluster $[Os_3(\mu\text{-}H)(OPh)(CO)_{10}]$ **4.1** was refluxed in xylene under nitrogen for 7 hours, the dihydride complex $[Os_3(\mu\text{-}H)_2(OC_6H_4)(CO)_9]$ **4.2** (5%) was obtained in a low yield. The yellow complex $[Os_3(\mu\text{-}H)_2(OC_6H_4)(CO)_9]$ **4.2** had been reported by previous workers using a different method.[42] It has been shown that carbon bridges the two metal atoms of the cluster, and not oxygen, as was initially thought by Deeming and co-workers.

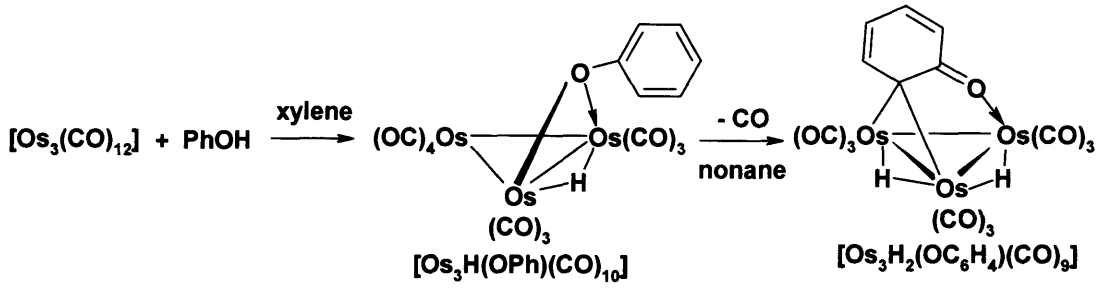

4.1 **4.2**

We studied the reactions of **4.2** with acid, to establish the nucleophilic sites within the cluster. The complex **4.2**, when dissolved in dichloromethane or $CDCl_3$, can be protonated easily by adding a couple of drops of trifluoroacetic acid (CF_3CO_2H). We have shown that protonation takes place at the oxygen rather than at the metal, by both infrared and ^1H NMR spectroscopy. We postulated that if protonation occurred at the oxygen or at a carbon atom of the C_6H_4O ligand, there would be an increase in IR ν(CO) frequencies by about 5-13 cm^{-1}, a much smaller shift than if protonation had

taken place at the metal (typically an increase of 20-30 cm^{-1}). We observed changes in the frequencies of the main absorptions in the spectrum from 2112(w), 2083(s), 2054(vs), 2033(m), 1996(m) cm^{-1} to 2121(w), 2093(s), 2065(s), 2043(m), 2009(m) cm^{-1}, an increase of 8-13 cm^{-1}, consistent with protonation at the ligand. The ^1H NMR spectrum shifts also increased by about δ 0.4 from those of the starting material but there were no other changes in the four signals for the ligand. This was consistent with protonation at the oxygen, with deshielding on protonation. It appear that the protonation at the oxygen is rapid and reversible, since removing the solvent and re-recording the IR spectrum in the absence of CF_3CO_2H showed the formation of the starting material. In the presence of CF_3CO_2H, however, protonation is complete since there are no absorptions for **4.2**. We could not detect any ^1H NMR spectrum signal for the C=OH group which may have indicated rapid exchange of the H atom on C=OH with those of the CF_3CO_2H.

In order to determine if an initial fast protonation at the oxygen would lead subsequently to slow conversion to an isomeric form which would be protonated at osmium, a solution of $[Os_3(\mu\text{-}H)_2(OC_6H_4)(CO)_9]$ in *d*-chloroform containing a few drops of trifluoroacetic acid was left standing in a sealed NMR tube. After 2 weeks the NMR spectrum showed no change, thus indicating no transformation had occurred. However, it is possible that the process is very slow and requires more time (**Scheme 4.1**). This result is surprising because the protonation of Os_3 clusters normally leads to protonation at the metal atoms. Since we had established that protonation occurs at the ketonic CO group, we wished to explore the possibility of the addition of other electrophiles at the oxygen atom. Another less likely possibility is protonation at the carbon ring. However, the ^1H NMR spectrum would then be more complex, and this was not observed.

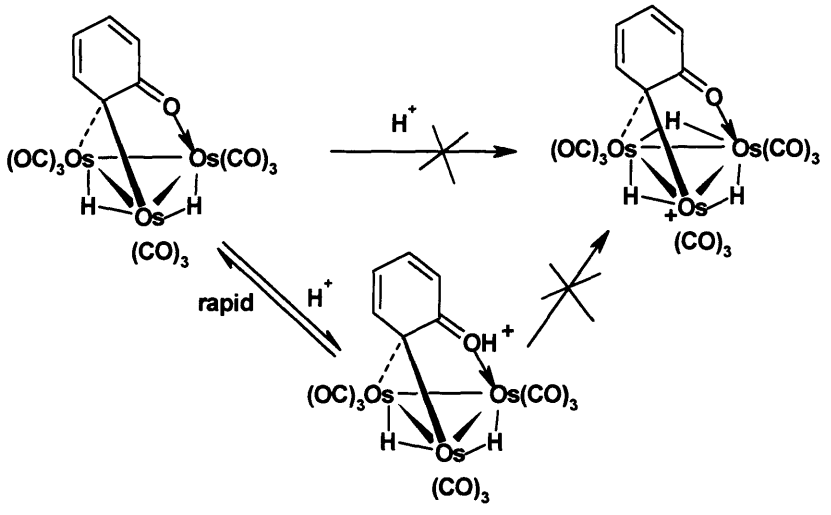

Scheme 4.1. Showing the protonation of phenol.

The reaction of $(CH_3)_3SiCl$ with $[Os_3(\mu\text{-}H)_2(OC_6H_4)(CO)_9]$ did not take place in CH_2Cl_2 at room temperature. Such lack of reactivity is surprising because of the high stability of Si-O bonds. This lack of reactivity could be due to steric reasons, as the small oxygen atom bonded to Os cannot donate two electrons to the silicon atom as the $SiMe_3$ is too large and bulky. However this is unlikely in view of the widespread use of $(CH_3)_3Si$ as a protecting group at the oxygen sites in organic chemistry. This result is unfortunate as this reaction was expected to form a stable product, and open up a gateway to some new and interesting chemistry involving the modification of phenol rings.

We have seen that phenol forms a non-aromatic dienone structure **4.2** in preference to the aromatic form. We will now look at the reactions of phenol with electron-withdrawing (fluorophenol) and donating (methoxyphenol) substituents and look at the effect, if any, they have on reactions with triosmium clusters and whether an aromatic form might be favoured.

4.2.2 Fluorophenol derivatives

The reaction of 4-fluorophenol with cluster **1.1** in refluxing xylene gave complexes analogous to the corresponding phenol derivatives as expected. Once again, the products $[Os_3(\mu\text{-}H)(OC_6H_4F)(CO)_{10}]$ **4.3** (22%) and $[Os_3(\mu\text{-}H)_2(OC_6H_3F)(CO)_9]$ **4.4** (<5%) were obtained in low yields. Also, additional TLC bands were obtained in trace amounts, which could not be characterized. In an attempt to see if we could isolate the trace products in large enough yields, we carried out the reaction between fluorophenol and $[Os_3(MeCN)_2(CO)_{10}]$ **1.2** under milder conditions, for example, in refluxing dichloromethane for 1 hour. No reaction was observed. However, carrying out the reaction in refluxing cyclohexane for 3 hours, gave three products. One was the expected decacarbonyl derivative **4.3**, displaying a sharp hydride peak at δ -12.2. Electron Ionisation mass spectroscopy (EI) indicated a mass of *m/z* = 968 (cal. 968), and the sequential loss of ten carbonyl ligands was observed. Deeming *et al.* previously reported complexes **4.3** and **4.4**.[128]

The ^1H NMR spectra of both other bands **4a** and **4b** showed no protons in the arene region, however, both bands gave a singlet hydride signal. Band **4a** showed a peak at δ -14.4, while band **4b** gave a peak at δ -27.6. The infrared spectrum of band **4a** showed absorption at 2115(w), 2076(s), 2068(m), 2034(w), 2027(vs), 2014(m), 2002(br), 1992(w, br) and 1989(w, br), cm^{-1}. Band **4b** also showed a similar pattern. This type of pattern is not characteristic of any phenol derivative. This puzzled us a little, until we examined the EIMS results. The spectrum of band **4a** indicated a mass of *m/z* = 892 with the sequential loss of ten carbonyls, while band **4b** gave a mass of *m/z* = 912 with the loss of 12 carbonyl ligands. We characterized compound **4a** as $[Os_3(\mu\text{-}H)(\mu\text{-}Cl)(CO)_{10}]$ **4.5**, and the parent ion showed the expected isotopic distribution for this species. The chlorine must have been derived from the dichloromethane solution. Johnson *et al.* have previously reported this type of complex.[129]

We believe the yellow compound **4b**, to be a mixture of the starting material **1.1** and an unknown hydrido cluster which remains uncharacterised. TLC could have separated the mixture further, however this was not investigated due to the very low yield of the product.

The product $[Os_3(\mu\text{-}H)_2(OC_6H_3F)(CO)_9]$ **4.4** was easily protonated by dissolving it in dichloromethane and by adding a few drops of trifluoroacetic acid. As in the phenol case, the n(C-O) stretching frequency increased by 8-10 cm^{-1} from that of the starting material **4.4**, thus indicating protonation at the oxygen atom rather than at the metal.

4.2.3 Methoxyphenol derivatives

A solution of 4-methoxyphenol and **1.1** in refluxing xylene gave, after TLC, the expected derivatives $[Os_3(\mu\text{-}H)(OC_6H_4OMe)(CO)_{10}]$ **4.6** (50%) and $[Os_3(\mu\text{-}H)_2(OC_6H_3OMe)(CO)_9]$ **4.7** (27%) in rather better yields. The infrared spectras of **4.6** and **4.7** are very similar to those of the corresponding fluorophenol derivatives, with absorption bands occurring at slightly lower frequencies for **4.6**: 2112(w), 2070(s), 2062(m), 2035(w), 2023(vs), 2004(m), 1989w(br) and 1985w(br), cm^{-1} (**Table 4.1, Appendix**). This is because an OMe can donate electron density to the cluster via π-interactions, which strengthens the M-C bonds and weakens the C-O bonds for the carbonyl ligands, whereas the fluorine withdraws electron density away from the ligands. The ^1H NMR spectra of **4.6** gave signals at δ -12.23 (s, OsH), δ 3.6 (s, MeO), and the arene protons gave signals at δ 6.64 (dd, 2H) and 6.62 (dd, 2H), a characteristic AA'BB' pattern. The EIMS spectrum gave *m/z* = 981 (calc: 981). The complex **4.7** gave signals in the appropriate region of the spectrum, but the two hydride signals at δ -11.6 and -13.8 were slightly broad.

By repeating the reaction several times, we managed to synthesize cluster **4.7** in larger quantities (160 mg). This was done to carry out a detailed study of the cluster by variable-temperature NMR. We wished to study: (a) the mobility of the hydride, (b) the carbonyl exchange process and (c) whether or not the arene ligand rotates with respect to the Os_3 triangle. We suspect that process (c) would be difficult to establish

without the detection of ^{187}Os splitting of the ^{13}C signals of the ligand. Such coupling had not been previously detected.

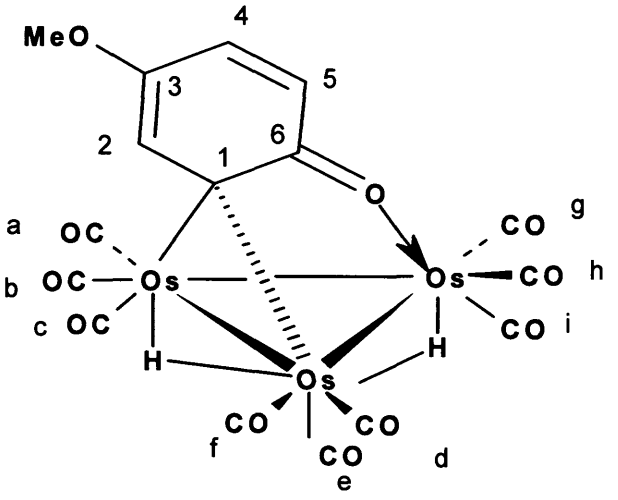

Structure of $[Os_3(\mu\text{-}H)_2(OC_6H_3OMe)(CO)_9]$ 4.7.

4.2.3.1 X-ray crystal structure of $[Os_3(\mu\text{-}H)_2(OC_6H_3OMe)(CO)_9]$ 4.7

The solid-state structure of $[Os_3(\mu\text{-}H)_2(OC_6H_3OMe)(CO)_9]$ **4.7** is shown in **Figure 4.3** with selected bond lengths given in **Table 4.3**. Crystallographic data are shown in **Table 4.4a**. The bond lengths and angles are given in **Table 4.4b (Appendix)**. The structure consists of an Os_3 triangle with three distinctly different metal-metal bonds: Os(1)-Os(3) = 2.7831(3) Å, Os(1)-Os(2) = 2.8116(3) Å and Os(2)-Os(3) = 2.9549(3) Å respectively. The shortest metal-metal bond is for that without a hydride bridge and the two long metal-metal bonds are for those associated with the bridging hydride ligands. Os(1)-Os(2) is not so long as Os(1)-Os(3) because the bridging alkylidene carbon C(6) restricts its ability to lengthen even though it is bridged by a hydride. The two bridging hydride ligands have been derived from O-H and C-H bond cleavage with metallation. There are nine terminal carbonyl ligands distributed evenly between three osmium atoms. The organic ligand is coordinated to the cluster through the oxygen lone pair and the doubly-bridging alkylidene group C(6). The methoxyphenol C-C single and C=C double bond lengths for C(1)-C(2) and C(2)-C(3) are 1.410(7) and 1.372(7) Å, indicating the structure to be non-aromatic with alternating single and double bonds, as found in $[Os_3(\mu\text{-}H)_2(OC_6H_3CH_2Ph)(CO)_9]$ and $[Os_3(\mu\text{-}H)_2(C_6H_4O)(CO)_9]$.[133, 131] The C(1)-O(1) bond length of 1.310(7) Å, is totally consistent with a ketonic group so that the ligand could be considered a dimetallated cyclohexadienone ring.

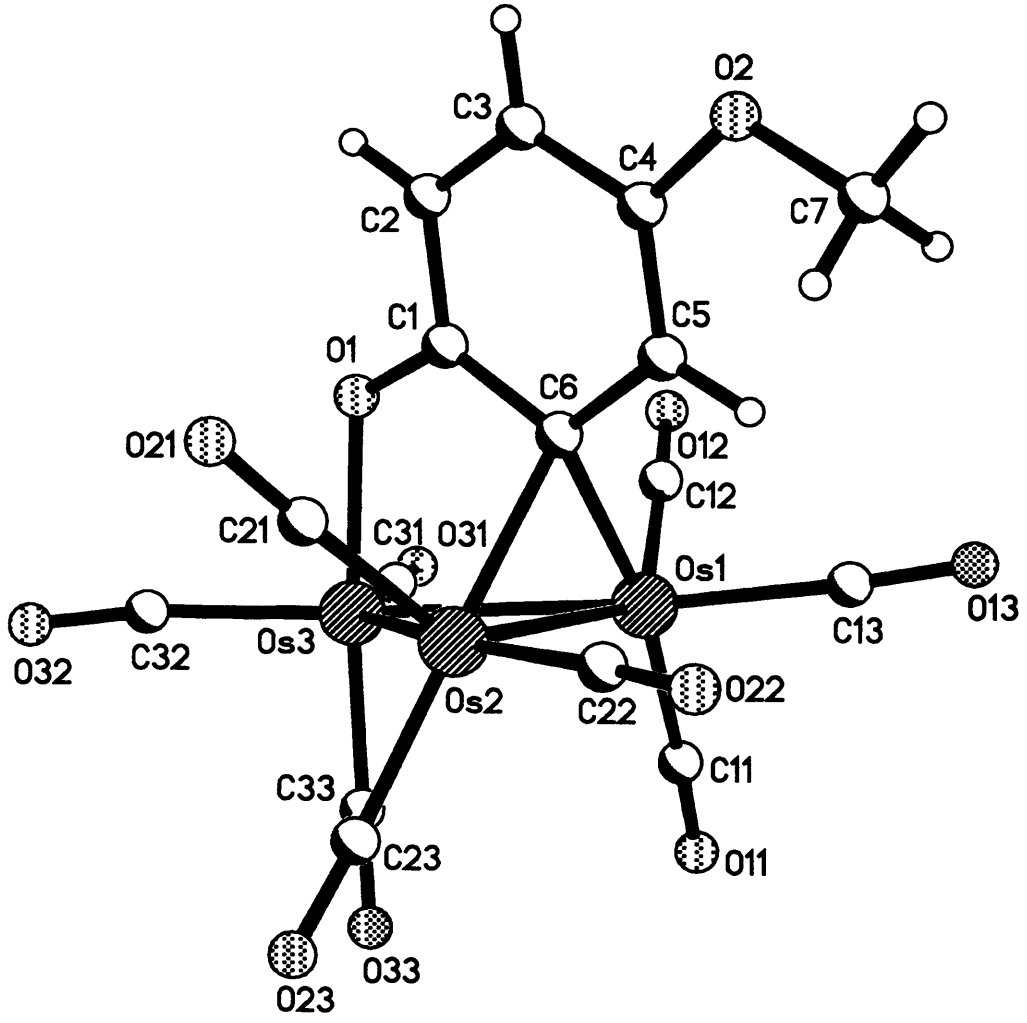

Figure 4.1. The solid-state structure of $[Os_3(\mu\text{-}H)_2(OC_6H_3OMe)(CO)_9]$ 4.7.

Table 4.3. Selected bond lengths [Å] for $[Os_3(\mu\text{-}H)_2(OC_6H_3OMe)(CO)_9]$ 4.7.

Os (1) – Os (3)	2.7831(3)	C (3) – C (4)	1.402(8)
Os (1) – Os (2)	2.8116(3)	C (4) – C (5)	1.364(7)
Os (2) – Os (3)	2.9549(3)	C (5) – C (6)	1.457(7)
C (1) – C (2)	1.410(7)	C (1) – C (6)	1.446(7)
C (2) – C (3)	1.372(7)	C (1) – O (1)	1.310(7)

4.2.3.2 ^{13}C NMR of $[Os_3(\mu\text{-}H)_2(OC_6H_3OMe)(CO)_9]$ 4.7

The ^{13}C NMR spectrum at room temperature showed the presence of five different carbonyl ligand sites in the region δ 160–85 **(Figure 4.1)**. This implied the hydride is rapidly mobile to give a time-averaged plane of symmetry, otherwise nine CO signals should have been observed. This was also supported by the broad hydride signals of complex **4.7** at room temperature. The five carbonyl signals cannot be assigned accurately. However, we can say that axial peaks normally come at a higher field than the equatorial ones. The peak at δ 211.3 is assigned to C^1, and the remaining five signals are due to the ring carbon atoms: δ 174.9 (C^6); 148.3 (C^4); 139.0, 131.9, and 123.8 due to C^2, C^3 and C^5 respectively. The peak at δ 54.2 is assigned to the methyl carbon (CH_3). We could not say that the assignments were definitely correct for each aromatic carbon, so we carried out a NOSY NMR experiment to correlate the results, which confirmed our assignment of the carbons to be correct, **Figure 4.3**.

We also carried out variable high-temperature ^{13}C NMR in order to determine if the carbonyls were migrating or if the ligand was rotating around the cluster; unfortunately we have found no evidence for this phenomena in this case. We were unable to record spectra at a temperature high enough to observe coalescence of CO signals.

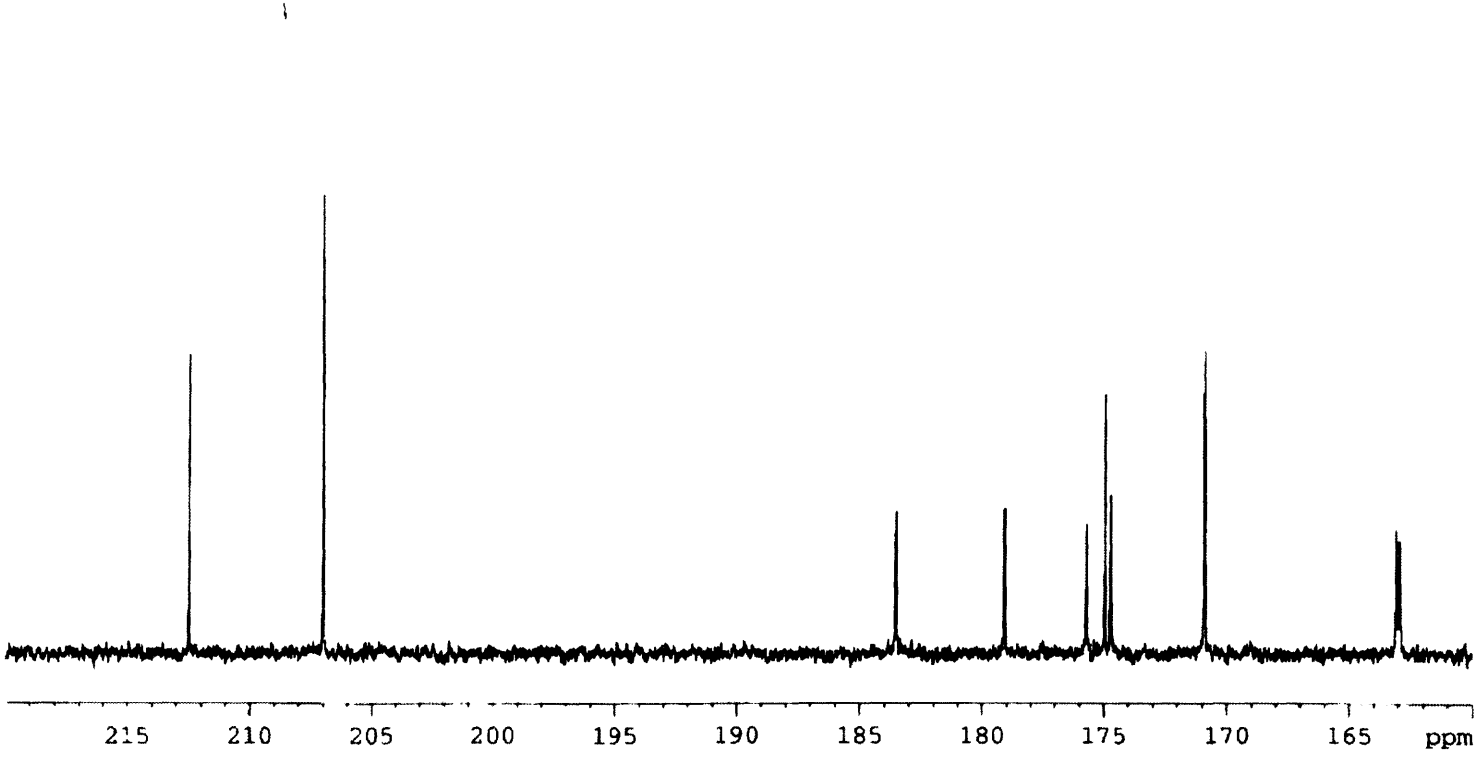

Figure 4.2. The ^{13}C NMR spectrum of cluster $[Os_3(\mu\text{-}H)_2(OC_6H_3OMe)(CO)_9)]$ 4.7, showing all the C-13 signals.

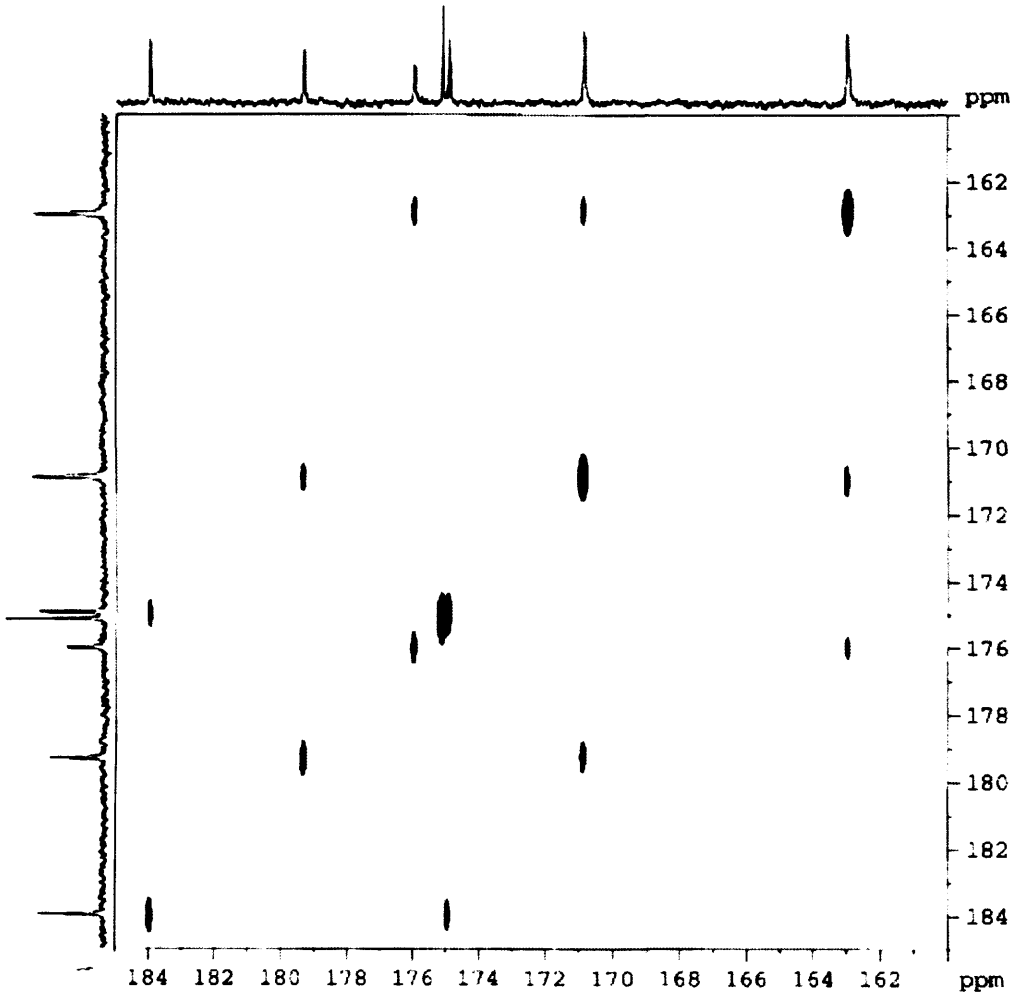

Figure 4.3. The NOSY ^{13}C NMR spectrum of cluster $[Os_3(\mu\text{-}H)_2(OC_6H_3OMe)(CO)_9]$ 4.7.

4.2.3.3 The V.T. ^{1}H NMR spectra of $[Os_3(\mu\text{-}H)_2(OC_6H_3OMe)(CO)_9]$ 4.7

Having carefully examined the room temperature ^{1}H NMR spectra of cluster $[Os_3(\mu\text{-}H)_2(\mu\text{-}OC_6H_3OMe)(CO)_9]$ **4.7**, it appeared that the hydride signals were slightly broad. The mobility of hydride ligands on osmium clusters has been reported as early as the 1960s. On cooling the solution to 213 K, we observed that the two hydride singlets at δ -11.60 and -13.80 were slightly sharper than the signals at 298 K. As the temperature was raised slowly from 213 K to 353 K, the two hydride signals broadened which implies that the two hydride ligands were exchanging slowly across the Os_3 cluster framework. Finally, at 373 K, the two hydride ligands were exchanging so fast that the two broad signals at 353 K coalesced to one broad signal at 373 K. The evidence can be explained by mechanism A together with mechanism B, but it is not possible to rule out C.

Mechanism A. No hydride exchange, but pair wise exchange of CO ligands. Axial CO^i does not exchange. This appears to be the fastest intramolecular process.

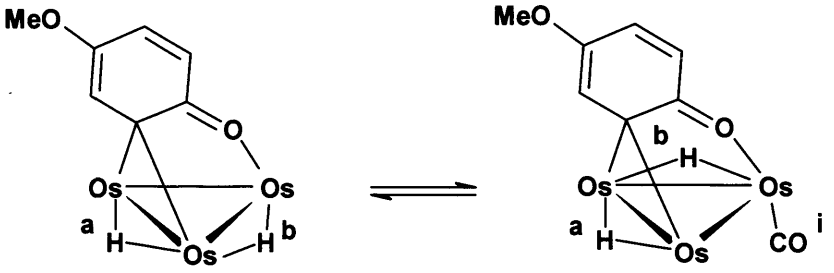

Mechanism B. H^a-H^b exchange plus pairwise CO exchange. This process will be slower than in **Mechanism A**.

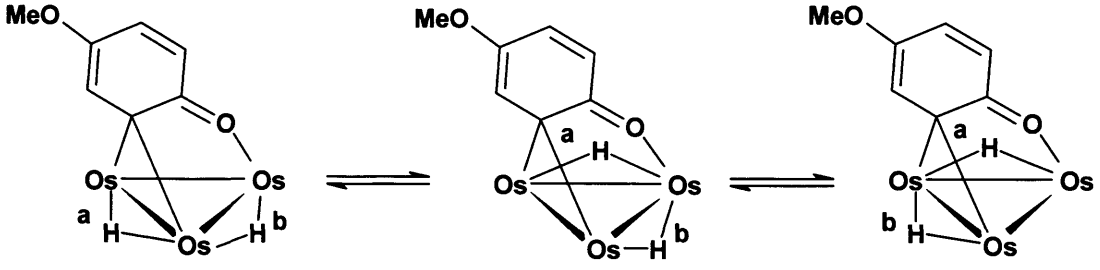

Mechanism C. Complete rotation of ligand. Exchange of H^a-H^b plus CO exchange to give axial-equatorial signals in the ratio of 1:2.

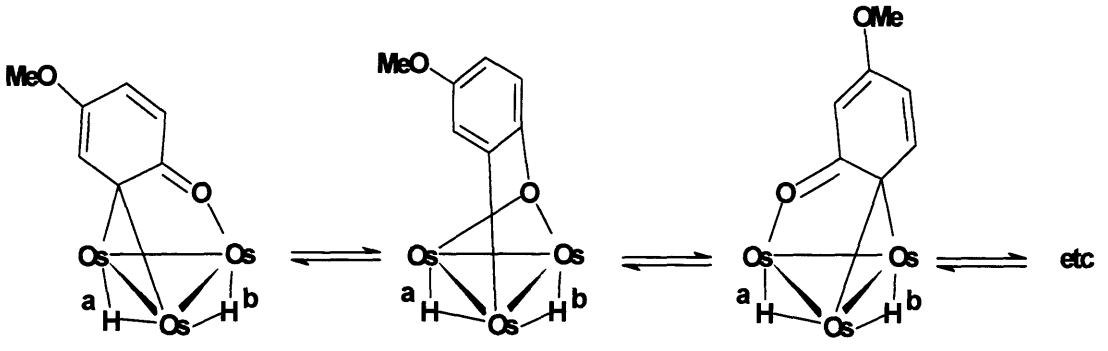

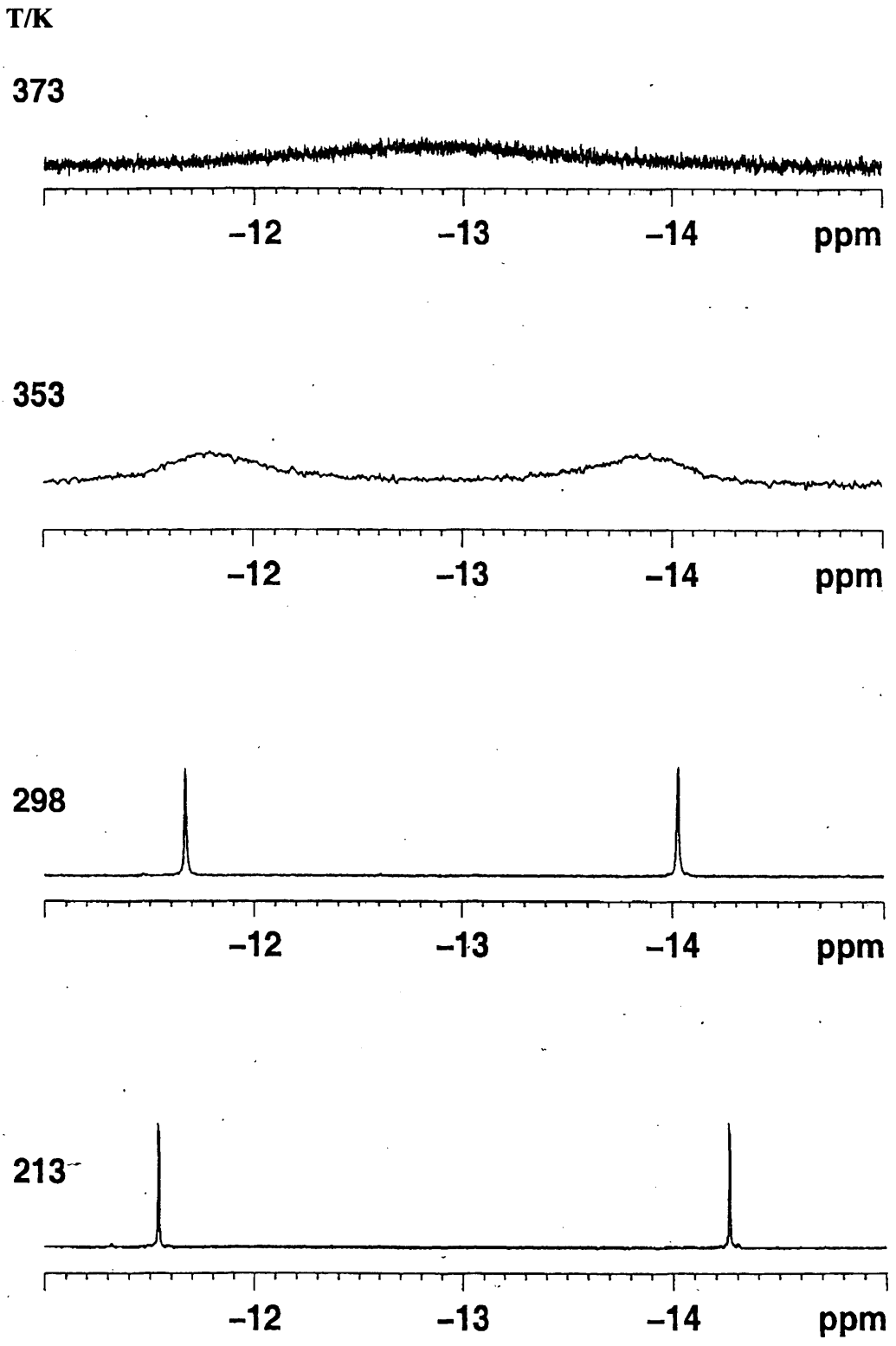

Figure 4.4. The variable temperature ^1H NMR of $[Os_3(\mu\text{-}H)_2(OC_6H_3OMe)(CO)_9]$ 4.7.

4.2.4 Hydroquinone (para-dihydroxybenzene) derivatives

Having shown the effects on the coordination of both electron-withdrawing and electron-donating phenols to triosmium clusters, we were interested in investigating whether the coordination of osmium clusters could occur at both ends of the functional groups linked by an arene. If the synthesis of the ligand-bridge dicluster system was successful, we could look at the degree of electronic communication, if any, between the linked clusters. In order to investigate this, we recognised that we would require functional groups that are good at forming bridges with metal atoms. For this we chose hydroquinone. We hoped to form the bis[$Os_3(CO)_9$] system rather than the bis[$Os_3(CO)_{10}$], as only in the bis[$Os_3(CO)_9$] system would the arene be bridged through carbon atoms by two Os_3 cluster units. There are four possible forms of the bis[$Os_3(CO)_9$] system, but we believe that only three are feasible as shown below. Form A and B are equivalent except that the roles of the two Os_3 clusters are reversed.

The fourth form (shown below) is very unlikely because one cannot place a C=C in the ring. It would seem that both clusters cannot have a bridging μ-C but both can have two μ-O or one μ-O and the other μ-C (as above). We set [{$Os_3(H)_2(CO)_9$}$_2$($C_6H_2O_2$)] as a target molecule.

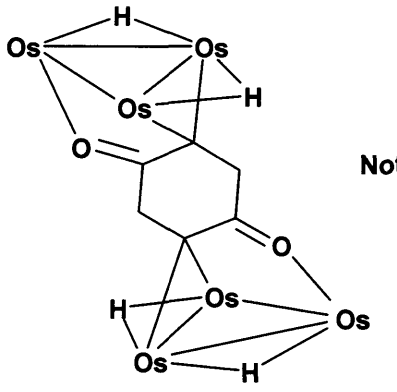

Not possible!

The direct reaction of $[Os_3(CO)_{12}]$ **1.1** with hydroquinone gave three products, which were $[Os_3(\mu\text{-}H)(OC_6H_4OH)(CO)_{10}]$ **4.8** (20%), along with $[Os_3(\mu\text{-}H)_2(OC_6H_3OH)(CO)_9]$ **4.9** (10%) and the arene bridged cluster $[Os_6(\mu\text{-}H)_3(C_6H_3O_2)(CO)_{19}]$ **4.10** (2%). All the complexes had been previously prepared from the reaction of $[Os_3(CO)_{12}]$ and hydroquinone using robust conditions.[131] Repeating the reaction between $[Os_3(CO)_{12}]$ and hydroquinone in refluxing xylene over a longer time period (48 hours) did not increase the yield of the products. Our primary objective was to make $[Os_6(\mu\text{-}H)_4(C_6H_2O_2)(CO)_{18}]$ but there was no evidence for this. Heating at the same temperature for a longer period of time resulted in cluster degradation. All the clusters have been characterized by infrared, ^1H NMR and mass spectroscopy. There was a perfect match between published and experimental data. It may be possible to form more di-cluster systems by reacting **4.8** or **4.9** with more Os_3 cluster units. There was no evidence for the loss of CO from **4.10** to form our target molecule.

The reaction between hydroquinone and the labile cluster $[Os_3(MeCN)_2(CO)_{10}]$ **1.2** in refluxing cyclohexane under nitrogen for 2 hours, gave the known clusters $[Os_3(\mu\text{-}H)(OC_6H_4OH)(CO)_{10}]$ **4.8** (2%) and $[Os_3(CO)_{12}]$ **1.1** in low yields.

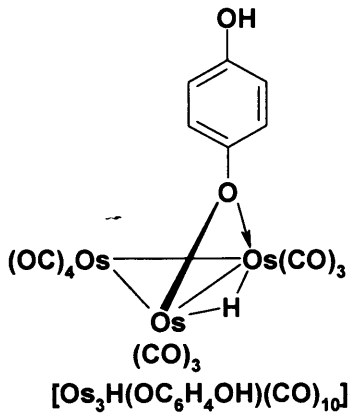

$[Os_3H(OC_6H_4OH)(CO)_{10}]$

4.8

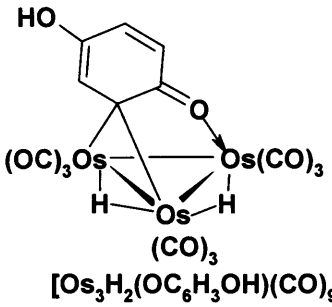

$[Os_3H_2(OC_6H_3OH)(CO)_9]$

4.9

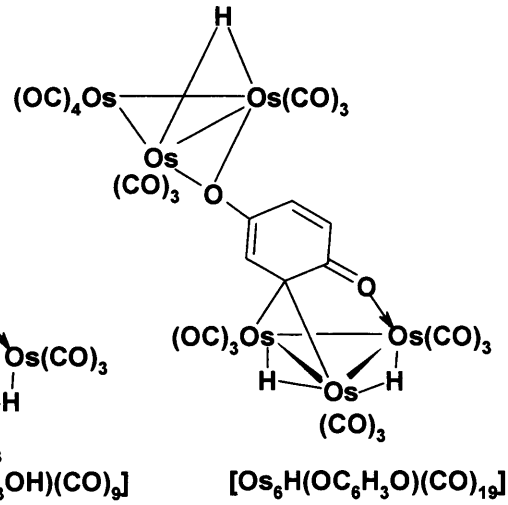

$[Os_6H(OC_6H_3O)(CO)_{19}]$

4.10

4.2.5 ortho-Dihydroxybenzene (catechol) derivatives

ortho-Dihydroxybenzene (catechol) could in theory form five-membered chelate rings incorporating both oxygen atoms. Catecholate chelates are well known with mononuclear complexes. However, the only product isolated from the reaction of catechol with the bis-acetonitrile complex **1.2** in cyclohexane, was $[Os_3(\mu\text{-}H)(OC_6H_4OH)(CO)_{10}]$ **4.11** (85 %). The compound has an IR spectrum similar to that of its analogues, $[Os_3(\mu\text{-}H)(CO)_{10}(OC_6H_4OH)]$ **4.8**, $[Os_3(\mu\text{-}H)(OC_{10}H_7)(CO)_{10}]$ **4.12**, $[Os_3(\mu\text{-}H)(OCH_2Ph)(CO)_{10}]$ **4.13** and $[Os_3(\mu\text{-}H)(OCHMePh)(CO)_{10}]$ **4.14**. The υ(CO) absorption data for $[Os_3(\mu\text{-}H)(OC_6H_4OH)(CO)_{10}]$ **4.11**: 2110(w), 2074(vs), 2059(m), 2025(vs), 2014(m), 2002(s), 1989(w,br) and a broad υ(OH) band at 3441 cm^{-1} are consistent with the formulae given for **4.11**. The υ(CO) absorption data are approximately 3-4 cm^{-1} lower than those for compounds **4.12**, **4.13** and **4.14**, indicating that the ligand is a somewhat better donor.

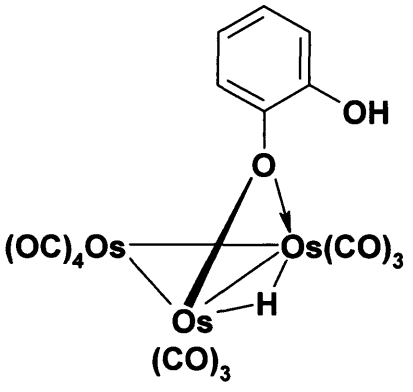

4.11

The ^1H NMR spectrum of **4.11** showed the presence of a single hydride ligand at δ -11.53, a free OH proton at δ 20.34 with the four ring protons giving two doublets of triplets at δ 6.70 and 6.62, and two doublets of doublets at δ 6.56 and 6.38 respectively. If however, both oxygen atoms were coordinated equivalently to metal, we would have observed an AA'BB' spectrum, which is clearly not the case. EIMS gave *m/z* = 966 (calc. 966), showed the successive loss of 10 carbonyl ligands leaving no doubt that the structure is as formulated.

Deeming had previously synthesised compound $[Os_3(\mu\text{-}H)_2(OC_6H_3OH\text{-}o)(CO)_9]$ from $[Os_3(CO)_{12}]$ **1.1** in refluxing xylene.[128] He postulated that this was formed *via* $[Os_3(\mu\text{-}$

H)(OC_6H_4OH)$(CO)_{10}$] **4.11**, with the second hydrogen being transferred from the *ortho*-carbon rather than the *ortho*-hydroxy group. We have now shown that this must be the case, from the synthesis of **4.11** under mild conditions. Interestingly, our attempts to cleave the second OH bond using more robust conditions, for example, by repeating the reaction in higher boiling solvents and also by carrying out the reaction in a Carius tube, were unsuccessful.

4.2.6 Benzoquinone derivatives

Benzoquinone ($C_6H_4O_2$) is formed by double oxidation of hydroquinone. Previously, Deeming *et al.* have shown that tropone (C_7H_6O) reacts with the labile and unsaturated clusters [Os_3(MeCN)$(CO)_{11}$] **1.2** and [$Os_3(\mu$-H$)_2(CO)_{10}$] **1.6** to give the decacarbonyl tropone derivative that loses a CO ligand on heating to give the nonacarbonyl derivative (**Scheme 4.2**).

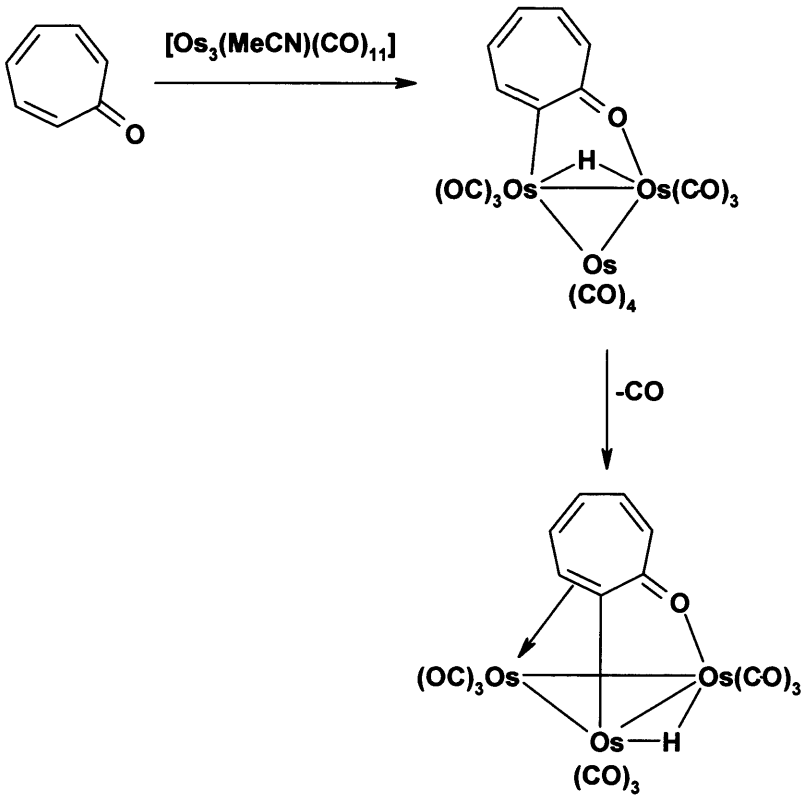

Scheme 4.2. Shows the formation of tropone derivatives

Unlike tropone, benzoquinone has two ketonic groups at the 1 and 4 positions, which could potentially bridge two triosmium clusters. Each could, in principle, coordinate to an Os_3 unit as does tropone. Benzoquinone could form the corresponding deca and nonacarbonyl derivatives, which could then possibly react further with more Os_3 clusters to give the hexanuclear osmium cluster, **Scheme 4.3**.

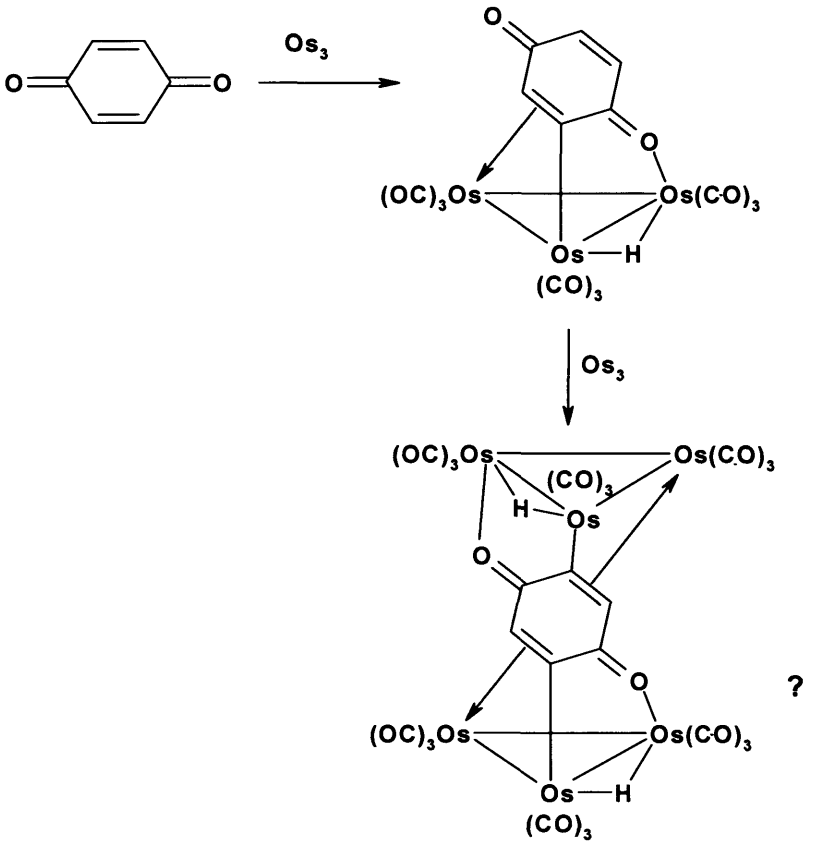

Scheme 4.3. Shows the possible formation of benzoquinone derivatives.

Unfortunately, no products were isolated from the reaction of $[Os_3(CO)_{12}]$ **1.1** with benzoquinone in xylene (143 °C) after 2 hours of reflux. We then carried out the reaction using milder conditions. For this we decided to use the unsaturated purple cluster $[Os_3(\mu\text{-}H)_2(CO)_{10}]$. The reaction of $[Os_3(\mu\text{-}H)_2(CO)_{10}]$ and benzoquinone in refluxing cyclohexane after 1 hour, 30 minutes gave a red solution. The main red product obtained was $[Os_3(\mu\text{-}H)(OC_6H_5O)(CO)_{10}]$ **4.15** (69%). The infrared spectrum of this cluster was unlike other decacarbonyl derivatives of fluorophenol, methoxyphenol and hydroquinone, *etc.* However, the υ(CO) spectrum was very similar to that of compound $[Os_3(\mu\text{-}H)(OC_6H_7)(CO)_{10}]$ **4.16**.[130] The ^1H NMR

spectrum showed only one hydride singlet at δ -12.6 and it also showed a complex spectrum in the range of δ 2.4-3.1, **Figure 4.5**. This complex set of multiplets is attributed to four non-equivalent coupled protons (**1-4**). Each of the signals at δ 2.47, 2.59, 2.82, and 2.97 can be analysed as a double, double doublet. The signal for H^5 appeared at δ 7.59 as a singlet. The EIMS spectrum gave the parent ion at *m/z* = 965 (calc: 965), and the successive loss of ten carbonyl ligands were also apparent. Further refluxing did not cause the free oxygen to coordinate to the cluster. Repeating the reaction with 2 moles of the cluster to 1 mole of the ligand was also unsuccessful.

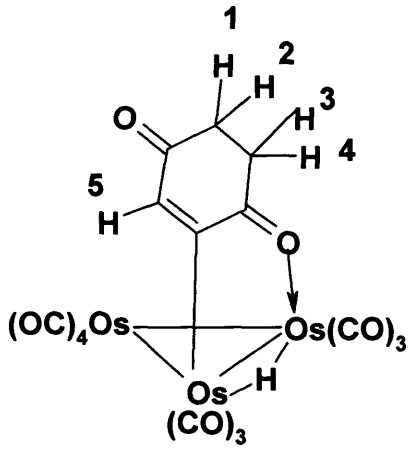

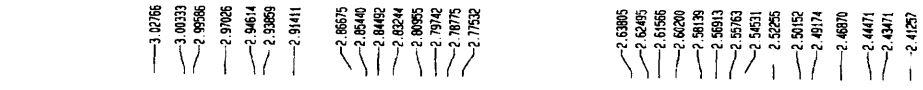

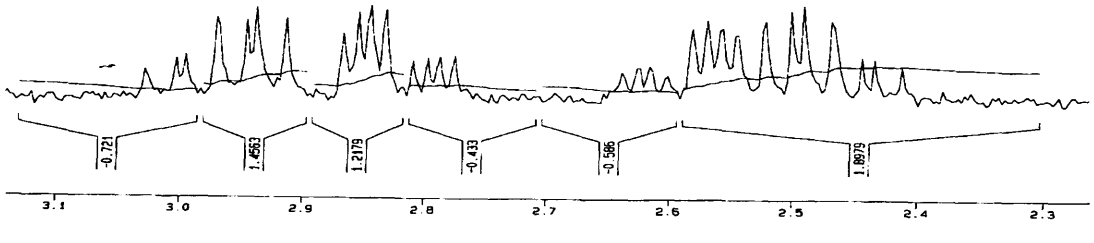

Figure 4.5. The ^{1}H NMR data for protons 1 to 4 of cluster $[Os_3(\mu\text{-}H)(OC_6H_5O)(CO)_{10}]$ 4.15.

The possible mechanism for the formation of $[Os_3(\mu\text{-}H)(OC_6H_5O)(CO)_{10}]$ **4.15**.

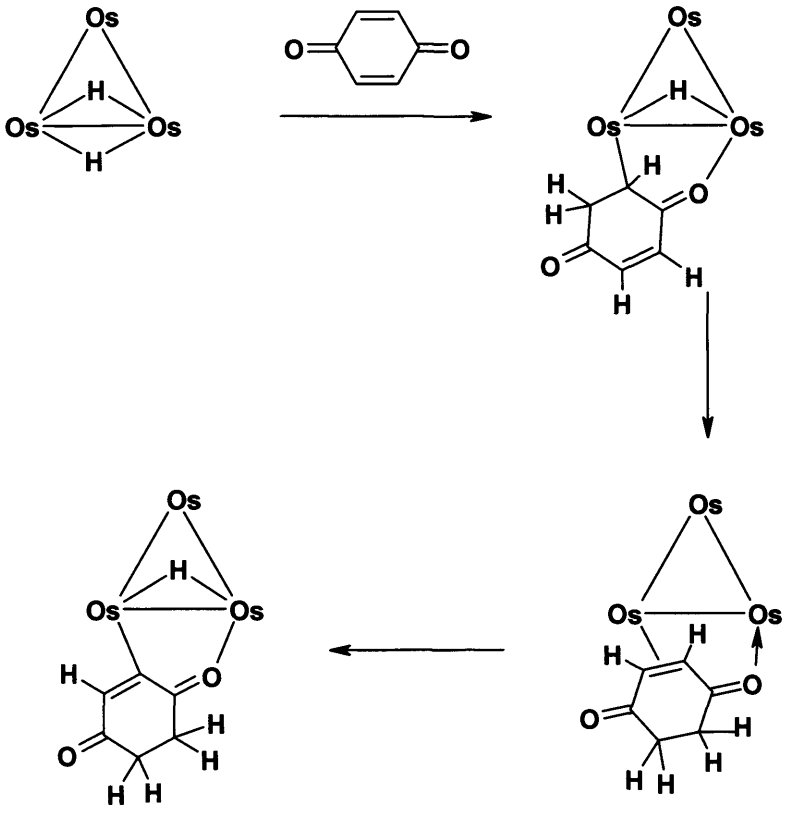

The reaction must proceed by the successive transfer of two Os hydrides to one C=C double bond, followed by oxidative addition with C-H cleavage at the other C=C bond. It is difficult to appreciate why the final stage is not mirrored in the reaction of benzoquinone with $[Os_3(MeCN)_2(CO)_{10}]$.

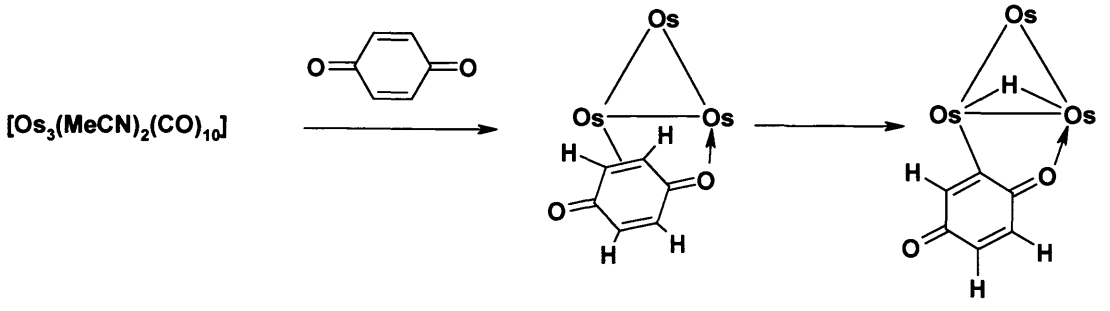

4.2.7 4-Aminophenol derivatives

The reaction between $[Os_3(CO)_{12}]$ **1.1** and 4-aminophenol ($H_2NC_6H_4OH$) can form a number of products. There is the possibility of forming linked clusters by coordinating through both ends of the molecule. The amino and hydroxy groups in aniline and phenol could oxidatively add to different triosmium clusters, to subsequently give the corresponding deca- and nona-carbonyl clusters. Interestingly, aminophenol could just react at one end of the ligand in which case we wished to know whether the primary reaction was at OH or NH_2.

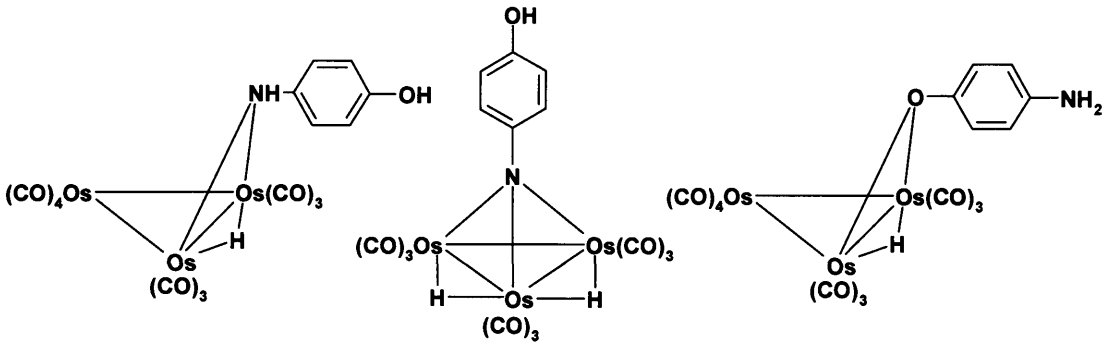

4.17 **4.18** **4.19**

The triosmium cluster $[Os_3(CO)_{12}]$ **1.1** reacted with 4-aminophenol in a Carius tube at 180° C, to give an inseparable mixture of compounds $[Os_3(\mu\text{-}H)(HNC_6H_4OH)(CO)_{10}]$ **4.17** and $[Os_3(\mu\text{-}H)_2(NC_6H_4OH)(CO)_9]$ **4.18** in the ratio of 6:1, and also pure $[Os_3(\mu\text{-}H)(OC_6H_4NH_2)(CO)_{10}]$ **4.19** (5%). The υ(CO) absorptions for compounds **4.17** and **4.18** are *ca.* 2-3 cm^{-1} lower than for compounds $[Os_3(\mu\text{-}H)(C_6H_5NH)(CO)_{10}]$ **4.20** and $[Os_3(\mu\text{-}H)_2(NPh)(CO)_9]$ **4.21**, derived from aniline.[131,132] The ^1H NMR showed two hydride signals consisting of a doublet and a singlet at δ -14.15 and -18.35 for **4.17** and **4.18** respectively. The doublet at δ -14.15 is due to the hydride being coupled to the NH proton in cluster **4.17** and the singlet is due to the equivalent hydrides in **4.18**. The hydride signals match very closely two those of **4.20** and **4.21**. The AA'BB' multiplet for the C_6H_4 proton of cluster **4.17** appears at δ 6.63 and 6.70 (J = 3.1 Hz), and the AA'BB'multiplet pattern of cluster **4.18** appears at δ 6.58 and 7.02. The NH

group gives a broad singlet at δ 5.78, and the OH signal comes at δ 4.67. Attempts to separate the mixture were unsuccessful. Unlike compound **4.17** and **4.18**, structure **4.19** has the ligand coordinated through the oxygen atom, only to give the analogue of **4.17**, $[Os_3(\mu\text{-}H)(OC_6H_4NH_2)(CO)_{10}]$ **4.19**. The υ(CO) absorption for **4.19** is on average 3-4 cm^{-1} lower than for $[Os_3(\mu\text{-}H)(OPh)(CO)_{10}]$ **4.1**, derived from phenol.[130,133]

The mass spectroscopic data (EIMS) for **4.17** and **4.18** gave *m/z* = 965 (calc. 965) for $[Os_3(\mu\text{-}H)(HNC_6H_4OH)(CO)_{10}]$ and *m/z* = 937 (calc.937) for $[Os_3(\mu H)_2(CO)_9(NC_6H_4OH)]$, with the successive loss of their respective carbonyl ligands. For cluster $[Os_3(\mu\text{-}H)(OC_6H_4NH_2)(CO)_{10}]$ **4.19**, *m/z* = 965 (calc.965).

These results indicate that there is a competitive reaction of the OH and the NH_2 groups at the triosmium clusters but with greater preference for reaction at the NH_2.

4.2.8 para-phenylenediamine derivatives

The reaction between aminophenol and $[Os_3(CO)_{12}]$ **1.1** did not form the desired linked cluster and showed that reactions are more favourable at the amine end of the substituted arene. Therefore we carried out a reaction between *para*-phenylenediamine ($4\text{-}H_2NC_6H_4NH_2$) and $[Os_3(CO)_{12}]$ **1.1** to see whether disubstituted amine makes any difference to the product formation. The cluster **1.1** reacted with *para*-phenylenediamine in a Carius tube at 180° C to give the cluster $[Os_3(\mu\text{-}H)(NC_6H_4NH_2)(CO)_{10}]$ **4.22** (10%). Prolonged heating of **4.22** with more **1.1** did not form the linked cluster but gave the product $[Os_3(\mu\text{-}H)_2(NC_6H_4NH_2)(CO)_9]$ **4.23** (< 3%). The ^1H NMR spectrum of **4.22** showed a doublet at δ -14.15 for the hydride being coupled to the NH ligand. NH and NH_2 showed two broad singlets at δ 5.83 and 3.56 respectively in the ratio of 2:1. The AA'BB' pattern for the C_6H_4 ligand was observed as two double doublets at δ 6.61 and 6.49 respectively. The ^1H NMR spectrum of **4.23** was almost identical to that of **4.22**, except for the two identical hydride (OsH) ligands, which gave a singlet at δ -18.36.

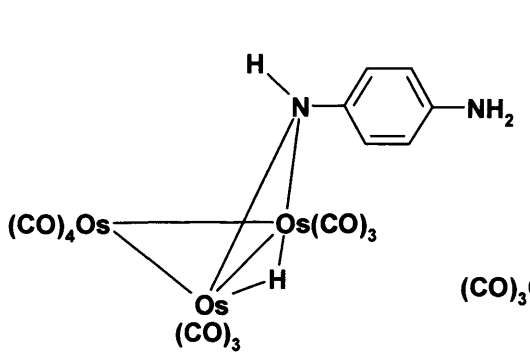

4.22

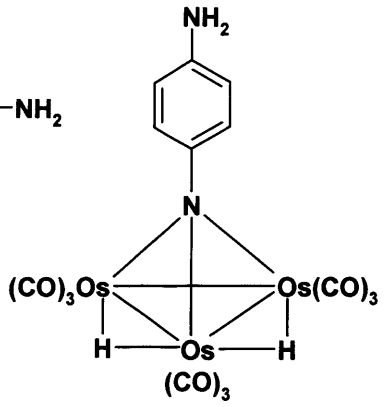

4.23

The reaction of $[Os_3(CO)_{12}]$ **1.1** with 4-aminophenol was more selective towards the amine group, as shown by the product formation of **4.19**. Coordination of the cluster did not take place at both ends of the ligand as in the hydroquinone case; it always occurred at only one of the two ends, with preference for the amine. Why the coordination only occurred at one end is not fully understood. Why coordination was preferred at the amine end could simply be that amine is more basic than OH, thus a reaction was more favourable at the amine end. On the other hand, it is also possible that when a reaction had occurred at one end of the ligand there was deactivation at the opposite end, thus making it unreactive. Chatt and co-workers in 1964, noted a similar effect during their studies on the synthesis of rhenium(V) imido complexes, which utilised the addition of aniline to $[ReOCl_3(PEt_2Ph)_2]$ **4.24**. They found that while the addition of aniline itself afforded the phenylimido complex $[Re(NPh)Cl_3(PEt_2Ph)_2]$ **4.25**, the reaction with *para*-phenylenediamine only afforded the *para*-substituted imido complex $[Re(p\text{-}NC_6H_4NH_2)Cl_3(PEt_2Ph)_2]$ **4.26**.[134] More recently, Hogarth and co-workers have found that an attempt to link molybdenum(VI) units together *via* the reaction of $[MoOCl_2(S_2CNEt_2)_2]$ **4.27** with *para*-phenylene diamine, did not lead to products with molybdenum(VI) centres at both ends. Coordination of one molybdenum centre deactivated the second towards further metal coordination, resulting from delocalisation of the lone pair towards the electron-deficient molybdenum(IV) centre.[135] In contrast, attempts at adding one single tungsten centre to *para*-phenylene diisocyanate, results in the formation of a 50:50 mixture. The coordination of one tungsten(IV) group to the isocyanate activates the

second group towards oxidative addition and provides some evidence of communication through the π-conjugated backbone.[136]

4.2.8.1 Crystal structure of $[Os_3(\mu\text{-}H)(NHC_6H_4NH_2)(CO)_{10}]$ 4.22

The crystal structure of $[Os_3(\mu\text{-}H)(NHC_6H_4NH_2)(CO)_{10}]$ **4.22** is shown in **Figure 4.6**. Crystallographic data are given in **Table 4.5a** and bond lengths and angles are given in **Table 4.5b**. The crystal structure consists of an Os_3 unit, which is bridged by nitrogen N(1) at the osmium atoms Os(1) and Os(2). The three metal bond distances of Os(1)-Os(2), Os(2)-Os(3) and Os(1)-Os(3) are 2.7834(6), 2.8452(6) and 2.8486(7) Å respectively. The Os-N bond distances are 2.1457(7) and 2.134(7) Å. There are ten terminal carbonyl ligands, which are distributed in units of 4, 3, and 3.

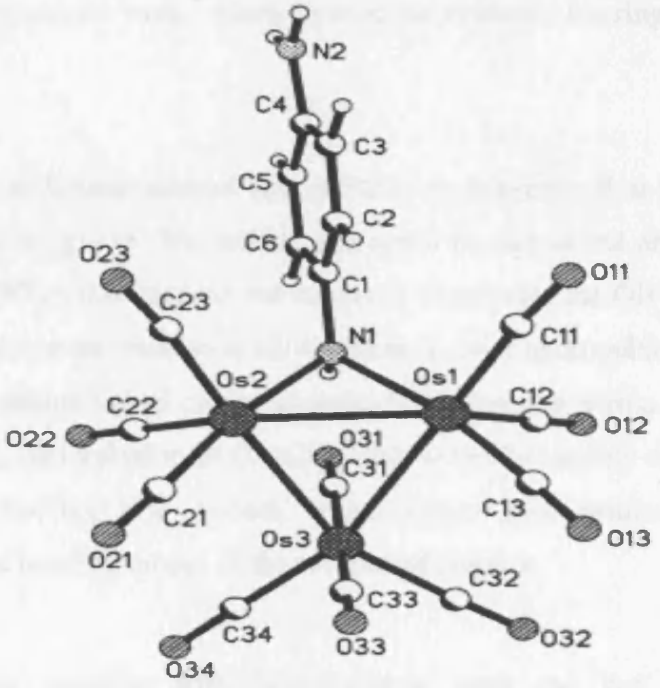

Figure 4.6. The molecular structure of $[Os_3(\mu\text{-}H)(NHC_6H_4NH_2)(CO)_{10}]$ 4.22.

4.3 Conclusions

In all of the reactions that we have performed with substituted phenols, the hydrogen of the heteroatom (oxygen or nitrogen) was metallated initially as had been found in other systems. Thus, there is initially oxidative addition of the ROH or RNH_2 groups with cleavage of the OH or NH bonds. The decacarbonyl cluster formed in this way undergoes further oxidative addition with C-H cleavage, to give a μ_3-ligand bond through both the oxygen and carbon atoms.

We have shown for the first time, with a series of substituted and di-substituted phenols, that phenols with electron-accepting or electron-donating substituents always form the dienone structure in preference to the aromatic form. With methoxyphenol the product has the dienone structure, with the hydride being mobile at room temperature leading to five ^{13}C signals in the aromatic region. We have also determined the crystal structure of $[Os_3(\mu\text{-}H)_2(CO)_9(OC_6H_3OMe)]$ and carried out detailed low-temperature work, which showed no evidence for ring rotation around the cluster.

We have found with aminophenol that substitution is preferred at the amine rather than at the hydroxy group. We believe this could be due to the amine being more basic than OH. When this happens we believe it deactivates the OH end leading to a very slow reaction or no reaction at all. Conversely, with hydroquinone, we managed to synthesise a unique linked cluster containing six osmium atoms. This compound has an $Os_3(CO)_{10}$ unit linked to an $Os_3(CO)_9$ unit, but unfortunately we were unable to synthesise the bis$[Os_3(CO)_9]$ system, which would have resulted in interesting differences in the bonding modes of the two linked clusters.

Interestingly, the reaction with benzoquinone gave the red cluster $[Os_3(\mu\text{-}H)(CO)_{10}(OC_6H_5O)]$ **4.11**, which is unlike other decacarbonyl phenol derivatives. The dihydride derivatives of phenol and substituted phenol can be protonated easily by trifluoroacetic acid. There is a rapid equilibrium between the protonated and deprotonated forms.

4.4 General synthetic details

All the reactions were carried out under an atmosphere of nitrogen unless otherwise stated. The subsequent purification of the products was carried out by thin layer chromatography (TLC) on silica-coated plates using standard laboratory grade solvents, without precaution taken to exclude air. The infrared spectra were recorded on a Shimadzu 8700 Fourier transform instrument. All the ^1H NMR spectra were recorded on either Bruker 300, 400 or 500 MHz instruments. The UCL service department carried out all the mass spectroscopy and elemental analyses. The trimethylamine *N*–oxide hydrate ($Me_3NO.2H_2O$) was dried before use to exclude water and the acetonitrile (MeCN) was distilled before use. The other reagents hydroquinone, methoxyphenol, fluorophenol, aminophenol and benzoquinone were purchased from Aldrich and used as supplied. The complex $[Os_3(MeCN)_2(CO)_{10}]$ **1.3** was synthesized using a method from literature.[18]

4.4.1 Synthesises of $[Os_3(MeCN)_2(CO)_{10}]$ 1.3

The yellow solid $[Os_3(CO)_{12}]$ **1.1** (0.4102 g, 0.4498 mmol) was ground into a fine powder and dichloromethane (400 cm^3) was added and then the solution was stirred until most of **1.1** had dissolved. Acetonitrile (10 cm^3) was added, and then the trimethylamine *N*-oxide hydrate was slowly added and the solution was stirred slowly until the loss of two CO ligands was observed by infrared spectroscopy. The solution was passed through a bed of silica and the solvent was removed under vacuum, to give **1.3** as a yellow crystalline solid (80 %).

4.4.2 Reaction of $[Os_3(CO)_{12}]$ with phenol in xylene

The yellow solid $[Os_3(CO)_{12}]$ **1.1** (0.5852 g, 0.6417 mmol) and an excess of phenol (1.4556 g, 15.4851 mmol) were added to xylene (65 cm^3) and the solution was refluxed for 10 hour. The solution changed colour from yellow to brown after 10 minutes. The solvent was removed *in vacuo* and the residue was chromatographed using petroleum spirit (b.p. 40-60 °C) – dichloromethane (4 : 1 v/v) as eluent. Five

significant products were observed of which two have been identified as $[Os_3(\mu\text{-}H)(OPh)(CO)_{10}]$ **4.1** (0.0892 g, 15%) and the starting material $[Os_3(CO)_{12}]$ **1.1**.

4.4.2.1 Protonation of $[Os_3(\mu\text{-}H)_2(OC_6H_4)(CO)_9]$

The yellow complex $[Os_3(\mu\text{-}H)_2(OC_6H_4)(CO)_9]$ (0.0030 g, 0.0033 mmol) was dissolved in dichloromethane (3 cm^3) and five drops of trifluoroacetic acid were added using a pipette. The solution was shaken and left standing for a few minutes. The infrared spectrum showed a complete change to give $[Os_3(\mu\text{-}H)_2(OC_6H_4)(CO)_9]$ **4.2** in a high yield (90 %).

4.4.3 Thermal treatment of $[Os_3(\mu\text{-}H)(OPh)(CO)_{10}]$ in refluxing xylene

The yellow complex $[Os_3(\mu\text{-}H)(OPh)(CO)_{10}]$ (0.040 g, 0.0421 mmol) was refluxed in xylene (20 cm^3) for 7 hour. The solvent was removed *in vacuo* and the solid was chromatographed using petroleum spirit (b.p. 40-60 °C) – dichloromethane (3 : 1 v/v) as eluent. One product was isolated, $[Os_3(\mu\text{-}H)_2(OC_6H_4)(CO)_9]$ **4.2** (< 5 %).

4.4.4 Reaction of $[Os_3(\mu\text{-}H)_2(OC_6H_4)(CO)_9]$ with $(CH_3)_3SiCl$

The cluster $[Os_3(\mu\text{-}H)_2(OC_6H_4)(CO)_9]$ (0.002 g, 0.0022 mmol) was dissolved in dichloromethane (2 cm^3) and 4 drops of $(CH_3)_3SiCl$ were added. The solution was shaken, and left standing for 5 minutes. The infrared spectrum showed no change. After several hours still no change was observed.

4.4.5 Reaction of $[Os_3(CO)_{12}]$ with fluorophenol

A solution of the yellow cluster $[Os_3(CO)_{12}]$ **1.1** (0.2360 g, 0.2587 mmol) and fluorophenol (0.0291 g, 0.2553 mmol) was refluxed in xylene (50 cm^3) for 14 hour. The solution changed colour from yellow to orange/yellow. The solvent was removed under vacuum and TLC was carried out using dichloromethane-petroleum spirit (40-60 °C) (1 : 4 v/v) as eluent. Seven significant bands were obtained, of which two have been identified as $[Os_3(\mu\text{-}H)(OC_6H_4F)(CO)_{10}]$ **4.3** (22%) and $[Os_3(\mu\text{-}H)_2(OC_6H_3F)(CO)_9]$ **4.4** (< 5 %). Complex **4.4** was only characterised by infrared spectroscopy.

4.4.6 Reaction of $[Os_3(MeCN)_2(CO)_{10}]$ with fluorophenol

A solution of the yellow cluster $[Os_3(MeCN)_2(CO)_{10}]$ **1.3** (0.050 g, 0.0533 mmol) and fluorophenol (0.0194 g, 0.1702 mmol) in dichloromethane (15 cm^3) was refluxed for 2 hours. The infrared spectra showed no change. The solvent was removed and the reaction carried out in cyclohexane. After refluxing in cyclohexane (30 cm^3) for 3 hours, the solvent was removed under vacuum and TLC was carried out using dichloromethane-petroleum spirit (40-60 °C) (1: 3 v/v) as eluent. Three bands were obtained of which two have been identified as $[Os_3(\mu\text{-}H)(OC_6H_4F)(CO)_{10}]$ **4.3** (22%) and $[Os_3(\mu\text{-}H)(\mu\text{-}Cl)(CO)_{10}]$ **4.5** (5%) in low yield.

4.4.6.1 Protonation of $[Os_3(\mu\text{-}H)_2(OC_6H_3F)(CO)_9]$ 4.4

The cluster $[Os_3(\mu\text{-}H)_2(OC_6H_3F)(CO)_9]$ **4.4** (0.003 g, 0.0032 mmol) was dissolved in dichloromethane (4 cm^3), then trifluoroacetic acid (4 drops) was added and the solution was shaken. The infrared spectrum showed a complete change from the starting material. The protonated compound was characterized by infrared spectroscopy only.

4.4.7 Reaction of $[Os_3(CO)_{12}]$ with methoxyphenol

The yellow complex $[Os_3(CO)_{12}]$ **1.1** (0.1271 g, 0.1394 mmol) and methoxyphenol (0.0411 g, 0.3262 mmol) were refluxed in xylene (50 cm^3) for 22 hours. The solution changed colour from yellow to dark orange. The solvent was removed under vacuum and TLC was carried out using dichloromethane-petroleum spirit (40-60 °C) (1:3 v/v) as eluent. Two bands were obtained of which two have been identified as $[Os_3(\mu\text{-}H)(OC_6H_4OMe)(CO)_{10}]$ **4.6** (51%) and $[Os_3(\mu\text{-}H)_2(OC_6H_3OMe)(CO)_9]$ **4.7** (20%). Red crystals of complex **4.7** were grown in heptane-dichloromethane (95:5); the solution was left standing for over 24 hours.

4.4.8 Reaction of $[Os_3(MeCN)_2(CO)_{10}]$ with hydroquinone

A solution of cyclohexane (20 cm^3) containing the labile cluster $[Os_3(MeCN)_2(CO)_{10}]$ (0.0110 g, 0.0177 mmol) and hydroquinone (0.004 g, 0.0357 mmol) was refluxed for 2 hours. The solvent was removed under vacuum and TLC was carried out using dichloromethane-petroleum spirit (40-60 °C) (1:3 v/v) as eluent. Two significant bands were obtained of which two have been identified as $[Os_3(\mu\text{-}H)(OC_6H_4OH)(CO)_{10}]$ **4.8** (2%) and the starting material $[Os_3(CO)_{12}]$.

4.4.9 Reaction of $[Os_3(MeCN)_2(CO)_{10}]$ with catechol

The yellow labile cluster $[Os_3(MeCN)_2(CO)_{10}]$ (0.040 g, 0.0426 mmol) and crystalline catechol (0.0335 g, 0.2991 mmol) were refluxed in cyclohexane (20 cm^3) for 2 hours. The colour changed from yellow to green. The solution was cooled and the solvent was removed. The solid was re-dissolved in dichloromethane and then passed through silica to get rid of excess catechol. TLC was carried out using petroleum spirit (40-60 ° C)-dichloromethane (5:2 v/v) as eluent. Only one major yellow band was isolated and identified as $[Os_3(\mu\text{-}H)(OC_6H_4OH)(CO)_{10}]$ **4.11** (85%).

4.4.10 Reaction of $[Os_3(\mu\text{-}H)_2(CO)_{10}]$ with benzoquinone

A solution of the dihydrido-complex $[Os_3(\mu\text{-}H)_2(CO)_{10}]$ (0.160 g, 0.1865mmol) and benzoquinone (0.0817 g, 0.7565 mmol) in cyclohexane (20 cm^3), was refluxed for 1 hour and 30 minutes, by which time the purple solution had become pale red. The solvent was removed *in vacuo* and the residue was separated by TLC using petroleum spirit (40-60 °C)-dichloromethane (2:3 v/v) as eluent, to give one red band which was characterised as $[Os_3(\mu\text{-}H)(OC_6H_5O)(CO)_{10}]$ **4.15** (69%). Repeating the reaction using an excess of the cluster did not form the linked cluster as we had anticipated.

4.4.11 Reaction of $[Os_3(CO)_{12}]$ with 4-Aminophenol

The cluster $[Os_3(CO)_{12}]$ (0.2949 g, 0.3234 mmol) and 4-aminophenol (0.03459 g, 0.3224 mmol) in xylene (20 cm^3) were sealed under vacuum and placed in the oven at 180 °C for 20 hours. The colour changed from yellow to orange. Some white solid was deposited at the bottom of the tube. The tube was cooled, the seal was broken, and the solution was filtered. The solvent was removed and the residue separated by TLC using petroleum spirit (40-60 °C)-dichloromethane (3:1 v/v) as eluent, to give three bands of which two have been identified. One was a mixture of $[Os_3(\mu\text{-}H)(HNC_6H_4OH)(CO)_{10}]$ **4.17** and $[Os_3(\mu\text{-}H)_2(NC_6H_4OH)(CO)_9]$ **4.18** ($\approx$ 65 %) in the ratio of 6:1, and the other band gave pure $[Os_3(\mu\text{-}H)(OC_6H_4NH_2)(CO)_{10}]$ **4.19** in a low yield (< 5 %).

4.4.12 Reaction of $[Os_3(CO)_{12}]$ with para-Phenylenediamine

The cluster $[Os_3(CO)_{12}]$ (0.2100 g, 0.2303 mmol) and *para*-Phenylenediamine (0.0235 g, 0.2313 mmol) in xylene (20 cm^3) were sealed under vacuum and placed in the oven at 180 °C for 20 hours. The colour changed from yellow to orange. The tube was cooled, the seal was broken, and the solution was filtered. The solvent was removed and the residue separated by TLC using petroleum spirit (b.p. 40-60 °C)-dichloromethane (3:1 v/v) as eluent, to give $[Os_3(\mu\text{-}H)(NHC_6H_4NH_2)(CO)_{10}]$ **4.22** (10%) and $[Os_3(\mu\text{-}H)_2(NHC_6H_4NH_2)(CO)_9]$ **4.23** (< 3 %).

Table 4.1. Infrared data for hydroxy and amino arene derivatives

Compound	υ (CO)/ cm^{-1} (cyclohexane)
$[Os_3(\mu\text{-}H)(OPh)(CO)_{10}]$ **4.1**	2112w, 2073s, 2064m, 2034w, 2025vs, 2007m, 1991w, 1986w
$[Os_3(\mu\text{-}H)_2(OC_6H_4)(CO)_9]$ **4.2**	2112w, 2086vs, 2058s, 2036m, 2030vs, 2015m, 2004m, 1988w,1981w
$[Os_3(\mu\text{-}H)_2(HOC_6H_4)(CO)_9]^+$ Protonated **4.2**	2121w, 2093s, 2065vs, 2046m(br), 2009m(br)
$[Os_3(\mu\text{-}H)(OC_6H_4F)(CO)_{10}]$ **4.3**	2112w, 2072s, 2063m, 2035w, 2024vs, 2005m, 1991w(br), 1987w(br)
$[Os_3(\mu\text{-}H)_2(OC_6H_3F)(CO)_9]$ **4.4**	2113w, 2086vs, 2058vs, 2035s, 2025s, 2015m, 2005m, 1988w(br), 1979w(br)
$[Os_3(\mu\text{-}H)(Cl)(CO)_{10}]$ **4.5**	2115w, 2076s, 2068m, 2035w, 2027vs, 2014m, 2002w(sh), 1992w(br), 1989w(br)
$[Os_3(\mu\text{-}H)(OC_6H_4OMe)(CO)_{10}]$ **4.6**	2111w, 2070vs, 2062s, 2035w, 2023vs, 2004m, 1989w (br), 1985w(br)
$[Os_3(\mu\text{-}H)_2(OC_6H_3OMe)(CO)_9]$ **4.7**	2108m, 2082vs, 2054vs, 2031s, 2022m, 2011m, 2000s, 1983w(br), 1977m
$[Os_3(\mu\text{-}H)(OC_6H_4OH)(CO)_{10}]$ **4.8**	2111w, 2072s, 2063m, 2023vs, 2005m, 1990w(br), 1987w(br)
$[Os_3(\mu\text{-}H)_2(OC_6H_3OH)(CO)_9]$ **4.9**	2109w, 2083vs, 2055vs, 2033s, 2024m, 2012m, 1985w(br), 1978w(br)
$[Os_6(\mu\text{-}H)_3(C_6H_3O)(CO)_{19}]$ **4.10**	2113w, 2109w, 2084s, 2073s, 2063m, 2057m, 2036m, 2023vs, 2014w, 2002m, 1991w(br), 1988w(br) 1980w(sh)
$[Os_3(\mu\text{-}H)(OC_6H_4OH)\ (CO)_{10}]$ **4.11**	2110w, 2074vs, 2059m, 2025vs, 2014m, 2002s, 1989w(br) and (OH) at 3441

Table 4.1. Infrared data for hydroxy and amino arene derivatives continued.

$[Os_3(\mu\text{-}H)(OC_6H_5O)(CO)_{10}]$ **4.15**	2105w, 2071s, 2055m, 2015vs, 1995m(br), 1976br (sh)
$[Os_3(\mu\text{-}H)(HNC_6H_4OH)(CO)_{10}]$ **4.17**	2104w, 2066vs, 2051s, 2021vs, 2003vs, 1993s, 1983w, 1974w.
$[Os_3(\mu\text{-}H)_2(NC_6H_4OH)(CO)_9]$ [a] **4.18**	2113w, 2080w, 2030w
$[Os_3(\mu\text{-}H)(OC_6H_4NH_2)(CO)_{10}]$ **4.19**	2106w, 2069vs, 2059vs, 2024vs, 2016s, 2000s, 1984w, br
$[Os_3(\mu\text{-}H)(NHC_6H_4NH_2)(CO)_{10}]$ **4.22**	2103w, 2066vs, 2050s, 2017m, 2001m, 1989w.
$[Os_3(\mu\text{-}H)_2(NHC_6H_4NH_2)(CO)_9]$ [a] **4.23**	2114w, 2077s,

[a] Dichloromethane

vs = very strong, s = strong, m = medium, w = weak, vw = very weak and br = broad peak

Table 4.2. The ^{1}H NMR data for hydroxy and amino arene derivatives.

Compounds	Chemical shifts (δ)	Intensities	Assignments
$[Os_3(\mu\text{-}H)(OPh)(CO)_{10}]$ **4.1**	7.00 (m)	2	H^3-H^5
	6.43 (d)	2	H^2, H^6
	-12.2 (s)	1	OsH
$[Os_3(\mu\text{-}H)_2(OC_6H_4)(CO)_9]$ **4.2**	7.67 (ddd)	1	H^5
	7.20 (dd)	1	H^3
	6.37 (d)	1	H^6
	6.01 (ddd)	1	H^4
	-11.73 (s)	1	OsH
	-14.12 (s)	1	OsH
$[Os_3(\mu\text{-}H)_2(HOC_6H_4)(CO)_9]^+$ (protonated)	8.06 (ddd)	1	H^5
	7.68 (dd)	1	H^3
	6.71 (d)	1	H^6
	6.46 (t)	1	H^4
	*	1	OH
	-11.40 (d)	1	OsH
	-14.03 (d)	1	OsH
$[Os_3(\mu\text{-}H)(OC_6H_4F)(CO)_{10}]$ **4.3**	6.81(m)	2	H^3, H^5
	6.35(m)	2	H^2, H^6
	-12.2(s)	1	OsH
$[Os_3H(Cl)(CO)_{10}]$ **4.5**	-14.36(s)	1	OsH
$[Os_3(\mu\text{-}H)(OC_6H_4OMe)(CO)_{10}]$ **4.6**	6.64(dd)	2	H^3, H^5
	6.34(dd)	2	H^2, H^6
	3.65(s)	3	OMe
	-12.23(s)	1	OsH
$[Os_3(\mu\text{-}H)_2(OC_6H_3OMe)(CO)_9]$ **4.7**	7.54 (dd)	1	H^3
	6.47 (dd)	2	H^4,
	6.63(dd)	1	H^6
	3.63 (s)	1	OMe
	-11.58 (s)	1	OsH
	-13.78 (s)	1	OsH
$[Os_3(\mu\text{-}H)(OC_6H_4OH)(CO)_{10}]$ **4.8**	6.59 (m)	2	H^3, H^5
	6.32 (m)	2	H^2, H^6
	4.34 (s)	1	OH
	-12.23(s)	1	OsH
$[Os_3(\mu\text{-}H)_2(OC_6H_3OH)(CO)_9]$ **4.9**	7.42 (dd)	1	H^3
	6.52(d)	1	H^6
	6.36(d)	1	H^4
	4.13(s)	1	OH
	-11.63(s)	1	OsH
	-13.92(s)	1	OsH

Table 4.2. The ^1H NMR data for hydroxy and amino arene derivatives continued.

$[Os_6(\mu\text{-}H)_3(C_6H_3O)(CO)_{19}]$ **4.10**	6.98 (dd)	1	H^3
	6.25(dd)	2	H^4, H^6
	-11.58(d)	1	OsH
	-12.31(s)	1	OsH
	-13.92(d)	1	OsH
$[Os_3(\mu\text{-}H)(OC_6H_4OH)(CO)_{10}]$ **4.11**	6.70 (dt)	1	H^2
	6.62 (dt)	1	H^3
	6.56 (dd)	1	H^4
	6.38 (dd)	1	H^1
	20.34(s)	1	OH
	-11.53 (s)	1	OsH
$[Os_3(\mu\text{-}H)(OC_6H_5O)(CO)_{10}]$ **4.15**	2.47(dd)	1	H^1
	2.59(dd)	1	H^4
	2.82(dd)	1	H^2
	2.97(d)	1	H^3
	7.59(s)	1	H^5
	12.6(s)	1	OsH
$[Os_3(\mu\text{-}H)(HNC_6H_4OH)(CO)_{10}]$ **4.17**	6.70 (m)	2	H^2-H^6
	6.63(m)	2	H^3-H^5
	5.78 (s, br)	1	NH
	4.37(s)	1	OH
	-14.15 (d)	1	OsH
$[Os_3(\mu\text{-}H)_2(NC_6H_4OH)(CO)_9]$ **4.18**	7.02 (dd)	2	H^2-H^6
	6.58(dd)	2	H^3-H^5
	4.67	1	OH
	18.35	2	OsH
$[Os_3(\mu\text{-}H)(OC_6H_4NH_2)(CO)_{10}]$ **4.19**	6.99(dd)	2	H^2-H^6
	6.35(dd)	2	H^3-H^5
	4.2(s,br)	2	NH_2
	-14.69(s)	1	OsH
$[Os_3(\mu\text{-}H)(NHC_6H_4NH_2)(CO)_{10}]$ **4.22**	6.61 (dd)	2	H^3-H^5
	6.49 (dd)	2	H^2-H^6
	5.83 (s,br)	1	NH
	3.56 (s, br)	2	NH_2
	-14.15 (s)	1	OsH
$[Os_3H_2(NHC_6H_4NH_2)(CO)_9]$ **4.23**	6.97 (dd)	2	H^3-H^5
	6.42 (dd)	2	H^2-H^6
	3.56 (s, br)	2	NH_2
	5.82(s, br)	1	NH
	-18.36 (s)	1	OsH

* not observed – most probably due to the exchange of OH molecules with the solvent.

Chapter 5. Reactions of triosmium clusters with dipyridyl disulfides

5.1 Introduction

Transition metal complexes containing disulfide ligands exhibit a range of interesting reactivity at the sulfur atoms. There is great interest in the synthesis of high-nuclearity transition metal carbonyl clusters via sulfides. The simplest disulfide of iron carbonyl $[Fe_2(\mu\text{-}S)_2(CO)_6]$, was first reported by Hieber in 1958.[137] It has rich reaction chemistry and has been extensively studied over the years.[138,139] The chemistry of $[Fe_2(\mu\text{-}S)_2(CO)_6]$ is dominated by reaction at the sulfur atoms, in which S-S bond cleavage occurs as the molecule oxidatively adds to the metal complexes ML_n.[138, 139]

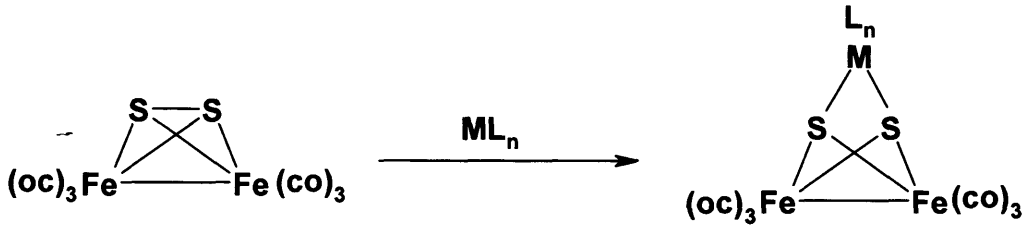

Scheme 5.1. Shows the cleavage of the S-S bond in $[Fe_2(\mu\text{-}S)_2(CO)_6]$.

Because of the use of bridging sulfido and pyridine ligands in the synthesis of polynuclear metal complexes, we set out to explore the chemistry of linked clusters through the use of both sulfur and pyridine as bridging groups. In a continuation of

our studies of the chemistry of linking triosmium clusters, we investigated the reactions of tetramethylthiuram disulfide, 4-mercaptopyridine and 4,4-dipyridyl disulfide with labile triosmium clusters. Previously, disulfides were only known to coordinate to triosmium clusters through the cleavage of sulfur-sulfur bonds (see Chapter 2). Herein, we report the interesting results obtained from the reactions of $[Os_3(MeCN)_2(CO)_{10}]$ with the disulfides shown below, and show for the first time how high nuclearity clusters can be synthesised at low temperatures.

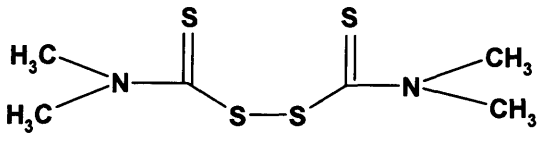

Tetramethylthiuram disulfide

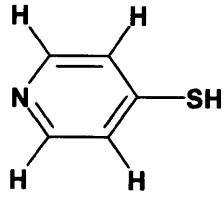

4-mercaptopyridine

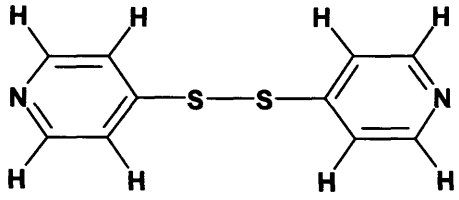

4,4'-dipyridyl disulfide

5.2 Results and discussion

5.2.1 Tetramethylthiuram disulfide derivatives

The unsaturated purple cluster $[Os_3(\mu\text{-}H)_2(CO)_{10}]$ quickly reacted with tetramethylthiuram disulfide in toluene at 80° C to give the mononuclear compound

$[Os(Me_2NCS_2)_2(CO)_3]$ **5.1** (26%). Crystallographic data are given in **Table 5.1a** and bond lengths and angles are given in **Table 5.1b**. The unit cell contained two structurally similar but independent molecules. An ORTEP drawing of both molecules is shown in **Figure 5.1**. The sulfur–osmium bond distances are Os(1)-S(1) = 2.4457(14), Os(1)-S(2) = 2.4485(17) and Os(1)-S(3) = 2.4236(17) Å respectively; [Os(2)-S(5) = 2.4484 (18), Os(2)-S(6) = 2.4448(14) and Os(2)-S(7) = 2.4233(17) Å respectively]. Values in brackets correspond to the second molecule in the crystal. Similar ruthenium-sulfur bond distances were found in the ruthenium cluster $[Ru(MeNCS_2)_2(CO)_2]$.[140] The crystal structure showed that the ligand $(Me_2NCS_2)_2$ had cleaved at the S-S bond to give two sets of Me_2NCS_2 ligands, which coordinated the osmium atom differently. In one case both sulfur atoms are coordinated, while in the other case only one sulfur atom is coordinated while the other remains free. The compound contains three terminal *fac*-carbonyl ligands, which are *trans* to the three sulfur atoms.

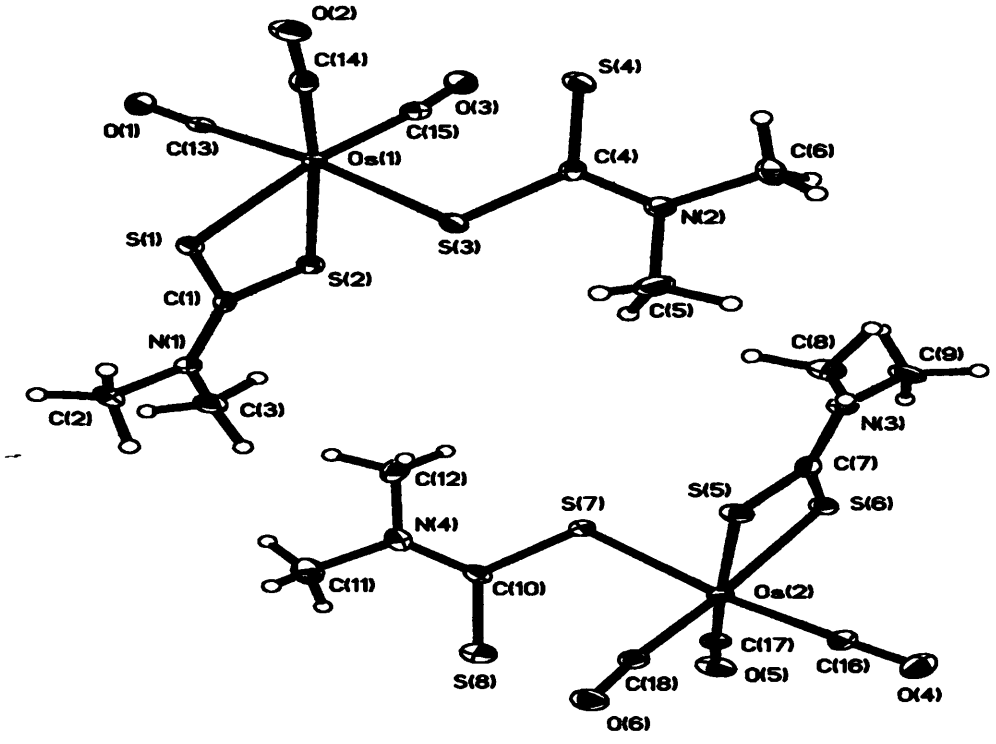

Figure 5.1. The molecular structure of the cluster $[Os(Me_2NCS_2)_2(CO)_3]$ 5.1 showing two independent molecules.

The infrared spectrum showed the presence of two carbonyl absorptions bands at 2100(s) and 2030(s) cm^{-1}, consistent with an approximate C_{3v} geometry for the $Os(CO)_3$ set of atoms. The lack of 3-fold symmetry in the $Os(CO)_3$ is not apparent in the spectrum since the lower symmetry would lead to three IR active CO bands. The ^1H NMR spectrum of $[Os(Me_2NCS_2)_2(CO)_3]$ **5.1**, showed four signals due to the four CH_3 groups, in the intensity ratio of 1:1:1:1 at δ 3.63, 3.22, 3.21 and 3.20. This indicated the 4 different environments of the CH_3 protons. We could not assign signals to the different protons. The EI mass spectrum gave m/z = 516 (calc. 516) with the successive loss of three carbonyl ligands from the parent molecular ion,

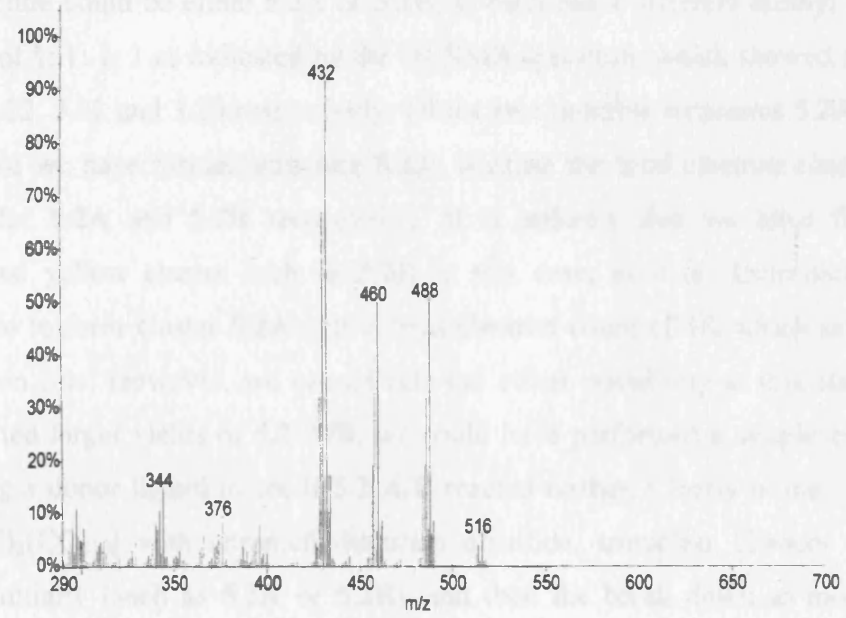

Figure 5.2. EIMS of cluster $[Os(Me_2NCS_2)_2(CO)_3]$ 5.1

We also isolated another cluster from the reaction of $[Os_3(\mu\text{-}H)_2(CO)_{10}]$ with tetramethylthiuram disulfide in a trace amount (<2 %). The EI-MS gave m/z = 1012/1013. There are at least two possible structures (shown below) for cluster $[Os_3(Me_2NCS_2)_2(CO)_7]$ **5.2**.

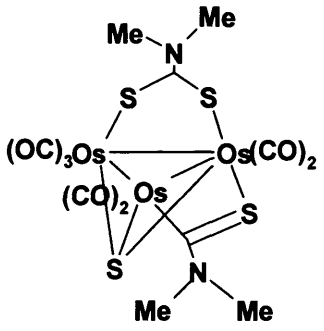

5.2A

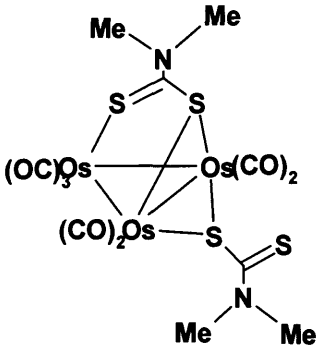

5.2B

The structure could be either **5.2A** or **5.2B**, as each has 4 different methyl groups in the ratio of 1: 1: 1: 1 as indicated by the ^{1}H NMR spectrum, which showed singlets at δ 3.24, 3.22, 3.21 and 3.20 respectively. Of the two possible structures **5.2A** or **5.2B**, we believe we have formed structure **5.2A**, because the total electron counts are 48 and 46 for **5.2A** and **5.2B** respectively. It is unlikely that we have formed an unsaturated yellow cluster such as **5.2B** in this case, as it is electronically more favourable to form cluster **5.2A** with a total electron count of 48, which satisfies the 18-electron rule. However, we cannot rule out either possibility at this stage. If we had isolated larger yields of **5.2 A/B**, we could have performed a simple experiment by adding a donor ligand to see if **5.2 A/B** reacted further. Clearly in the reaction of $[Os_3(\mu\text{-}H)_2(CO)_{10}]$ with tetramethylthiuram disulfide, trinuclear clusters would be formed initially (such as **5.2A** or **5.2B**), and then the break down to mononuclear species would occur subsequently.

The thermolysis of compound $[Os(Me_2NCS_2)_2(CO)_3]$ **5.1** in refluxing xylene gave the compound $[Os(Me_2NCS_2)_2(CO)_2]$ **5.3** (2%). The compound was characterised by IR and EI-MS method only. The IR indicated the presence of two CO peaks at 2017(s) and 1943(m) cm^{-1} as expected. These two peaks are at lower wave number than those observed for $[Os(Me_2NCS_2)_2(CO)_3]$ **5.1**, since $[Os(Me_2NCS_2)_2(CO)_2]$ **5.3** contains more donor atoms coordinated to the metal with greater resultant back-donation to CO. Previously, the ruthenium analogue of **5.3** was synthesised in this group by Deeming *et al.* The spectroscopic data matches well with that of our compound.[141]

The EI-MS gave m/z = 488 (calc. 488) for the parent molecular ion, with the successive loss of two CO ligands. In our attempts at similar reactions of $[Os_3(\mu\text{-}H)_2(CO)_{10}]$ with tetramethylthiuram monosulfide, we obtained complex mixtures, which could not be separated satisfactorily.

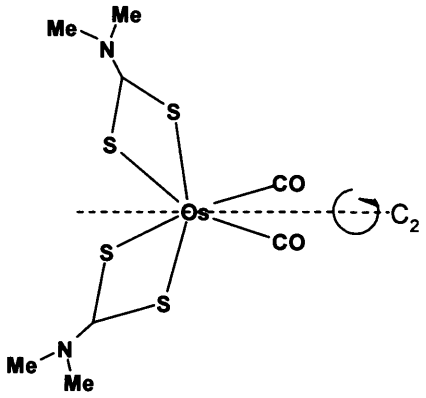

In our effort to explore the chemistry of nitrogen, oxygen and sulfur containing arenes to form bridging linked clusters, we treated 4-mercaptopyridine (NC_5H_4SH) with the labile bis-acetonitrile cluster $[Os_3(MeCN)_2(CO)_{10}]$ **1.3**. We knew from research carried out in our laboratory and work published in literature that both pyridine and sulfur ligands readily react with cluster **1.3**. The only problem that we could foresee was that the reaction would only take place at one function of the molecule, thus deactivating others as previously shown in Chapter 4 for other bifunctional ligands.

5.2.2 4-Mercaptopyridine derivatives

The treatment of 2 moles of cluster **1.3** with 1 mole of 4-mercaptopyridine at 30 °C in acetonitrile yielded the linked yellow cluster $[Os_6(\mu\text{-}H)_2(NC_5H_3S)(CO)_{20}]$ **5.4** (42%) in a moderate yield. The same reaction also worked well in dichloromethane.

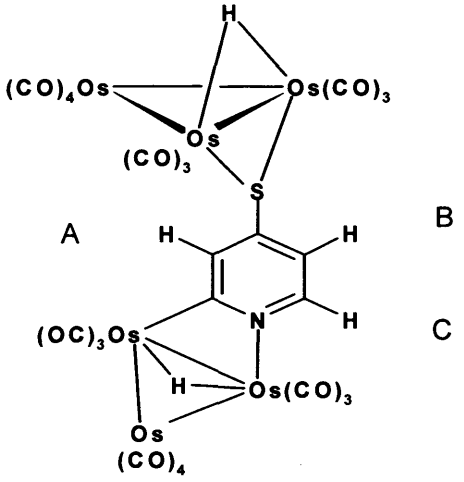

5.4

The complex IR spectrum told us straight away that two cluster units are present. The infrared spectrum in cyclohexane gave absorptions at 2112(w), 2104(w), 2071(vs), 2065(s), 2054(m), 2027(vs), 2020(m), 2009(w), 2002(m), 1992(m) and 1978(w,br) cm^{-1}. The sulfur end of the cluster matches well with IR data for cluster $[Os_3(\mu\text{-}H)(OPh)(CO)_{10}]$, giving absorptions at 2112(w), 2073(s), 2064(m), 2034(w), 2025(v)s, 2007(m), 1991(w) and 1986(w) cm^{-1}, and likewise the pyridine bound Os_3 unit matches well with that of the cluster $[Os_3(\mu\text{-}H)(C_5H_3N)(CO)_{10}]$. The ^1H NMR spectrum shown below (**Figure 5.3**) showed the presence of only five protons consistent with the formulae $[Os_6(\mu\text{-}H)_2(NC_5H_3S)(CO)_{20}]$ **5.4**. A doublet was observed at δ 7.90 due to proton C, a narrow doublet at δ 7.03 due to proton A and a double doublet at δ 6.61 due to proton B. Two sharp hydride signals were also observed at δ -14.79 (py end) and -17.23 (S end) in the ratio of 1:1. EI-MS gave m/z = 1823 (calc. 1823).

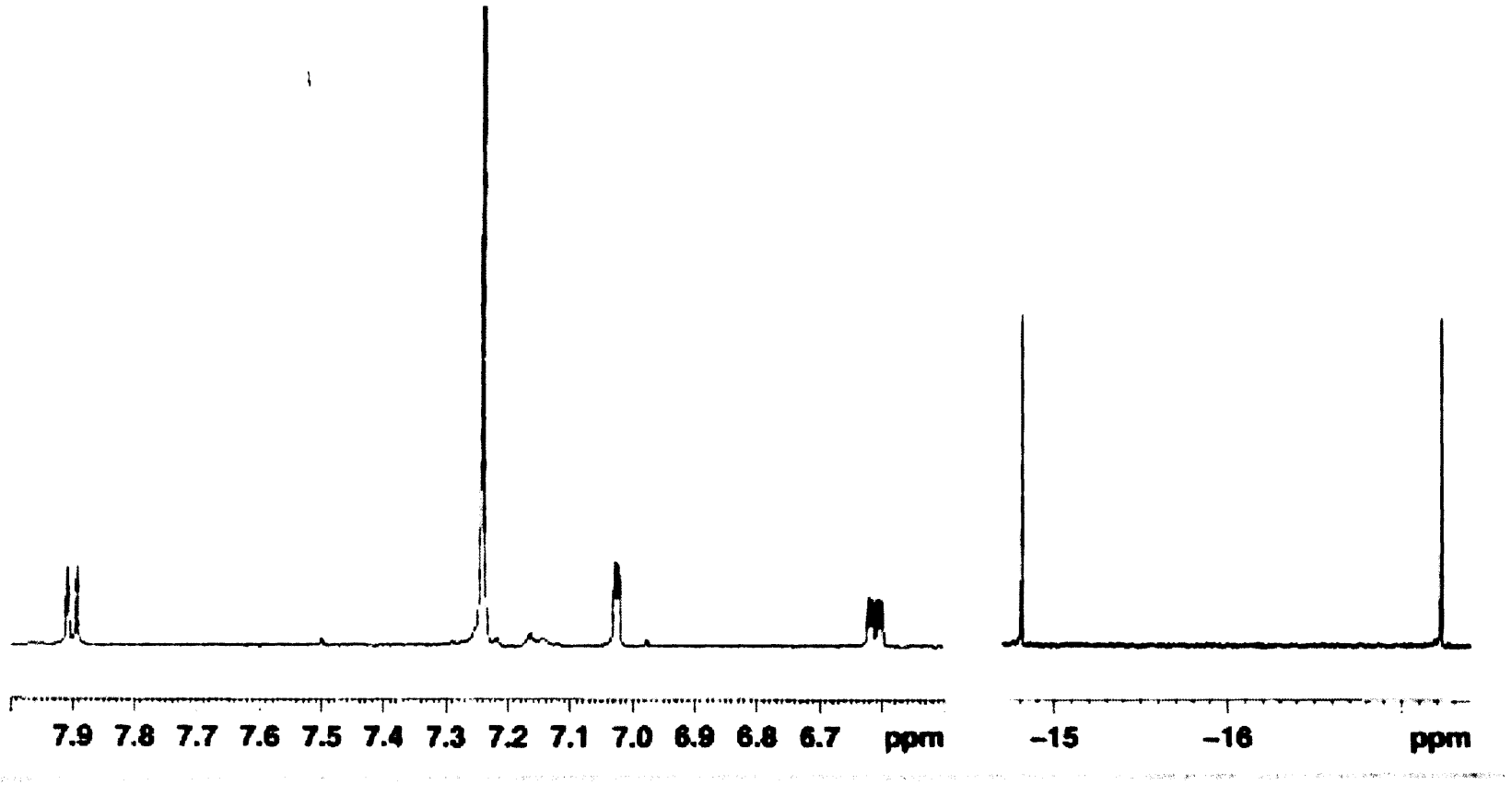

***Figure 5.3. The ^{1}H NMR spectrum of cluster $[Os_6(\mu\text{-}H)_2(NC_5H_3S)(CO)_{20}]$* 5.4 in $CDCl_3$ solution.**

5.2.3 4,4-dipyridyl disulfide derivatives

Since the reaction between cluster **1.3** and 4-mercaptopyridine was successfully carried out, we pursued the corresponding reaction with the ligand 4,4-dipyridyl disulfide (aldothiol) ($NC_5H_4S_2C_5H_4N$) shown below. There were a number of things that could have happened: (a) we could get a reaction at just one pyridine ligand leaving the other free; (b) reaction could occur at both pyridine rings; or (c) cleavage of the S-S bond could occur, as in the benzyl disufide case described in Chapter 2. In fact any combination of C-H cleavage of the pyridine or S-S cleavage of the disulfide could occur.

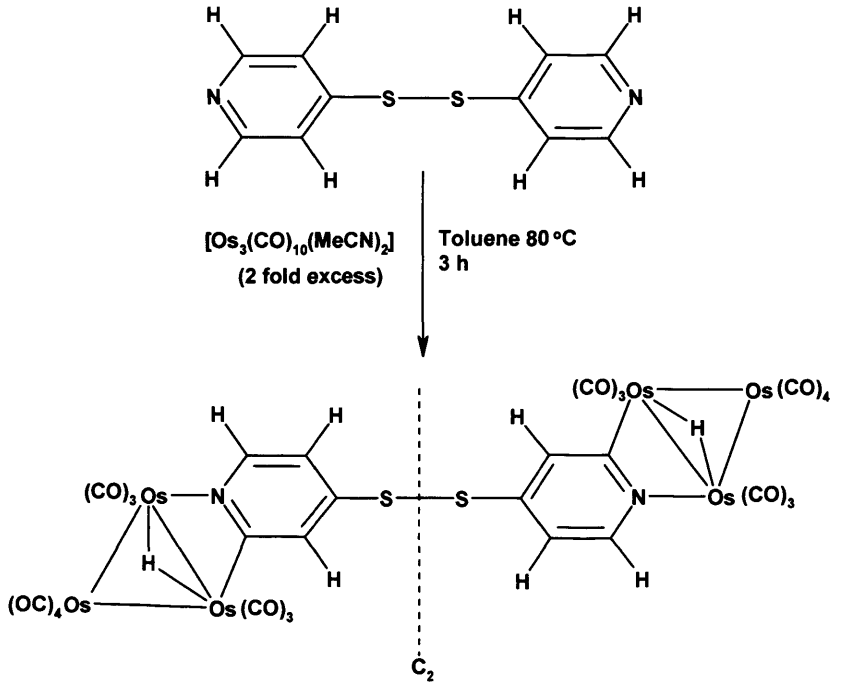

The 4,4-dipyridyl disulfide ligand readily reacted with cluster **1.3**. When a 2-fold excess of the cluster was added, the major product isolated was the hexanuclear cluster $[Os_6(\mu\text{-}H)_2\{(NC_5H_3)_2S_2\}(CO)_{20}]$ **5.5** (34%). In the ^1H NMR spectrum (**Figure. 5.4**) we see the presence of two isomers in the ratio of 6:4. The major isomer gives two doublets at δ 7.95 and 7.31 and also a double doublet at δ 6.69, while the minor isomer gave a similar pattern with two doublets at δ 7.94 and 7.37 and a double doublet at 6.70. Two hydride signals were also observed at δ -14.84 and -14.83 in the

ratio of 6:4. Clearly the two sets of NMR signals are very similar. Each cluster sub-unit is chiral with stereochemistry that might be labelled Δ or Λ. Hence, in the dicluster unit there are two diastereomers possible, each with equivalent ligand sets; one diastereoisomer exists as a racemic mixture of a pair of enantiomers but the other is a meso isomer.

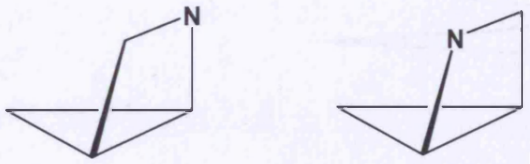

Δ Λ

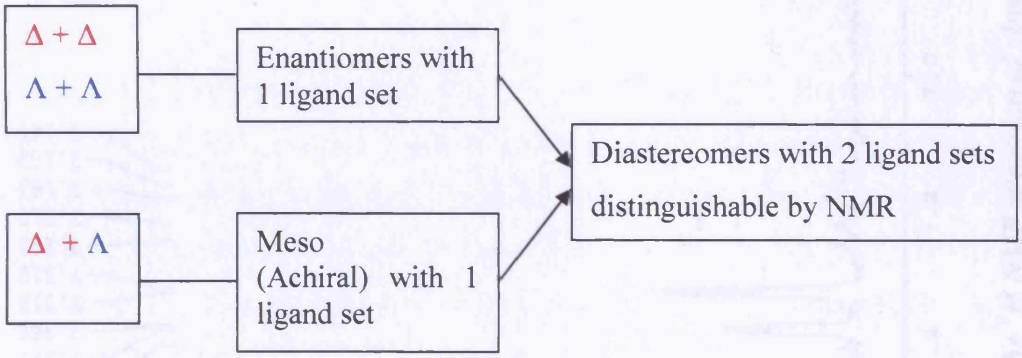

The two enantiomers (ΔΔ and ΛΛ) will have the same ^{1}H NMR spectra but different from that of the diastereomeric meso form (ΔΛ). That is why we observed the presence of two species in the ratio of 6:4. Unfortunately, we cannot determine whether the major peaks are due to the meso or racemic forms.

Diastereomer 1: Δ Δ + Λ Λ enantiomeric pair (racemic mixture)

Diastereomer 2: Δ Λ Meso isomer (contains centre of symmetry)

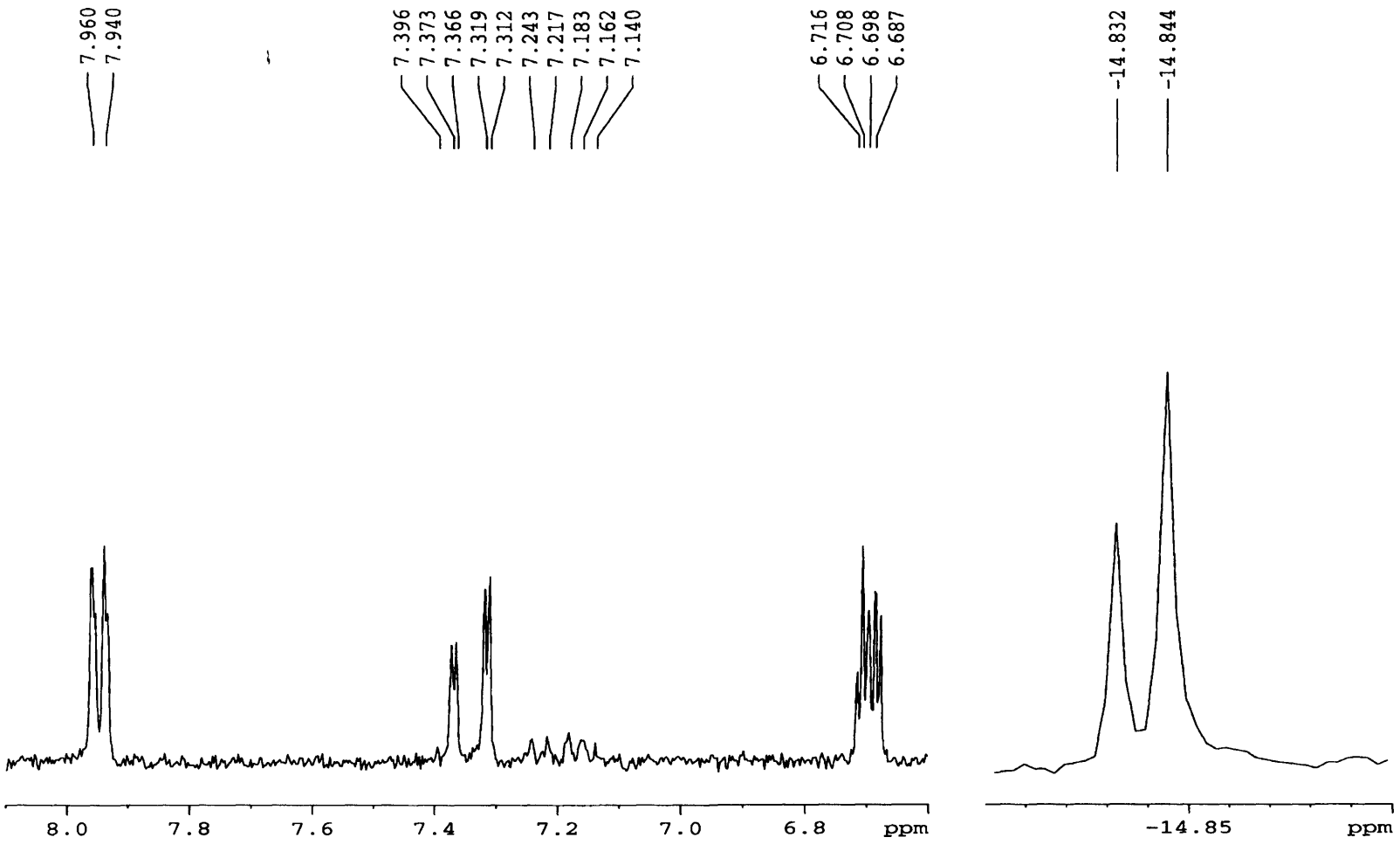

Figure 5.4. The ^{1}H NMR spectrum of cluster $[Os_6(\mu\text{-}H)_2\{(NC_5H_3)S_2\}(CO)_{20}]$ 5.5 showing the major and the minor isomers.

We can conclude that both ends of the ligand have coordinated, otherwise we would have observed the coordinated end to have three proton signals in the ratio of 1:1:1 with the non-coordinated end giving an AA'BB' spectrum. If that were the case, we would have also observed the presence of one hydride signal only, which is clearly not the case. Wong and co-workers recently isolated the linked cluster $[Os_3(\mu\text{-}H)(CO)_{10}(\mu\text{-}NC_5H_3N{=}NC_5H_3N)Os_3(\mu\text{-}H)(CO)_{10}]$ from the reaction of $[Os_3(MeCN)_2(CO)_{10}]$ and 4,4'-azopyridine ($NC_5H_4N{=}NC_5H_4N$). The linked cluster showed a single set of NMR signals unlike the 4,4-dipyridyl disulfide case.[142]

The IR spectrum looked similar to that of a single *ortho*-metallated pyridine cluster, such as $[Os_3(\mu\text{-}H)(\mu\text{-}C_5H_4N)(CO)_{10}]$. This is because in this case both ends of the molecule are essentially equivalent, thus giving rise to a simple IR spectrum. The FAB-MS gave m/z = 1934 (calc.1934), with the successive loss of CO ligands.

5.2.4 X-ray crystal structure of $[Os_6(\mu\text{-}H)_2(\mu\text{-}S_2(C_5H_3N)_2(CO)_{20}]$ 5.5

The molecular structure of $[Os_6(\mu\text{-}H)_2(\mu\text{-}S_2(C_5H_3N)_2CO)_{20}]$ is shown in **Figure 5.5**. The crystallographic data are given in **Table 5.2a** and bond lengths and angles are given in **Table 5.2b** (Appendix). The solid-state structure gives a molecule with C_2 symmetry. The structure shown in **Figure 5.5** has the Λ Λ form. The structure consists of two Os_3 triangles each linked to two *ortho*-metallated pyridine ligands, which are bridged by two sulfur atoms, with their sulfur-sulfur bond still intact. The six metal-metal bonds are very similar. However, we believe the hydride ligands are located between Os(1)-Os(2) and Os(4)-Os(5), and have a slightly longer metal-metal bond distances of 2.8891(10) and 2.9035(10) Å, associated with the bridging hydride ligands which lie above the Os_3 plane. There are ten terminal carbonyl ligands at each Os_3 cluster that are distributed in units of 4, 3, and 3. The S(1)-S(2) bond length of 2.009(7) Å is similar to those found in the dinuclear iron and manganese carbonyls, $[Fe_2(\mu\text{-}S_2)(CO)_6]$[143], $[Mn_2(\mu\text{-}SMe_2)(\mu\text{-}S_2)(CO)_6]$, $[Mn_2(\mu\text{-}SCH_2CH_2CH_2)(\mu\text{-}S_2)(CO)_6]$ and $[Mn_2(\mu\text{-}2S_3)(\mu\text{-}S_2)(CO)_6]$, with bond lengths of 2.021(3), 2.0471(7), 2.0459(11) and 2.0448(9) Å respectively.[144] The Os(1)-N(1) and Os(4)-N(2) bond lengths of 2.107(14) and 2.088(13) Å are similar to those found in $[Os_3(\mu\text{-}H)(\mu\text{-}NC_5H_4S)(CO)_9]$.

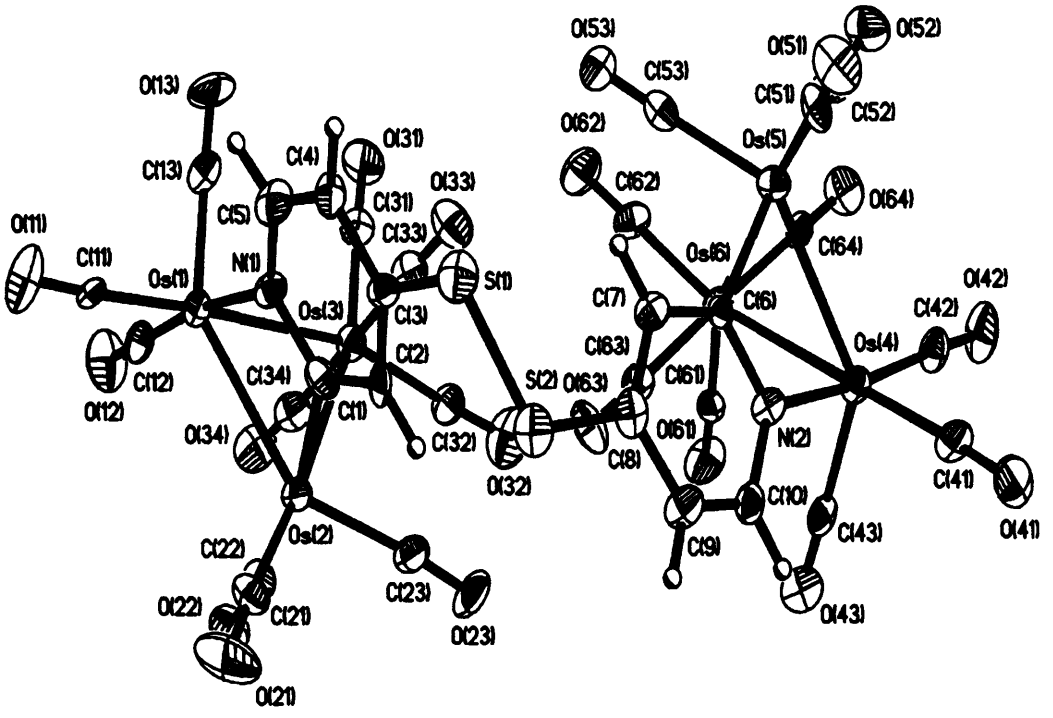

Figure 5.5. The molecular structure of the linked cluster $[Os_6(\mu\text{-}H)_2\{(NC_5H_3)_2S_2\}(CO)_{20}]$ 5.5, with the S-S bond intact.

The bond angles for C(8)-S(2)-S(1) of 107.7(6)° and C(3)-S(1)-S(2) of 105.7(6)°, indicate that the sulfur-sulfur bond is distorted. The angles of C(1)-N(1)-Os(1) and C(6)-N(2)-Os(4) are identical (111.9°), consistent with C_2 symmetry. The gauche arrangement about the S-S bond brings the Os_3 cluster quite close together. We believe this closeness results in the NMR differences between the isomers, with one cluster in each isomer being sensitive to the stereochemistry of the other.

Having synthesised a very interesting and uniquely linked cluster from 4,4-dipyridyl disulfide, which left the sulfur-sulfur bond intact, we carried out further reactions of cluster $[Os_6(\mu\text{-}H)\{(NC_5H_3)_2S_2\}(CO)_{20}]$ **5.5** with **1.3**, in an attempt to oxidatively add **5.5** to the other cluster with cleavage of the sulfur-sulfur bond. Adams has inserted metal-containing groups into the sulfur-sulfur bond in manganese, iron and mixed metal compounds.[145,146,147] The chemistry of the S-S bond should parallel that

described in Chapter 2. The direct reaction of the cluster $[Os_6(\mu\text{-}H)_2\{(NC_5H_3)_2S_2\}(CO)_{20}]$ **5.5** with one mole of $[Os_3(MeCN)_2(CO)_{10}]$ at room temperature yielded the new cluster $[Os_9(\mu\text{-}H)_2(NC_5H_3S)_2(CO)_{30}]$ **5.6**, in 29% yield. This product was also obtained from the reaction of a 3-fold excess of cluster **1.3** with 4,4-dipyridyl disulfide. The cluster $[Os_9(\mu\text{-}H)_2(NC_5H_3S)_2(CO)_{30}]$ **5.6** was isolated by TLC using a hexane/CH_2Cl_2 solvent mixture. The situation was now much more complex than in cluster $[Os_6(\mu\text{-}H)_2\{(NC_5H_3)_2S_2\}(CO)_{20}]$ **5.5**. All three Os_3 clusters are different and each is asymmetric. The direct reaction of $[Os_3(CO)_{12}]$ with 4,4-dipyridyl disulfide also yielded cluster **5.5** in a very low yield.

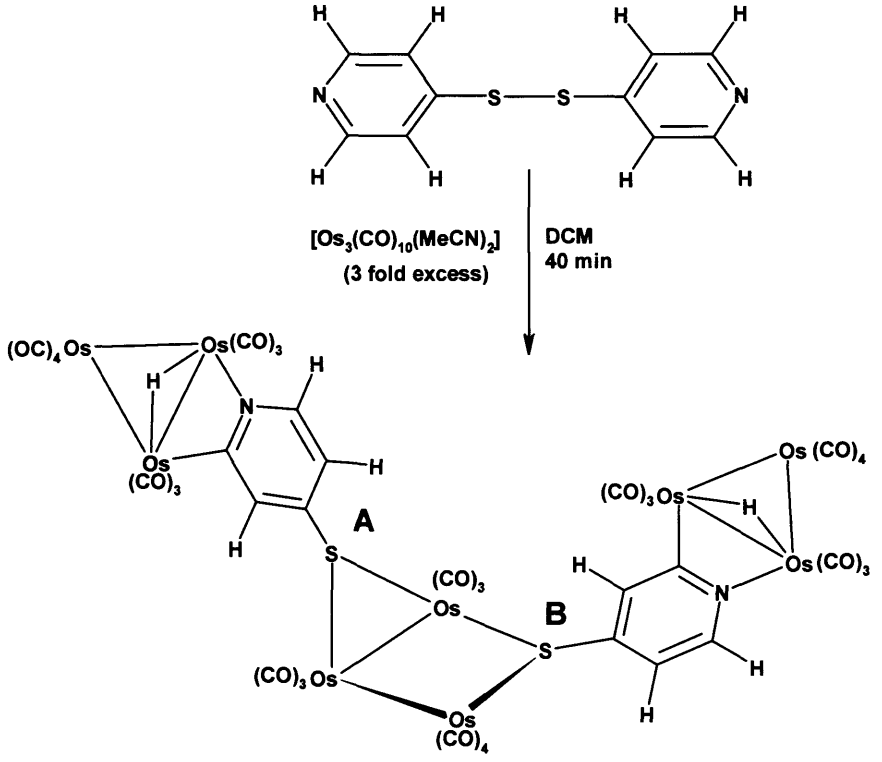

The infrared spectrum of compound $[Os_9(\mu\text{-}H)_2(NC_5H_3S)_2(CO)_{30}]$ **5.6** gave a complex absorption pattern in the carbonyl region. The absorptions occur at: 2121(w), 2014(w), 2075(w), 2065(vs), 2055(m), 2041(w), 2023(vs), 2016(vw) 2001(m), 1990(v,sh), 1977(w,sh) and 1966(w,sh) cm^{-1}. This complex spectrum can be rationalised by comparing the infrared spectrum of the unsymmetrical cluster $[Os_3(SCH_2Ph)_2(CO)_{10}]$ **2.7** along with the osmium pyridine cluster $[Os_3(\mu\text{-}$

H)(NC_5H_4)$(CO)_{10}$], as the combination of the IR spectra of both clusters matches closely to that of [$Os_9(\mu\text{-}H)_2(NC_5H_3S)_2(CO)_{30}$] **5.6**. The EI-MS gave m/z = 2788 (calc. 2788) with the successive loss of CO, pyridine and osmium atoms.

The ^{1}H NMR spectrum of cluster [$Os_9(\mu\text{-}H)_2(NC_5H_3S)_2(CO)_{30}$] **5.6** exhibited 4 sets of signals with each set giving a total of 8 signals. In the hydride region we observed eight separate singlet hydride signals, two for each of the four isomers, **Figure 5.8**. The ^{1}H NMR data for [$Os_9(\mu\text{-}H)_2(NC_5H_3S)_2(CO)_{30}$] **5.6** is given below:

Set 1 protons. δ	Set 2 protons. δ	Set 3 protons. δ	Set 4 protons. δ	Hydride δ
6.47(d)	6.79(d)	7.27(d)	7.88(d)	-14.79 (s,OsH)
6.48(d)	6.80(d)	7.30(d)	7.89(d)	-14.80 (s,OsH)
6.52(d)	6.81(d)	7.38(d)	7.90(d)	-14.81 (s,OsH)
6.53(d)	6.82(d)	7.42(d)	7.92(d)	-14.82 (s,OsH)
6.58(d)	6.84(d)	7.45(d)	7.93(d)	-14.88 (s,OsH)
6.58(d)	6.85(d)	7.48(d)	7.94(d)	-14.89 (s,OsH)
6.62(d)	6.86(d)	7.50(d)	7.95(d)	-14.90 (s,OsH)
6.63(d)	6.87(d)	7.59(d)	7.96(d)	-14.91 (s,OsH)

We also observed signals for another very minor species, which have been assigned δ 6.51 (d, 1H), 6.52 (d, 1H), 7.19 (s, 1H), 7.28 (s, 1H), 7.81 (d, 1H), 7.82 (d, 1H), -14.94 (OsH). This corresponds possibly to an isomer of **5.6** with equivalent SR groups as in [$Os_3(SCH_2Ph)_2(CO)_{10}$], isomer **2.4**.

Interestingly, as with cluster [$Os_6(\mu\text{-}H)_2\{(NC_5H_3)S_2\}(CO)_{20}$] **5.5**, we now have a number of possible combinations. If the stereochemistries of the three clusters are described as Δ or Λ and the non-equivalent attachments of pyS at the central cluster as **A** and **B**, we then have eight distinct arrangements:

Δ **A** Δ **B** Δ Δ **A** Δ **B** Λ Δ **A** Λ **B** Λ Δ **A** Λ **B** Δ

Λ **A** Λ **B** Λ Λ **B** Λ **B** Δ Λ **A** Δ **B** Δ Λ **A** Δ **B** Λ

There are four diastereomers each having two enantiomers, which implies we should observe 4 sets of hydride and pyridine NMR signals. Note that ^{1}H NMR cannot be used to distinguish between enantiomers. We clearly observed ^{1}H NMR signals for 4 sets of diastereomers, each being associated with 2 hydride ligands, thus, giving rise to 8 hydride singlets. From the ^{1}H NMR spectrum, we could not assign signals to the particular diastereomeric forms. Attempts to separate the four diastereomers are in principle possible, especially in view of their well-separated NMR signals, which indicate that each cluster is sensitive to the stereochemistries of the others. However, we only observed a single band by TLC and did not attempt any other method of separation such as HPLC.

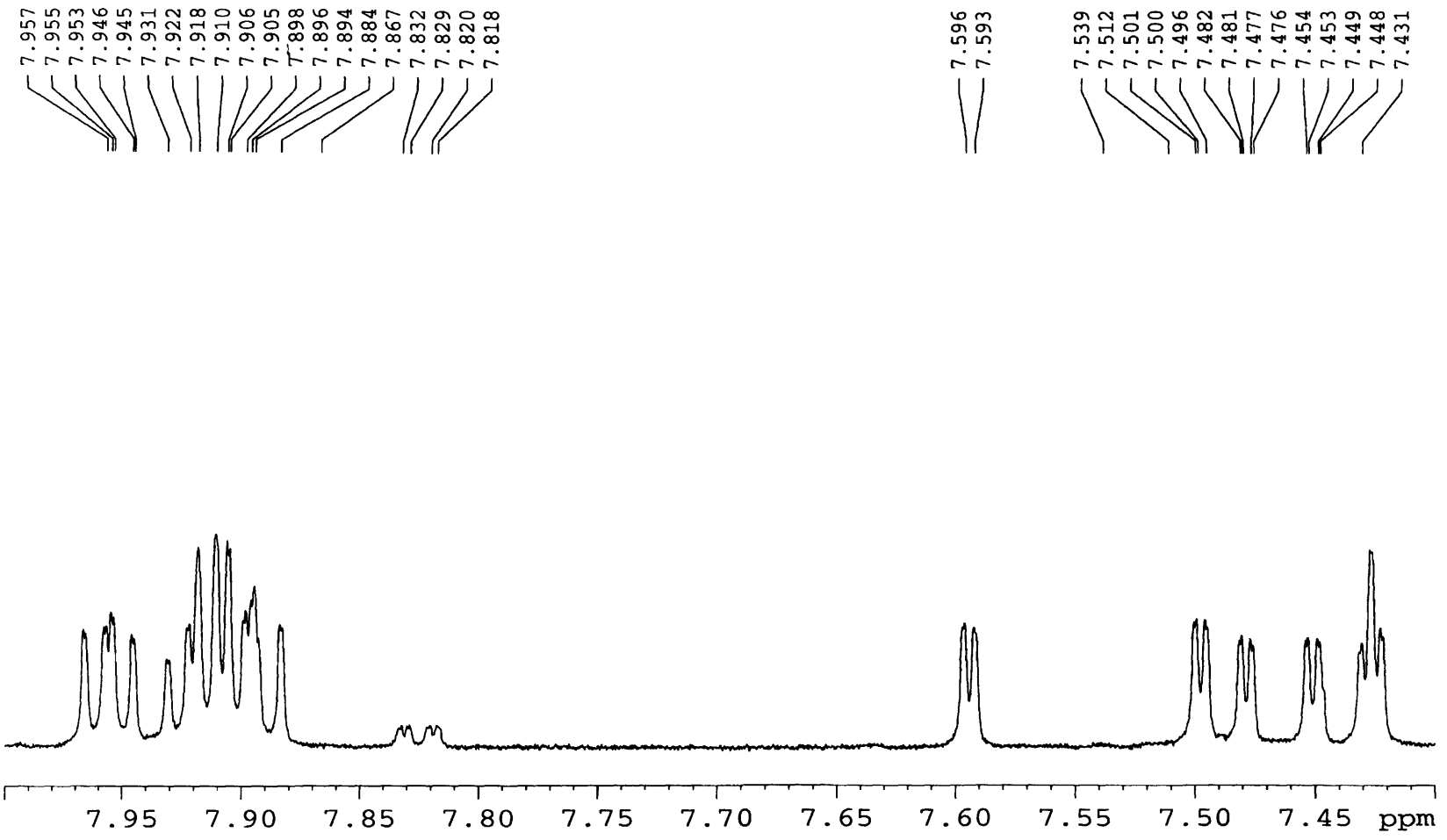

Figure 5.6. Part of the ^{1}H NMR of $[Os_9(\mu\text{-}H)_2(NC_5H_3S)_2(CO)_{30}]$ 5.6.

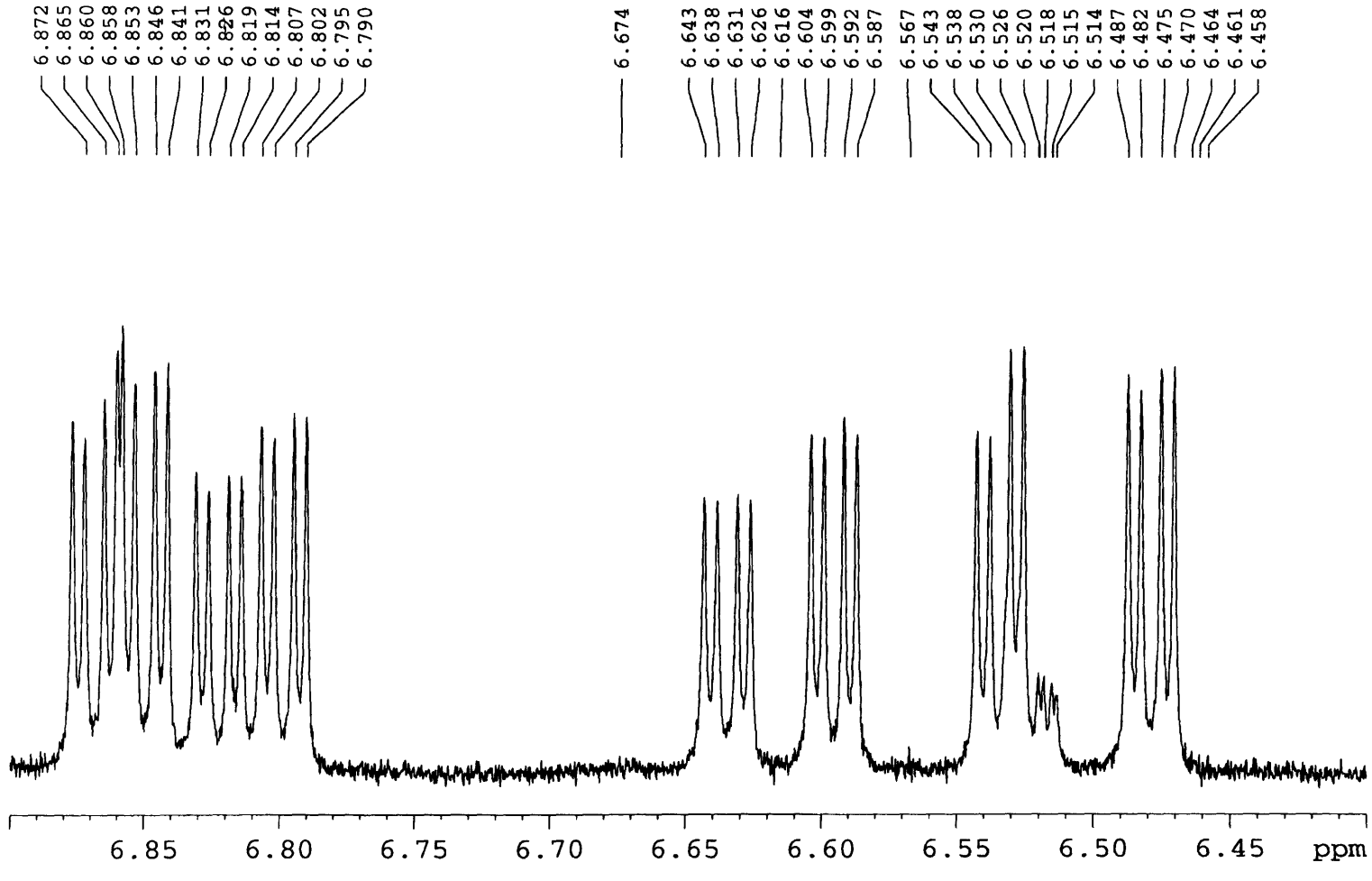

Figure 5.7. Part of the ^{1}H NMR of $[Os_9(\mu\text{-}H)_2(NC_5H_3S)_2(CO)_{30}]$ 5.6.

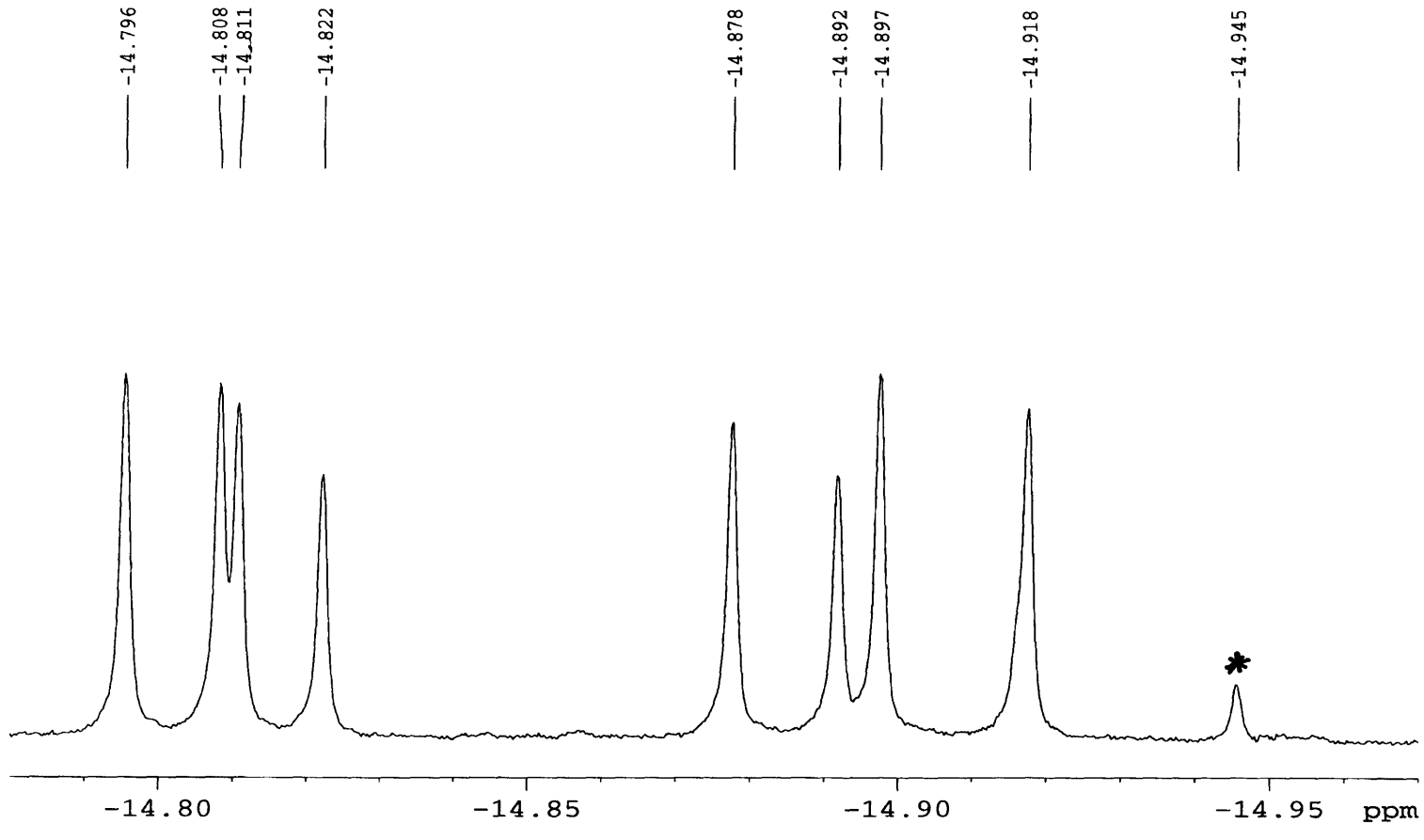

Figure 5.8. Part of the ^{1}H NMR of $[Os_9(\mu\text{-}H)_2(NC_5H_3S)_2(CO)_{30}]$ 5.6, showing the eight hydride signals along with the isomer hydride. * = impurity

5.3 Conclusions

In summary, the use of pyridine sulfides is a very useful method for the synthesis of linked clusters starting from $[Os_3(MeCN)_2(CO)_{10}]$ **1.3**. The direct reaction of an excess of **1.3** with 4-mercaptopyridine or 4,4-dipyridyl disulfide in dichloromethane solvent at room temperature yielded the new linked clusters, $[Os_6(\mu\text{-}H)_2(NC_5H_3S)(CO)_{20}]$ **5.4**, $[Os_6(\mu\text{-}H)_2\{(NC_5H_3)_2S_2\}(CO)_{20}]$ **5.5**, and $[Os_9(\mu\text{-}H)_2(NC_5H_3S)_2(CO)_{30}]$ **5.6**. These products were not expected, since under similar conditions the reactions of **1.3** with aminophenol and phenylene diamine did not produce the desired linked clusters in Chapter 4.

Interestingly, the reaction of 4-mercaptopyridine with an excess of cluster **1.3** readily yields the linked cluster $[Os_6(\mu\text{-}H)_2(NC_5H_3S)(CO)_{20}]$, with the cleavage of the S-H and C-H bonds. In this case, we found no evidence for the reaction at one end of the molecule deactivating the other. In the 4,4-dipyridyl disulfide case, initial reaction is always preferred at the two nitrogen ends leaving the S-S bond intact. It is quite remarkable that C-H bond activation is preferred to that of S-S activation. However, a further reaction with one mole of the cluster easily cleaves this S-S bond to give a unique Os_9 cluster. The crystal structure of $[Os_6(\mu\text{-}H)_2\{(NC_5H_3)_2S_2\}(CO)_{20}]$ **5.5** has also been determined, which gives a structure with C_2 symmetry. We assumed that this diastereomer is less soluble than the other or we were just fortuitous in picking the crystal from a mixture of the crystalline diastereomers.

Overall, we have found a simple and convenient method for the synthesis of high-nuclearity osmium clusters at room temperature. This method can be applied to other transition metals to yield linked clusters, mixed metal clusters or to form even larger clusters. The ability to form high nuclearity osmium clusters at room temperature is unprecedented. The chemistry of cluster $[Os_6(\mu\text{-}H)_2\{(C_5H_3N)_2S_2\}(CO)_{20}]$ could be further developed by investigating the reaction at the S-S bond with other transition metals, as this could play a key role in understanding the chemistry of metal sulfides which plays an important role in both industry and biology.

5.4 Experimental

The bis-acetonitrile cluster $[Os_3(MeCN)_2(CO)_{10}]$ was prepared by published methods.[18] Tetramethylthiuram disulfide, 4-mercaptopyridine, and 4-4-dipyridyl disulfide were purchased from Aldrich plc and used without further purification. The ^1H NMR spectra were recorded on a Bruker AMX300 MHz, AMX400 MHz or AMX 500 MHz spectrometer and the data was processed using XWIN-NMR. Electron Ionisation (EI) and Fast Atom Bombardment (FAB) mass spectra were acquired from the UCL mass spectrometry service. IR spectra were recorded on a Shimadzu 8700 FT-IR spectrometer. Preparative Thin Layer Chromatography (TLC) (silica gel 60 HF_{254} with fluorescent indicator E. Merck, Germany) was prepared as aqueous slurry and was either dried in the air or in the oven at 100 °C overnight before use. All the reactions were carried out under nitrogen gas unless otherwise stated.

5.4.1 Reactions of $[Os_3(\mu\text{-}H)_2(CO)_{10}]$ with tetramethylthiura disulfide

The purple unsaturated cluster (0.0801 g, 0.0934 mmol) and tetramethylthiuram disulfide (0.0734 g, 0.0306 mmol) in toluene (20 cm^3) was heated at 80° C for 30 minutes. The colour changed from purple to bright yellow. TLC using petroleum spirit (40-60 °C): dichloromethane (4:1 v/v) as eluent, gave three bands. The major band separated as an impure compound, which was unable to be purified further by TLC. We purified the major band by crystallisation using three solvent mixtures: dichloromethane, acetonitrile and heptane, in the ratio of 1:1:1, which yielded some yellow crystals which were separated by filtration. The yellow filtrate was left at room temperature for further crystallisation. However, this was unsuccessful. The yellow crystals were characterised as $[Os(Me_2NCS_2)_2(CO)_3]$ **5.1** (0.0241 g, 26%), and from the remaining bands we characterised $[Os_3(\mu\text{-}S_2CNMe_2)(\mu\text{-}S)(\mu\text{-}S{=}CNMe_2)(CO)_7]$ **5.2** (< 2%) in trace amounts.

IR (dichloromethane): cluster $[Os(Me_2NCS_2)_2(CO)_3]$ **5.1**, 2100(s), 2030(s) cm^{-1}. ^1H NMR ($CDCl_3$, 25 °C): δ 3.63 (s, 3H, CH_3), 3.22 (s, 3H, CH_3), 3.21(s, 3H, CH_3), 3.20

(s, 3H, CH_3). EI-MS: m/z = 516, with the successive loss of CO ligands. C, 20.71; H, 2.36; N, 5.32; S, 22.23. Calc. C, 21.00; H, 2.34; N, 5.40; S, 24.90.

IR υ(CO) (dichloromethane): cluster $[Os_3(\mu\text{-}S_2CNMe_2)(\mu\text{-}S)(\mu\text{-}S{=}CNMe_2)(CO)_7]$ **5.2**. ^1H NMR ($CDCl_3$, 25 °C): δ 3.63 (s, 3H, CH_3), 3.2 (s, 3H, CH_3), 3.21(s, 3H, CH_3), 3.20 (s, 3H, CH_3). EI-MS: m/z = 1012/1012.

5.4.2 Thermolysis of $[Os(Me_2NCS_2)_2(CO)_3]$.

A solution of $[Os(Me_2NCS_2)_2(CO)_3]$ **5.1** (0.0150 g, 0.0291 mmol) in xylene (15 cm^3) was refluxed for 3 hours. The colour changed from yellow to orange/yellow. TLC using petroleum spirit (40-60° C): dichloromethane (4:1 v/v) as eluent, gave three bands of which two have been characterised as $[Os(Me_2NCS_2)_2(CO)_2]$ (0.0003 g, 2%) and the starting material $[Os_3(CO)_{12}]$.

IR υ(CO) (dichloromethane): cluster $[Os(Me_2NCS_2)_2(CO)_2]$ **5.3**, 2017(s), 1943(m) cm^{-1}. EI-MS gave m/z = 488 (calc. 488), with the successive loss of two CO ligands.

5.4.3 Reaction of $[Os_3(MeCN)_2(CO)_{10}]$ with 4-Mercaptopyridine

4-Mercaptopyridine (0.0062 g, 0.0558 mmol) was dissolved in acetonitrile (30 cm^3) under nitrogen by stirring for 5 minutes. $[Os_3(MeCN)_2(CO)_{10}]$ (0.1059 g, 0.1128 mmol) was partially dissolved in acetonitrile (10 cm^3) and added slowly to the 4-mercaptopyridine solution over a 5 minute period. The solution was left at 30° C for 1 hour. TLC using hexane: dichloromethane (4:1v/v) as eluent gave two bands. The major band was characterised as $[Os_6(\mu\text{-}H)_2(\mu\text{-}SC_5H_3N)_2(CO)_{20}]$ **5.4** (0.0874 g, 42%). The minor band was not characterised as it was only obtained in trace amounts.

IR υ(CO) (cyclohexane): cluster $[Os_6(\mu\text{-}H)_2(\mu\text{-}SC_5H_3N)_2(CO)_{20}]$ **5.4**, 2112(w), 2104(w), 2071(vs), 2065(s), 2054(m), 2027(vs), 2020(m), 2009(w), 2002(m) 1992(m), 1978(w,br) cm^{-1}. ^1H NMR ($CDCl_3$, 25 °C): δ 7.90 (d, 1H, *J* 6.03 Hz), 7.03 (d, 1H, *J* 2.31), 6.61 (dd, 1H, *J* 2.31 and 6.08), -14.79 (s, 1H, μ-H), -17.23 (s, 1H, μ-H). EI-MS, m/z = 1823 (calcd. 1823) with the loss of CO ligands. EA for $[Os_6(\mu\text{-}$

$H)_2(\mu\text{-}SC_5H_3N)_2(CO)_{20}]$ **5.4**: C, 16.62; H, 0.13; N, 0.58; S, 0.60. Calc. C, 16.46; H, 0.27; N, 0.77; S, 1.76.

5.4.4 Reaction of 4,4-dipyridyl disulfide with 2-fold excess of $[Os_3(CO)_{10}(MeCN)_2]$

The labile cluster $[Os_3(MeCN)_2(CO)_{10}]$ (0.1340 g, 0.1423 mmol, 2 fold excess) and 4,4-dipyridyl disulfide (0.0258 g, 0.1172 mmol) in toluene (20 cm^3) were heated at 80° C for 3 hours. Some brown material precipitated out. The solvent was removed under reduced pressure, and TLC using petroleum spirit (40-60° C): dichloromethane (4:1 v/v) as eluent, gave four bands of which one has been characterised as $[Os_6(\mu\text{-}H)_2\{(NC_5H_3)_2S_2\}(CO)_{20}]$ **5.5** (0.0941 g, 34%, g). Crystals were grown from a dichloromethane/heptane solution by slow evaporation at room temperature. IR υ(CO) (cyclohexane): 2104(w), 2064(vs), 2053(s), 2023(vs), 2009(m), 2003(m), 1992(m), 1977(w) cm^{-1}. ^1H NMR ($CDCl_3$, 25°C): δ 7.95 (d, 1H, *J* 6.20 Hz), 7.31 (d, 1H, *J* 2.25 Hz), 6.69 (dd, 1H, *J* 6.20 Hz), -14.84 (1H, OsH)). The minor isomer gave, ^1H NMR ($CDCl_3$, 25°C): δ 7.94 (d, 1H) 7.37 (d, 1H), 6.70 (dd, 1H), -14.83 (1H, μ-H). FAB-MS gave m/z = 1934 (calc.1934), with the successive loss of CO ligands. EA for $[Os_6(\mu\text{-}H)_2\{(NC_5H_3)_2S_2\}(CO)_{20}]$ **5.5**: C, 19.14; H, 0.41; N, 1.25; S, 1.62. Calc. C, 18.74; H, 0.41; N, 1.45; S, 3.36.

5.4.5 Reaction of 4,4-dipyridyl disulfide with a 3-fold excess of $[Os_3(MeCN)_2(CO)_{10}]$

4,4-dipyridyl disulfide (0.0067 g, 0.0304 mmol) was dissolved in dichloromethane by stirring for 5 minutes. Cluster $[Os_3(MeCN)_2(CO)_{10}]$ (0.0875 g, 0.0932 mmol, 3-fold excess) was dissolved in a minimum amount of dichloromethane (2 cm^3) and the yellow solution was added slowly to the 4,4 dipyridyl disulfide solution over a 5 minute period. The solution was left stirring at room temperature for 40 minutes after which time the IR indicated a complete reaction. TLC using dichloromethane: hexane (1:2 v/v) as eluent, isolated three bands of which one has been characterised as $[Os_9(\mu\text{-}H)_2(C_5H_3NS_2C_5H_3N)(CO)_{30}]$ **5.6** (0.0243g, 29%).

IR υ(CO) (cyclohexane): cluster $[Os_9(\mu\text{-}H)_2(C_5H_3NS_2C_5H_3N)(CO)_{30}]$ **5.6**, 2121(w), 2014(w), 2075(w), 2065(vs), 2055(m), 2041(w), 2023(vs), 2016(vw) 2001(m), 1990(v,sh), 1977(w, sh) and 1966(w, sh) cm^{-1}. EI-Maldi, gave m/z = 2788 (calc.2788). ^1H NMR ($CDCl_3$, 25 °C) for $[Os_9(\mu\text{-}H)_2(NC_5H_3S_2C_5H_3N)(CO)_{30}]$ **5.6** is shown below.

Set 1 protons. δ	Set 2 protons. δ	Set 3 protons. δ	Set 4 protons. δ	Hydride δ
6.47(d,1H)	6.79(d,1H)	7.27(d, 1H)	7.88(d, 1H)	-14.79 (s,OsH)
6.48(d, 1H)	6.80(d, 1H)	7.30(d, 1H)	7.89(d, 1H)	-14.80 (s,OsH)
6.52(d, 1H)	6.81(d, 1H)	7.38(d, 1H)	7.90(d, 1H)	-14.81 (s,OsH)
6.53(d, 1H)	6.82(d, 1H)	7.42(d, 1H)	7.92(d, 1H)	-14.82 (s,OsH)
6.58(d, 1H)	6.84(d, 1H)	7.45(d, 1H)	7.93(d, 1H)	-14.88 (s,OsH)
6.58(d, 1H)	6.85(d, 1H)	7.48(d, 1H)	7.94(d, 1H)	-14.89 (s,OsH)
6.62(d, 1H)	6.86(d, 1H)	7.50(d, 1H)	7.95(d, 1H)	-14.90 (s,OsH)
6.63(d, 1H)	6.87(d, 1H)	7.59(d, 1H)	7.96(d, 1H)	-14.91 (s,OsH)

Other minor species ^1H NMR ($CDCl_3$, 25 °C): δ 6.51(d, 1H), 6.52(d, 1H), 7.19(s, 1H), 7.28(s, 1H), 7.81(d, 1H), 7.82(d, 1H), -14.94(OsH).

5.4.6 Reaction of $[Os_3(CO)_{12}]$ with 4,4-dipyridyl disulfide.

The yellow cluster $[Os_3(CO)_{12}]$ (0.0881 g, 0.0967 mmol) and 4,4 dipyridyl disulfide (0.01062 g, 0.0483 mmol) in xylene (20 cm^3) were refluxed for 48 hours, after which time the reaction went cloudy. The reaction was cooled and the solvent removed under reduced pressure using a rotary evaporator. TLC using petroleum spirit (40-60° C): dichloromethane (4:1 v/v) as eluent, isolated two bands in small yields, which have been characterised as $[Os_6(\mu\text{-}H)_2\{(NC_5H_3)_2S_2\}(CO)_{20}]$ **5.5** but this was not 100% pure. IR υ(CO) (cyclohexane): cluster **5.5**, 2104(w), 2064(vs), 2053(s), 2023(vs), 2009(m), 2004(m), 1992(m), 1977(w,br) cm^{-1}. The cluster was characterised by its infrared spectrum only.

References

1. (a) A. J. Deeming. *Adv. Organomet. Chem.* 1986, **26**, 1. (b) A. J. Deeming. *Comprehensive Organomet. Chem.* E. W. Abel, F. G. A. Stone and G. Wilkinson. 1986, **2**, 683.
2. K. Burgess. *Polyhedron* 1984, **3**, 1175.
3. R. D. Adams. *Acc. Chem. Res.* 1983, **16**, 67.
4. Edited by B. F. G. Johnson. *Transition Metal Clusters* 1980, John Wiley and Sons, London and New York.
5. B. F. G. Johnson, J. Lewis and P. A. Kilty. *J. Chem. Soc. (A).* 1968, 2859
6. C. W. Bradford and R. S. Nyholm. *J. Chem. Soc. Chem. Commun.* 1976, 384.
7. S. R. Drake and P. A. Loveday. *Inorg. Synth.* 1990, **28**, 230.
8. M. I. Bruce, C. M. Jensen and N. L. Jones. *Inorg. Synth.* 1990, **28**, 216.
9. C. E. Housecroft, M. E. O'Neill, K. Wade and B. C. Smith. *J. Organomet. Chem.* 1981, **213**, 35.
10. H. K. Sanati, A. Becalska, A. K. Ma and R. K. Pomeroy. *J. Chem. Soc. Chem. Commun.* 1990, 197.
11. B. F. G. Johnson, J. Lewis and P.A. Kilty. *J. Chem. Soc. (A).* 1968, 2854.
12. A. J. Deeming, B. F. G. Johnson and J. Lewis. *J. Organomet. Chem.* 1969, **17**, 40.
13. B. F. G. Johnson and A. Bott. *J. Chem. Soc. Dalton Trans.* 1990, 2437.
14. C. E. Housecroft, K. Wade and B. C. Smith. *J. Chem. Soc. Chem. Commun.* 1978, 765.
15. N. E. Leadbeater. *J. Organomet. Chem.* 1999, **573**, 211.
16. C. H. Wei and L. F. Dahl. *J. Am. Chem. Soc.* 1969, **91**, 1351.
17. Y. Shvo and E. Hazum. *J. Chem. Soc. Chem. Commun.* 1974, 336.
18. B. F. G. Johnson, J. Lewis and D. A. Pippard. *J. Organomet. Chem.* 1978, **145**, C4.

19. K. Burgess, B. F. G. Johnson, J. Lewis and P. R. Raithby. *J. Chem. Soc. Dalton Trans.* 1982, 2085.

20. M. Tachikawa and J. R. Shapley. *J. Organomet. Chem.* 1977, **124**, C19.

21. S. R. Drake and R. Khatter. *Organomet. Synth.* 1988, **4**, 234

22. J. N. Nicholls and M. D. Vargas. *Inorg. Synth.* 1990, **28**, 232.

23. B. F. G. Johnson, J. Lewis and D. A. Pippard. *J. Chem. Soc. Dalton Trans.* 1981, 407.

24. S. R. Drake and R. Khatter. *Organomet. Synth.* 1988, **4**, 234

25. H. G. Ang, W. L. Kwik and W. K. Leong. *J. Organomet. Chem.* 1989, **379**, 325.

26. N. E. Leadbeater. *J. Organomet. Chem.* 1999, 211.

27. G. R. Frauenhoff, S. R. Wilson and J. R. Shapley. *Inorg. Chem.* 1991, 30.

28. A. J. Edwards, N. E. Leadbeater, J. Lewis and P. R. Raithby. *J. Organomet. Chem.* 1995, **15**, 513.

29. H. D. Kaesz. *Inorg. Synth.* 1990, **28**, 219.

30. S. F. A. Kettle and P. L. Stanghellini. *Inorg. Chem.* 1982, **2**, 1447.

31. D. E. Sherwood Jr. and M. B. Hall. *Inorg. Chem.* 1982, **21**, 3458.

32. G. E. Hawkes, E. W. Randell, S. Aime, D. Osella and J. E. Elliot. *J. Chem. Soc. Dalton Trans.* 1984, 279.

33. A. J. Deeming and S. Hasso. *J. Organomet. Chem.* 1975, **88**, C21.

34. A. J. Deeming and S. Hasso. *J. Organomet. Chem.* 1976, **114**, 313.

35. N. E. Leadbeater, J. Lewis and P. R. Raithby. *J. Organomet. Chem.* 1997, **543**, 251.

36. B. F. G. Johnson, P. A. Kilty, and J. Lewis. *Chem. Comm.* 1968, 180.

37. G. R. Crooks, B. F. G. Johnson, J. Lewis, and I. G. Williams. *J. Chem. Soc. (A).* 1969, 797.

38. (a) R. Mason. *Pure Appl. Chem.* 1973, **33**, 513. (b) R. Mason and D. M. P. Mingos. *J. Organomet. Chem.* 1973, **50**, 53.

39. A. J. Deeming and M. Underhill. *J. Organomet. Chem.* 1972, **42**, C60.

40. A. J. Deeming and M. Underhill. *J. Chem Soc. Chem. Commun.* 1973, 277.

41. A. J. Canty, B. F. G. Johnson, and J. Lewis. *J. Organomet. Chem.* 1972, **36**, C35.

42. A. J. P. Domingos, B. F. G. Johnson, and J. Lewis, *J. Organomet. Chem.* 1972, **36**, C43.

43. A. J. Deeming and M. Underhill. *J. Chem. Soc. Dalton Trans.* 1973, 2727.

44. D. Braga, P. J. Dyson, F. Grepioni and B. F. G. Johnson. *Chem. Rev.* 1994, **94**, 1585.

45. M. P. Gomez-Sal, B. F. G. Johnson, J. Lewis, P. R. Raithby and A. H. Wright, *J. Chem. Soc. Chem. Commun.* 1985, 1862.

46. (a) E. G. Bryan, B. F. G. Johnson, J. Lewis and M. McPartlin. *J. Chem. Soc. Dalton Trans.* 1976, 254. (b) E. G. Bryan, B. F. G. Johnson and J. Lewis. *J. Chem. Soc. Dalton Trans.* 1977, 1328.

47. B. F. G. Johnson, J. Lewis, M. Martinelli, A. H. Wright, D. Braga and F. Grepioni. *J. Chem. Soc. Chem. Commun.* 1990, 364.

48. A. J. Blake, P. J. Dyson, B. F. G. Johnson, C. M. Martin, J. G. M. Nairn, E. Parisini and J. Lewis. *J. Chem. Soc. Dalton Trans.* 1993, 981.

49. K. A. Azam, A. J. Deeming, R. E. Kimber and P. R. Shukla. *J. Chem. Soc. Dalton Trans.* 1976, 1853.

50. C. Choo Yin and A. J. Deeming. *J. Chem. Soc. Dalton Trans.* 1974, 1013.

51. A. J. Deeming, P. J. Manning, I. P. Rothwell, M. B. Hursthouse and N. P. C. Walker. *J. Chem. Soc. Dalton Trans.* 1984, 2039.

52. K. A. Azam, A. J. Deeming, I. P. Rothwell, M. B. Hursthouse and J. D. J. Backer-Dirks. *J. Chem. Soc. Dalton Trans.* 1981, 2039.

53. D. S. Bohle and H. Vahrenkamp. *Angew. Chem. Int. Ed. Engl.* 1990, **29**, 198.

54. P. Sundberg. *J. Chem. Soc. Chem. Commun.* 1987, 1307.

55. A. J. Deeming. Multiple interaction between arenes and metal atoms. *UCL Inorganic Lecture*, 2000.

56. R. D. Adams, D. Manning and B. E. Segmuller. *Organometallics* 1983, **2**, 149.

57. R. D. Adams and I. T. Horvath. *J. Am. Chem. Soc.* 1984, **106**, 1869.

58. E. W. Ainscough, A. M. Brodie, R. K. Coll, T. G. Kotch, A. J. Lees, A. J. A. Mair and J. M. Waters. *J. Organomet. Chem.* 1996, 517.

59. B. F. G. Johnson and A. Bott. *J. Chem. Soc. Dalton Trans.* 1990, 2437.

60. R. F. Alex and R. K. Pomeroy. *Organometallics* 1982, **1**, 452.

61. A. J. Deeming, S. Donovan-Mtunzi and S. E. Kabir. *J. Organomet. Chem.* 1985, 281.

62. A. J. Deeming, S. Donovan-Mtunzi, S. E. Kabir and P. J. Manning. *J. Chem. Soc. Dalton Trans.*1985, 1037.

63. M. I. Bruce, M. J. Liddell, C. A. Hughes, B. W. Skelton and A. H. White. *J. Organomet. Chem.*1988, **347**, 157.

64. M. R. Churchill and B. G. DeBoer. *Inorg. Chem.* 1977, **16**, 2397.

65. R. E. Benfield, B. F. G. Johnson, P. R. Raithby and G. M. Sheldrick. *Acta Crystallogr. Sect. B: Struct. Crystallogr. Cryst. Chem.* 1978, **B34**, 666.

66. R. D. Adams and N. M. Golembeski. *Inorg. Chem.*1979, **18**, 1909.

67. M. A. Gallop, B. F. G. Johnson and J. Lewis. *J. Chem. Soc. Chem. Commum.* 1987, 1831.

68. A. J. Deeming and M. B. Smith. *J. Chem. Soc. Chem. Commum.* 1993, 844.

69. J. McMurry. *Organic Chemistry.* 1995, **4**, 1070.

70. J. McMurry. *Organic Chemistry.* 1995, **4**, 512.

71. E. L. Muetterties, R. R. Burch and A. M. Stolzenberg. *Ann. Rev. Phys. Chem.* **1982**, 33, 89.

72. H. Vahrenkamp. *Angew. Chem. Int. Ed. Engl.* 1978, **17**, 379.

73. P. Chini, G. Longoni and V. G. Albano. *Adv. Organomet. Chem.* 1976, **14**, 285.

74. T. J. Meyer. *Prog. Inorg. Chem.* 1975, **19**, 1.

75. A. J. Carty. *Pure Appl. Chem.* 1972, **42**, C60.

76. H. Vahrenkamp. *Angew. Chem. Int. Ed. Engl.* 1975, **14**, 322.

77. A. J. Deeming. Triosmium Clusters, *Comprehensive Organometallic Chemistry II*; E. W. Abel, F. G. A. Stone and G. Wilkinson. 1995, **7**, 726.

78. R. D. Adams. *Polyhedron* 1985, **4**, 2003.

79. R. D. Adams and I. T. Horváth. *Prog. Inorg. Chem.* 1985, **33**, 127.

80. R. D. Adams and I. T. Horváth. *Inorg. Synth.* 1989, **26**, 3003.

81. P. V. Broadhurst, B. F. G. Johnson and J. Lewis, *J. Chem. Soc. Dalton Trans.* 1982, 1881.

82. A. J. Arce, P. Arrojo, Y. De Sanctis, A. J. Deeming and D. J. West. *Polyhedron* 1991, **11**, 1013.

83. A. J. Deeming, R. Vaish, A. J. Arce, P. Arrojo and Y. De Sanctis. *Polyhedron* 1994, **13**, 3285.

84. E. W. Abel, R. Khan, K. Kite, K. G. Orrell and V. Šik. *J. Chem. Soc. Dalton Trans.* 1980, 2220

85. A. B. Ali. *MSc Thesis*. UCL. University of London, 2000.

86. G. R. Crooks, B. F. G. Johnson, J. Lewis and I. G. Williams. *J. Chem. Soc. (A)*. 1969, 797.

87. B. F. G. Johnson, J. Lewis and P. A. Kilty. *J. Chem. Soc. (A)*. 1968, 2859.

88. R. D. Adams, G. Chen, S. Sun and T. A. Wolfe. *J. Am. Chem. Soc.* 1990, **112**, 868.

89. E. W. Abel, S. K. Bhargava, K. G. Orrell, A. W. G. Platt, V. Šik and T. S. Cameron. *J. Chem. Soc. Dalton Trans.* 1985, 345.

90. E. W. Abel, R. P. Bush, F. J. Hopton and J. Jenkins. *J. Chem. Soc. Chem. Commun.* 1966, 58.

91. G. Hunter and R. C. Massey. *J. Chem. Soc. Dalton Trans.* 1976, 2007.

92. G. Hunter and R. C. Massey. *J. Chem. Soc. Dalton Trans.* 1976, 205.

93. R. J. Cross, G. Hunter and R. C. Massey. *J. Chem. Soc. Dalton Trans.* 1976, 2015.

94. E. W. Abel, K. M. Higgins, K. G. Orrell and V. Šik. *J. Chem. Soc. Dalton Trans.* 1985, 2195.

95. E. W. Abel, R. P. Bush, F. J. Hopton and J. Jenkins. *J. Chem. Soc. Chem. Commun.*1966, 58.

96. A. Eisenstadt, C. M. Giandomenico, M. F. Frederick and R. M. Laine, *Organometallics* 1985, **4**, 2033.

97. A. J. Deeming. *Adv. Organomet. Chem.* 1986, **26**, 1.

98. S. Shouheng, L. K. Yeung, D. A. Sweigart, T. Y. Lee, S. S. Lee, Y. K. Chung, S. R. Switzer and R. D. Pike. *Organometallics* 1995, **14**, 2613.

99. M. F. Semmelhack, G. R. Clark, D. C. Garcia, J. J. Harrison, Y. Thebtarnonth, W. A. Wuff and A. Yamashita. *Tetrahedron* 1981, **37**, 3957.

100. E. C. Constable. *Polyhedron* 1984, **3**, 1037.

101. Md. J. Abedin, B. Bergman, R. Holmquist, R. Smith, E. Rosenberg, J. Ciurash, K. Hardcastle, J. Roe, V. Vazquez, C. Roe, S. E. Kabir, S. Alam and K. A. Azam. *Coord. Chem. Rev.* 1999, **190-192**, 975.

102. S. E. Kabir, D. S. Kolwaite, E. Rosenberg, K. Hardcastle, W. Cresswell and J. Grindstaff. *Organometallics* 1995, **14**, 3611.

103. E. Rosenberg, Md. J. Abedin, D. Rokhsana, D. Osella, L. Milone, C. Nervi and J. Fielder. *Inorg. Chim. Acta.* 2000, **300-302**, 769.

104. C. Choo Yin and A. J. Deeming. *J. Chem. Soc. Dalton Trans.* 1975, 2091.

105. C. Choo Yin. *Ph.D. Thesis.* UCL. University of London, 1975.

106. J. A. Van Doorn and P.W. N. M. Van Leeuwen. *J. Organomet. Chem.* 1981, **222**, 299.

107. D. Roberto, E. Lucenti, C. Roveda and R. Ugo. *Organometallics* 1997, **16**, 5974.

108. J. R. Moss and W. A. G. Graham. *J. Organomet. Chem.* 1970, **23**, C47.

109. S. A. R. Knox, J. W. Koepke, M. A. Andrews and H. D. Kaesz. *J. Am. Chem. Soc.* 1975, **97**, 3942.

110. B. F. G. Johnson, J. Lewis, P. R. Raithby, G. M. Sheldrick, K. Wong and M. McPartlin. *J. Chem. Soc. Dalton Trans.* 1978, 673.

111. C. Dossi, R. Psaro, D. Roberto, R. Ugo and G. M. Zanderighi. *Inorg. Chem.* 1990, **29**, 4368.

112. A. J. Deeming and I. P. Rothwell. *J. Chem. Soc. Dalton Trans.* 1980, 1259.

113. M. Chao, S. Kumaresen, Y. Wen, S. Lin, J. R. Hwu and K. Lu. *Organometallics* 2000, **19**, 714.

114. V. F. Allen, R. Mason and P. B. Hitchcock. *J. Organomet. Chem.* 1977, **140**, 297.

115. J. R. Norton, J. P. Collmann, G. Dolcetti and W. T. Robinson. *Inorg. Chem.* 1972, **11**, 382.

116. A. M. Clark, C. E. F. Rickard, W. R. Roper and L. J. Wright. *J. Organomet. Chem.* 1997, **545-546**, 619.

117. B. F. G. Johnson, J. Lewis, P. R. Raithby, G. M. Sheldrick, K. Wong and M. McPartlin. *J. Chem. Soc. Dalton Trans.* 1978, 673.

118. H. Wadepohl. *Angew Chem. Int. Ed. Engl.* 1992, **31**, 247.

119. F. Hein. *Chem. Ber.* 1919, **52**, 195.

120. H. H. Zeiss and M. Tsutsui. *126 th Meet. Am. Chem. Soc.* 1954; *J. Am. Chem. Soc.* 1957, **79**, 3062.

121. E. O. Fischer and W. Hafner. *Z. Naturforsch.* 1955, **10**, 665.

122. E. O. Fischer and K. Öfele. *Chem. Ber.* 1957, **90**, 2532.

123. H. Wadepohl, K. Büchner, M. Herrmann and H. Pritzkow. *Organometallics* 1991, **10**, 861.

124. W. Weng, T. Bartik and J. A. Gladysz. *Angew. Chem. Int. Ed. Engl.* 1994, **33**, 2199.

125. W. Weng and J. A. Gladysz. *J. Chem. Soc. Chem. Commun.* 1994, 2655.

126. F. Coat and C. Lapinte. *Organometallics* 1996, **15**, 477.

127. E. W. Ainscough, A. M. Brodie, R. K. Coll, T. G. Kotch, A. J. Lees, A. J. A. Mair and J. M. Waters. *J. Organomet. Chem.* 1996, **517**, 173.

128. K. A. Azam, A. J. Deeming, R. E. Kimber and P. R. Shukla. *J. Chem. Soc. Dalton Trans.* 1976, 1853

129. B. F. G. Johnson, J. Lewis and D. A. Pippard. *J. Chem. Soc. Dalton Trans.* 1981, 407.

130. K. A. Azam, A. J. Deeming and I. P. Rothwell. *J. Chem. Soc. Dalton Trans.* 1981, 91.

131. K. A. Azam, A. J. Deeming, I. P. Rothwell, M. B. Hursthouse and J. D. J. Backer-Dirks. *J. Chem. Soc. Dalton Trans.* 1981, 2039.

132. C. Choo Yin and A. J. Deeming. *J. Chem. Soc. Dalton Trans.* 1973, 1013.

133. K. A. Azam, A. J. Deeming, I. P. Rothwell, M. B. Hursthouse and L. New. *J. Chem. Soc. Chem. Commun.* 1978, 1086.

134. J. Chatt, J. D. Garforth, N. P. Johnson and G. A. Rowe. *J. Chem. Soc.Chem. Commun* 1964, 1012.

135. G. Hogarth, T. Norman and S. P. Redmond. *Polyhedron* 1999, **18**, 1221.

136. G. Hogarth, D. G. Humphrey, N. Kaltsoyannis, W.-S. Kim, M.-Y. (Venus) Lee, T. Norman and S. P. Redmond. *J. Chem. Soc. Dalton Trans.* 1999, 2705.

137. W. Heiber and J. Z. Gruber. *Anorg. Allg. Chem.* 1958, **269**, 91.

138. K. H. Whitmire, Iron compounds without hydrocarbon ligands, *Comprehensive Organometallics Chemistry II*; G. Wilkinson, F. G. A. Stone and E. W. Abel., Eds; Pergamon Press: New York, 1995; vol. 7, Chapter 1.

139. L.-C. Song, G.-L. Lu, O.-T. Hu, H.-T. Fan, Y. Chen and J. Sun. *Organometallics* 1999, **18**, 3258, and references therein.

140. R. R. D. M. Speel and A. J. Deeming. *UCL.* unpublished.

141. H. H. Murray, L. W. Wei, S. E. Sherman, M. A. Eriksen, B. Carstensen, T. R. Halbert and E. I. Stiefel. *Inorg. Chem.* 1995, **34**, 841.

142. W.-Y. Wong, S.-H. Cheung, S.-M. Lee and S.-Y. Leung. *J. Organomet. Chem.* 2000, **596**, 36.

143. R. Minkwitz, H. Borrmann and J. Nowicki. *Z. Naturforsch.* 1992, **47**, 915.

144. R. D. Adams, O.-S. Kwon and M. D. Smith. *Inorg. Chem.* 2002, **41**, 5525.

145. R. D. Adams, O.-S. Kwon and M. D. Smith. *Organometallics* 2002, **21**,1960.

146. R. D. Adams, O.-S. Kwon and M. D. Smith. *Organometallics* 2002, **41**,1658.

147. R. D. Adams, B. Captain, O.-S. Kwon and S. Miao. *Inorg. Chem.* 2003, **42**, 3356.

Appendix - Crystallographic data

Table 2.4a. Crystallographic data for $[Os_3(\mu\text{-}SCH_2Ph)_2(CO)_{10}]$ 2.2.

Chemical formula	$C_{24}H_{14}O_{10}Os_3S_2$	
Formula weight	1097.07	
Temperature	150(2) K	
Radiation, wavelength	MoKα, 0.71073 Å	
Crystal system, space group	monoclinic, $P2_1$	
Unit cell parameters	a = 9.6956(10) Å	α = 90°
	b = 14.8885(16) Å	β = 99.481(2)°
	c = 9.8411(10) Å	γ = 90°
Cell volume	1401.2(3) $Å^3$	
Z	2	
Calculated density	2.600 g/cm^3	
Absorption coefficient μ	13.770 mm^{-1}	
F(000)	996	
Crystal colour and size	pale yellow, 0.44 × 0.18 × 0.17 mm^3	
Data collection method	Bruker SMART APEX diffractometer	
	ω rotation with narrow frames	
θ range for data collection	2.10 to 28.25°	
Index ranges	h −12 to 12, k −19 to 19, l −13 to 13	
Completeness to θ = 26.00°	100.0 %	
Reflections collected	12340	
Independent reflections	6392 (R_{int} = 0.0244)	
Reflections with $F^2>2\sigma$	6312	
Absorption correction	semi-empirical from equivalents	
Min. and max. transmission	0.0646 and 0.2030	
Structure solution	direct methods	
Refinement method	Full-matrix least-squares on F^2	
Weighting parameters a, b	0.0332, 10.2279	
Data / restraints / parameters	6392 / 1 / 353	
Final R indices [$F^2>2\sigma$]	R1 = 0.0279, wR2 = 0.0694	
R indices (all data)	R1 = 0.0284, wR2 = 0.0696	
Goodness-of-fit on F^2	1.029	
Absolute structure parameter	0.538(11)	
Extinction coefficient	0.00000(10)	
Largest and mean shift/su	3.884 and 0.011	
Largest diff. peak and hole	2.101 and −1.229 e $Å^{-3}$	

Table 2.4b. Bond lengths [Å] and angles [°] for[$Os_3(\mu\text{-}SCH_2Ph)_2(CO)_{10}$] 2.2.

Os(1)–C(12)	1.899(9)
Os(1)–C(13)	1.915(9)
Os(1)–C(11)	1.935(9)
Os(1)–S(1)	2.3729(19)
Os(1)–S(2)	2.440(2)
Os(2)–C(21)	1.910(9)
Os(2)–C(22)	1.940(9)
Os(2)–C(24)	1.949(9)
Os(2)–C(23)	1.973(9)
Os(2)–S(2)	2.438(2)
Os(2)–Os(3)	2.9109(5)
Os(3)–C(33)	1.893(10)
Os(3)–C(31)	1.897(10)
Os(3)–C(32)	1.905(9)
Os(3)–S(1)	2.3874(19)
S(1)–C(40)	1.828(9)
S(2)–C(50)	1.836(9)
C(40)–C(41)	1.495(12)
C(41)–C(42)	1.373(13)
C(41)–C(46)	1.412(14)
C(42)–C(43)	1.389(14)
C(43)–C(44)	1.364(17)
C(44)–C(45)	1.400(17)
C(45)–C(46)	1.375(14)
C(50)–C(51)	1.520(12)
C(51)–C(52)	1.390(13)
C(51)–C(56)	1.391(14)
C(52)–C(53)	1.384(14)
C(53)–C(54)	1.359(15)
C(54)–C(55)	1.396(15)
C(55)–C(56)	1.367(14)
C(11)–O(11)	1.125(11)
C(12)–O(12)	1.133(12)
C(13)–O(13)	1.138(12)
C(21)–O(21)	1.143(12)
C(22)–O(22)	1.142(11)
C(23)–O(23)	1.124(11)
C(24)–O(24)	1.134(11)
C(31)–O(31)	1.139(13)
C(32)–O(32)	1.146(12)
C(33)–O(33)	1.152(12)
C(12)–Os(1)–C(13)	92.8(4)
C(12)–Os(1)–C(11)	90.3(4)
C(13)–Os(1)–C(11)	101.3(4)
C(12)–Os(1)–S(1)	95.2(3)
C(13)–Os(1)–S(1)	148.9(3)
C(11)–Os(1)–S(1)	108.7(3)
C(12)–Os(1)–S(2)	178.2(3)
C(13)–Os(1)–S(2)	88.2(3)
C(11)–Os(1)–S(2)	91.0(3)

Table 2.4b. Bond lengths [Å] and angles [°] for[$Os_3(\mu\text{-}SCH_2Ph)_2(CO)_{10}$] 2.2 continued.

S(1)–Os(1)–S(2)	83.22(7)
C(21)–Os(2)–C(22)	96.4(4)
C(21)–Os(2)–C(24)	91.1(4)
C(22)–Os(2)–C(24)	93.5(4)
C(21)–Os(2)–C(23)	90.3(4)
C(22)–Os(2)–C(23)	95.9(4)
C(24)–Os(2)–C(23)	170.3(3)
C(21)–Os(2)–S(2)	167.5(3)
C(22)–Os(2)–S(2)	93.7(3)
C(24)–Os(2)–S(2)	95.7(3)
C(23)–Os(2)–S(2)	81.2(2)
C(21)–Os(2)–Os(3)	87.7(3)
C(22)–Os(2)–Os(3)	173.5(3)
C(24)–Os(2)–Os(3)	81.3(3)
C(23)–Os(2)–Os(3)	89.1(3)
S(2)–Os(2)–Os(3)	82.95(5)
C(33)–Os(3)–C(31)	90.6(4)
C(33)–Os(3)–C(32)	100.2(4)
C(31)–Os(3)–C(32)	94.5(4)
C(33)–Os(3)–S(1)	159.0(3)
C(31)–Os(3)–S(1)	95.1(3)
C(32)–Os(3)–S(1)	99.5(3)
C(33)–Os(3)–Os(2)	86.2(3)
C(31)–Os(3)–Os(2)	175.8(3)
C(32)–Os(3)–Os(2)	88.8(3)
S(1)–Os(3)–Os(2)	86.98(5)
C(40)–S(1)–Os(1)	113.7(3)
C(40)–S(1)–Os(3)	110.7(3)
Os(1)–S(1)–Os(3)	72.94(5)
C(50)–S(2)–Os(2)	111.0(3)
C(50)–S(2)–Os(1)	108.3(3)
Os(2)–S(2)–Os(1)	106.35(8)
C(41)–C(40)–S(1)	109.8(6)
C(42)–C(41)–C(46)	118.9(9)
C(42)–C(41)–C(40)	121.5(9)
C(46)–C(41)–C(40)	119.6(8)
C(41)–C(42)–C(43)	121.4(10)
C(44)–C(43)–C(42)	119.7(11)
C(43)–C(44)–C(45)	120.1(10)
C(46)–C(45)–C(44)	120.2(10)
C(45)–C(46)–C(41)	119.6(10)
C(51)–C(50)–S(2)	110.4(6)
C(52)–C(51)–C(56)	118.6(9)
C(52)–C(51)–C(50)	120.3(8)
C(56)–C(51)–C(50)	121.1(8)
C(53)–C(52)–C(51)	119.7(9)
C(54)–C(53)–C(52)	121.2(9)
C(53)–C(54)–C(55)	119.7(9)
C(56)–C(55)–C(54)	119.5(9)
C(55)–C(56)–C(51)	121.3(9)

Table 2.4b. Bond lengths [Å] and angles [°] for $[Os_3(\mu\text{-}SCH_2Ph)_2(CO)_{10}]$ 2.2 continued.

O(11)–C(11)–Os(1)	175.8(8)
O(12)–C(12)–Os(1)	176.7(9)
O(13)–C(13)–Os(1)	176.7(10)
O(21)–C(21)–Os(2)	175.7(9)
O(22)–C(22)–Os(2)	175.1(9)
O(23)–C(23)–Os(2)	178.2(8)
O(24)–C(24)–Os(2)	176.9(7)
O(31)–C(31)–Os(3)	175.2(8)
O(32)–C(32)–Os(3)	177.3(9)
O(33)–C(33)–Os(3)	179.3(8)

Table 2.5a. Crystallographic data for $[Os_3(\mu\text{-}S^tBu)_2(CO)_{10}]$ 2.6.

Chemical formula	$C_{18}H_{18}O_{10}Os_3S_2$
Formula weight	1029.04
Temperature	293(2) K
Radiation, wavelength	MoKα, 0.71073 Å
Crystal system, space group	triclinic, P-1
Unit cell parameters	a = 8.7581(7) Å α = 81.8870(10)°
	b = 10.7875(9) Å β = 86.4370(10)°
	c = 14.5669(12) Å γ = 73.1180(10)°
Cell volume	1303.44(18) $Å^3$
Z	2
Calculated density	2.622 g/cm^3
Absorption coefficient μ	14.793 mm^{-1}
F(000)	932
Crystal colour and size	yellow, 0.43 x 0.34 x 0.13 mm^3
Data collection method	Bruker SMART APEX diffractometer
	ω rotation with narrow frames
θ range for data collection	1.99 to 28.34°
Index ranges	h -11 to 11, k -14 to 13, l -18 to 18
Completeness to θ = 26.00°	98.4 %
Reflections collected	11026
Independent reflections	5920 (R_{int} = 0.0377)
Reflections with $F^2>2\sigma$	5300
Absorption correction	semi-empirical from equivalents
Min. and max. transmission	0.0608 and 0.2552
Structure solution	direct methods
Refinement method	Full-matrix least-squares on F^2
Weighting parameters a, b	0.0614, 0.0000
Data / restraints / parameters	5920 / 0 / 304
Final R indices [$F^2>2\sigma$]	R1 = 0.0430, wR2 = 0.1111
R indices (all data)	R1 = 0.0470, wR2 = 0.1143
Goodness-of-fit on F^2	1.053
Largest and mean shift/su	0.001 and 0.000
Largest diff. peak and hole	3.216 and -2.583 e $Å^{-3}$

Table 2.5b. Bond lengths [Å] and angles [°] for $[Os_3(\mu\text{-}S^tBu)_2(CO)_{10}]$ 2.6.

Os(1)-C(12)	1.882(8)
Os(1)-C(13)	1.910(9)
Os(1)-C(11)	1.914(8)
Os(1)-S(1)	2.3861(19)
Os(1)-S(2)	2.4564(18)
Os(1)-Os(3)	2.8477(4)
Os(2)-C(21)	1.911(9)
Os(2)-C(22)	1.926(9)
Os(2)-C(24)	1.946(9)
Os(2)-C(23)	1.964(9)
Os(2)-S(2)	2.4593(18)
Os(2)-Os(3)	2.9332(4)
Os(3)-C(31)	1.883(8)
Os(3)-C(33)	1.891(9)
Os(3)-C(32)	1.903(9)
Os(3)-S(1)	2.3892(19)
S(1)-C(1)	1.859(9)
S(2)-C(5)	1.880(7)
C(1)-C(4)	1.471(17)
C(1)-C(2)	1.504(17)
C(1)-C(3)	1.524(16)
C(5)-C(7)	1.504(12)
C(5)-C(8)	1.528(11)
C(5)-C(6)	1.535(13)
C(11)-O(11)	1.142(10)
C(12)-O(12)	1.134(11)
C(13)-O(13)	1.141(10)
C(21)-O(21)	1.131(11)
C(22)-O(22)	1.143(11)
C(23)-O(23)	1.117(10)
C(24)-O(24)	1.145(10)
C(31)-O(31)	1.145(11)
C(32)-O(32)	1.137(11)
C(33)-O(33)	1.154(10)
C(12)-Os(1)-C(13)	89.0(4)
C(12)-Os(1)-C(11)	92.1(4)
C(13)-Os(1)-C(11)	100.3(4)
C(12)-Os(1)-S(1)	99.2(3)
C(13)-Os(1)-S(1)	157.9(3)
C(11)-Os(1)-S(1)	99.9(3)
C(12)-Os(1)-S(2)	169.3(4)
C(13)-Os(1)-S(2)	84.4(3)
C(11)-Os(1)-S(2)	97.4(3)
S(1)-Os(1)-S(2)	84.23(6)
C(12)-Os(1)-Os(3)	89.1(3)
C(13)-Os(1)-Os(3)	106.7(3)
C(11)-Os(1)-Os(3)	153.0(3)
S(1)-Os(1)-Os(3)	53.44(4)
S(2)-Os(1)-Os(3)	84.79(4)

Table 2.5b. Bond lengths [Å] and angles [°] for $[Os_3(\mu\text{-}S^tBu)_2(CO)_{10}]$ 2.6 continued.

C(21)-Os(2)-C(22)	93.8(4)
C(21)-Os(2)-C(24)	90.3(4)
C(22)-Os(2)-C(24)	95.5(4)
C(21)-Os(2)-C(23)	91.1(4)
C(22)-Os(2)-C(23)	95.1(4)
C(24)-Os(2)-C(23)	169.1(3)
C(21)-Os(2)-S(2)	165.3(3)
C(22)-Os(2)-S(2)	97.9(3)
C(24)-Os(2)-S(2)	97.3(2)
C(23)-Os(2)-S(2)	79.2(3)
C(21)-Os(2)-Os(3)	85.8(3)
C(22)-Os(2)-Os(3)	176.7(3)
C(24)-Os(2)-Os(3)	81.2(3)
C(23)-Os(2)-Os(3)	88.2(2)
S(2)-Os(2)-Os(3)	82.92(4)
C(31)-Os(3)-C(33)	87.7(4)
C(31)-Os(3)-C(32)	94.4(4)
C(33)-Os(3)-C(32)	98.4(4)
C(31)-Os(3)-S(1)	99.9(3)
C(33)-Os(3)-S(1)	161.4(3)
C(32)-Os(3)-S(1)	97.9(3)
C(31)-Os(3)-Os(1)	92.8(3)
C(33)-Os(3)-Os(1)	109.8(3)
C(32)-Os(3)-Os(1)	151.2(3)
S(1)-Os(3)-Os(1)	53.34(4)
C(31)-Os(3)-Os(2)	170.7(3)
C(33)-Os(3)-Os(2)	84.1(3)
C(32)-Os(3)-Os(2)	91.2(3)
S(1)-Os(3)-Os(2)	86.68(4)
Os(1)-Os(3)-Os(2)	85.796(12)
C(1)-S(1)-Os(1)	120.3(3)
C(1)-S(1)-Os(3)	120.0(3)
Os(1)-S(1)-Os(3)	73.22(5)
C(5)-S(2)-Os(1)	116.3(3)
C(5)-S(2)-Os(2)	118.7(3)
Os(1)-S(2)-Os(2)	106.38(7)
C(4)-C(1)-C(2)	114.6(15)
C(4)-C(1)-C(3)	107.5(12)
C(2)-C(1)-C(3)	106.4(14)
C(4)-C(1)-S(1)	117.7(8)
C(2)-C(1)-S(1)	105.0(8)
C(3)-C(1)-S(1)	104.7(7)
C(7)-C(5)-C(8)	112.3(7)
C(7)-C(5)-C(6)	108.5(8)
C(8)-C(5)-C(6)	111.3(7)
C(7)-C(5)-S(2)	107.8(6)
C(8)-C(5)-S(2)	111.8(5)
C(6)-C(5)-S(2)	104.8(6)
O(11)-C(11)-Os(1)	173.3(9)
O(12)-C(12)-Os(1)	175.1(10)

Table 2.5b. Bond lengths [Å] and angles [°] for $[Os_3(\mu\text{-}S^tBu)_2(CO)_{10}]$ 2.6 continued.

O(13)-C(13)-Os(1)	177.0(8)
O(21)-C(21)-Os(2)	177.4(8)
O(22)-C(22)-Os(2)	172.9(11)
O(23)-C(23)-Os(2)	179.0(8)
O(24)-C(24)-Os(2)	176.6(7)
O(31)-C(31)-Os(3)	173.3(10)
O(32)-C(32)-Os(3)	176.8(9)
O(33)-C(33)-Os(3)	179.1(9)

Table 2.6a Crystallographic data for $[Os_3(\mu\text{-}SPhCH_2)_2(CO)_{10}]$ (equivalent $PhCH_2S$ ligands) 2.4.

Chemical formula	$C_{24}H_{14}O_{10}Os_3S_2$
Formula weight	1097.07
Temperature	293(2) K
Radiation, wavelength	MoKα, 0.71073 Å
Crystal system, space group	monoclinic, $P2_1/m$
Unit cell parameters	a = 9.0625(5) Å α = 90°
	b = 15.0949(9) Å β = 97.3560(10)°
	c = 10.1246(6) Å γ = 90°
Cell volume	1373.62(14) $Å^3$
Z	2
Calculated density	2.652 g/cm^3
Absorption coefficient μ	14.047 mm^{-1}
F(000)	996
Crystal colour and size	very pale yellow, 0.34 × 0.28 × 0.11 mm^3
Data collection method	Bruker SMART APEX diffractometer
	ω rotation with narrow frames
θ range for data collection	2.44 to 28.25°
Index ranges	h −11 to 11, k −19 to 19, l −13 to 12
Completeness to θ = 28.25°	94.6 %
Reflections collected	12042
Independent reflections	3333 (R_{int} = 0.0387)
Reflections with $F^2>2\sigma$	3108
Absorption correction	semi-empirical from equivalents
Min. and max. transmission	0.0869 and 0.3072
Structure solution	direct methods
Refinement method	Full-matrix least-squares on F^2
Weighting parameters a, b	0.0475, 2.6543
Data / restraints / parameters	3333 / 0 / 193
Final R indices [$F^2>2\sigma$]	R1 = 0.0321, wR2 = 0.0794
R indices (all data)	R1 = 0.0346, wR2 = 0.0811
Goodness-of-fit on F^2	1.058
Largest and mean shift/su	0.001 and 0.000
Largest diff. peak and hole	2.709 and −2.575 e $Å^{-3}$

Table 2.6b. Bond lengths [Å] and angles [°] for $[Os_3(\mu\text{-}SPhCH_2)_2(CO)_{10}]$ (equivalent $PhCH_2S$ ligands) 2.4.

Os(1)–C(11a)	1.906(7)
Os(1)–C(11)	1.906(7)
Os(1)–C(12)	1.929(8)
Os(1)–S(1)	2.4298(14)
Os(1)–S(1a)	2.4298(13)
Os(1)–Os(3)	2.8926(4)
Os(2)–C(22)	1.905(9)
Os(2)–C(21)	1.922(6)
Os(2)–C(21a)	1.922(6)
Os(2)–S(1a)	2.4330(14)
Os(2)–S(1)	2.4330(13)
Os(2)–Os(3)	2.8917(4)
Os(3)–C(33)	1.916(9)
Os(3)–C(32)	1.929(9)
Os(3)–C(31)	1.951(6)
Os(3)–C(31a)	1.951(6)
S(1)–C(1)	1.831(6)
C(1)–C(2)	1.506(8)
C(2)–C(7)	1.387(9)
C(2)–C(3)	1.388(9)
C(3)–C(4)	1.380(10)
C(4)–C(5)	1.381(11)
C(5)–C(6)	1.367(12)
C(6)–C(7)	1.363(10)
C(11)–O(11)	1.136(8)
C(12)–O(12)	1.119(10)
C(21)–O(21)	1.122(8)
C(22)–O(22)	1.135(10)
C(31)–O(31)	1.128(8)
C(32)–O(32)	1.130(11)
C(33)–O(33)	1.142(11)
C(11a)–Os(1)–C(11)	93.7(4)
C(11a)–Os(1)–C(12)	94.4(3)
C(11)–Os(1)–C(12)	94.4(3)
C(11a)–Os(1)–S(1)	166.42(19)
C(11)–Os(1)–S(1)	90.1(2)
C(12)–Os(1)–S(1)	98.34(19)
C(11a)–Os(1)–S(1a)	90.1(2)
C(11)–Os(1)–S(1a)	166.42(19)
C(12)–Os(1)–S(1a)	98.34(19)
S(1)–Os(1)–S(1a)	83.45(6)
C(11a)–Os(1)–Os(3)	87.41(19)
C(11)–Os(1)–Os(3)	87.41(19)
C(12)–Os(1)–Os(3)	177.4(2)
S(1)–Os(1)–Os(3)	79.72(3)
S(1a)–Os(1)–Os(3)	79.72(3)
C(22)–Os(2)–C(21)	96.1(2)
C(22)–Os(2)–C(21a)	96.1(2)
C(21)–Os(2)–C(21a)	91.1(4)

Table 2.6b. Bond lengths [Å] and angles [°] for $[Os_3(\mu\text{-}SPhCH_2)_2(CO)_{10}]$ (equivalent $PhCH_2S$ ligands) 2.4 continued.

C(22)–Os(2)–S(1a)	94.34(18)
C(21)–Os(2)–S(1a)	168.79(18)
C(21a)–Os(2)–S(1a)	91.83(19)
C(22)–Os(2)–S(1)	94.34(18)
C(21)–Os(2)–S(1)	91.83(18)
C(21a)–Os(2)–S(1)	168.79(18)
S(1a)–Os(2)–S(1)	83.31(6)
C(22)–Os(2)–Os(3)	171.9(2)
C(21)–Os(2)–Os(3)	89.52(18)
C(21a)–Os(2)–Os(3)	89.52(18)
S(1a)–Os(2)–Os(3)	79.68(3)
S(1)–Os(2)–Os(3)	79.68(3)
C(33)–Os(3)–C(32)	103.5(4)
C(33)–Os(3)–C(31)	91.07(18)
C(32)–Os(3)–C(31)	91.99(18)
C(33)–Os(3)–C(31a)	91.07(18)
C(32)–Os(3)–C(31a)	91.99(19)
C(31)–Os(3)–C(31a)	174.9(3)
C(33)–Os(3)–Os(2)	94.4(3)
C(32)–Os(3)–Os(2)	162.0(3)
C(31)–Os(3)–Os(2)	87.62(18)
C(31a)–Os(3)–Os(2)	87.62(18)
C(33)–Os(3)–Os(1)	165.7(3)
C(32)–Os(3)–Os(1)	90.7(3)
C(31)–Os(3)–Os(1)	88.39(18)
C(31a)–Os(3)–Os(1)	88.39(17)
Os(2)–Os(3)–Os(1)	71.309(11)
C(1)–S(1)–Os(1)	114.4(2)
C(1)–S(1)–Os(2)	111.4(2)
Os(1)–S(1)–Os(2)	87.79(4)
C(2)–C(1)–S(1)	111.6(4)
C(7)–C(2)–C(3)	118.0(6)
C(7)–C(2)–C(1)	121.0(6)
C(3)–C(2)–C(1)	121.0(6)
C(4)–C(3)–C(2)	121.1(7)
C(3)–C(4)–C(5)	119.2(7)
C(6)–C(5)–C(4)	120.4(7)
C(7)–C(6)–C(5)	120.2(7)
C(6)–C(7)–C(2)	121.2(7)
O(11)–C(11)–Os(1)	178.8(6)
O(12)–C(12)–Os(1)	175.1(8)
O(21)–C(21)–Os(2)	178.4(6)
O(22)–C(22)–Os(2)	179.2(7)
O(31)–C(31)–Os(3)	175.7(5)
O(32)–C(32)–Os(3)	179.2(9)
O(33)–C(33)–Os(3)	177.7(9)

Table 3.3a. Crystallographic data for $Os(C_9H_6NO)_2(CO)_2]$ (C_1 isomer) 3.1.

Chemical formula	$C_{20}H_{12}N_2O_4Os$
Formula weight	534.52
Temperature	293(2) K
Radiation, wavelength	MoKα, 0.71073 Å
Crystal system, space group	monoclinic, $P2_1/c$
Unit cell parameters	a = 9.5887(12) Å α = 90°
	b = 14.1983(18) Å β = 100.339(2)°
	c = 12.6275(16) Å γ = 90°
Cell volume	1691.2(4) $Å^3$
Z	4
Calculated density	2.099 g/cm^3
Absorption coefficient μ	7.570 mm^{-1}
F(000)	1016
Crystal colour and size	yellow, 0.42 ′ 0.13 ′ 0.03 mm^3
Data collection method	Bruker SMART APEX diffractometer
	ω rotation with narrow frames
θ range for data collection	2.16 to 28.35°
Index ranges	h -12 to 12, k -18 to 18, l -16 to 16
Completeness to θ = 26.00°	99.8 %
Reflections collected	14814
Independent reflections	4079 (R_{int} = 0.0412)
Reflections with $F^2>2\sigma$	3458
Absorption correction	semi-empirical from equivalents
Min. and max. transmission	0.1444 and 0.8047
Structure solution	direct methods
Refinement method	Full-matrix least-squares on F^2
Weighting parameters a, b	0.0332, 0.7301
Data / restraints / parameters	4079 / 0 / 244
Final R indices [$F^2>2\sigma$]	R1 = 0.0327, wR2 = 0.0724
R indices (all data)	R1 = 0.0413, wR2 = 0.0763
Goodness-of-fit on F^2	1.026
Largest and mean shift/su	0.001 and 0.000
Largest diff. peak and hole	1.526 and -1.168 e $Å^{-3}$

Table 3.3b. Bond lengths [Å] and angles [°] for $[Os(C_9H_6NO)_2(CO)_2]$ 3.1 (C_1 isomer).

Os(1)-C(1)	1.857(6)
Os(1)-C(2)	1.876(6)
Os(1)-O(4)	2.054(3)
Os(1)-N(1)	2.071(3)
Os(1)-O(3)	2.086(3)
Os(1)-N(2)	2.114(4)
N(1)-C(3)	1.325(6)
N(1)-C(11)	1.365(5)
N(2)-C(12)	1.319(6)
N(2)-C(20)	1.362(6)
O(1)-C(1)	1.136(6)
O(2)-C(2)	1.132(6)
O(3)-C(10)	1.317(6)
O(4)-C(19)	1.297(7)
C(3)-C(4)	1.376(7)
C(4)-C(5)	1.358(7)
C(5)-C(6)	1.408(7)
C(6)-C(11)	1.405(6)
C(6)-C(7)	1.415(7)
C(7)-C(8)	1.368(8)
C(8)-C(9)	1.400(8)
C(9)-C(10)	1.375(7)
C(10)-C(11)	1.425(6)
C(12)-C(13)	1.389(8)
C(13)-C(14)	1.345(10)
C(14)-C(15)	1.413(10)
C(15)-C(20)	1.408(8)
C(15)-C(16)	1.426(10)
C(16)-C(17)	1.332(11)
C(17)-C(18)	1.411(11)
C(18)-C(19)	1.389(7)
C(19)-C(20)	1.421(8)
C(1)-Os(1)-C(2)	88.7(2)
C(1)-Os(1)-O(4)	96.14(18)
C(2)-Os(1)-O(4)	95.6(2)
C(1)-Os(1)-N(1)	97.29(17)
C(2)-Os(1)-N(1)	94.71(19)
O(4)-Os(1)-N(1)	163.19(16)
C(1)-Os(1)-O(3)	174.69(16)
C(2)-Os(1)-O(3)	95.81(19)
O(4)-Os(1)-O(3)	86.18(14)
N(1)-Os(1)-O(3)	79.63(13)
C(1)-Os(1)-N(2)	92.54(17)
C(2)-Os(1)-N(2)	175.89(19)
O(4)-Os(1)-N(2)	80.33(15)
N(1)-Os(1)-N(2)	89.00(14)
O(3)-Os(1)-N(2)	83.12(13)
C(3)-N(1)-C(11)	118.6(4)
C(3)-N(1)-Os(1)	128.6(3)

Table 3.3b. Bond lengths [Å] and angles [°] for $[Os(C_9H_6NO)_2(CO)_2]$ 3.1 (C_1 isomer) continued.

C(11)-N(1)-Os(1)	112.3(3)
C(12)-N(2)-C(20)	120.8(4)
C(12)-N(2)-Os(1)	129.2(4)
C(20)-N(2)-Os(1)	110.0(3)
C(10)-O(3)-Os(1)	112.0(3)
C(19)-O(4)-Os(1)	112.2(3)
O(1)-C(1)-Os(1)	178.1(5)
O(2)-C(2)-Os(1)	178.9(5)
N(1)-C(3)-C(4)	122.9(5)
C(5)-C(4)-C(3)	119.5(4)
C(4)-C(5)-C(6)	120.0(4)
C(11)-C(6)-C(5)	117.1(4)
C(11)-C(6)-C(7)	118.3(4)
C(5)-C(6)-C(7)	124.6(5)
C(8)-C(7)-C(6)	119.0(5)
C(7)-C(8)-C(9)	122.4(5)
C(10)-C(9)-C(8)	120.7(5)
O(3)-C(10)-C(9)	123.7(4)
O(3)-C(10)-C(11)	118.9(4)
C(9)-C(10)-C(11)	117.4(4)
N(1)-C(11)-C(6)	121.8(4)
N(1)-C(11)-C(10)	116.0(4)
C(6)-C(11)-C(10)	122.2(4)
N(2)-C(12)-C(13)	120.9(6)
C(14)-C(13)-C(12)	120.4(6)
C(13)-C(14)-C(15)	120.1(6)
C(20)-C(15)-C(14)	117.1(6)
C(20)-C(15)-C(16)	117.9(6)
C(14)-C(15)-C(16)	125.0(6)
C(17)-C(16)-C(15)	118.9(7)
C(16)-C(17)-C(18)	123.7(7)
C(19)-C(18)-C(17)	120.2(7)
O(4)-C(19)-C(18)	123.0(6)
O(4)-C(19)-C(20)	120.6(4)
C(18)-C(19)-C(20)	116.4(6)
N(2)-C(20)-C(15)	120.7(5)
N(2)-C(20)-C(19)	116.3(5)
C(15)-C(20)-C(19)	122.9(5)

Table 3.5a. Crystallographic data for $[Os(C_9H_6NO)_2(CO)_2]$ 3.5 (C_2 isomer) with N trans to N).

Identification code	str0097	
Chemical formula	$C_{20}H_{12}N_2O_4Os$	
Formula weight	534.52	
Temperature	293(2) K	
Radiation, wavelength	MoKα, 0.71073 Å	
Crystal system, space group	monoclinic, $P2_1/c$	
Unit cell parameters	a = 7.0173(4) Å	α = 90°
	b = 28.1652(14) Å	β = 98.3460(10)°
	c = 8.6771(4) Å	γ = 90°
Cell volume	1696.81(15) $Å^3$	
Z	4	
Calculated density	2.092 g/cm^3	
Absorption coefficient μ	7.545 mm^{-1}	
F(000)	1016	
Crystal colour and size	yellow, 0.47 ′ 0.33 ′ 0.33 mm^3	
Data collection method	Bruker SMART APEX diffractometer	
	ω rotation with narrow frames	
θ range for data collection	2.48 to 28.30°	
Index ranges	h -9 to 9, k -37 to 37, l -11 to 11	
Completeness to θ = 28.30°	96.8 %	
Reflections collected	14915	
Independent reflections	4088 (R_{int} = 0.0178)	
Reflections with $F^2>2\sigma$	3799	
Absorption correction	semi-empirical from equivalents	
Min. and max. transmission	0.1269 and 0.1910	
Structure solution	direct methods	
Refinement method	Full-matrix least-squares on F^2	
Weighting parameters a, b	0.0145, 1.8023	
Data / restraints / parameters	4088 / 0 / 244	
Final R indices [$F^2>2\sigma$]	R1 = 0.0194, wR2 = 0.0410	
R indices (all data)	R1 = 0.0221, wR2 = 0.0418	
Goodness-of-fit on F^2	1.097	
Largest and mean shift/su	0.002 and 0.000	
Largest diff. peak and hole	1.080 and -0.625 e $Å^{-3}$	

Table 3.5b. Bond lengths [Å] and angles [°] for $[Os(C_9H_6NO)_2(CO)_2]$ 3.5 (C_2 isomer with N trans to N).

Os(1)-C(2)	1.868(3)	Os(1)-C(1)	1.870(3)
Os(1)-O(3)	2.062(2)	Os(1)-O(4)	2.0664(19)
Os(1)-N(1)	2.073(2)	Os(1)-N(2)	2.080(2)
N(1)-C(3)	1.323(4)	N(1)-C(11)	1.368(4)
N(2)-C(12)	1.323(3)	N(2)-C(20)	1.369(4)
O(3)-C(10)	1.325(3)	O(4)-C(19)	1.325(3)
C(3)-C(4)	1.393(4)	C(4)-C(5)	1.351(5)
C(5)-C(6)	1.410(5)	C(6)-C(7)	1.404(5)
C(6)-C(11)	1.413(4)	C(7)-C(8)	1.364(5)
C(8)-C(9)	1.399(5)	C(9)-C(10)	1.375(4)
C(10)-C(11)	1.418(4)	C(12)-C(13)	1.395(4)
C(13)-C(14)	1.346(5)	C(14)-C(15)	1.405(4)
C(15)-C(16)	1.401(5)	C(15)-C(20)	1.414(4)
C(16)-C(17)	1.359(5)	C(17)-C(18)	1.395(5)
C(18)-C(19)	1.379(4)	C(19)-C(20)	1.415(4)
C(1)-O(1)	1.145(4)	C(2)-O(2)	1.137(4)

C(2)-Os(1)-C(1)	89.80(14)	C(2)-Os(1)-O(3)	92.35(12)
C(1)-Os(1)-O(3)	175.95(10)	C(2)-Os(1)-O(4)	173.86(11)
C(1)-Os(1)-O(4)	95.55(11)	O(3)-Os(1)-O(4)	82.49(8)
C(2)-Os(1)-N(1)	94.70(11)	C(1)-Os(1)-N(1)	96.44(11)
O(3)-Os(1)-N(1)	79.97(8)	O(4)-Os(1)-N(1)	87.70(8)
C(2)-Os(1)-N(2)	96.60(11)	C(1)-Os(1)-N(2)	95.44(11)
O(3)-Os(1)-N(2)	87.72(8)	O(4)-Os(1)-N(2)	79.93(8)
N(1)-Os(1)-N(2)	163.60(9)	C(3)-N(1)-C(11)	119.2(2)
C(3)-N(1)-Os(1)	128.5(2)	C(11)-N(1)-Os(1)	112.24(17)
C(12)-N(2)-C(20)	118.9(2)	C(12)-N(2)-Os(1)	129.5(2)
C(20)-N(2)-Os(1)	111.45(16)	C(10)-O(3)-Os(1)	112.95(17)
C(19)-O(4)-Os(1)	112.31(16)	N(1)-C(3)-C(4)	122.3(3)
C(5)-C(4)-C(3)	119.6(3)	C(4)-C(5)-C(6)	120.4(3)
C(7)-C(6)-C(5)	125.1(3)	C(7)-C(6)-C(11)	118.0(3)
C(5)-C(6)-C(11)	116.9(3)	C(8)-C(7)-C(6)	119.3(3)
C(7)-C(8)-C(9)	122.8(3)	C(10)-C(9)-C(8)	120.1(3)
O(3)-C(10)-C(9)	123.8(3)	O(3)-C(10)-C(11)	118.6(2)
C(9)-C(10)-C(11)	117.6(3)	N(1)-C(11)-C(6)	121.6(3)
N(1)-C(11)-C(10)	116.2(2)	C(6)-C(11)-C(10)	122.2(3)
N(2)-C(12)-C(13)	122.2(3)	C(14)-C(13)-C(12)	120.0(3)
C(13)-C(14)-C(15)	120.1(3)	C(16)-C(15)-C(14)	124.9(3)
C(16)-C(15)-C(20)	117.9(3)	C(14)-C(15)-C(20)	117.2(3)
C(17)-C(16)-C(15)	119.8(3)	C(16)-C(17)-C(18)	122.4(3)
C(19)-C(18)-C(17)	120.3(3)	O(4)-C(19)-C(18)	123.7(3)
O(4)-C(19)-C(20)	118.7(2)	C(18)-C(19)-C(20)	117.6(3)
N(2)-C(20)-C(15)	121.5(2)	N(2)-C(20)-C(19)	116.5(2)
C(15)-C(20)-C(19)	122.0(3)	O(1)-C(1)-Os(1)	176.4(3)
O(2)-C(2)-Os(1)	176.7(3)		

Table 3.6a. Crystallographic data for $[Os_3H(C_9H_6NO)(CO)_9]$ 3.7.

Chemical formula	$C_{18}H_7NO_{10}Os_3$
Formula weight	967.85
Temperature	150(2) K
Radiation, wavelength	MoKα, 0.71073 Å
Crystal system, space group	triclinic, $P\bar{1}$
Unit cell parameters	a = 9.8056(7) Å α = 81.3170(10)°
	b = 10.3276(8) Å β = 79.6810(10)°
	c = 10.7233(8) Å γ = 81.9230(10)°
Cell volume	1048.91(14) $Å^3$
Z	2
Calculated density	3.064 g/cm^3
Absorption coefficient μ	18.182 mm^{-1}
F(000)	860
Crystal colour and size	yellow, 0.50 ′ 0.29 ′ 0.06 mm^3
Data collection method	Bruker SMART APEX diffractometer
	ω rotation with narrow frames
θ range for data collection	2.61 to 28.29°
Index ranges	h -12 to 12, k -13 to 13, l 0 to 14
Completeness to θ = 28.29°	87.8 %
Reflections collected	4576
Independent reflections	4576 (R_{int} = 0.0000)
Reflections with $F^2>2\sigma$	4238
Absorption correction	DIFABS
Min. and max. transmission	0.0397 and 0.4134
Structure solution	Patterson synthesis
Refinement method	Full-matrix least-squares on F^2
Weighting parameters a, b	0.1029, 0.0000
Data / restraints / parameters	4576 / 2 / 292
Final R indices [$F^2>2\sigma$]	R1 = 0.0542, wR2 = 0.1424
R indices (all data)	R1 = 0.0565, wR2 = 0.1444
Goodness-of-fit on F^2	1.048
Largest and mean shift/su	0.033 and 0.001
Largest diff. peak and hole	3.800 and -3.401 e $Å^{-3}$

Table 3.6b. Bond lengths [Å] and angles [°] for $[Os_3H(C_9H_6NO)(CO)_9]$ 3.7.

Os(1)-C(12)	1.910(11)
Os(1)-C(11)	1.918(10)
Os(1)-C(13)	1.938(9)
Os(1)-C(14)	1.956(10)
Os(1)-Os(2)	2.7797(5)
Os(1)-Os(3)	2.8162(5)
Os(2)-C(22)	1.873(10)
Os(2)-C(21)	1.879(11)
Os(2)-H(8)	1.78(8)
Os(2)-N(1)	2.147(8)
Os(2)-O(1)	2.147(6)
Os(2)-Os(3)	2.8108(5)
Os(3)-H(8)	1.56(8)
Os(3)-C(32)	1.883(10)
Os(3)-C(31)	1.915(9)
Os(3)-C(33)	1.936(10)
Os(3)-O(1)	2.160(6)
N(1)-C(1)	1.336(12)
N(1)-C(9)	1.388(11)
O(1)-C(8)	1.365(12)
C(1)-C(2)	1.401(15)
C(2)-C(3)	1.342(15)
C(3)-C(4)	1.439(14)
C(4)-C(9)	1.375(14)
C(4)-C(5)	1.415(14)
C(5)-C(6)	1.357(15)
C(6)-C(7)	1.406(15)
C(7)-C(8)	1.375(12)
C(8)-C(9)	1.423(13)
C(11)-O(11)	1.143(13)
C(12)-O(12)	1.164(13)
C(13)-O(13)	1.148(12)
C(14)-O(14)	1.123(12)
C(21)-O(21)	1.148(13)
C(22)-O(22)	1.139(12)
C(31)-O(31)	1.141(12)
C(32)-O(32)	1.137(12)
C(33)-O(33)	1.146(12)
C(12)-Os(1)-C(11)	102.6(5)
C(12)-Os(1)-C(13)	95.6(4)
C(11)-Os(1)-C(13)	93.8(4)
C(12)-Os(1)-C(14)	95.6(4)
C(11)-Os(1)-C(14)	92.8(4)
C(13)-Os(1)-C(14)	165.4(4)
C(12)-Os(1)-Os(2)	158.9(3)
C(11)-Os(1)-Os(2)	98.5(3)
C(13)-Os(1)-Os(2)	82.6(3)
C(14)-Os(1)-Os(2)	83.5(3)
C(12)-Os(1)-Os(3)	98.7(3)
C(11)-Os(1)-Os(3)	158.6(3)
C(13)-Os(1)-Os(3)	86.5(3)

Table 3.6b. Bond lengths [Å] and angles [°] for $[Os_3H(C_9H_6NO)(CO)_9]$ 3.7 continued.

C(14)-Os(1)-Os(3)	82.6(3)
Os(2)-Os(1)-Os(3)	60.300(13)
C(22)-Os(2)-C(21)	87.9(4)
C(22)-Os(2)-H(8)	100(4)
C(21)-Os(2)-H(8)	168(3)
C(22)-Os(2)-N(1)	103.1(4)
C(21)-Os(2)-N(1)	102.4(4)
H(8)-Os(2)-N(1)	84(4)
C(22)-Os(2)-O(1)	170.4(4)
C(21)-Os(2)-O(1)	101.5(3)
H(8)-Os(2)-O(1)	70(4)
N(1)-Os(2)-O(1)	77.4(3)
C(22)-Os(2)-Os(1)	94.4(3)
C(21)-Os(2)-Os(1)	90.5(3)
H(8)-Os(2)-Os(1)	81(4)
N(1)-Os(2)-Os(1)	158.4(2)
O(1)-Os(2)-Os(1)	83.23(17)
C(22)-Os(2)-Os(3)	121.4(3)
C(21)-Os(2)-Os(3)	138.1(3)
H(8)-Os(2)-Os(3)	30(3)
N(1)-Os(2)-Os(3)	99.2(2)
O(1)-Os(2)-Os(3)	49.46(17)
Os(1)-Os(2)-Os(3)	60.492(12)
H(8)-Os(3)-C(32)	99(5)
H(8)-Os(3)-C(31)	169(4)
C(32)-Os(3)-C(31)	89.6(4)
H(8)-Os(3)-C(33)	88(4)
C(32)-Os(3)-C(33)	94.6(4)
C(31)-Os(3)-C(33)	97.8(4)
H(8)-Os(3)-O(1)	74(4)
C(32)-Os(3)-O(1)	168.6(3)
C(31)-Os(3)-O(1)	96.5(3)
C(33)-Os(3)-O(1)	94.0(3)
H(8)-Os(3)-Os(2)	35(3)
C(32)-Os(3)-Os(2)	120.4(3)
C(31)-Os(3)-Os(2)	133.8(3)
C(33)-Os(3)-Os(2)	112.4(3)
O(1)-Os(3)-Os(2)	49.06(16)
H(8)-Os(3)-Os(1)	83(4)
C(32)-Os(3)-Os(1)	88.2(3)
C(31)-Os(3)-Os(1)	90.5(3)
C(33)-Os(3)-Os(1)	171.2(3)
O(1)-Os(3)-Os(1)	82.13(17)
Os(2)-Os(3)-Os(1)	59.207(12)
C(1)-N(1)-C(9)	117.0(8)
C(1)-N(1)-Os(2)	128.5(7)
C(9)-N(1)-Os(2)	114.5(6)
C(8)-O(1)-Os(2)	113.6(5)
C(8)-O(1)-Os(3)	116.0(5)

Table 3.6b. Bond lengths [Å] and angles [°] for $[Os_3H(C_9H_6NO)(CO)_9]$ 3.7 continued.

Os(2)-O(1)-Os(3)	81.5(2)
N(1)-C(1)-C(2)	122.6(9)
C(3)-C(2)-C(1)	120.3(9)
C(2)-C(3)-C(4)	119.4(10)
C(9)-C(4)-C(5)	118.9(9)
C(9)-C(4)-C(3)	116.9(9)
C(5)-C(4)-C(3)	124.1(9)
C(6)-C(5)-C(4)	121.0(10)
C(5)-C(6)-C(7)	119.9(9)
C(8)-C(7)-C(6)	120.8(9)
O(1)-C(8)-C(7)	122.4(9)
O(1)-C(8)-C(9)	119.0(8)
C(7)-C(8)-C(9)	118.6(9)
C(4)-C(9)-N(1)	123.6(9)
C(4)-C(9)-C(8)	120.9(9)
N(1)-C(9)-C(8)	115.5(8)
O(11)-C(11)-Os(1)	176.5(9)
O(12)-C(12)-Os(1)	178.6(9)
O(13)-C(13)-Os(1)	177.7(8)
O(14)-C(14)-Os(1)	178.5(9)
O(21)-C(21)-Os(2)	173.8(9)
O(22)-C(22)-Os(2)	177.1(10)
O(31)-C(31)-Os(3)	178.7(9)
O(32)-C(32)-Os(3)	179.1(9)
O(33)-C(33)-Os(3)	175.4(9)

Table 3.7a. Crystallographic data for $[Os_4H(C_9H_6NO)(CO)_{11}]\cdot 0.5C_7H_{16}$ 3.8.

Chemical formula	$C_{23.50}H_{15}NO_{12}Os_4$	
Formula weight	1264.17	
Temperature	293(2) K	
Radiation, wavelength	MoKα, 0.71073 Å	
Crystal system, space group	triclinic, P-1	
Unit cell parameters	a = 11.7882(8) Å	α = 74.6510(10)°
	b = 11.9497(8) Å	β = 64.3960(10)°
	c = 12.0180(8) Å	γ = 87.6400(10)°
Cell volume	1467.00(17) Å^3	
Z	2	
Calculated density	2.862 g/cm^3	
Absorption coefficient μ	17.326 mm^{-1}	
F(000)	1126	
Crystal colour and size	pale yellow, 0.48 × 0.26 × 0.11 mm^3	
Data collection method	Bruker SMART APEX diffractometer	
	ω rotation with narrow frames	
θ range for data collection	1.77 to 28.29°	
Index ranges	h -15 to 15, k -15 to 15, l -16 to 15	
Completeness to θ = 28.29°	92.9 %	
Reflections collected	12911	
Independent reflections	6762 (R_{int} = 0.0400)	
Reflections with $F^2>2\sigma$	5764	
Absorption correction	semi-empirical from equivalents	
Min. and max. transmission	0.0443 and 0.2634	
Structure solution	direct methods	
Refinement method	Full-matrix least-squares on F^2	
Weighting parameters a, b	0.0422, 0.0000	
Data / restraints / parameters	6762 / 2 / 391	
Final R indices [$F^2>2\sigma$]	R1 = 0.0400, wR2 = 0.0928	
R indices (all data)	R1 = 0.0458, wR2 = 0.0949	
Goodness-of-fit on F^2	1.034	
Largest and mean shift/su	0.001 and 0.000	
Largest diff. peak and hole	2.522 and -3.563 e Å^{-3}	

Table 3.7b. Bond lengths [Å] and angles [°] for $[Os_4H(C_9H_6NO)(CO)_{11}]\cdot 0.5\ C_7H_{16}$ 3.8.

Os(1)-C(12)	1.862(9)
Os(1)-C(11)	1.882(10)
Os(1)-H(8)	1.95(7)
Os(1)-O(1)	2.103(5)
Os(1)-N(1)	2.110(6)
Os(1)-Os(4)	2.9719(4)
Os(1)-Os(3)	3.0462(5)
Os(2)-C(23)	1.874(9)
Os(2)-C(21)	1.902(9)
Os(2)-C(22)	1.938(9)
Os(2)-O(1)	2.190(5)
Os(2)-Os(3)	2.8295(5)
Os(2)-Os(4)	2.9605(5)
Os(3)-C(31)	1.870(11)
Os(3)-C(32)	1.901(10)
Os(3)-C(33)	1.903(10)
Os(3)-Os(4)	2.8033(5)
Os(4)-C(41)	1.905(11)
Os(4)-C(43)	1.903(10)
Os(4)-C(42)	1.904(10)
N(1)-C(1)	1.331(10)
N(1)-C(9)	1.363(10)
O(1)-C(8)	1.357(9)
C(1)-C(2)	1.411(13)
C(2)-C(3)	1.313(14)
C(3)-C(4)	1.424(12)
C(4)-C(5)	1.389(12)
C(4)-C(9)	1.424(11)
C(5)-C(6)	1.365(13)
C(6)-C(7)	1.406(12)
C(7)-C(8)	1.349(11)
C(8)-C(9)	1.412(10)
C(11)-O(11)	1.145(11)
C(12)-O(12)	1.141(10)
C(21)-O(21)	1.133(10)
C(22)-O(22)	1.119(10)
C(23)-O(23)	1.116(10)
C(31)-O(31)	1.159(12)
C(32)-O(32)	1.145(11)
C(33)-O(33)	1.130(11)
C(41)-O(41)	1.149(12)
C(42)-O(42)	1.129(11)
C(43)-O(43)	1.137(11)
C(51)-C(52)	1.33(6)
C(51)-C(56)	1.68(12)
C(51)-C(51A)	1.65(6)
C(52)-C(56)	1.02(10)
C(52)-C(55)	1.1(2)
C(52)-C(53)	1.66(7)
C(53)-C(54)	0.95(9)

Table 3.7b Bond lengths [Å] and angles [°] for $[Os_4H(C_9H_6NO)(CO)_{11}]0.5C_7H_{16}$ 3.8 continued.

C(53)-C(56)	0.81(13)
C(53)-C(55)	1.14(15)
C(54)-C(55)	1.5(2)
C(54)-C(56)	1.71(15)
C(55)-C(56)	1.09(19)
C(12)-Os(1)-C(11)	89.7(4)
C(12)-Os(1)-H(8)	102(2)
C(11)-Os(1)-H(8)	162(2)
C(12)-Os(1)-O(1)	176.0(3)
C(11)-Os(1)-O(1)	94.3(3)
H(8)-Os(1)-O(1)	74(2)
C(12)-Os(1)-N(1)	100.8(3)
C(11)-Os(1)-N(1)	91.9(3)
H(8)-Os(1)-N(1)	72(2)
O(1)-Os(1)-N(1)	78.6(2)
C(12)-Os(1)-Os(4)	93.4(2)
C(11)-Os(1)-Os(4)	109.1(3)
H(8)-Os(1)-Os(4)	85(2)
O(1)-Os(1)-Os(4)	85.78(13)
N(1)-Os(1)-Os(4)	154.74(18)
C(12)-Os(1)-Os(3)	95.5(3)
C(11)-Os(1)-Os(3)	163.9(3)
H(8)-Os(1)-Os(3)	30(2)
O(1)-Os(1)-Os(3)	80.76(14)
N(1)-Os(1)-Os(3)	101.97(19)
Os(4)-Os(1)-Os(3)	55.508(10)
C(23)-Os(2)-C(21)	90.4(4)
C(23)-Os(2)-C(22)	89.7(4)
C(21)-Os(2)-C(22)	96.6(4)
C(23)-Os(2)-O(1)	176.1(3)
C(21)-Os(2)-O(1)	92.3(3)
C(22)-Os(2)-O(1)	92.7(3)
C(23)-Os(2)-Os(3)	92.8(3)
C(21)-Os(2)-Os(3)	86.0(3)
C(22)-Os(2)-Os(3)	176.4(2)
O(1)-Os(2)-Os(3)	84.65(13)
C(23)-Os(2)-Os(	91.6(3)
C(21)-Os(2)-Os(4)	143.9(3)
C(22)-Os(2)-Os(4)	119.5(3)
O(1)-Os(2)-Os(4)	84.58
(13)Os(3)-Os(2)-Os(4)	57.862(11)
C(31)-Os(3)-C(32)	98.2(4)
C(31)-Os(3)-C(33)	92.9(4)
C(32)-Os(3)-C(33)	92.0(4)
C(31)-Os(3)-Os(4)	159.6(3)
C(32)-Os(3)-Os(4)	99.8(3)
C(33)-Os(3)-Os(4)	96.0(3)
C(31)-Os(3)-Os(2)	97.9(3)
C(32)-Os(3)-Os(2)	162.8(3)
C(33)-Os(3)-Os(2)	93.1(3)

Table 3.7b. Bond lengths [Å] and angles [°]for $[Os_4H(C_9H_6NO)(CO)_{11}]0.5\ C_7H_{16}$ 3.8 continued.

Os(4)-Os(3)-Os(2)	63.414(12)
C(31)-Os(3)-Os(1)	107.6(3)
C(32)-Os(3)-Os(1)	96.4(3)
C(33)-Os(3)-Os(1)	156.4(3)
Os(4)-Os(3)-Os(1)	60.902(11)
Os(2)-Os(3)-Os(1)	72.971(11)
C(41)-Os(4)-C(43)	95.4(4)
C(41)-Os(4)-C(42)	96.9(4)
C(43)-Os(4)-C(42)	90.9(4)
C(41)-Os(4)-Os(3)	172.0(3)
C(43)-Os(4)-Os(3)	90.1(3)
C(42)-Os(4)-Os(3)	88.8(3)
C(41)-Os(4)-Os(2)	115.1(3)
C(43)-Os(4)-Os(2)	92.3(3)
C(42)-Os(4)-Os(2)	147.4(3)
Os(3)-Os(4)-Os(2)	58.724(11)
C(41)-Os(4)-Os(1)	110.4(3)
C(43)-Os(4)-Os(1)	153.6(3)
C(42)-Os(4)-Os(1)	91.3(2)
Os(3)-Os(4)-Os(1)	63.590(11)
Os(2)-Os(4)-Os(1)	72.267(10)
C(1)-N(1)-C(9)	120.5(7)
C(1)-N(1)-Os(1)	126.9(6)
C(9)-N(1)-Os(1)	112.6(5)
C(8)-O(1)-Os(1)	113.5(4)
C(8)-O(1)-Os(2)	121.5(4)
Os(1)-O(1)-Os(2)	109.1(2)
N(1)-C(1)-C(2)	120.0(9)
C(3)-C(2)-C(1)	120.7(9)
C(2)-C(3)-C(4)	121.9(8)
C(5)-C(4)-C(3)	126.0(8)
C(5)-C(4)-C(9)	118.9(8)
C(3)-C(4)-C(9)	115.2(8)
C(6)-C(5)-C(4)	119.5(8)
C(5)-C(6)-C(7)	121.8(8)
C(8)-C(7)-C(6)	120.3(8)
C(7)-C(8)-O(1)	123.8(7)
C(7)-C(8)-C(9)	119.2(7)
O(1)-C(8)-C(9)	117.1(7)
N(1)-C(9)-C(8)	118.0(7)
N(1)-C(9)-C(4)	121.7(7)
C(8)-C(9)-C(4)	120.3(7)
O(11)-C(11)-Os(1)	178.1(8)
O(12)-C(12)-Os(1)	178.3(8)
O(21)-C(21)-Os(2)	177.9(8)
O(22)-C(22)-Os(2)	172.7(8)
O(23)-C(23)-Os(2)	178.1(9)
O(31)-C(31)-Os(3)	178.7(10)
O(32)-C(32)-Os(3)	179.4(9)
O(33)-C(33)-Os(3)	177.5(9)

Table 3.7b. Bond lengths [Å] and angles [°]for $[Os_4H(C_9H_6NO)(CO)_{11}]0.5C_7H_{16}$ 3.8 continued.

O(41)-C(41)-Os(4)	179.1(10)
O(42)-C(42)-Os(4)	177.8(9)
O(43)-C(43)-Os(4)	178.6(9)
C(52)-C(51)-C(56)	37(4)
C(52)-C(51)-C(51A)	119(4)
C(56)-C(51)-C(51A)	156(4)
C(56)-C(52)-C(55)	63(10)
C(56)-C(52)-C(51)	90(9)
C(55)-C(52)-C(51)	142(8)
C(56)-C(52)-C(53)	22(9)
C(55)-C(52)-C(53)	43(7)
C(51)-C(52)-C(53)	112(5)
C(54)-C(53)-C(56)	154(10)
C(54)-C(53)-C(55)	89(10)
C(56)-C(53)-C(55)	66(10)
C(54)-C(53)-C(52)	128(9)
C(56)-C(53)-C(52)	28(10)
C(55)-C(53)-C(52)	40(10)
C(53)-C(54)-C(55)	51(6)
C(53)-C(54)-C(56)	12(8)
C(55)-C(54)-C(56)	39(6)
C(52)-C(55)-C(56)	56(10)
C(52)-C(55)-C(53)	97(9)
C(56)-C(55)-C(53)	43(8)
C(52)-C(55)-C(54)	137(9)
C(56)-C(55)-C(54)	83(10)
C(53)-C(55)-C(54)	40(9)
C(52)-C(56)-C(53)	130(10)
C(52)-C(56)-C(55)	61(10)
C(53)-C(56)-C(55)	71(10)
C(52)-C(56)-C(51)	52(7)
C(53)-C(56)-C(51)	175(10)
C(55)-C(56)-C(51)	109(10)
C(52)-C(56)-C(54)	118(10)
C(53)-C(56)-C(54)	14(10)
C(55)-C(56)-C(54)	58(10)
C(51)-C(56)-C(54)	164(10)

Table 4.4a. Crystallographic data for $[Os_3(\mu\text{-}H)_2(OC_6H_3OMe)(CO)_9]$ 4.7.

Formula weight	944.81
Temperature	150(2) K
Radiation, wavelength	MoKα, 0.71073 Å
Crystal system, space group	monoclinic, $P2_1/n$
Unit cell parameters	a = 7.4064(4) Å α = 90°
	b = 8.7999(5) Å β = 93.0780°
	c = 29.4394(17) Å γ = 90°
Cell volume	1915.96(19) $Å^3$
Z	4
Calculated density	3.275 g/cm^3
Absorption coefficient μ	19.905 mm^{-1}
F(000)	1672
Crystal colour and size	orange, 0.21 × 0.05 × 0.05 mm^3
Data collection method	Bruker SMART APEX diffractometer
	ω rotation with narrow frames
θ range for data collection	2.42 to 28.29°
Index ranges	h −9 to 9, k −11 to 11, l −38 to 38
Completeness to θ = 26.00°	99.8 %
Reflections collected	16365
Independent reflections	4553 (R_{int} = 0.0273)
Reflections with $F^2>2\sigma$	4254
Absorption correction	semi-empirical from equivalents
Min. and max. transmission	0.1026 and 0.4360
Structure solution	direct methods
Refinement method	Full-matrix least-squares on F^2
Weighting parameters a, b	0.0174, 11.1112
Data / restraints / parameters	4553 / 0 / 272
Final R indices [$F^2>2\sigma$]	R1 = 0.0252, wR2 = 0.0519
R indices (all data)	R1 = 0.0280, wR2 = 0.0530
Goodness-of-fit on F^2	1.085
Extinction coefficient	0.00034(3)
Largest and mean shift/su	0.001 and 0.000
Largest diff. peak and hole	2.094 and −1.592 e $Å^{-3}$

Table 4.4b. Bond lengths [Å] and angles [°] for $[Os_3(\mu\text{-}H)_2(OC_6H_3OMe)(CO)_9]$ 4.7.

Os(1)–C(12)	1.904(5)	Os(1)–C(11)	1.912(5)
Os(1)–C(13)	1.937(5)	Os(1)–C(6)	2.204(5)
Os(1)–Os(3)	2.7831(3)	Os(1)–Os(2)	2.8116(3)
Os(2)–C(21)	1.912(5)	Os(2)–C(22)	1.933(6)
Os(2)–C(23)	1.936(5)	Os(2)–C(6)	2.236(5)
Os(2)–Os(3)	2.9549(3)	Os(3)–C(33)	1.887(6)
Os(3)–C(31)	1.926(6)	Os(3)–C(32)	1.937(6)
Os(3)–O(1)	2.098(3)	O(1)–C(1)	1.310(6)
O(2)–C(4)	1.373(6)	O(2)–C(7)	1.426(7)
C(1)–C(2)	1.410(7)	C(1)–C(6)	1.446(7)
C(2)–C(3)	1.372(7)	C(3)–C(4)	1.402(8)
C(4)–C(5)	1.364(7)	C(5)–C(6)	1.457(7)
C(11)–O(11)	1.142(7)	C(12)–O(12)	1.138(6)
C(13)–O(13)	1.131(7)	C(21)–O(21)	1.135(6)
C(22)–O(22)	1.119(7)	C(23)–O(23)	1.123(6)
C(31)–O(31)	1.136(7)	C(32)–O(32)	1.140(7)
C(33)–O(33)	1.142(7)		

C(12)–Os(1)–C(11)	92.8(2)	C(12)–Os(1)–C(13)	94.3(2)
C(11)–Os(1)–C(13)	94.6(2)	C(12)–Os(1)–C(6)	93.3(2)
C(11)–Os(1)–C(6)	168.9(2)	C(13)–Os(1)–C(6)	94.2(2)
C(12)–Os(1)–Os(3)	88.27(15)	C(11)–Os(1)–Os(3)	93.11(15)
C(13)–Os(1)–Os(3)	171.74(16)	C(6)–Os(1)–Os(3)	77.83(13)
C(12)–Os(1)–Os(2)	137.08(15)	C(11)–Os(1)–Os(2)	119.08(15)
C(13)–Os(1)–Os(2)	109.62(15)	C(6)–Os(1)–Os(2)	51.21(14)
Os(3)–Os(1)–Os(2)	63.758(7)	C(21)–Os(2)–C(22)	93.2(2)
C(21)–Os(2)–C(23)	95.3(2)	C(22)–Os(2)–C(23)	91.7(2)
C(21)–Os(2)–C(6)	91.2(2)	C(22)–Os(2)–C(6)	95.7(2)
C(23)–Os(2)–C(6)	169.8(2)	C(21)–Os(2)–Os(1)	139.39(15)
C(22)–Os(2)–Os(1)	101.82(15)	C(23)–Os(2)–Os(1)	121.31(15)
C(6)–Os(2)–Os(1)	50.21(13)	C(21)–Os(2)–Os(3)	104.54(16)
C(22)–Os(2)–Os(3)	159.29(15)	C(23)–Os(2)–Os(3)	97.07(16)
C(6)–Os(2)–Os(3)	73.69(13)	Os(1)–Os(2)–Os(3)	57.652(7)
C(33)–Os(3)–C(31)	93.3(2)	C(33)–Os(3)–C(32)	92.8(2)
C(31)–Os(3)–C(32)	95.0(2)	C(33)–Os(3)–O(1)	171.74(19)
C(31)–Os(3)–O(1)	92.72(19)	C(32)–Os(3)–O(1)	92.35(18)
C(33)–Os(3)–Os(1)	89.78(16)	C(31)–Os(3)–Os(1)	91.23(16)
C(32)–Os(3)–Os(1)	173.12(15)	O(1)–Os(3)–Os(1)	84.43(10)
C(33)–Os(3)–Os(2)	89.20(16)	C(31)–Os(3)–Os(2)	149.73(16)
C(32)–Os(3)–Os(2)	115.03(16)	O(1)–Os(3)–Os(2)	82.75(10)
Os(1)–Os(3)–Os(2)	58.589(7)	O(1)–C(1)–C(2)	116.5(5)
C(1)–O(1)–Os(3)	118.2(3)	O(1)–C(1)–C(2)	116.5(5)
C(4)–O(2)–C(7)	117.0(4)	C(2)–C(1)–C(6)	120.4(5)
O(1)–C(1)–C(6)	123.1(5)	C(2)–C(3)–C(4)	121.4(5)
C(3)–C(2)–C(1)	120.3(5)		

Table 4.4b. Bond lengths [Å] and angles [°] for $[Os_3(\mu\text{-}H)_2(OC_6H_3OMe)(CO)_9]$ 4.7 continued.

C(5)–C(4)–O(2)	125.5(5)	C(5)–C(4)–C(3)	120.0(5)
O(2)–C(4)–C(3)	114.5(5)	C(4)–C(5)–C(6)	121.9(5)
C(1)–C(6)–C(5)	115.9(4)	C(1)–C(6)–Os(1)	115.0(3)
C(5)–C(6)–Os(1)	120.1(3)	C(1)–C(6)–Os(2)	110.1(3)
C(5)–C(6)–Os(2)	110.4(3)	Os(1)–C(6)–Os(2)	78.58(17)
O(11)–C(11)–Os(1)	177.9(5)	O(12)–C(12)–Os(1)	178.2(5)
O(13)–C(13)–Os(1)	174.7(5)	O(21)–C(21)–Os(2)	177.4(5)
O(22)–C(22)–Os(2)	177.0(5)	O(23)–C(23)–Os(2)	177.2(5)
O(31)–C(31)–Os(3)	178.8(5)	O(32)–C(32)–Os(3)	172.4(5)
O(33)–C(33)–Os(3)	175.4(5)		

Table 4.5a. Crystallographic data for $[Os_3(\mu\text{-}H)(NHC_6H_4NH_2)(CO)_{10}]$ 4.22.

Chemical formula	$C_{16}H_7N_2O_{10}Os_3$	
Formula weight	957.84	
Temperature	150(2) K	
Radiation, wavelength	MoKα, 0.71073 Å	
Crystal system, space group	monoclinic, $P2_1/n$	
Unit cell parameters	a = 13.863(3) Å	α = 90°
	b = 9.1433(17) Å	β = 109.237(3)°
	c = 17.226(3) Å	γ = 90°
Cell volume	2061.5(7) $Å^3$	
Z	4	
Calculated density	3.086 g/cm^3	
Absorption coefficient μ	18.501 mm^{-1}	
F(000)	1700	
Crystal colour and size	orange, 0.48 ´ 0.48 ´ 0.36 mm^3	
Data collection method	Bruker SMART APEX diffractometer	
	ω rotation with narrow frames	
θ range for data collection	2.30 to 28.26°	
Index ranges	h -18 to 17, k 0 to 12, l 0 to 22	
Completeness to θ = 26.00°	98.8 %	
Reflections collected	17931	
Independent reflections	4844 (R_{int} = 0.1322)	
Reflections with $F^2>2\sigma$	4360	
Absorption correction	semi-empirical from equivalents	
Min. and max. transmission	0.0408 and 0.0575	
Structure solution	direct methods	
Refinement method	Full-matrix least-squares on F^2	
Weighting parameters a, b	0.0850, 1.2427	
Data / restraints / parameters	4844 / 0 / 230	
Final R indices [$F^2>2\sigma$]	R1 = 0.0541, wR2 = 0.1365	
R indices (all data)	R1 = 0.0588, wR2 = 0.1394	
Goodness-of-fit on F^2	1.097	
Largest and mean shift/su	0.001 and 0.000	
Largest diff. peak and hole	5.448 and -3.816 e $Å^{-3}$	

Table 4.5b. Bond lengths [Å] and angles [°] for[$Os_3(\mu\text{-}H)(NHC_6H_4NH_2)(CO)_{10}$] 4.22.

Os(1)-C(12)	1.889(10)	C(12)-Os(1)-C(13)	92.2(4)
Os(1)-C(11)	1.899(11)	C(13)-Os(1)-C(11)	89.2(5)
Os(1)-Os(2)	2.7834(6)	C(13)-Os(1)-N(1)	168.4(4)
Os(2)-C(21)	1.896(11)	C(12)-Os(1)-Os(2)	134.0(3)
Os(2)-C(23)	1.929(11)	C(11)-Os(1)-Os(2)	116.7(3)
Os(2)-Os(3)	2.8452(6)	C(12)-Os(1)-Os(3)	90.9(3)
Os(3)-C(31)	1.911(11)	C(11)-Os(1)-Os(3)	173.6(3)
Os(3)-C(33)	1.961(12)	Os(2)-Os(1)-Os(3)	60.674(16)
N(2)-C(4)	1.412(13)	C(21)-Os(2)-C(23)	90.8(4)
C(1)-C(6)	1.406(13)	C(21)-Os(2)-N(1)	170.4(3)
C(3)-C(4)	1.401(13)	C(23)-Os(2)-N(1)	94.8(3)
C(5)-C(6)	1.388(12)	C(22)-Os(2)-Os(1)	133.0(3)
C(12)-O(12)	1.135(12)	N(1)-Os(2)-Os(1)	49.59(19)
C(21)-O(21)	1.142(13)	C(22)-Os(2)-Os(3)	90.2(3)
C(23)-O(23)	1.129(13)	N(1)-Os(2)-Os(3)	84.83(19)
C(32)-O(32)	1.126(13)	C(34)-Os(3)-C(31)	94.8(5)
C(34)-O(34)	1.138(14)	C(31)-Os(3)-C(32)	93.7(5)
Os(1)-C(13)	1.900(10)	C(31)-Os(3)-C(33)	171.4(5)
Os(1)-N(1)	2.145(7)	C(34)-Os(3)-Os(2)	102.0(3)
Os(1)-Os(3)	2.8486(7)	C(32)-Os(3)-Os(2)	156.8(4)
Os(2)-C(22)	1.902(12)	C(34)-Os(3)-Os(1)	160.5(3)
Os(2)-N(1)	2.134(7)	C(32)-Os(3)-Os(1)	98.3(4)
Os(3)-C(34)	1.906(11)	Os(2)-Os(3)-Os(1)	58.530(12)
Os(3)-C(32)	1.929(10)	C(1)-N(1)-Os(1)	124.4(6)
N(1)-C(1)	1.455(11)	C(2)-C(1)-C(6)	120.0(9)
C(1)-C(2)	1.365(14)	C(6)-C(1)-N(1)	116.1(8)
C(2)-C(3)	1.404(13)	C(4)-C(3)-C(2)	119.3(10)
C(4)-C(5)	1.376(14)	C(5)-C(4)-N(2)	120.2(9)
C(11)-O(11)	1.145(13)	C(4)-C(5)-C(6)	119.7(9)
C(13)-O(13)	1.142(12)	O(11)-C(11)-Os(1)	173.5(9)
C(22)-O(22)	1.111(14)	O(13)-C(13)-Os(1)	176.8(9)
C(31)-O(31)	1.149(13)	O(22)-C(22)-Os(2)	178.4(10)
C(33)-O(33)	1.124(14)	O(31)-C(31)-Os(3)	177.2(10)

Table 4.5b. Bond lengths [Å] and angles [°] for $[Os_3(\mu\text{-}H)(NHC_6H_4NH_2)(CO)_{10}]$ ***4.22 continued.***

O(33)-C(33)-Os(3)	179.0(10)
C(12)-Os(1)-C(11)	94.6(4)
C(12)-Os(1)-N(1)	96.3(3)
C(11)-Os(1)-N(1)	97.9(4)
C(13)-Os(1)-Os(2)	119.3(3)
N(1)-Os(1)-Os(2)	49.3(2)
C(13)-Os(1)-Os(3)	87.5(3)
N(1)-Os(1)-Os(3)	84.6(2)
C(21)-Os(2)-C(22)	92.0(5)
C(22)-Os(2)-C(23)	95.8(5)
C(22)-Os(2)-N(1)	95.2(4)
C(21)-Os(2)-Os(1)	120.9(3)
C(23)-Os(2)-Os(1)	114.5(3)
C(21)-Os(2)-Os(3)	88.8(3)
C(23)-Os(2)-Os(3)	174.0(3)
Os(1)-Os(2)-Os(3)	60.796(16)
C(34)-Os(3)-C(32)	101.2(5)
C(34)-Os(3)-C(33)	90.3(5)
C(32)-Os(3)-C(33)	92.1(5)
C(31)-Os(3)-Os(2)	86.1(3)
C(33)-Os(3)-Os(2)	86.1(3)
C(31)-Os(3)-Os(1)	84.9(3)
C(33)-Os(3)-Os(1)	87.9(4)
C(1)-N(1)-Os(2)	121.9(6)
Os(2)-N(1)-Os(1)	81.2(2)
C(2)-C(1)-N(1)	123.9(8)
C(1)-C(2)-C(3)	120.2(9)
C(5)-C(4)-C(3)	120.5(9)
C(3)-C(4)-N(2)	119.2(9)
C(5)-C(6)-C(1)	120.2(9)
O(12)-C(12)-Os(1)	176.8(9)
O(21)-C(21)-Os(2)	177.8(8)
O(23)-C(23)-Os(2)	172.6(9)
O(32)-C(32)-Os(3)	177.9(11)
O(34)-C(34)-Os(3)	177.1(11)

Table 5.1a. Crystallographic data for $[Os(Me_2NCS_2)_2(CO)_3]$ 5.1.

Chemical formula	$C_9H_{12}N_2O_3OsS_4$	
Formula weight	514.65	
Temperature	150(2) K	
Radiation, wavelength	MoKα, 0.71073 Å	
Crystal system, space group	orthorhombic, $Pca2_1$	
Unit cell parameters	a = 29.8531(19) Å	α = 90°
	b = 6.5510(4) Å	β = 90°
	c = 15.8913(10) Å	γ = 90°
Cell volume	3107.8(3) $Å^3$	
Z	8	
Calculated density	2.200 g/cm^3	
Absorption coefficient μ	8.746 mm^{-1}	
F(000)	1952	
Crystal colour and size	very, 0.336 x 0.142 x 0.088 mm^3	
Data collection method	Bruker SMART APEX diffractometer	
	ω rotation with narrow frames	
θ range for data collection	1.87 to 28.30°	
Index ranges	h -39 to 38, k -8 to 8, l -20 to 20	
Completeness to θ = 26.00°	99.9 %	
Reflections collected	26191	
Independent reflections	7402 (R_{int} = 0.0350)	
Reflections with $F^2>2\sigma$	6964	
Absorption correction	semi-empirical from equivalents	
Structure solution	direct methods	
Refinement method	Full-matrix least-squares on F^2	
Weighting parameters a, b	0.0268, 1.7061	
Data / restraints / parameters	7402 / 1 / 351	
Final R indices [$F^2>2\sigma$]	R1 = 0.0287, wR2 = 0.0652	
R indices (all data)	R1 = 0.0312, wR2 = 0.0661	
Goodness-of-fit on F^2	1.117	
Absolute structure parameter	0.00	
Largest and mean shift/su	0.009 and 0.000	
Largest diff. peak and hole	1.498 and -0.730 e Å	

Table 5.1b. Bond lengths [Å] and angles [°] for [Os(Me$_2$NCS$_2$)$_2$(CO)$_3$] 5.1.

Os(1)-C(13)	1.904(7)
Os(1)-C(14)	1.918(7)
Os(1)-C(15)	1.939(6)
Os(1)-S(3)	2.4236(17)
Os(1)-S(1)	2.4457(14)
Os(1)-S(2)	2.4485(17)
Os(2)-C(16)	1.908(7)
Os(2)-C(17)	1.915(7)
Os(2)-C(18)	1.925(6)
Os(2)-S(7)	2.4233(17)
Os(2)-S(6)	2.4448(14)
Os(2)-S(5)	2.4484(18)
S(1)-C(1)	1.725(6)
S(2)-C(1)	1.733(6)
S(3)-C(4)	1.755(6)
S(4)-C(4)	1.676(7)
S(5)-C(7)	1.716(6)
S(6)-C(7)	1.728(7)
S(7)-C(10)	1.760(6)
S(8)-C(10)	1.667(7)
N(1)-C(1)	1.315(7)
N(1)-C(3)	1.461(9)
N(1)-C(2)	1.469(8)
N(2)-C(4)	1.331(8)
N(2)-C(6)	1.450(9)
N(2)-C(5)	1.470(9)
N(3)-C(7)	1.317(8)
N(3)-C(8)	1.455(9)
N(3)-C(9)	1.474(8)
N(4)-C(10)	1.328(9)
N(4)-C(12)	1.460(9)
N(4)-C(11)	1.472(9)
C(13)-O(1)	1.138(8)
C(14)-O(2)	1.145(8)
C(15)-O(3)	1.133(8)
C(16)-O(4)	1.133(8)
C(17)-O(5)	1.144(8)
C(18)-O(6)	1.132(8)
C(13)-Os(1)-C(14)	92.8(3)
C(13)-Os(1)-C(15)	89.9(3)
C(14)-Os(1)-C(15)	91.7(3)
C(13)-Os(1)-S(3)	172.68(19)
C(14)-Os(1)-S(3)	91.9(2)
C(15)-Os(1)-S(3)	95.57(19)
C(13)-Os(1)-S(1)	91.71(19)
C(14)-Os(1)-S(1)	98.73(19)
C(15)-Os(1)-S(1)	169.35(19)
S(3)-Os(1)-S(1)	82.03(6)
C(13)-Os(1)-S(2)	88.9(2)

Table 5.1b. Bond lengths [Å] and angles [°] for [Os(Me$_2$NCS$_2$)$_2$(CO)$_3$] 5.1 continued.

C(14)-Os(1)-S(2)	170.85(19)
C(15)-Os(1)-S(2)	97.30(19)
S(3)-Os(1)-S(2)	85.62(6)
S(1)-Os(1)-S(2)	72.22(5)
C(16)-Os(2)-C(17)	94.4(3)
C(16)-Os(2)-C(18)	91.2(3)
C(17)-Os(2)-C(18)	92.6(3)
C(16)-Os(2)-S(7)	172.8(2)
C(17)-Os(2)-S(7)	90.3(2)
C(18)-Os(2)-S(7)	94.0(2)
C(16)-Os(2)-S(6)	89.2(2)
C(17)-Os(2)-S(6)	97.6(2)
C(18)-Os(2)-S(6)	169.8(2)
S(7)-Os(2)-S(6)	84.78(6)
C(16)-Os(2)-S(5)	89.4(2)
C(17)-Os(2)-S(5)	168.9(2)
C(18)-Os(2)-S(5)	97.8(2)
S(7)-Os(2)-S(5)	85.06(6)
S(6)-Os(2)-S(5)	71.97(6)
C(1)-S(1)-Os(1)	87.5(2)
C(1)-S(2)-Os(1)	87.2(2)
C(4)-S(3)-Os(1)	112.5(2)
C(7)-S(5)-Os(2)	87.5(2)
C(7)-S(6)-Os(2)	87.3(2)
C(10)-S(7)-Os(2)	111.7(2)
C(1)-N(1)-C(3)	122.6(5)
C(1)-N(1)-C(2)	121.2(5)
C(3)-N(1)-C(2)	115.8(5)
C(4)-N(2)-C(6)	120.7(6)
C(4)-N(2)-C(5)	123.0(6)
C(6)-N(2)-C(5)	116.3(6)
C(7)-N(3)-C(8)	122.8(6)
C(7)-N(3)-C(9)	120.1(6)
C(8)-N(3)-C(9)	116.8(6)
C(10)-N(4)-C(12)	122.7(6)
C(10)-N(4)-C(11)	120.1(6)
C(12)-N(4)-C(11)	117.1(6)
N(1)-C(1)-S(1)	124.0(5)
N(1)-C(1)-S(2)	122.9(5)
S(1)-C(1)-S(2)	113.1(3)
N(2)-C(4)-S(4)	122.9(5)
N(2)-C(4)-S(3)	113.9(5)
S(4)-C(4)-S(3)	123.2(4)
N(3)-C(7)-S(5)	122.7(5)
N(3)-C(7)-S(6)	124.0(5)
S(5)-C(7)-S(6)	113.2(4)
N(4)-C(10)-S(8)	121.8(5)
N(4)-C(10)-S(7)	114.0(5)
S(8)-C(10)-S(7)	124.2(4)
O(1)-C(13)-Os(1)	177.0(6)

Table 5.1b. lengths [Å] and angles [°] for [Os(Me$_2$NCS$_2$)$_2$(CO)$_3$] 5.1 continued.

O(2)-C(14)-Os(1)	175.5(6)
O(3)-C(15)-Os(1)	170.7(6)
O(4)-C(16)-Os(2)	178.0(6)
O(5)-C(17)-Os(2)	177.8(6)
O(6)-C(18)-Os(2)	172.1(6)

Table 5.2a. Crystallographic data for [{$Os_3H(CO)_{10}(NC_5H_3S)$}$_2$] 5.5 (C_2 symmetry).

Chemical formula	$C_{30}H_8N_2O_{20}Os_6S_2$	
Formula weight	1921.70	
Temperature	293(2) K	
Radiation, wavelength	MoKα, 0.71073 Å	
Crystal system, space group	triclinic, P-1	
Unit cell parameters	a = 9.1394(13) Å	α = 104.799(3)°
	b = 12.7677(17) Å	β = 96.663(3)°
	c = 18.342(3) Å	γ = 92.012(3)°
Cell volume	2050.7(5) $Å^3$	
Z	2	
Calculated density	3.112 g/cm^3	
Absorption coefficient μ	18.697 mm^{-1}	
F(000)	1700	
Crystal colour and size	pale, 0.20 x 0.19 x 0.02 mm^3	
Data collection method	Bruker SMART APEX diffractometer	
	ω rotation with narrow frames	
θ range for data collection	1.65 to 28.39°	
Index ranges	h -11 to 12, k -16 to 16, l -24 to 24	
Completeness to θ = 26.00°	99.3 %	
Reflections collected	18465	
Independent reflections	9531 (R_{int} = 0.0723)	
Reflections with $F^2>2\sigma$	5826	
Absorption correction	semi-empirical from equivalents	
Min. and max. transmission	0.1149 and 0.7668	
Structure solution	direct methods	
Refinement method	Full-matrix least-squares on F^2	
Weighting parameters a, b	0.0536, 0.0000	
Data / restraints / parameters	9531 / 0 / 541	
Final R indices [$F^2>2\sigma$]	R1 = 0.0658, wR2 = 0.1273	
R indices (all data)	R1 = 0.1176, wR2 = 0.1502	
Goodness-of-fit on F^2	0.925	
Largest and mean shift/su	0.001 and 0.000	
Largest diff. peak and hole	2.705 and -1.513 e $Å^{-3}$	

Table 5.2b. Bond lengths [Å] and angles [°] for [{$Os_3H(CO)_{10}(NC_5H_3S)$}$_2$] 5.5 (C_2 symmetry).

Os(1)-C(13)	1.87(2)
Os(1)-C(12)	1.91(2)
Os(1)-C(11)	1.912(19)
Os(1)-N(1)	2.107(14)
Os(1)-Os(3)	2.8730(11)
Os(1)-Os(2)	2.8891(10)
Os(2)-C(21)	1.92(2)
Os(2)-C(22)	1.93(2)
Os(2)-C(23)	1.94(2)
Os(2)-C(1)	2.124(17)
Os(2)-Os(3)	2.8808(10)
Os(3)-C(32)	1.88(2)
Os(3)-C(34)	1.90(2)
Os(3)-C(31)	1.94(2)
Os(3)-C(33)	1.94(3)
S(1)-C(3)	1.786(17)
S(1)-S(2)	2.009(7)
N(1)-C(1)	1.36(2)
N(1)-C(5)	1.37(2)
C(3)-C(2)	1.38(2)
C(3)-C(4)	1.39(2)
C(4)-C(5)	1.36(2)
C(11)-O(11)	1.13(2)
C(12)-O(12)	1.15(2)
C(13)-O(13)	1.16(2)
C(21)-O(21)	1.12(2)
C(22)-O(22)	1.17(2)
C(23)-O(23)	1.08(2)
C(31)-O(31)	1.12(2)
C(32)-O(32)	1.16(2)
C(33)-O(33)	1.17(2)
C(34)-O(34)	1.18(2)
Os(4)-C(41)	1.918(18)
Os(4)-C(43)	1.92(2)
Os(4)-C(42)	1.95(2)
Os(4)-N(2)	2.088(13)
Os(4)-Os(6)	2.8736(10)
Os(4)-Os(5)	2.9035(10)
Os(5)-C(51)	1.92(2)
Os(5)-C(52)	1.93(2)
Os(5)-C(53)	1.94(2)
Os(5)-C(6)	2.111(16)
Os(5)-Os(6)	2.8769(10)
Os(6)-C(62)	1.888(18)
Os(6)-C(61)	1.936(19)
Os(6)-C(64)	1.969(19)
Os(6)-C(63)	2.01(2)
S(2)-C(8)	1.771(19)
N(2)-C(6)	1.365(18)
N(2)-C(10)	1.38(2)

Table 5.2b. Bond lengths [Å] and angles [°] for [{$Os_3H(CO)_{10}(NC_5H_3S)$}$_2$] 5.5 (C_2 symmetry).

C(6)-C(7)	1.41(2)
C(7)-C(8)	1.40(2)
C(8)-C(9)	1.35(2)
C(9)-C(10)	1.32(2)
C(41)-O(41)	1.131(19)
C(42)-O(42)	1.11(2)
C(43)-O(43)	1.15(2)
C(51)-O(51)	1.11(2)
C(52)-O(52)	1.15(2)
C(53)-O(53)	1.10(2)
C(61)-O(61)	1.112(19)
C(62)-O(62)	1.15(2)
C(63)-O(63)	1.07(2)
C(64)-O(64)	1.10(2)
C(1)-C(2)	1.43(2)
C(13)-Os(1)-C(12)	90.1(9)
C(13)-Os(1)-C(11)	96.5(7)
C(12)-Os(1)-C(11)	94.1(8)
C(13)-Os(1)-N(1)	96.5(7)
C(12)-Os(1)-N(1)	172.7(7)
C(11)-Os(1)-N(1)	88.1(6)
C(13)-Os(1)-Os(3)	87.7(6)
C(12)-Os(1)-Os(3)	89.9(6)
C(11)-Os(1)-Os(3)	174.2(5)
N(1)-Os(1)-Os(3)	87.4(4)
C(13)-Os(1)-Os(2)	144.1(6)
C(12)-Os(1)-Os(2)	104.0(6)
C(11)-Os(1)-Os(2)	114.8(5)
N(1)-Os(1)-Os(2)	68.8(4)
Os(3)-Os(1)-Os(2)	59.99(2)
C(21)-Os(2)-C(22)	92.1(7)
C(21)-Os(2)-C(23)	96.4(9)
C(22)-Os(2)-C(23)	91.1(8)
C(21)-Os(2)-C(1)	89.4(7)
C(22)-Os(2)-C(1)	170.6(8)
C(23)-Os(2)-C(1)	98.0(8)
C(21)-Os(2)-Os(3)	174.4(6)
C(22)-Os(2)-Os(3)	91.3(5)
C(23)-Os(2)-Os(3)	88.0(6)
C(1)-Os(2)-Os(3)	86.5(5)
C(21)-Os(2)-Os(1)	115.1(6)
C(22)-Os(2)-Os(1)	102.2(6)
C(23)-Os(2)-Os(1)	144.9(6)
C(1)-Os(2)-Os(1)	68.9(5)
Os(3)-Os(2)-Os(1)	59.73(3)
C(32)-Os(3)-C(34)	91.6(9)
C(32)-Os(3)-C(31)	100.0(9)
C(34)-Os(3)-C(31)	92.7(9)

Table 5.2b. Bond lengths [Å] and angles [°] for [{$Os_3H(CO)_{10}(NC_5H_3S)\}_2$] 5.5 ($C_2$ symmetry).

C(32)-Os(3)-C(33)	90.8(8)
C(34)-Os(3)-C(33)	175.8(8)
C(31)-Os(3)-C(33)	90.2(9)
C(32)-Os(3)-Os(1)	157.8(6)
C(34)-Os(3)-Os(1)	90.0(6)
C(31)-Os(3)-Os(1)	102.0(7)
C(33)-Os(3)-Os(1)	86.5(5)
C(32)-Os(3)-Os(2)	97.6(6)
C(34)-Os(3)-Os(2)	89.1(6)
C(31)-Os(3)-Os(2)	162.2(7)
C(33)-Os(3)-Os(2)	87.2(5)
Os(1)-Os(3)-Os(2)	60.28(3)
C(3)-S(1)-S(2)	105.7(6)
C(1)-N(1)-C(5)	118.7(16)
C(1)-N(1)-Os(1)	111.9(11)
C(5)-N(1)-Os(1)	129.4(12)
C(2)-C(3)-C(4)	122.5(16)
C(2)-C(3)-S(1)	124.9(12)
C(4)-C(3)-S(1)	112.6(12)
C(5)-C(4)-C(3)	116.3(16)
C(4)-C(5)-N(1)	124.7(18)
O(11)-C(11)-Os(1)	176.7(17)
O(12)-C(12)-Os(1)	180(2)
O(13)-C(13)-Os(1)	177.2(18)
O(21)-C(21)-Os(2)	176(2)
O(22)-C(22)-Os(2)	173.2(19)
O(23)-C(23)-Os(2)	174(2)
O(31)-C(31)-Os(3)	177(2)
O(32)-C(32)-Os(3)	177(2)
O(33)-C(33)-Os(3)	174.1(17)
O(34)-C(34)-Os(3)	175.9(18)
C(41)-Os(4)-C(43)	97.7(7)
C(41)-Os(4)-C(42)	91.5(7)
C(43)-Os(4)-C(42)	93.7(9)
C(41)-Os(4)-N(2)	89.1(6)
C(43)-Os(4)-N(2)	92.5(7)
C(42)-Os(4)-N(2)	173.6(7)
C(41)-Os(4)-Os(6)	177.5(6)
C(43)-Os(4)-Os(6)	83.6(4)
C(42)-Os(4)-Os(6)	90.6(5)
N(2)-Os(4)-Os(6)	88.7(3)
C(41)-Os(4)-Os(5)	118.3(6)
C(43)-Os(4)-Os(5)	137.9(5)
C(42)-Os(4)-Os(5)	105.8(6)
N(2)-Os(4)-Os(5)	68.5(4)
Os(6)-Os(4)-Os(5)	59.73(3)
C(51)-Os(5)-C(52)	93.0(7)
C(51)-Os(5)-C(53)	94.9(7)
C(52)-Os(5)-C(53)	95.4(8)

Table 5.2b. Bond lengths [Å] and angles [°] for [{$Os_3H(CO)_{10}(NC_5H_3S)\}_2$] 5.5 ($C_2$ symmetry).

C(51)-Os(5)-C(6)	89.6(7)
C(52)-Os(5)-C(6)	172.0(7)
C(53)-Os(5)-C(6)	91.9(7)
C(51)-Os(5)-Os(6)	174.0(6)
C(52)-Os(5)-Os(6)	91.8(5)
C(53)-Os(5)-Os(6)	88.3(5)
C(6)-Os(5)-Os(6)	85.1(4)
C(51)-Os(5)-Os(4)	115.6(6)
C(52)-Os(5)-Os(4)	103.8(5)
C(53)-Os(5)-Os(4)	142.5(5)
C(6)-Os(5)-Os(4)	68.3(4)
Os(6)-Os(5)-Os(4)	59.62(2)
C(62)-Os(6)-C(61)	100.9(8)
C(62)-Os(6)-C(64)	92.9(8)
C(61)-Os(6)-C(64)	92.4(8)
C(62)-Os(6)-C(63)	90.1(8)
C(61)-Os(6)-C(63)	91.6(8)
C(64)-Os(6)-C(63)	174.5(7)
C(62)-Os(6)-Os(4)	157.8(6)
C(61)-Os(6)-Os(4)	101.1(5)
C(64)-Os(6)-Os(4)	88.9(5)
C(63)-Os(6)-Os(4)	86.5(5)
C(62)-Os(6)-Os(5)	97.3(6)
C(61)-Os(6)-Os(5)	161.8(5)
C(64)-Os(6)-Os(5)	87.4(5)
C(63)-Os(6)-Os(5)	87.6(5)
Os(4)-Os(6)-Os(5)	60.65(2)
C(8)-S(2)-S(1)	107.7(6)
C(6)-N(2)-C(10)	119.2(14)
C(6)-N(2)-Os(4)	111.9(10)
C(10)-N(2)-Os(4)	128.8(11)
N(2)-C(6)-C(7)	119.2(14)
N(2)-C(6)-Os(5)	110.6(11)
C(7)-C(6)-Os(5)	129.5(12)
C(8)-C(7)-C(6)	119.4(16)
C(9)-C(8)-C(7)	118.1(17)
C(9)-C(8)-S(2)	117.8(14)
C(7)-C(8)-S(2)	124.1(14)
C(10)-C(9)-C(8)	122.5(18)
C(9)-C(10)-N(2)	121.4(17)
O(41)-C(41)-Os(4)	176.6(19)
O(42)-C(42)-Os(4)	174.7(18)
O(43)-C(43)-Os(4)	178.3(15)
O(51)-C(51)-Os(5)	174.4(17)
O(52)-C(52)-Os(5)	176.5(19)
O(53)-C(53)-Os(5)	177.9(17)
O(61)-C(61)-Os(6)	177.7(18)
O(62)-C(62)-Os(6)	177.9(18)
O(63)-C(63)-Os(6)	174.5(18)

Table 5.2b. Bond lengths [Å] and angles [°] for [{$Os_3H(CO)_{10}(NC_5H_3S)$}$_2$] 5.5 (C_2 symmetry).

O(64)-C(64)-Os(6)	178.8(17)
N(1)-C(1)-C(2)	120.1(16)
N(1)-C(1)-Os(2)	110.4(12)
C(2)-C(1)-Os(2)	129.3(14)
C(3)-C(2)-C(1)	117.7(16)